Dynamic Nature of Multispecies Biofilm Under Stress

A thesis presented in partial fulfilment of the requirements for the degree of

Doctor of Philosophy

In

Food Microbiology

At Massey University, Manawatu Campus, New Zealand

Krisha Pant

2026

Highlights

- The biofilm formation and interaction between *P. fluorescens*, *S. aureus*, and *L. monocytogenes* are dependent on the nutrient concentration, with higher nutrient levels leading to higher biofilm formation, greater exopolysaccharide production, enhanced tolerance to sanitisers, and synergistic interactions.

- The shear stress impacts the biofilm formation in both single and multi-species biofilm. *L. monocytogenes* showed weak biofilm formation (cell counts) under flow but increased in dual species and triple species biofilm where *P. fluorescens* was present.

- Filament-like structures formed with *L. monocytogenes* in a single species biofilm under turbulent flow (shear stress), which were absent in dual species biofilm (with *P. fluorescens*), indicating better adaptation in a multispecies arrangement compared to a single species under shear stress.

- The dual-species biofilm formed by *P. fluorescens* and *L. monocytogenes* is significantly impacted by the sequence of colonisation. *L. monocytogenes* showed significantly higher attachment (30 min) and biofilm formation when introduced to a pre-formed *P. fluorescens* biofilm (48 h).

Abstract

Multispecies biofilms are an arrangement of sessile communities of multiple species of bacteria, embedded within the 3D structure of the extracellular matrix produced by multiple microorganisms in the community. These biofilms can be found in many natural environments, such as food, clinical, and natural surfaces. When multiple species of bacteria come together, the interactions between these bacteria define the evolution of the biofilm, including pathogenicity and response to cleaning and sanitizing agents. The existing research focus has been extensively on single-species biofilm, as these are simpler to study. However, in a natural environment, multi-species biofilm is the most common. The variables present in the environment can impact the complex interactions in multispecies biofilms. This study hypothesized that multispecies biofilms have different biofilm properties compared to their single-species counterparts, and common variables encountered in the food industry, such as nutrients and flow, significantly impact both single and multispecies biofilm formation.

For the first research objective, single, dual, and triple species biofilm from a combination of spoilage and pathogenic bacteria relevant to food processing, *P. fluorescens*, *S. aureus*, and *L. monocytogenes,* were studied for changes in the interactions under different nutrient environments on polystyrene surfaces. The crystal violet values ($O.D_{590}$ nm) and interaction equations showed that the interactions between the bacteria can develop into competition under nutrient limitation (10% TSB), in contrast to synergy under nutrient abundance (full-strength TSB). These observations were supported by higher biofilm formation based on total biomass and higher exopolysaccharide under nutrient-abundant conditions. Since the cell concentrations between the bacteria formed under both nutrient conditions were comparable, it may be possible that under low nutrient conditions, the bacteria are focused on survival rather than on matrix overproduction as observed in nutrient-abundant conditions (**Chapter 3**). All three bacteria involved showed increased tolerance against sodium hypochlorite sanitizer in the multispecies arrangement compared with their single-species counterparts, more so prominent in *L. monocytogenes* with 1.1 $\log_{10}$ reduction in multispecies compared to its single species tolerance (4.3 $\log_{10}$ reduction), indicating added protection in multispecies biofilm.

The next objective examined biofilm formation on an industrially relevant surface, stainless-steel, under the influence of turbulent flow (Reynold number > 4000). The impact of flow in single and multispecies biofilm formation was analysed using the Centre for Disease Control

and Prevention (CDC) bioreactor. Both single and multispecies biofilm formation were significantly impacted by the turbulent flow, with higher exopolysaccharide (EPS) and increased tolerance to sodium hypochlorite sanitizer in biofilm formed under flow compared to the static system. Epifluorescence microscopy revealed structural variation, with interstitial voids present in the three-species biofilm, which was not observed in the static system (**Chapter 4**). The impact of turbulence was more pronounced for single and dual species combinations of *S. aureus* and *L. monocytogenes*, with observations such as macroscopic threads and microscopic filaments and low cell concentrations in both single and dual species biofilm. In the presence of *P. fluorescens*, both these structures were absent, and the cell concentrations increased significantly ($p<0.05$) in the multispecies biofilm.

The filamentous cell formation in single species and its absence, followed by a significant increase in *L. monocytogenes* cells in the dual species biofilm with *P. fluorescens* under turbulent flow, were further analysed. Preliminary analysis found that the cell concentration of *L. monocytogenes* in a single species was limited to 5.1 $\log_{10}$ CFU/cm^2 after 48 h, where filamentous cells (27.7 µm in length) were observed. In dual species with *P. fluorescens*, the cell concentration reached 8.7 $\log_{10}$ CFU/cm^2, and no filaments were observed. Gene expression analysis showed significant ($p<0.001$) downregulation of *motB* (motility), *sigB* (stress), and cell division (*ftsX* and *ftsW*), and upregulation of *mpl* (adhesion) and *rodA* (rod shape), indicating *L. monocytogenes* adaptation to shear stress (**Chapter 5**). While the gene expression and motility studies provide insight into stress adaptation and filament formation, further insights into the significantly higher cell concentration of *L. monocytogenes* in dual-species biofilm with *P. fluorescens* can be understood through sequential biofilm formation.

For the final chapter, the sequence of attachment and biofilm formation in a dual species biofilm of *P. fluorescens* and *L. monocytogenes* under both static and turbulent flow conditions was investigated to further understand why *L. monocytogenes* cells show a spike in cell concentration under turbulent flow in dual-species biofilms. Results showed that this significant spike can be observed within 48 h in 2 conditions: when both bacteria are co-inoculated, and secondly, when *L. monocytogenes* was added into the 48 h preformed *P. fluorescens* biofilm. The preformed *P. fluorescens* biofilm also correlated with higher attachment (30 min) of *L. monocytogenes* cells (**Chapter 6**). Interestingly, the conditioning of the stainless-steel surfaces by freeze-dried and rehydrated exopolysaccharides (0-27.5 µg/mL) extracted from *P. fluorescens* biofilm did not affect the attachment of *L. monocytogenes*, indicating other factors, such as biofilm structure, other biofilm components, or the presence

of *P. fluorescens* cells, could be at play. While the initial attachment of *P. fluorescens* was negatively affected by the *Listeria* preformed biofilm formed under flow, the overall biofilm (cell concentration) was not affected by either the flow or the colonisation order. This chapter provides insight into the significantly higher growth of *L. monocytogenes* in multispecies biofilm under turbulent flow, also observed in the previous chapter.

Overall, the presence of multiple bacteria in the three species biofilm selected for this study altered the cell composition of the biofilm, the exopolysaccharide concentration, stress adaptation, and the tolerance to sanitizers, indicating the importance of studying multispecies biofilm as the natural state of biofilm in the environment. This is the first reported study on biofilms in these three species to examine the nutrient and flow variables and to provide insights into how the interaction between bacteria varies in response to these external variables.

Thesis Overview

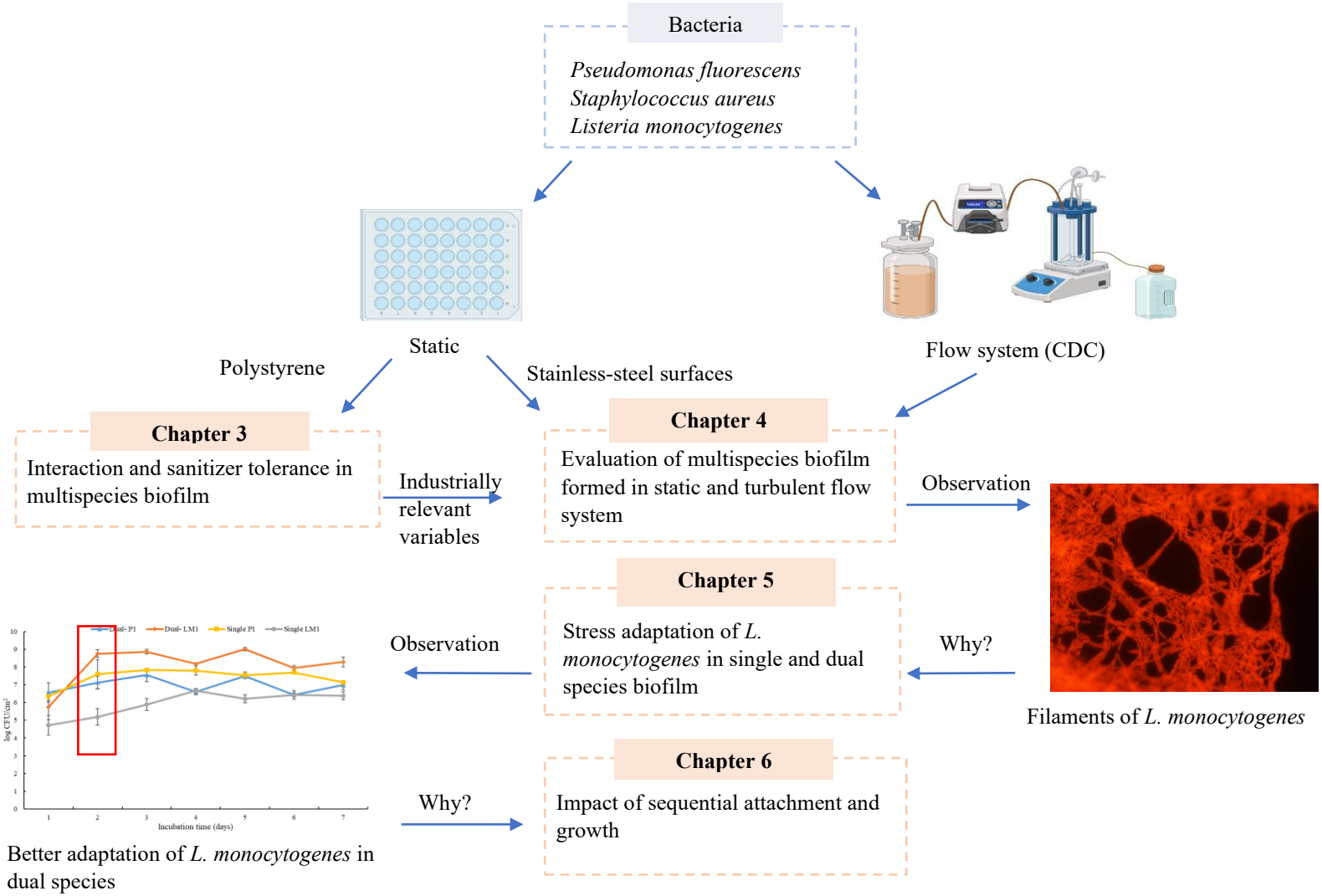

Acknowledgements

I would like to thank my supervisor, Steve, for his excellent support and advice, both within and beyond research. I'll always be grateful for your kind words and contagious curiosity in research. Thank you, Jon, for your brilliant ideas, for being the voice of logic, and for your overall support during the study. These years would not have gone so smoothly without the immense support and guidance from my supervisors. A grateful thank you also goes to Massey University for the Massey Doctoral Scholarship Award, which made all this possible.

I would also like to thank Ann-Marie and Baizura for creating a positive and productive microbiology lab environment. I will always remember the time spent in the lab fondly. Thank you, Anja, from Molecular Cell Biology at Massey, for your training and insights into genetic analysis. A special thank you to Simon from the mechatronics workshop at Massey for helping us with the coupons and holders, which turned out to be a vital component of this thesis. I would like to express my sincere gratitude to all my lab mates for their help and support during the studies.

I would like to take this opportunity to thank Gloria and Yalda for joining me on adventures through amazing hikes and weekend brunches. Special thanks to my wonderful officemates, Ili and Srinithi, for their baked goods, chats, and advice. Thank you, Ashmita and Deny, for being comrades and advisors on this journey and for being home away from home. I couldn't have asked for better people to share this journey of intellectual and personal growth.

My deepest gratitude goes to my parents for instilling and nurturing a love of science that set me on this path of exploration. To my sister Nisha for being patient with me on both good and bad days. I owe my sense of wonder and positivity to my family.

I gratefully acknowledge Bledisloe Park, whose quiet paths and riverbanks shaped the way I approach failed experiments and complicated manuscripts. I am incredibly grateful for all the other people I met during this journey. Thank you for being wonderful teachers; I learned something from all of you.

Publications and Conference Presentations

Publications

Pant, K., Palmer, J., & Flint, S. (2026). Sequential Attachment and *Listeria* Predominance Under Turbulent Flow. *Biofouling*, 1-16.

Pant, K., Palmer, J., & Flint, S. (2026). Conditional synergy: Impact of nutrient abundance on multispecies biofilm formation and sanitiser tolerance. *Food Microbiology*, 104952.

Pant, K., Palmer, J., & Flint, S. (2025). Shear stress adaptation of *Listeria monocytogenes* in mono and dual-species biofilms. *Food Research International*, 117190.

Pant, K., Palmer, J., & Flint, S. (2025). Multispecies biofilm cities and the importance of the order of colonisation. *Food Control*, 111319.

Pant, K., Palmer, J., & Flint, S. (2025). Evaluation of single and multispecies biofilm formed in the static and continuous systems. *International Journal of Food Microbiology*, 429, 111030.

Conference Presentations

Friends under crisis: *Listeria* Stress Adaptation in dual species biofilms. *Oral presentation*, 2025 New Zealand Microbiology Society Conference, 17-20 November, Rotorua, New Zealand.

Listeria: The ultimate shapeshifter. *3M presentation* (Student Finalist), 2025 New Zealand Microbiology Society Conference, 17-20 November, Rotorua, New Zealand.

Gold Digging in Biofilms: In it for Snacks and Networking. *Poster Presentation*, 2025 New Zealand Microbiology Society Conference, 17-20 November, Rotorua, New Zealand.

Turbulence and Teamwork: A Study on Multispecies Biofilm Formed Under Turbulent Flow. *Poster Presentation*, 2025 New Zealand Institute of Food Science and Technology Conference, 24-26 June, Palmerston North, New Zealand.

Friendly Interactions and Sanitiser Tolerance in Multispecies Biofilm. *Poster Presentation*, 2024 New Zealand Institute of Food Science and Technology Conference, 2-4 July, Hamilton, New Zealand.

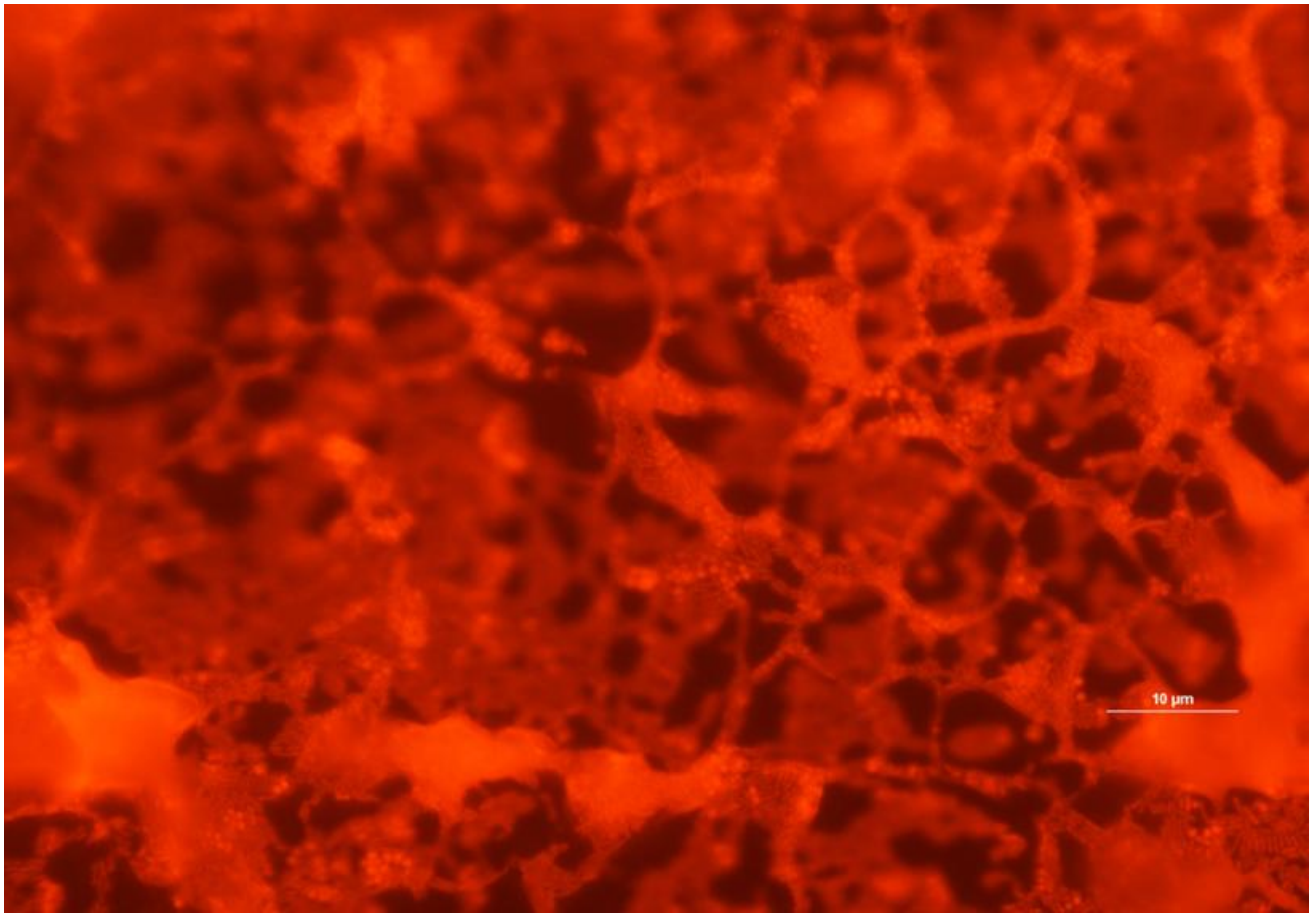

Frontispiece Epifluorescence image of three-species biofilm (*P. fluorescens*, *S. aureus*, and *L. monocytogenes*) formed under turbulent flow (CDC bioreactor) on a stainless-steel surface at 72 h in 10% TSB and 30°C (Stained with Acridine Orange).

Table of Contents

List of Figures

Chapter 2

Chapter 3

Chapter 4

Chapter 5

Chapter 6

List of Tables

Chapter 2

Chapter 3

Chapter 4

Chapter 5

Chapter 1. Introduction

1.1 Background

Biofilm is composed of microbial cells embedded in the extracellular polysaccharide matrix produced by bacteria and is attached to biotic/abiotic surfaces (Rodríguez-Melcón, Alonso-Hernando, et al., 2021). Bacteria rarely exist by themselves in any relevant environment, including, but not limited to, food contact surfaces (Zhou, Dong, et al., 2024), natural environments (Raghupathi et al., 2018), waste-water treatment plants (Huang et al., 2019), medical equipment and surfaces (Maillard & Centeleghe, 2023), and marine fouling (Park et al., 2025). The number of bacteria in these multispecies arrangements can range from dual species to hundreds, residing in the same community and undergoing different interactions (Tan et al., 2017). The beneficiaries are decided through bacterial interactions and spatial structures equipped with an array of channels for the distribution of nutrients and removal of waste materials (Pang et al., 2017; Sauer et al., 2007). The evolution of planktonic cells to sessile cells benefits the bacteria by providing increased resistance to stressors (antibiotics, antimicrobials, and host immunity), and an organised distribution of nutrients (Bottery et al., 2021; Donlan, 2001; Shrout et al., 2011), stable spatial arrangement for metabolites and genetic material exchange (Molin & Tolker-Nielsen, 2003), and mechanical stability (Mosteller & Bishop, 1993). Multispecies biofilm formation on any biotic/abiotic surface takes place through various stages, initiated by the irreversible attachment of one or more bacteria to the surface, followed by the production of extracellular matrix (ECM), microcolony formation, maturation, and sequential dispersal of biofilms (Jahid & Ha, 2014). The major constituents of the extracellular matrix in the biofilm are extracellular polysaccharides (EPS), enzymes, bacteriocins, proteinaceous substances, and nucleic acids (Hobley et al., 2015; Schilcher & Horswill, 2020).

Pseudomonas, *Staphylococcus*, and *Listeria* are among the most frequently isolated bacteria from industrial surfaces, both in single-species and multispecies communities (Dong et al., 2022; Kart et al., 2014; Zhou, Dong, et al., 2024). There have been reports of the enhanced attachment and growth of *Listeria* in the presence of specific *Pseudomonads* (Norwood & Gilmour, 2000; Rodríguez-López et al., 2022), and *Staphylococcus* being the precursor/signalling microorganisms to test for the presence of *Listeria* specific to the dairy industry when sampled in 15 dairy plants (Frank et al., 1990). These arrangements can result in a complex biofilm with a complicated spatial structure and emergent properties, rendering the single-species targeted antimicrobials less effective or even ineffective (Alonso et al., 2020;

Tadielo et al., 2022; Wang et al., 2021; L. Yuan, M. F. Hansen, et al., 2020). The interaction between these multiple bacteria in the biofilm directly affects the formation and maturation through interspecies interactions, such as neutral, antagonistic, or synergistic (Elias & Banin, 2012). While the neutral interaction has no specific effect on the bacteria present, the synergistic interaction can result in the formation of persistent biofilms with emergent and functional properties, distinct from those of a single species (Wicaksono et al., 2022). These interactions have been hypothesized to be impacted by the environmental factors that are universal in natural/food processing environments (Guillonneau et al., 2018; Luo et al., 2022).

When the dynamic nature of these interactions is taken into consideration, biofilm properties such as population diversity, spatial arrangement, exopolysaccharide networks, and the response to sanitizers cannot be predicted from the fixed condition biofilms (Røder et al., 2020; Tan et al., 2017). This research aims to understand the biofilm formation, properties, and response of bacteria in multispecies biofilms under environment-dependent factors, such as nutrient variation, substrate, shear stress, and the sequence of colonization. This information will aid in understanding the evolution of biofilm in such habitats and the repercussions these could have on overall diversity and the persistence of biofilm.

1.2 Research questions

a) Does the nutrient availability and substrate material influence the biofilm formation of *Pseudomonas fluorescens* 2614, *Staphylococcus aureus* subsp. *aureus* Rosenbach (ATCC 9144), and *Listeria monocytogenes* H1 in a single, dual, and triple species biofilm? Are the interactions between these bacteria fixed or dynamic, depending upon these variables?

b) Do the hydrodynamics (shear stress) of the media impact the biofilm formation in single and multispecies? How does *L. monocytogenes* H1 adapt to hydrodynamic stress, especially in multispecies biofilm?

c) Is there an optimal order of colonization of the surface by the bacteria for the best fitness of the multispecies biofilm? Is attachment, maturation, or detachment impacted by the presence of preformed conditioned biofilm on a surface?

1.3 Objectives

The primary objective of this study is to evaluate and understand the interspecies interactions between bacteria: *Pseudomonas fluorescens* 2614, *Staphylococcus aureus* subsp. *aureus* Rosenbach (ATCC 9144), *and Listeria monocytogenes* H1 in a multispecies biofilm under variables relevant to food industry surfaces.

a) To understand the impact of nutrient variation on the biofilm formation, interaction, and sanitizer tolerance between *Pseudomonas fluorescens* 2614, *Staphylococcus aureus* subsp. *aureus* Rosenbach (ATCC 9144), and *Listeria monocytogenes* H1.

b) To analyse the impact of turbulent flow on the single and multispecies biofilm formation.

c) To assess the impact of sequential colonization on the dual-species biofilm formation by *P. fluorescens* 2614 and *L. monocytogenes* H1.

1.4 Hypotheses for the research

The biofilm formation and interactions between bacteria are significantly influenced by variables such as nutrient content, hydrodynamic conditions, and the sequence of colonisation, and are vital to understand for the control of multispecies biofilms.

Chapter 2. Literature Review

This chapter contains material that was published as a peer-reviewed article:

Pant, K., Palmer, J., & Flint, S. (2025). Multispecies biofilm cities and the importance of the order of colonization. *Food Control*, 111319.

2.1 Introduction

Biofilms are sessile communities of cells embedded in the extracellular matrix of polysaccharides, formed to protect from adverse conditions (Ramstedt & Burmølle, 2022). Biofilms are often considered a stress response to environmental changes. In food, environments, and industrial settings, the probability of bacteria existing in multispecies communities is higher than that of bacteria existing by themselves (Lee et al., 2014; Liu et al., 2018; Wang et al., 2021). By existing in a mixed population, the bacteria gain the advantage of maximum exploitation of the current environment, as well as a competitive advantage over the co-existing bacteria in the biofilm (Natan et al., 2022). This is possible because of interspecies communication between bacteria via multiple pathways, including, but not limited to, genetic material transfer, quorum sensing, metabolic pathways, and physical interactions (Joshi et al., 2021). Understanding the interactions and communications between bacteria is vital to developing biocidal agents with increased effectiveness in biofilms (Kirisits & Parsek, 2006).

In food, several resident bacteria such as *Pseudomonas* spp, *Serratia*, *Staphylococcus*, *Stenotrophomonas* spp, and *Bacillus licheniformis* have been noted to thrive in the niches of industry surfaces, where they can attach themselves and enhance the chance of contamination through food that comes into contact with the surface (Cleto et al., 2012). *Pseudomonas fluorescens* is a gram-negative, rod-shaped, motile, spoilage bacterium and is extensively studied in biofilm research as a model organism for single-species biofilm formation (Kumar et al., 2019). *P. fluorescens* is a challenging bacterium in the food industry (milk and milk products, meat products, and vegetable processing industries) for its ability to grow in a wide range of temperatures and the production of heat-resistant spoilage enzymes (proteases, lipases, lecithinases), volatile compounds, and pigments (Decimo et al., 2014). *P. fluorescens* can attach to several substrates (milk tankers, drains, conveyor belts) of varying materials and form biofilm, and enhance its tolerance to chemical (disinfectants) and environmental stress (desiccation) (Rossi et al., 2016). *Staphylococcus aureus* is a gram-positive, non-motile, coccus-shaped, food-borne pathogen capable of producing enterotoxins (Léguillier et al., 2024). The enterotoxins are resistant to proteolytic enzymes in the human gastrointestinal tract, allowing them to cross the gastrointestinal barrier and enter the blood, resulting in nausea, abdominal pain, diarrhoea, and fever 12-48 h after 8 h of consuming contaminated food. The consumption of *S. aureus*-contaminated foods can result in mild food poisoning to life-

threatening illnesses (Bencardino et al., 2021). *Listeria monocytogenes* is a gram-positive, rod-shaped, motile pathogen involved in several foodborne outbreaks over the years because of its ability to survive low temperatures (0-4°C), high salt, and pH environments (<4.4) (Colagiorgi et al., 2016). The consumption of *L. monocytogenes*-contaminated food can result in 'listeriosis', and although rare, it can be fatal to immunocompromised individuals, such as pregnant women, infants, and older people, making it a public health concern (Liu et al., 2024). *L. monocytogenes* can form biofilm on multiple surfaces relevant to food industries (glass, plastic, polypropylene, rubber, and stainless-steel) and show higher tolerance to chemical disinfectants when embedded in its exopolysaccharide matrix (Bonsaglia et al., 2014).

The biofilm is a complex structural formation where the cells are in a sessile form in their own matrix of components consisting of polysaccharides, proteins, enzymes, and other metabolites (Røder et al., 2016). The presence of bacteria in the biofilm (oral) is limited to 5-25% of the volume, the bulk (75-95%) being exopolysaccharides (Huang et al., 2011). These components are known to assist in the adhesion and maturation of biofilms at different stages of biofilm formation. In addition, the EPS provides physical support and protection against desiccation and osmotic pressure changes while acting as a warehouse for the nutrients, trace minerals, and cell-promoting metabolites (Schlafer & Meyer, 2017). The composition of the biofilm matrix of *Staphylococcus aureus* in tryptone soy broth (TSB) consists of protein (82.5%), polysaccharides (82.5%), and extracellular DNA (8.9%), respectively. Similarly, the matrix of a mature *L. monocytogenes* biofilm formed in TSB supplemented with 0.3% w/v yeast extract consists of proteins (83.3%), polysaccharides (10.9%), and extracellular DNA (5.67%) (Cervantes-Huamán et al., 2022).

P. fluorescens, *S. aureus*, and *L. monocytogenes* have several colonisation and nutritional niches (meat, dairy, fresh cut fruits and vegetables processing surfaces) in common, which result in a multispecies biofilm complex along with other background micro-organisms (Figure 2.1). The food safety risk increases when pathogens such as *S. aureus* and *L. monocytogenes* are capable of hiding in the matrix formed by higher biofilm formers, such as *P. fluorescens,* and survive strategies employed to remove them from food contact surfaces (Carrascosa et al., 2021; Fagerlund et al., 2021).

In mixed species biofilm, these bacteria that colonize the surface first and regulate the interactions with the secondary bacteria are also referred to as resident microbiota (Hascoët et al., 2019), founder bacteria (Clarke, 2016; Eigentler et al., 2022), pioneer bacteria (Lapointe et

al., 2019), or promoter bacteria (Prabhukhot, Eggleton, Kim, & Patel, 2024). The impact of early colonizers on later colonizers can be either inhibitory or facilitative, also termed as 'priority effects' (Fukami, 2015; Olsen et al., 2019). These priority effects define the composition and interactions among bacteria in the biofilm (Fukami, 2015). In facilitative conditions, the resident microbiota create a microenvironment that allows the second pathogen to acquire nutrients/metabolites. More recently, under inhibitory conditions, the concept of biocontrol by using a non-pathogen as a primary colonizer has also been explored (Angoshtari et al., 2023).

The impacts of multispecies biofilms have been studied extensively in the human gut (Debray et al., 2022; Gensollen et al., 2016; Gibbons et al., 2017; Lee et al., 2013), and nature (soil/plants) (Eng et al., 2020; von Gillhaussen et al., 2014). Microbes on food surfaces also follow similar patterns of biofilm assembly (Pang & Yuk, 2019). With the added complexities of biotic (multiple strains/species/kingdom) and abiotic (food industry surface, wastewater treatment surface, medical implants in clinical settings) variables, the biofilm formation, spatial arrangements, and the interactions between the bacteria discussed in the literature will vary from case to case (Sauer et al., 2022). Multispecies biofilms have been described as similar to cities (Clarke, 2016) with their own architecture, cross-feeding, and microenvironment maintenance within the biofilm (Paula et al., 2020). This chapter explores biofilm formation in single and multispecies arrangements, their interactions and spatial arrangements, the impact of colonisation sequence, and the removal of multispecies biofilm from industrially relevant surfaces.

B

- Dairy industry surfaces (Meesilp & Mesil, 2019)
- Whey RO membranes (Anand et al., 2014)
- Sausage production facility (Gounadaki et al., 2008)

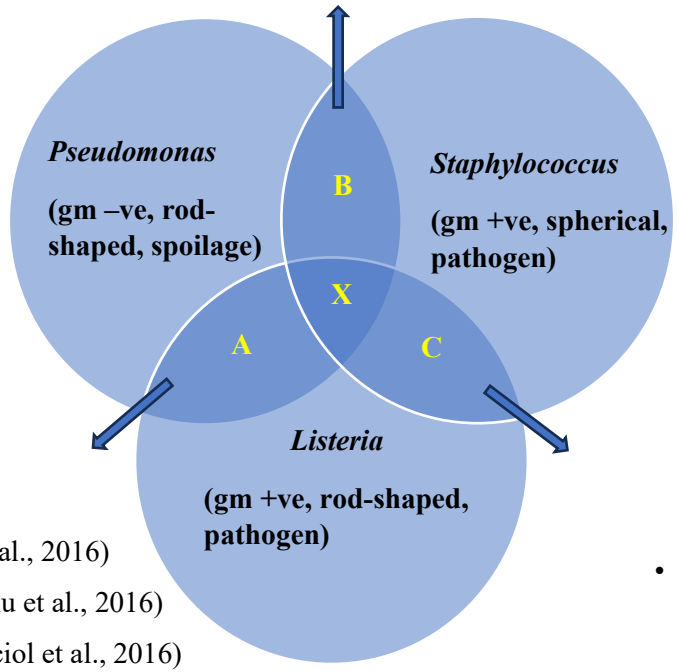

X

- Meat processing plant (Rodríguez-López et al., 2015)
- Drains of meat processing plant (Fagerlund et al., 2025)

A

- Salmon processing plant (Langsrud et al., 2016)
- Drains of food processing facilities (Liu et al., 2016)
- Cheese production- floor drains (Dzieciol et al., 2016)
- Iberian pig processing plant (Hascoët et al., 2019)
- Fruit packing facilities (Rolon et al., 2023)

C

- Seafood processing plant (Rodríguez-López et al., 2015)

Figure 2.1 Co-occurrence of *Pseudomonas*, *Staphylococcus*, and *Listeria* in multispecies arrangements in food processing industries

2.2 Biofilm formation

There are five stages of biofilm formation according to the single-species model: a) Reversible attachment b) Irreversible attachment c) Maturation d) Microcolony formation and e) Detachment (Sauer et al., 2022). When multiple bacterial species approach a surface, they can form a multispecies biofilm. However, simultaneous attachment of multiple species of bacteria at the same time is rarely observed. The variation in the formation steps can be observed with the assumption of sequential colonisation as represented in Figure 2.2: a) primary coloniser attaching to the surface, b) microcolony formation by the primary coloniser, c) attachment of secondary bacteria on the microcolonies formed by the primary coloniser, and d) sequential dispersion of the biofilm (Cheah & Bae, 2023). In the presence of multispecies bacteria, higher biofilm-forming bacteria/fast colonisers become the primary colonizers, often easing the attachment of the lower biofilm-forming bacteria. For example, in multispecies biofilm containing *Pseudomonas*, early attachment of *Pseudomonads* is observed frequently, owing to their ability to form higher biofilm (Periasamy et al., 2015).

a) Attachment

The first stage of biofilm formation requires the contact between biotic and abiotic surfaces and bacteria, facilitated by the flow of the media, electrostatic forces, Brownian motion of the particles in the media, sedimentation, in addition to the structural characteristics of bacteria such as flagella and pili, proteins, and surface polysaccharides (Floyd et al., 2017; Luo et al., 2022). The impact of these forces can be predicted using DLVO (Derjaguin, Landau, Verwey, and Overbeek) theory, which summarises the interaction of van der Waals forces (attraction) and electrostatic forces (repulsion at neutral pH). In addition, the presence of food and non-food components settled on surfaces from the bulk flow can alter surface properties (hydrophobicity, electrostatic charges) through the formation of a conditioning film and subsequently impact bacterial attachment (Palmer et al., 2007). The attachment step is reversible and can be affected by insufficient adhesive compounds in the combined flow patterns. In addition to the surface attachment, the formation of a microcolony requires the attachment of bacteria to the adjacent cells (autoaggregation or coaggregation) and the immobilized cells on the surface (co-adhesion) (Foster & Kolenbrander, 2004; Joshi et al., 2021; Kolenbrander et al., 2010; Yao et al., 2022). Similar to a single species attachment, the attachment of a second bacterium to the primary microcolony also requires coaggregation

between the bacteria (Clarke, 2016). This coaggregation was observed to be higher for dual species biofilm of *L. monocytogenes* and *Myroides odoratus* compared to their single species counterparts (Jacobs & Chenia, 2009). Sequential attachment and ecological succession of the bacteria were observed in dual-species biofilm of *E. coli* and *P. aeruginosa,* with *E.coli* attaching first (fast coloniser) but being overpowered by *P. aeruginosa,* which attached itself to the *E. coli* biofilm in the later stages (slow coloniser) (Wetherington et al., 2022). After surface attachment, bacteria multiply within the matrix, laying the foundation for biofilm maturation. The accumulation of loosely adhered exopolysaccharides is required around the polar region of the cell to form a stable arrangement and an irreversible structure. The bacterial composition of the biofilm at the time of attachment can differ significantly from that of the mature multispecies biofilm, depending on the microbes involved and internal and external stimuli (Clarke, 2016).

b) Maturation

A mature biofilm consists of compact layers of multiple species of bacteria embedded in the extracellular matrix with microenvironments suitable for each bacteria and linked with interstitial channels throughout the layers, providing access of nutrients to cells under the layers and an outlet for waste metabolites (Yao et al., 2022). The properties and constituents of a mature biofilm can be vastly different depending on the complexities of bacterial species in the biofilm (Eigentler et al., 2022). The relative abundance of bacteria in a mature biofilm is determined by their ability to replace themselves while withstanding various stresses, including nutrient gradients, environmental factors (temperature, oxygen, pH, shear), and other metabolic challenges. Due to these variables, the question of how the founding cell impacts the mature biofilm and the intercellular interactions remains a mystery on many levels (Eigentler et al., 2022). In a 79-day biofilm maturation study, most (six out of nine) of the founder bacteria abundant (>5%) at 8 days were replaced by minority species at the 79-day endpoint. Additionally, the bacteria that dominated the overall multispecies biofilm were observed in significant concentrations only from the 56-day mark of the 79-day study (Brislawn et al., 2019). Hence, the higher abundance of a single bacterium type is not guaranteed and has been reported to fluctuate as the biofilm matures. The presence of multispecies also impacts the properties of a mature biofilm. The time taken for the maturation of dual species biofilm of *Shewanella baltica* and *P. fluorescens* was found to be longer despite the decreased thickness, biomass, and polysaccharide content compared to their single species counterparts (Zhu et al., 2019).

A mature biofilm is a complex structural formation where the cells are in a sessile form in their own matrix of components commonly known as extracellular matrix, which includes polysaccharides, proteins, enzymes, and other metabolites (Røder et al., 2016). The exopolysaccharide provides physical support and protection against desiccation and osmotic pressure changes, meanwhile acting as a warehouse for the nutrients, trace minerals, and cell-promoting metabolites (Schlafer & Meyer, 2017).

c) Dispersal

Dispersion of the biofilm is often triggered by external stimuli/stress factors, such as nutrients, pH, oxygen availability, and temperature (Roy et al., 2021), as well as internal agitation between bacteria, facilitated by the release of dispersal enzymes (Rumbaugh & Sauer, 2020). In multiple species, the dispersion of a bacterium from the biofilm can create opportunities for other bacteria to attach to the hollow voids left behind and colonise the space (Culotti & Packman, 2014). In a three-species biofilm composed of *P. aeruginosa*, *E. coli*, and *E. faecalis*, *P. aeruginosa* dispersal was higher in biovolume than in the other two species, allowing all three bacteria to maintain their populations and coexist in the biofilm. In the lack of dispersion, *P. aeruginosa* dominated the biofilm, displacing both *E. coli* and *E. faecalis*. The periodic dispersal of *P. aeruginosa* cells allowed the coexistence and population boom of other bacteria in the multispecies biofilm (Holt et al., 2024). While there are assumptions that the dispersal of higher EPS-producing bacteria that produce surfactants, such as rhamnolipid, is also capable of removing other bacteria from the biofilm (Wood et al., 2018). This is highly dependent on the spatial arrangement and location of the bacteria within the biofilm. It can also be assumed that the bacteria embedded in the *Pseudomonas* biofilm layers might be removed during the dispersal of *Pseudomonas* biofilm, allowing the rare species on the outskirts an opportunity to multiply and flourish (Holt et al., 2024). In addition to the natural biofilm cycle, the removal of predominant bacteria (*Stenotrophomonas maltophilia*) through antimicrobial treatment increased the abundance of an antimicrobial-resistant, smaller bacterial community (*E. faecium* and *Stenotrophomonas haemolyticus*) in a multispecies biofilm (Wicaksono et al., 2022). In addition to the presence of multiple species of bacteria already existing in the biofilm, the attachment of new bacteria to the remnants of EPS produced by the primary after dispersion or cleaning is very much a possibility (Puga et al., 2018). Either way, the dispersal of bacteria in multispecies biofilm is closely related to the concept of competition-colonization trade-off in multispecies bacteria competing for space and resources in the biofilm (Wetherington et al., 2022).

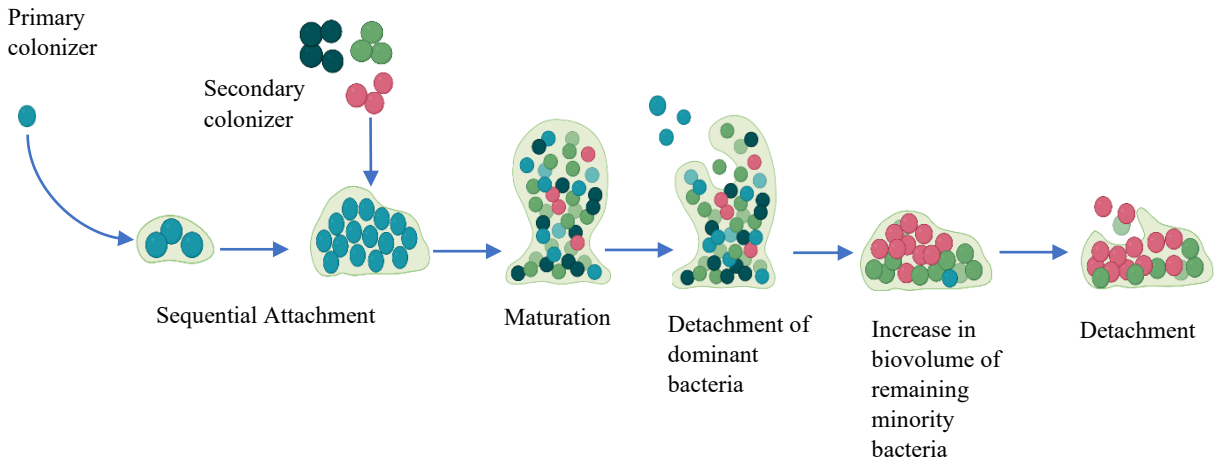

Figure 2.2 Multispecies biofilm formation steps with sequential colonisation and sequential detachment

2.3 Quorum sensing in multispecies biofilm

In a biofilm, communication between bacteria is facilitated by the secretion and reception of specific effector molecules, also known as auto-inductors (Elias & Banin, 2012). These effector molecules significantly impact the bacterial attachment, nutrient uptake, and virulence in biofilms (Hosni et al., 2011). Currently, three quorum-sensing molecules are known to mediate this type of communication. Acyl Homoserine lactones (AHLs) (specific for gram-negative bacteria), autoinducer peptide compounds (AIP), and autoinducer-2 (AI-2) for gram-positive and interspecies communication between bacteria. Autoinducer-2 (AI-2) is a universal interspecies communication molecule present in bacteria, which gives rise to signalling pathways (Bai & Rai, 2011; Miller & Bassler, 2001; Schauder & Bassler, 2001). The concentration of these autoinducers is a deciding factor in the expression of genes responsible for EPS production and biofilm formation. In a three-species biofilm comprising *P. aeruginosa*, *P. protegens*, and *K. pneumoniae*, the AHL molecule produced by *P. aeruginosa* was detected as a community modulating (higher biomass and tolerance to chemical stress) quorum-sensing molecule (Subramoni et al., 2021). When *P. aeruginosa* in the biofilm was replaced with QS mutants, the community's stress resistance was lost, indicating that a single bacterium can act as a keystone species regardless of its proportion in the biofilm (Subramoni et al., 2021). In the antagonistic dual-species biofilm of *Salmonella* and *P. aeruginosa*, AHLs produced by *P. aeruginosa* interrupt the cell division process and adhesion properties of *Salmonella*, resulting

in the inhibition of *Salmonella* in the dual-species biofilm (Wang et al., 2013). The *P. aeruginosa lasI* mutant produced flat, unstructured biofilms with reduced tolerance to detergents (sodium dodecyl sulphate), compared to the large aggregate structures typically observed in wild-type strains (Passos da Silva et al., 2017). In the dual species oral biofilm of *Actinomyces naeslundii* and *Streptococcus oralis*, communication between the bacteria during coaggregation was mediated by the autoinducer-2 (AI-2) (Hardie & Heurlier, 2008). This communication via AI-2 can inhibit or promote the bacteria involved in biofilm formation. In the dual species biofilm of *Streptococcus mitis* and *P. aeruginosa*, *S. mitis* produces the AI-2 molecule, which promotes the growth, biofilm formation, and pathogenicity of *P. aeruginosa* (Wang et al., 2016). Depending on the bacteria, AI-2 can also influence motility and exopolysaccharide production in the biofilms (Hardie & Heurlier, 2008).

2.4 Biofilm formation systems

Most of the research in single and multispecies biofilm has been focused on static systems for the higher degree of control over factors such as nutrient conditions, metabolic interactions, and substrates (Buckingham-Meyer et al., 2007; Diarra et al., 2023) (Figure 2.3). In the food processing industries, there are unit operations such as 'fresh-cut' in the minimal processing vegetables (MPV) sector (Cunault et al., 2015), storage (transport) tanks in the dairy sector (Alabdullatif, 2024), spray drying systems (Al-Sharify et al., 2025), and flow through stainless-steel tubes (Perni et al., 2006), where the impact of hydrodynamic conditions can be observed (Szlavik et al., 2012). Depending upon the hydrodynamic conditions of the biofilm formation environment, the structure, population diversity, composition, and architecture of the biofilm can be impacted (Prabhukhot, Eggleton, Vinyard, & Patel, 2024). The bioreactor system (e.g. CDC), with its continuous supply of media and turbulent flow conditions, allows for a more robust biofilm formation that simulates the biofilms formed in food industries (Lindsay et al., 2022). These variables have been observed for biofilm formed in many food industries under flow and mixing, and hence, there is a need to understand the bacterial response under such conditions (Fysun et al., 2019). The bioreactor also provides flexibility to form biofilm of differing structures (thickness), function (nutrient consumption), and composition by altering the parameters of the system (Goeres et al., 2005).

Some of the different types of bioreactors designed to analyse single and multispecies biofilms have been summarised in Table 2.1. Among the systems used in the literature, the bioreactor

introduced by the Center for Disease Control and Prevention, also known as the CDC bioreactor, has been one of the most extensively studied for its biofilm formation and response to sanitisers for bacteria such as *L. monocytogenes* (Mendez et al., 2020), *P. aeruginosa* (Goeres et al., 2005), and *S. aureus* (Buckingham-Meyer et al., 2007). Depending on the target environment, the fluid dynamics of the CDC bioreactor can be operated to form strong biofilms with greater mass (turbulent flow) or porous biofilm with weaker attachment (static or laminar flow) (Simões et al., 2022). The bioreactor consists of 4 components (Figure 2.3.C) (Lindsay et al., 2022),

A) Sterile inlet media tank: The type of media in this tank depends on the requirements of biofilm formation. Some of the commonly used media for biofilm formation for continuous systems are: 1% (300g/L) TSB for *P. aeruginosa* and *S. aureus* (single species) biofilm formation (Buckingham-Meyer et al., 2007), 0.1% (1g/L) of BHI for *L. monocytogenes* multi-strain biofilm (Mendez et al., 2020), 1% TSB for single species *L. monocytogenes* biofilm (Manville et al., 2023), and 10% TSB for dual species biofilm of *E. coli* and *L. monocytogenes* (Prabhukhot, Eggleton, Vinyard, & Patel, 2024).

B) Peristaltic pump: Connected to both the inlet media tank and the bioreactor, the flow rate of the media to the bioreactor is controlled by this pump. For steady-state biofilm formation, the residence time of planktonic cells (inoculated/shed) in the bioreactor should be shorter than the doubling time of the bacteria. Depending upon the doubling time of bacteria under the growth conditions (temperature), 11.46 mL/min for *P. aeruginosa* and 11.47 mL/min for *S. aureus* (1% TSB), 11 mL/min for *L. monocytogenes* (0.1% TSB) are some of the commonly used flow rates (Buckingham-Meyer et al., 2007; Mendez et al., 2020).

C) Bioreactor: The bioreactor consists of an impeller and the 8 rod holders. Each rod consists of 3 coupons, totalling 24 coupons in the bioreactor. The coupons, made of stainless steel, polystyrene, polypropylene, and glass, have been commonly used to observe the impact of substrate variables on biofilm formation. Depending on the impeller rpm, the flow can be classified as static (no flow), laminar (<2000 Reynolds number), transient (2000-4000 Reynolds number), or turbulent (>4000 Reynolds

number). Based on the Reynolds number, the shear stress (N/m^2) imposed on the coupon surface can also be calculated.

D) Outlet tank: This tank collects the waste media from the bioreactor.

Depending upon the velocity of flow, the shear stress can enhance both attachment and detachment; the balancing value between these two processes is called the 'critical shear stress' value (Nejadnik et al., 2008). The presence of shear stress during biofilm formation can promote biofilm formation (Tsagkari et al., 2022) and increase the resistance to the mechanical removal of the biofilm from the surface (Berne et al., 2018). This is the result of either a continuous supply of nutrients to the cells or of cell adaptation during biofilm formation, which is often observed in experimental studies. In addition to the number of cells, the dominating population in the polymicrobial biofilm, the spatial arrangement, and the biofilm properties, such as thickness and composition, can also be impacted by the shear stress (Stoodley et al., 1999). After the formation of biofilm, the sloughing off of the bacteria from the surface (Chawla et al., 2020), also known as 'washing' away of the quorum-sensing molecules, is one of the other factors impacted by the flow system. The sloughing off of the biofilm from the surface in the flow system should reduce the biofilm biomass, but some research shows that it increases instead, indicating that the biofilm formation rate is higher than the sloughing off through periodic dispersion (Rickard et al., 2004). Signalling molecules such as cyclic-di-GMP are expressed in shear stress for *P. aeruginosa,* and are indicated by the overproduction of EPS matrix in the biofilm (Rodesney et al., 2017). This overproduction of EPS acts as a physical barrier against stresses and protects the bacteria within, as noted in the dual species biofilm of *P. aeruginosa* and *E. coli* (Cheah & Bae, 2023).

Static systems

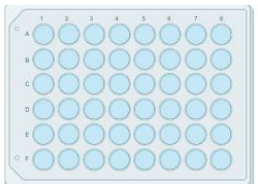

A. Polystyrene 96 well-plates (Diarra et al., 2023)

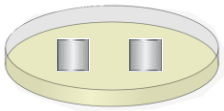

B. Stainless-steel coupons on petri plates / well-plates (Buckingham-Meyer et al., 2007)

Continuous system

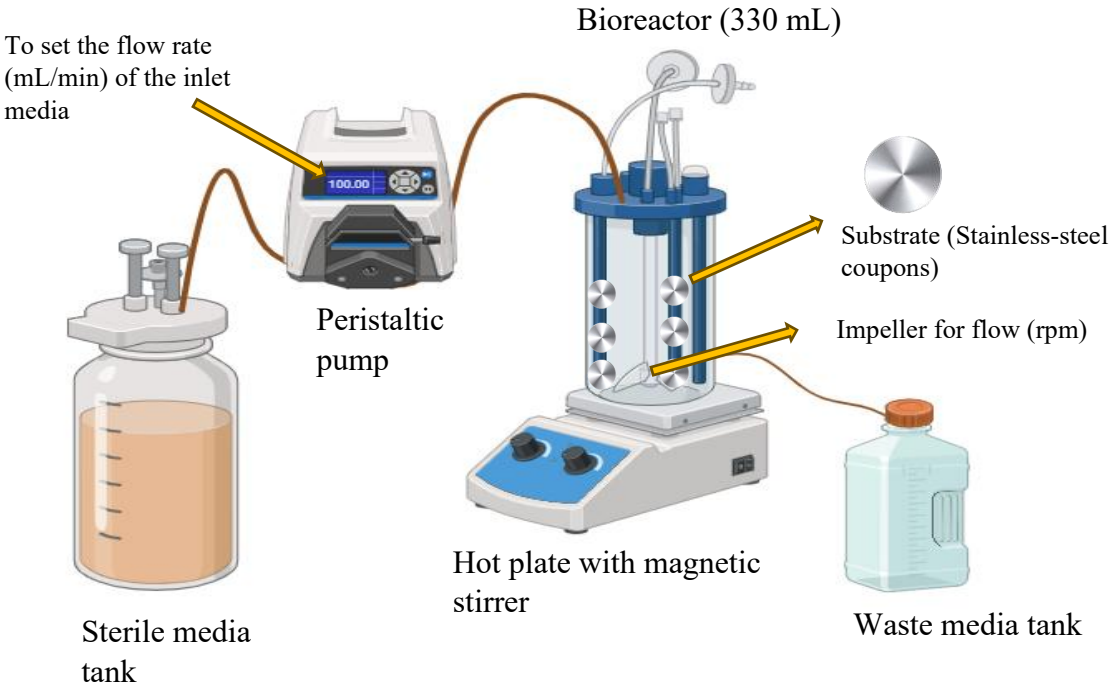

C. CDC bioreactor (Lindsay et al., 2022)

Figure 2.3 Some common systems used for multispecies biofilm analysis A) static and B) continuous systems. The image was created using Biorender.

Table 2.1 Biofilm formation systems used for single and multispecies biofilm formation

System	Flow in the system	Bacteria studied	Observation	References
Trickle-bed bioreactors	Transient flow	*Burkholderia* sp. and *Pseudomonas* sp.	Population diversity responds to environmental stresses	(Hekmat et al., 2006)
Microfluidic chamber	Static and Laminar flow	*P. fluorescens*	Higher diffusion of temporin-L (antibiofilm) under flow conditions	(Di Somma et al., 2020)
Flow cell reactors	Laminar and Turbulent flow	*P. fluorescens*	Higher biofilm mass/cm^2, cellular density, and protein content in turbulent flow	(Simões et al., 2007)
Flow through reactors	60 rpm	*L. monocytogenes* and *Flavobacterium* spp.	Higher cell concentration of *L. monocytogenes* in mixed species biofilm	(Bremer et al., 2001)
Rotating cylinder reactor (RCR)	Turbulent flow	*B. cereus* and *P. fluorescens*	High shear results in compressed biofilm	(Gomes et al., 2021)
CDC bioreactor	Laminar and Turbulent	*E. coli*, *L. monocytogenes* and *R. insidiosa*	Less ineffective chlorine treatment under turbulent flow	(Prabhukhot, Eggleton, Vinyard, & Patel, 2024)

2.5 Regulation of biofilm through the sequence of colonisation

In a multispecies biofilm arrangement, the co-attachment of multiple species of bacteria to the abiotic surface simultaneously would be rare. If the continuous influx of new colonisers in a multispecies biofilm is taken into account, significant changes in the biofilm composition, properties, and interactions can be observed (Sauer et al., 2022) (Table 2.2). This is also referred to as bacterial conditioning and impacts the attachment of the sequential bacterial species that come after the first attaching bacterial species (primary coloniser/resident microbiota) (Pang & Yuk, 2019). The resident microbiome can reduce the attachment and inhibit the growth of later attaching bacteria, or enhance it (Hascoët et al., 2021), through metabolic processes like niche pre-emption (depletion of resources by early colonisers), niche facilitative modification (early colonisers produce metabolites beneficial for later arriving microbes), and niche inhibitory modification (competition that prevents the attachment of later arriving microbes) (Debray et al., 2022). In synergistic interactions, multiple researchers have found that the presence of one bacterium species on the surface enhances the attachment of consecutive bacterial species (Lapointe et al., 2019).

In some cases, the predominance of certain isolates can be observed regardless of the biofilm stage at which the new coloniser was introduced (co-culture vs sequential). *E. coli* virulent serotypes can dominate the biofilm through competition regardless of the order of colonisation, which explains the frequent isolation of this specific serotype from food outbreaks (Wang et al., 2015). On the other hand, the production of biosurfactant by a primary coloniser such as *B. safensis* has been associated with the reduced attachment of secondary colonisers such as *L. monocytogenes* and *S. epidermidis* (Table 2.2) (Abdelli et al., 2019; Hascoët et al., 2021). A similar reduction in biofilm formation was observed for *L. monocytogenes* when inoculated to preformed *Lactobacillus sakei* biofilms (bacteriocin formers). In addition to the inhibitory compounds, the exopolysaccharide (negatively charged teichoic acid) produced by *L. sakei* has been assumed to inhibit adhesion of *L. monocytogenes* to preformed *Lactobacillus* biofilms (Leriche & Carpentier, 2000; Pérez-Ibarreche et al., 2016). The addition of bacteriocin carrier *B. thuringiensis* to a preformed *S. aureus* biofilm successfully removed the 24 h *S. aureus* biofilm and re-established a new biofilm consisting only of *B. thuringiensis*. This process was accelerated by the motility of *B. thuringiensis*, which created channels within the preformed *S. aureus* biofilm, facilitating the delivery of bacteriocin molecules (Houry et al., 2012). The three-species biofilm formed under shear stress (Centre for Disease Control Bioreactor- CDC)

showed that primary colonisation by either *P. fluorescens* or *Leuconostoc pseudomesenteroides* resulted in enhanced attachment of *L. plantarum,* indicating a synergistic interaction between the three bacteria enhanced by the amphiphilic nature of the EPS produced by *Pseudomonas* (Lapointe et al., 2019). Another interesting observation was made by Olsen et al., (2019), where the pre-colonisation by single species (good biofilm formers) did not affect the subsequent colonisers and overall biofilm formation. But when the surface was pre-colonised with dual species (good biofilm formers), the subsequent biofilm formation was higher compared to the four-species biofilm formed through co-inoculation (via drip flow reactor) comprising *Stenotrophomonas rhizophila*, *Xanthomonas retroflexus*, *Microbacterium oxydans,* and *Paenibacillus amylolyticus* (Table 2.2). This sheds light on another perspective on sequential biofilm formation when multispecies arrangements are concerned.

Table 2.2 Sequence of colonisation and its impact on biofilm composition in a multispecies biofilm system

Bacteria	Sequence of colonisation	Observation	Reference
E. coli (STEC) O157:H7 and *E. coli* O111:H8	Co-inoculation	Serotype O157:H7 outcompetes the O111:H8	(Wang et al., 2015)
	Pre-formed biofilm	Primary coloniser dominates the biofilm	
B. safensis and *L. monocytogenes*	Co-inoculation	Inhibition of *L. monocytogenes*	(Ripolles-Avila et al., 2022)
	B. safensis preformed (2 days / 7 days)	Inhibition of *L. monocytogenes*	(Hascoët et al., 2021)
L. monocytogenes and *L. sakei*	Co-cultured	Inhibition of *L. monocytogenes* biofilm formation	(Pérez-Ibarreche et al., 2016)
	Lactobacillus preformed (6 days)	Prevention of *L. monocytogenes* biofilm formation	
L. monocytogenes and *P. fluorescens*	Co-cultured (2 days)	Reduced growth of *L. monocytogenes*	(Puga et al., 2016b)
	Pseudomonas preformed	Higher cell concentration and matrix overproduction	(Puga et al., 2018)
B. thuringiensis and *S. aureus*	*S. aureus* preformed (1 day)	Complete eradication of *S. aureus* biofilm and replacement by *B. thuringiensis*	(Houry et al., 2012)

P. fluorescens, L. plantarum, and *L. pseudomesenteroides*	*P. fluorescens* or *L. pseudomesenteroides* preformed	Enhanced attachment of *L. plantarum*	(Lapointe et al., 2019)
Stenotrophomonas rhizophila, Xanthomonas retroflexus, Microbacterium oxydans and Paenibacillus amylolyticus	Co-inoculated	Synergistic interaction-higher biofilm	(Olsen et al., 2019)
	Preformed biofilm- *S. rhizophila* and *X. retroflexus*	Higher biofilm formation	
	Preformed biofilm- *M. oxydans* and *P. amylolyticus*	Lowered biofilm formation	

2.6 Spatial arrangement of bacteria in multispecies biofilm

The limited mobility of the bacteria embedded inside the biofilms results in a specific spatial arrangement commonly approached through microscopic observations and modelling (Bao et al., 2015). The metabolic function and the overall role of each bacterium regulate the spatial arrangement of the bacteria in a multispecies biofilm setup (Lee et al., 2014). The spatial location and density of the primary colonisers were significant in the competitive interactions between the bacteria in a multispecies biofilm (Eigentler et al., 2022). The higher biofilm-forming bacteria can be found around the top, and the bacteria that provide structural support are found at the bottom (Cheah & Bae, 2023). In addition, facultative anaerobes can be found in the bottom layers, covered by the species that require oxygen for growth and EPS production (Cheah & Bae, 2023). The bacterial population across the mature biofilm is also regulated by the gradients of nutrients, oxygen, and waste products across the plane (Serra & Hengge, 2014).

The spatial arrangement of the biofilm can be observed as microcolonies, co-growth microbial layering, and specific mixing patterns (Figure 2.4), depending on the metabolic requirements and the nutrient distribution in the media (Liu et al., 2018). Much of the spatial structure is associated with the extracellular matrix, which directly affects resilience, intercellular communication, nutrient distribution, and genetic material exchange between cells (Lee et al., 2014; Nadell et al., 2017). In dual species biofilm formed by *Pseudomonas spp*. and *L. monocytogenes*, the latter was found in the bottom layers of the biofilm, providing higher survival during surface sanitiser treatment (Puga et al., 2018; Ripolles-Avila et al., 2022). In addition to the co-culture, the sequentially added *L. monocytogenes* incorporated itself more deeply into the bottom layers of preformed *Pseudomonas* biofilm, with *Pseudomonas* forming a blanket-like layer of bacteria on top (Puga et al., 2018; Thomassen et al., 2023). The hollow voids left behind by *P. aeruginosa* during dispersion on the surface can be colonised by *E. coli*, leading to a similar 'blanket' layering of the *E. coli* (Culotti & Packman, 2014). When a higher EPS-producing spoilage microbe, such as *P. fluorescens,* is introduced into multi-strain biofilm environments, it initiates overproduction of EPS and migrates to the top of the biotic and abiotic layers to gain increased access to oxygen (W. Kim et al., 2014). The migration of bacteria within preformed biofilms is driven by gradients across the surface created by high cell density (in the centre of the biofilm) and by access to nutrients (at the edges and surface of the biofilm) (Xavier et al., 2009). A similar observation was made for four species of biofilm consisting of *Stenotrophomonas rhizophila*, *Xanthomonas retroflexus*, *Microbacterium oxydans*, and

Paenibacillus amylolyticus, where the pre-inoculation of bacteria did not affect the spatial arrangement despite causing significant changes in the biofilm biomass (Olsen et al., 2019). These observations show that the spatial distribution of bacteria in the biofilm depends on their inherent properties and metabolic requirements and can be independent of the sequence of colonisation.

In addition to the layering effect, the formation of individual microcolonies on the surface, with the primary coloniser inside and the second bacterium attached to the outside in layers, has also been observed. This spatial arrangement was observed for bacteria with high oxygen requirements, in which one microcolony maintains a safe distance from another, and each microcolony has two layers of bacteria, as observed in the dual species biofilm of *P. putida* and *Acinetobacter* sp. C6 (Haagensen et al., 2015) (Figure 2.4.C).

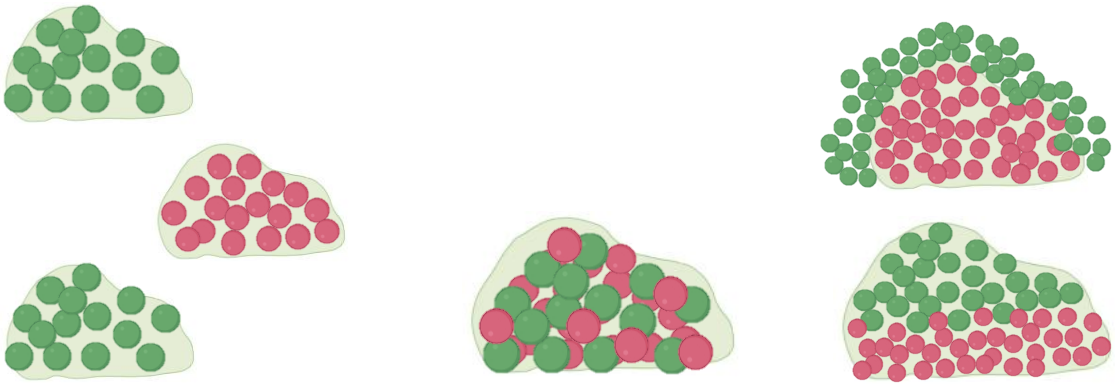

A

(Nielsen et al., 2000)

B

(Rodríguez-López et al., 2022)

C

(Haagensen et al., 2015) (Rodríguez-Melcón, Alonso-Hernando, et al., 2021)

Figure 2.4 The spatial arrangement of bacteria in biofilm A) single species microcolonies of *Pseudomonas* sp. and *Burkholderia* sp., B) Intermixed dual species biofilm of *P. fluorescens* and *L. monocytogenes*. C) Layered dual species biofilm of Salmonella and *E. faecium*. This image was created using Biorender.

2.7 Interaction between the bacteria in the multispecies biofilm

The high density of bacteria in biofilms and their spatial arrangement ensure both inter- and intra-species linking within the biofilms (Kreth et al., 2005). The interspecies interactions in multi-species biofilms are so intricately linked that these biofilms have often been referred to

as multicellular individuals (Yao et al., 2022). This coalescing can lead to various interactions, cooperative/synergistic, competitive/antagonistic, and neutral (Burmølle et al., 2014). The coaggregation leading to cooperative interactions has been extensively studied in dental biofilms (Kim et al., 2017; Kreth et al., 2005). To categorise the interactions between the bacteria, as a first step, biofilm biomass is compared under similar incubation and growth conditions between the single species and their combination (Ren et al., 2015). For example, the biomass of a multispecies biofilm will be higher than that of a single species, with the highest biofilm biomass for synergistic interaction. Similarly, for neutral and antagonistic biofilm, the biomass in the multispecies biofilm will be the same or lower than that of the single species with the highest value, respectively. These interactions are highly strain dependent (Sadiq et al., 2023). Based on similar measures, the interaction between bacteria in the biofilm can be broadly categorized into 3 types.

2.7.1 Synergistic Interactions

Synergistic interactions result in the protective effects against stressors for one or more bacteria in the biofilm (Bottery et al., 2022). In addition to the improved survival of bacteria in the mixed population, the overproduction of EPS and increased resistance to the antimicrobial compounds are some of the factors associated with synergistic interactions (Table 2.3) (Bottery et al., 2022). Multiple species of bacteria within the same biofilm can also alter the resistance of select bacteria to antibiotic treatments. Streptococcal protein A produced by *S. aureus* improved the biofilm formation and increased the tobramycin resistance of *P. aeruginosa* (Beaudoin et al., 2017). In exchange, 4-hydroxy-2-heptylquinoline-*N*-oxide and siderophores produced by *P. aeruginosa* increase the vancomycin resistance of *S. aureus* (Orazi & O'Toole, 2017). The higher biofilm biomass in the synergistic biofilm can also be the result of the production of limited metabolites (e.g., Vitamin B6 and iron) by multiple species of bacteria in the biofilm (Wicaksono et al., 2022). A three-fold increase in biofilm was observed for a four-species combination of dairy bacteria, *Stenotrophomonas rhizophila*, *Bacillus licheniformis*, *Microbacterium lacticum*, and *Calidifontibacter indicus* as the result of synergistic interactions (Sadiq et al., 2023).

When bacteria attach to surfaces in an ordered manner, the early colonisers can modify the environment, also known as 'niche modification', which eases the attachment and growth of secondary bacteria (Debray et al., 2022; Fukami, 2015). Also known as the facilitative priority

effect, this phenomenon has been studied as a synergistic interaction once the bacteria successfully attach to the surface. The presence of multiple species allows the use of available nutrients to produce a simplified carbon source termed 'cross-feeding', which normally is not possible for single-species communities (Joshi et al., 2021; Tan et al., 2017). The term 'public goods' was introduced to describe the synergistic cross-feeding in the multispecies biofilm, where substrates produced by one bacterium are utilised by another bacterium in proximity for their growth or defence (Evans et al., 2020). These 'goods' can be a composition of the matrix, such as exopolysaccharides or metabolic byproducts. In a multispecies oral biofilm consisting of *S. oralis* and *Veillonella* sp., the lactic acid produced by *S. oralis* is used by *Veillonella* sp. for growth in saliva (Periasamy & Kolenbrander, 2010).

2.7.2 Antagonistic interactions

Nutrient competition and negative metabolic interactions between multiple species of bacteria in the biofilm can favour the survival of dominant bacteria better suited to certain growth conditions (Burmølle et al., 2014). These interactions can be recurring when bacteria from different sources are introduced (Madsen et al., 2016). The antagonistic interaction can result in the reduction of tolerance against environmental or chemical stressors compared to synergistic interactions (Z. Zhu et al., 2020). There are exceptions to this, as some bacteria within the biofilm can produce a specific structure that resists chemical stress (chlorine), even during antagonistic interactions (Z. Zhu et al., 2020). These interactions are commonly the result of the production of antagonistic metabolites, which are used to outcompete other bacteria present in the biofilm. For example, when *B. cereus* and *L. monocytogenes* were introduced on the stainless-steel surface, the *B. cereus* produced metabolites that inhibited the growth and adherence of *L. monocytogenes* to the stainless-steel surface (Alonso et al., 2020) (Table 2.3). A similar observation was made in dual-species biofilm of *B. safensis* and *L. monocytogenes*, where the preformed biofilm significantly reduced the cell count of *L. monocytogenes* through competition for nutrients, space for attachment, and production of biosurfactant (Hascoët et al., 2021). Furthermore, the negative interaction between *Lactococcus piscium* and *L. monocytogenes* was found to require cell-to-cell contact, the mechanism of inhibition assumed as horizontal gene transfer via secretion pathways (types IV and VI) and nanotubes (Saraoui et al., 2016). In addition to the transfer of DNA and protein molecules, under nutrient-limiting conditions, the production of surface-inhibiting compounds (Bacteriocins CibA and CIbB) also inhibited secondary bacteria upon cell-to-cell contact with

S. pneumoniae (García-Curiel et al., 2021). The inhibition of bacteria in a multispecies environment also depends on physicochemical changes of the media (pH) and temperature. In a complex 4-species biofilm formed in microfiltered milk, the inhibition of *S. aureus* by the combination of *Lactococcus garvieae*, *Lactococcus lactis,* and *Enterococcus faecalis* co-incubation was a result of pH reduction (Alomar et al., 2008). The interaction between a dual-species biofilm of *Streptococcus* and *Lactobacillus* is defined by the metabolites produced by *Lactobacilli* that hinder the biofilm formation of *Streptococcus* on glass surfaces by altering the microenvironment's pH (Söderling et al., 2011). In a biofilm formed by multispecies bacteria such as *Enterococcus* and *Listeria* over 8 days, a reduction in pH (7 to 4.4) was found to be favourable for the growth of *Enterococcus* compared to *L. monocytogenes* (da Silva Fernandes et al., 2015). In sequential colonisation, the attachment prevention of the late colonisers can take place through 'niche pre-emption', where the resources available (nutrients/space) have already been utilised by the early colonisers, hence preventing the attachment of late-arriving species (Debray et al., 2022; Fukami, 2015).

2.7.3 Neutral Interactions

Another type of interaction is neutral interaction, which can be observed when the presence of one or more bacteria does not significantly impact the overall bacterial population in a multispecies biofilm. Depending on nutrient availability and incubation time, neutral interactions can shift to antagonistic interactions in which competition for nutrients leads to the domination of one or more bacteria over others in the population. This type of interaction has also been observed in the interaction in the biofilm (*Sphingomonas* + *Microbacterium*) when comparing 24 h (neutral) with 48 and 72 h (competitive) biofilms (Z. Zhu et al., 2020).

Some common examples of multispecies interactions in bacteria relevant to food industry surfaces are highlighted in Table 2.3.

Table 2.3 Multispecies and the result of their interaction in multispecies biofilms relevant to the food industry

Microbiological Niches	Microbes Involved	Interaction	Result of interaction	References
Pipe walls of drinking water	*Acinetobacter calcoaceticus* and *Stenotrophomonas maltophilia*	Synergistic	-Higher biofilm formation. -Increased sensitivity to sodium hypochlorite.	(Gomes et al., 2018)
Stainless-steel surfaces in the food industry	*P. aeruginosa* and *Salmonella*	Antagonistic	-Reduced biofilm formation.	(Pang et al., 2017)
Fish processing industry	*Shewanella baltica* and *P. fluorescens*	Antagonistic	-Lowered biomass and polysaccharides. -Longer time taken for the biofilm cycle. -Less compact biofilm in dual species biofilms.	(Zhu et al., 2019)
Meat processing conditions	*L. pseudomesenteroides, L. plantarum*, and *P. fluorescens*	Synergistic	-Enhanced attachment of *L. plantarum.* -Increased resistance of *Leuconostoc.*	(Lapointe et al., 2019)
Food processing facilities	*L. monocytogenes* and *Salmonella Typhimurium*	Neutral	-No changes in cell concentration.	(Tadielo et al., 2022)

Industrial juice filtration membranes	*Rhodotorula mucilaginosa, C. tropicalis, Candida krusei* and *Candida kefyr*	Neutral	-No changes in effect against farnesol, 2-phenyl ethanol.	(Agustín et al., 2019)
Poultry processing environment	*S. Enteritidis, C. jejuni,* and *C. perfringens*	Synergistic	-Increased cell concentration of *C. jejuni.*	(Kim & Oh, 2024b)
Food processing industry	*S. aureus* and *S. enterica, Raoultella planticola*	Competitive	-Decreased biofilm biomass in dual species biofilm containing *S. aureus.*	(Makovcova et al., 2017)
Fish juice	*P. fluorescens* and *S. aureus*	Competitive	-Dominance of *P. fluorescens.* -Increased sensitivity to carvacrol.	(Y. Wang et al., 2020)
Dairy surface	*Stenotrophomonas rhizophila, B. licheniformis, Microbacterium lacticum, and Calidifontibacter indicus*	Synergistic	-Elevation in biofilm formation (3.13-fold).	(Sadiq et al., 2023)

2.8 Factors affecting multispecies biofilm formation

2.8.1 Abiotic surfaces

Since attachment to a surface is the first stage of biofilm formation, the surface properties play a significant role in the overall biofilm formation (Abdallah et al., 2014). Some of the common surfaces where multispecies bacteria have been isolated from are: Meat processing surfaces (knives, tables, mincing machines) (Gounadaki et al., 2008), dairy processing industries (pasteurisation lines) (Sharma & Anand, 2002), salmon processing surfaces (conveyor belt) (Langsrud et al., 2016), fruit packing facility (floors under washing, drying, and waxing area, bristles of brushes) (Rolon et al., 2023) (Figure 2.1). The common materials used for these contact surfaces are stainless-steel (SS), polystyrene (PS), polyethylene (PE), silicone rubber (SR), polyethylene glycol (PEG), polyvinyl chloride (PVC), and polypropylene (PP). With extensive use, these common contact surfaces undergo surface degradation, which results in surfaces that enhance bacterial attachment upon contamination (Uneputty et al., 2022). The bacterial attachment to the surfaces is a complex process that depends on the surface properties (hydrophobicity, roughness), mass transfer (Van der Waals forces, electrostatic interactions, Brownian motion), and bacterial structure (pili, fimbriae, flagella), also summarised by the extended DLVO theory (Krsmanovic et al., 2021; Palmer et al., 2007).

In recent years, surface manipulation to prevent bacterial attachment and subsequent biofilm formation has been employed. Fabrication of an irregular nanostructure on the polyethylene surface successfully reduced the attachment of *E. coli* (Schwibbert et al., 2019). The fabrication of cones and holes, spherical nanostructures, copolymer brushes, changes in wettability (super-hydrophobicity), and the adoption of copper hydroxide nanowires are among the fabrication techniques successfully tested for reduced bacterial attachment (Uneputty et al., 2022). These surfaces can be impregnated with various antibiofilm/antibacterial compounds, such as nitric oxide on a polymer brush (Zhao et al., 2024), and with metal ions, such as copper, zinc, and silver on aquatic surfaces (Li et al., 2024). Between the natural (pebble/wood) and artificial (carbon fibre and polyvinyl chloride) substrates, the formation of biofilm was found to be more intricate, with high diversity and stability in the artificial substrate, with the increased ability to metabolise nitrogen, carbon, and arsenic sources in addition to resistance to extrinsic factors (Miao et al., 2021). Because of the greater smoothness of the plastic surfaces, bacteria were

retained less on the plastic surfaces as compared to the wooden surfaces with complex micro-topography (Gough & Dodd, 1998). But this can be highly dependent on the strain and the nature of the material because surfaces with higher smoothness, such as Titanium (Truong et al., 2010) and glass (Mitik-Dineva et al., 2009), can show higher bacterial attachment. In contrast, the increase in the roughness of the stainless-steel did not impact bacteria's adhesion (Hilbert et al., 2003).

2.8.2 Nutrient availability

The interaction between bacteria in the multispecies community is affected by the nutrient availability and the presence of antimicrobials during the formation of the biofilm (Parijs & Steenackers, 2018). In addition to growth, the nutrient conditions also impact the architecture of the biofilm. The biofilms formed under high nutrient availability have thicker biofilm and higher biovolume compared to low nutrient conditions (S. Yuan et al., 2020). At low glucose concentrations, *L. monocytogenes* biofilm surfaces were found to be rough and uneven (higher surface area) to increase the uptake of the nutrient for survival (Kyoui et al., 2016). *P. aeruginosa* formed mushroom-shaped biofilm under glucose minimal media, but flat non-structured biofilms in citrate or benzoate minimal media (Klausen et al., 2003). The biofilm formation of *L. monocytogenes* was found to be higher in 10× diluted brain heart infusion broth compared with full-strength BHI, owing to the compact structure of biofilms formed under stress for more efficient survival (Cherifi et al., 2017). The stress conditions, such as nutrient limitation and the presence of disinfectants in the medium, enhance biofilm formation. The low nutrient conditions can impact the interactions in multispecies biofilm formation, owing to the compatibility of the multispecies bacteria and varying community structure (Wicaksono et al., 2022). During the first stages of growth, the main carbon source, such as glucose, is metabolised for growth. In the lack of a continuous supply in multispecies biofilm, the main carbon source is replaced by the recalcitrant substrates, resulting in cross-feeding (Rivett et al., 2016). For example, after the depletion of the primary carbon sources, glycerol produced by *S. cerevisiae* can be utilized by *Lactobacillus* in fermentation, resulting in synergistic cross-feeding between the bacteria (Xu et al., 2021).

The presence of specific food constituents in milk, such as Ca^{++} and Mg^{++}, increases biofilm formation of *Geobacillus*, and lactose in *B. subtillis* and *S. aureus,* respectively (Dutra et al., 2018). A similar observation was made for *L. monocytogenes* biofilms in salmon broth (higher

biofilm formation) compared with diluted TSB (Pang et al., 2019). The conditioning (5% skim milk) of the polystyrene surface by a protein layer resulted in 8-13% higher biofilm formation of *L. monocytogenes* (Ripolles-Avila et al., 2018). This has been attributed to the conditioning layer formed by concentrated food constituents (nutrient layers) on the surface for enhanced biofilm formation (Mazaheri et al., 2023). In a study of *L. monocytogenes* biofilm formation on stainless-steel coupons, higher bacterial growth was observed on the non-preconditioned (6.63 ± 0.42 $\log_{10}$ CFU/cm^2) surface compared with the preconditioned (food residue) surface (5.71 ± 0.60 $\log_{10}$ CFU/cm^2). Depending on composition, the conditioning layers can impact the bacteria's binding behaviours and result in weaker biofilms (Paz-Méndez et al., 2017). The food constituents also influence the efficiency of cleaning compounds in the industry. The removal (alkaline chlorine) of *L. monocytogenes* was found to be higher for preconditioned surfaces in comparison to the non-preconditioned surfaces (Mazaheri et al., 2023). A similar observation was made by Hua et al., (2021), where the reduction of *L. innocua* was higher on preconditioned surfaces (apple juice coating) than on non-preconditioned surfaces when treated with saturated steam (100°C).

2.8.3 Temperature

Studies on the effect of temperature on the arrangement of bacteria embedded in the biofilm indicate the importance of temperature in interspecies interactions. In the specific case of *L. monocytogenes* and *Pseudomonas* biofilm, the low temperature stress (4°C) was found to be unfavourable to synergistic biofilm formation compared with higher temperatures (20°C) (Puga et al., 2016b). At low temperature, the biofilm matrix components varied, despite similar cell concentrations, which was hypothesised to impact the interactions between the species (Puga et al., 2016a). The temperature also determines the number of active bacteria in the biofilms and their EPS production. *P. fluorescens* cells were found to be more active in biofilms formed at 4°C than at 30°C. Similarly, the EPS production by the *P. extremaustralis* bacteria was higher at lower temperatures (10°C) than at higher temperatures (28°C) (Yuan et al., 2018). When dual-species biofilm formed by *Pseudomonas* and *Listeria* at two different temperatures (20°C and 4°C) was compared for its structural properties, the thickness of the higher temperature biofilm was found to be double that of the lower temperature. Hollow cavities could be observed for biofilm formed under higher temperature post-treatment with antibiofilm chitosan, as observed by confocal laser microscopy (Puga et al., 2016a).

2.8.4 Other environmental factors

Some of the other factors that impact the biofilm formation are oxygen level and pH (Abdallah et al., 2014). Each bacterium in a multispecies biofilm may have different oxygen requirements (aerobic/anaerobic), which is also one of the factors that determines the spatial arrangement in biofilm formation. In the dual-species biofilm formed by *P. putida* and *Acinetobacter*, *P. putida* forms its own microcolonies, owing to its high oxygen requirements. As the oxygen level decreases, the *P. putida* biofilm disperses, impacting both the spatial arrangement of the bacteria in the biofilm and interspecies interactions (Hansen et al., 2007). The commonly observed layered biofilm formation (Figure 2.4) is the result of bacteria with high oxygen requirements on the top layers, followed by bacteria that prefer/can survive on limited oxygen access on the bottom layers (Yao et al., 2022). In multispecies with aerobic requirements, the exhaustion of oxygen can result in oxygen gradients across the biofilm, directly evolving the biofilm interactions into competition (Pouget et al., 2020). The antagonistic interaction between the obligate aerobe *Brevibacillus* sp. and the facultative aerobe *Pseudoxanthomonas* sp. in dual species biofilm formed at the air-liquid interface results in the reduction of *Brevibacillus* as a result of competition for oxygen (Yamamoto et al., 2010).

In the biofilm formed by multispecies organisms like *Enterococcus* and *Listeria* over the period of 8 days, the reduction of pH (7 to 4.4) was found to be favourable for the growth of *Enterococcus* compared to *L. monocytogenes* (da Silva Fernandes et al., 2015). The pH variation of the dual species biofilm formed by *S. epidermis* and *S. aureus* resulted in predomination of *S. epidermis* at lowered pH (pH 5 and 6) and *S. aureus* at high pH (pH 8 and 9). At high pH values, *S. epidermis* does not fully integrate into the multispecies biofilm and remains as small microcolonies compared to large clusters of dominant *S. aureus* colonies (Stewart et al., 2017), indicating that, in addition to metabolic interactions, pH also impacts the spatial arrangements. Since pH adjustment has been used to disrupt the biofilm formation and disrupt the mechanical matrix, the impact of pH on the removal of the biofilm is significant (Stewart et al., 2015).

2.9 Challenges in biofilm control

Chemical (antimicrobials), physical (UV, cold plasma), and biological (bacteriophages, enzymes) measures are targeted towards dismantling the biofilm matrix and inhibiting the

bacteria embedded in the matrix, so that further attachment of the bacteria into new biotic and abiotic surfaces does not take place (Sadekuzzaman et al., 2015; Y. Zhu et al., 2020). The removal of mature biofilm depends on various factors, including, but not limited to, attachment strength to abiotic/biotic surfaces, surface roughness, the composition and properties (thickness) of the biofilm (Y. Zhu et al., 2020).

2.9.1 Chemical methods

Sodium hypochlorite, peracetic acid, and quaternary ammonium compounds are some of the commonly used sanitizers in the food industry for their high efficiency and low costs (Deng et al., 2020) (Table 2.4). Sodium hypochlorite affects the cell through oxidation of sulfhydryl groups of certain enzymes inside the cellular membrane efficiently, but has a limited effect on mature biofilm due to its interaction with organic compounds, which are major biofilm components (Rodríguez-Melcón et al., 2019). In contrast, peracetic acid has minimal effect on other biofilm components and works as an oxidizing agent of cellular compounds (Castro et al., 2021). Even though the peracetic was found to be more effective post-application, higher growth control was achieved with sodium hypochlorite in multispecies studies (Fernández-Gómez et al., 2023) (Table 2.4).

Since effective cleaning and sanitation requires access to the sessile cells embedded in the exopolysaccharide layers in the biofilm, the interaction of sanitizers with these layers can reduce their efficiency. Recent research on dual species biofilm of *Escherichia coli* O45 and *Salmonella enterica* serovar Typhimurium treated with 100 mg/L of sodium hypochlorite for 1 min, showed that there was a significant ($p<0.05$) increase in chlorine tolerance in dual species (0.70 and 1.17 $\log_{10}$ CFU reduction) as compared to single species (1.97 and 2.01 $\log_{10}$ CFU reduction) (Lin et al., 2022) (Table 2.4). A similar study on the sanitizer effects on multispecies biofilms based on ricotta processing areas for *E. faecium*, *E. faecalis*, and *L. monocytogenes* showed increased resistance in multispecies biofilms to sanitizers, sodium hypochlorite, and quaternary ammonium compounds compared to their single species counterparts (da Silva Fernandes et al., 2017). A protective observation was made for the dual species biofilm combinations of *S. rhizophila* with *B. licheniformis* or *M. lacticum*, where the spatial arrangement of *S. rhizophila* (on top layers) protected the dual species biofilms against cleaning and disinfection processes (Table 2.4) (Sadiq et al., 2024). The pre-colonisation of *P. fluorescens* in a dual-species biofilm with *L. monocytogenes* resulted in higher EPS production,

better attachment, and greater resistance to desiccation or disinfectant treatment for *L. monocytogenes* (Pang & Yuk, 2019).

The resistance of multispecies biofilm to chemical sanitizers has been attributed to the synergy between the bacteria in the biofilm, due to the increased EPS production and increased thickness, which resists the diffusion of chemicals through the layers (Cloete, 2003), in addition to the spatial localization of the bacteria in these EPS layers (Z. Zhu et al., 2020). Genetic characteristics (genes related to oxidative stress resistance), biofilm age, and metabolite interference are some of the additional measures taken by bacteria for resistance in multispecies biofilm (Li et al., 2021).

2.9.2 Alternate methods

Owing to the rise of multidrug-resistant bacteria, the application of plant-derived antibiofilm compounds has been effective. The impact of volatile compounds can be observed via their structural groups, representing bioactive compounds such as monoterpenes (carvacrol, thymol, linalool), sesquiterpenes, and phenylpropanoids in single and multispecies biofilms. The mechanism of inhibition of sessile bacteria in the biofilm was commonly found to be membrane injury (Klančnik et al., 2021). Multispecies biofilm formed by *E. coli*, *Salmonella* Typhimurium, and *L. monocytogenes* showed enhanced resistance to grapefruit seed extract compared to their mono-species counterparts (Kim & Oh, 2024a). More recently, the application of a combination of essential oils has been introduced to overcome limitations with the application of a single bioactive compound.

Among the molecules used for the communication between interspecies bacteria and intraspecific bacteria, N-acyl homoserine lactone (AHL) molecules have been noted in multispecies biofilm containing *P. aeruginosa*, *K. pneumoniae*, and *P. protegens* (Subramoni et al., 2021). These autoinducer molecules can be quenched to further avoid the formation of biofilm, as in the case of *P. chlororaphis* (Gannesen et al., 2015). Bacteriocins (Melian et al., 2019), essential oils (eg, black cardamom) (Abdullah et al., 2021), and organic acids (lactic acids, malic acids, acetic acids, cinnamic acids) (Almasoud et al., 2016) have been identified to be effective quorum quenchers against *L. monocytogenes*, *Salmonella* Typhimurium, and *E.coli,* respectively.

Table 2.4 Effect of antibiofilm agents on the multispecies biofilm

Niches	Microbes Involved	Treatment	Observation	References
Food processing surfaces-stainless-steel	*E. coli* O45 and *Salmonella enterica* serovar Typhimurium	100 mg/l sodium hypochlorite for 1 min	-Reduced log reduction in multispecies compared to single species- increased chlorine tolerance	(Lin et al., 2022)
Food contact surfaces	*P. fluorescens* and *Salmonella* Enteritidis	Quaternary ammonium compounds (20 ppm/5 days)	-Enhanced survival of *S.* Enteritidis	(Pang et al., 2020)
Food industry surfaces	*E. coli*, *S.* Typhimurium, and *L. monocytogenes*	Grapefruit seed extract	-Enhanced resistance in multi-species biofilm	(Kim & Oh, 2024a)
Dairy pasteurizer	*S. rhizophila, B. licheniformis,* and *M. lacticum*	Standard CIP* regime	-Protected against disinfection in multi-species	(Sadiq et al., 2024)
Fruit packing facilities	*L. monocytogenes, Pseudomonadaceae, Xanthomonadaceae, Microbacteriaceae,* and *Flavobacteriaceae*	Benzalkonium chloride (12.5 ppm/2h)	-Enhanced survival of *L. monocytogenes*	(Rolon et al., 2024)

*CIP: water rinse-1.5 % (w/v) sodium hydroxide at 60 °C /6.45 min-another water rinse-1.0 % nitric acid at 60 °C /4.45 min-water rinse-0.01 % peracetic acid/7.6 min-water rinse

2.10 Gaps in the literature

It has already been established in the literature that biofilm formation, interactions, and the efforts of removal are dependent on the environmental variables, such as nutrient conditions, substrates, hydrodynamics, and the presence of multiple species (Houry et al., 2012). The impact of the nutrition and substrate variables has been in focus in single-species biofilm research (Tamminen et al., 2022). While that provides fundamental information on the bacterial nature in biofilm, properties such as population diversity, the spatial arrangement, EPS networks, and sanitiser tolerance of biofilm formed under dynamic conditions cannot be predicted from the mono-species arrangement, formed under static conditions, with the assumptions of co-inoculation (Røder et al., 2020; Tan et al., 2017). This oversight might be the reason why, despite a continuous effort to curb contamination and spoilage in food industries through a large number of physical, chemical, and biological methods of cleaning and disinfecting, the persistence of specific bacteria to grow and form biofilms continues (Luo et al., 2022). Bioreactors have been used to mimic dynamic target environments to further understand the attachment and biofilm formation (Lindsay et al., 2022; Prabhukhot, Eggleton, Kim, & Patel, 2024). Shear stress (12-54 Pa) reduces the adhesion of different strains of bacteria on the surfaces (Busscher & Van Der Mei, 2006). But these observations are based on a single-species model (Nejadnik et al., 2008) and the response to shear might not be comparable in multispecies arrangements, especially in the presence of more stress-tolerant bacteria such as *Pseudomonas*. There is a lack of research in understanding the multispecies biofilm formation under stress, the effect on the biofilm components, and the underlying reasons for their persistence in their natural environment (Guillonneau et al., 2018; Luo et al., 2022).

The establishment of higher EPS producing bacteria on the surface might impact the 'critical shear stress' value of the later-arriving bacteria, which could result in enhancement of bacterial attachment, in contrast to the decrease we observe in the single species as a result of shear. In studies of a multispecies biofilm model, the conditioning by the primary coloniser is a reality that has been considered in a few interaction studies (Puga et al., 2018; Sasahara & Zottola, 1993). The colonisation sequence can impact the attachment and biofilm formation, which could impact the interspecies interactions and their response to antimicrobial agents as well (Puga et al., 2018). Further research is needed to understand how this priority-based assembly of the biofilm impacts functional properties of multispecies biofilm relevant to food surfaces.

These findings allow us to explore the biocontrol strategies to reduce microbial contaminants of food, as well as the interference that needs to be done before the keystone antimicrobial-resistant bacteria are cemented on the surface.

Chapter 3 Impact of nutrient abundance on multispecies biofilm formation

This chapter contains material that was published as a peer-reviewed article:

Pant, K., Palmer, J., & Flint, S. (2025). Conditional synergy: Impact of nutrient abundance on multispecies biofilm formation and sanitizer tolerance. *Food Microbiology*, 104952.

3.1 Introduction

The presence of multispecies bacteria in natural biofilms has been observed in a multitude of industrial settings and food processing areas, often leading to contamination and microbial corrosion (Bonneville et al., 2021; Di Pippo et al., 2018; Dula et al., 2021). Biofilm formers such as *P. fluorescens*, *S. aureus*, and *L. monocytogenes* have been isolated in combination from various food surfaces (Cherif-Antar et al., 2016) (Figure 2.1). *Staphylococcus* and *Pseudomonas* are good biofilm formers with common nutritional niches such as meat, dairy, fresh fruits, milk, and vegetables, with *Pseudomonas* causing spoilage and *Staphylococcus* capable of causing food poisoning (Xu et al., 2019). *L. monocytogenes* can adhere to, multiply, and show higher sanitizer tolerance on industrial surfaces in the presence of *Pseudomonas* (dos Santos et al., 2023; Fagerlund et al., 2017; Kocot & Olszewska, 2020; Thomassen et al., 2023). These multispecies biofilms show increased tolerance to cleaning agents compared to single-species biofilms, which has been associated with the exchange of public goods, quorum sensing between the bacteria involved, and added resistance provided by the biofilm matrix (Sanchez-Vizuete et al., 2015; Wicaksono et al., 2022; L. Yuan, M. F. Hansen, et al., 2020). The bacteria that survive these treatments on industrial processing surfaces can be released into the passing liquid, partly due to shear stress, and contaminate the food (Rückerl et al., 2014), which has been previously noted for pathogens such as *L. monocytogenes* (Rodríguez-Campos et al., 2019). The cross-contamination that leads from failure to remove biofilm on food industry surfaces has so far accounted for 25% of the world's food safety outbreak cases (Yushina et al., 2024).

The sanitizers commonly used in the food industry for cleaning and sanitation are quaternary ammonium compounds, peracetic acid, and chlorine compounds such as sodium hypochlorite (Chaves et al., 2024; Simões et al., 2010). The chlorine oxidizes the organic matter in the biofilm before diffusing into the layers for a bactericidal effect (Sarjit & Dykes, 2017) and can interact with proteins, enzymes, lipids, DNA, and RNA (Barnes & Greive, 2013; Ran et al., 2019). The recommended concentration of sanitizer, such as sodium hypochlorite (active chlorine 13%), ranges from 0.05-2%, depending on the intended application and treatment time (Aarnisalo et al., 2007). In the food industry, surfaces are cleaned and sanitized frequently, which results in a nutrient-depleted surface for the possible formation of bacterial biofilms. Hence, it is important to understand the responses of biofilm-forming bacteria under different nutrient conditions (Pang et al., 2019). The biofilm and its components, including

exopolysaccharides, proteins, and eDNA, are significantly affected by the nutrient conditions (Wang et al., 2022).

Previous biofilm research has extensively focused on single-species biofilm, largely due to the relative simplicity of investigations in a single species. However, bacteria on the food contact surfaces rarely exist by themselves (Sadiq et al., 2017) and the sanitizer response is defined by the complex interaction dynamics of the multiple bacteria present in the biofilm (L. Yuan, N. Wang, et al., 2020). Environmental variables such as temperature (Yushina et al., 2024), nutrients, and substrate (topography, material, and coating/conditioning) can impact the interspecies interaction in the biofilm (key species, chemical composition, and sanitizer resistance) (Ramstedt & Burmølle, 2022). Among them, nutrient concentration is a critical parameter for biofilm formation and is vital to understanding interspecies interactions in multispecies environments (Ibusquiza et al., 2012; Wang et al., 2022). This chapter aimed to understand the effect of nutrient variation on the single, dual, and triple-species biofilm formed by *P. fluorescens*, *S. aureus*, and *L. monocytogenes* and their tolerance to sub-lethal concentrations of sodium hypochlorite (50 ppm/5 min) on polystyrene surfaces.

3.2 Materials and Methods

3.2.1 Bacterial strains and culture media used

Stock cultures (-80°C) of *Pseudomonas fluorescens* 2614 (P1) (Dairy), *Staphylococcus aureus* subsp. aureus Rosenbach (ATCC 9144) (S2), and *Listeria monocytogenes* H1 (LM1) (Environment-soil) were streaked into tryptone soy agar (TSA) (Difco™, Becton, Dickinson and Company, USA) and incubated at 30°C for 24 h. All three bacteria are from a previously established culture collection of the Food Microbiology Lab, School of Natural Sciences and Food Technology, Massey University, Palmerston North, New Zealand. The colonies were then inoculated into tryptone soy broth (TSB) (Difco™, Becton, Dickinson and Company, USA) individually and incubated again in 15 mL centrifuge tubes (Falcon®, Corning, USA) for another 18 h at 30°C to prepare the working culture. After the secondary incubation, the cultures were centrifuged (Sigma® 6-16, John Morris Scientific Ltd., Germany) at 10000× g for 10 min at room temperature. The cell pellets after centrifugation were washed with sterile saline solution (0.85% w/v) via vortex mixing (30 s, highest setting) (Scilogex, Germany) and centrifugation (10000× g for 10 min). The concentrated cells were collected by removing the

saline solution and resuspending the final pellet into fresh sterile saline solution to the required cell concentration (CFU/mL). The cell concentration of each bacterium was set to 8 $\log_{10}$ CFU/mL for biofilm formation using a graph of O. D_{600nm} vs. cell concentration ($\log_{10}$ CFU/mL) (Appendix VI). The final cell concentration in the sample was fixed to 6 $\log_{10}$ CFU/mL using saline solution for dilution (×100 times).

3.2.2 Biofilm formation

Polystyrene 96-well plates (Falcon, USA) (0.34 cm^2) were used as substrates. For single species biofilm formation, 20 µl of bacteria in saline solution (8 $\log_{10}$ CFU/mL) was added to 180 µl of media (TSB or 10% TSB) in each well of the 96-well plate. For dual and triple species biofilm formation, *P. fluorescens*, *S. aureus*, and *L. monocytogenes* in 1:1 (10 µl each) and 1:1:1 (10 µl each) was added into the media (full strength TSB and 10% TSB) in single, dual, and triple species to 180 µl of media (TSB or 10% TSB). The final cell concentration was fixed at~6 $\log_{10}$ CFU/mL. The plates were incubated for 24 h at 30°C for cell quantification in the biofilm and 72 h for exopolysaccharide quantification. For blank samples, the respective sterile media were added to the wells.

3.2.3 Biofilm biomass

The biofilm biomass was determined according to Stepanović et al., (2004) with crystal violet dye (Acros Organics, USA). Crystal violet stains all biofilm components, including cells and extracellular components. The 24 h incubated plates from section 3.2.2 were washed with the saline solution (0.85%) and air-dried at room temperature for 20 min. Crystal violet dye (200 µl) (0.5% w/v in water) was added to each well in a 96-well plate and allowed to stain for 20 min before washing with saline solution until the water runs clear. The stained plate was allowed to air-dry at room temperature for 30 mins before adding 200 µl of 95% ethanol. After 20 min of ethanol extraction, the absorbance value was noted at an optical density of 590 nm using a spectrophotometer (Varioskan Lux 3020-1333, Thermo Fisher Scientific Ltd., USA).

Depending on the crystal violet value for the single and multispecies biofilm, the interaction was classified into synergistic, neutral, and antagonistic. For synergy to be effective, the absorbance for the multispecies biofilm (OD_{590} MS) needed to be higher than the absorbance obtained from the highest biofilm producer in the single-species biofilm (OD_{590} HS). This can be written as (OD_{590} MS- S.D) > (O.D_{590} HS + S.D), where S.D is the standard deviation of

respective values. Similarly for neutral interaction, (OD_{590} MS- S.D) = ($O.D_{590}$ HS + S.D) and for competitive interactions, (OD_{590} MS- S.D) < ($O.D_{590}$ HS + S.D) (Ren et al., 2015).

3.2.4 Sanitizer treatment

The response of single and multiple species bacteria in biofilm to sub-lethal concentrations of sodium hypochlorite sanitizer was analyzed according to Lin et al., (2022). After 24 h incubation at 30°C (section 3.2.2), the wells were washed with sterile saline solution (×2) to remove planktonic cells from the wells before treating with sodium hypochlorite (200 µl, 50 ppm, pH: 6.8-7) (Janola, Australia) for 5 min at room temperature immediately followed by 200 µl of 1% sodium thiosulphate neutralizer (AnalaR®, VWR International, England) for 2 mins. The wells were then promptly saline solution washed and air dried before swabbing with cotton buds (Citoswab® Citotest Labware, China) in saline solution and mixed by vortex (highest setting/1 min) to remove the cells to enable the number of cells in the biofilm after treatment to be determined. The serial 10-fold dilutions for plate counting were carried out using saline solution (0.85%) and plated on selective agar. *Pseudomonas* Isolation agar (Difco™, USA) for *P. fluorescens*, Mannitol salt agar (Oxoid, UK) for *S. aureus,* and Modified Oxford agar (HiMedia, USA) for *L. monocytogenes*.

3.2.5 Exopolysaccharide concentration

The biofilm matrix from the polystyrene surface was extracted using sonication and then quantified using phenol-sulphuric acid hydrolysis (Zhou, Dong et al., 2024). The 96-well plates with single and multispecies biofilms (72 h) from section 3.2.2 were washed (×3) with sterile saline (0.85%) solution to remove planktonic cells. Sterile distilled water (200 µl) was added into each well, and the wells were sealed using microplate sealing tape (Nunc™, Thermo Scientific™, Denmark) before sonication for 20 min (40 kHz) (Ultrasonic cleaner, DAIHAN Scientific Co., Ltd, Korea). The extraction process was completed by centrifugation (14,400× g /5 mins) of the sample solution collected from the wells. The supernatant was pooled from 96 wells in the plates and collected for filtration (0.20 µm) (Minisart, Sartorius, Germany), and the pellet was discarded. To 200 µl of filtrate, 100 µl of 6% phenol (Sigma-Aldrich, Germany) and 500 µl of 98% sulphuric acid (Ajax Finechem, Thermo Fischer Scientific, Australia) were added, and left to react for 20 min at room temperature. The optical density reading was taken

at O.D 490 nm using a spectrophotometer and compared with the standard curve for dextran (Appendix VII), and the EPS was determined as μg/cm^2 of the polystyrene surface.

To confirm the removal of biofilm from the well's surface through sonication, the wells incubated with the sample and blank were stained with crystal violet (0.5% w/v) after sonication and compared.

3.2.6 Gram staining and microscopic observation

The polystyrene surfaces for microscopy were prepared by laser cutting (EpilogLaser fusion 120 W, Alfex Laser, Australia) the polystyrene well plates into coupons of sizes of 10 mm×10 mm. The dual species biofilm was formed in 48 well plate (Falcon, USA) in 1:1 ratio and 10% TSB according to section 3.2.2. The 24 h dual species biofilm of *P. fluorescens*, *S. aureus*, and *L. monocytogenes* were washed with saline solution and prepared for gram staining by air-dying the surface. The surface dry coupons were introduced into 6-well plates containing crystal violet and dipped for 1 min, followed by washing. The coupons were then introduced in wells containing Gram's iodine (potassium iodide and iodine- Thermo Fisher, New Zealand) for 1 min, followed by rinsing and decolorization with ethanol for 20 sec. The coupons were then counterstained by Safranine (Baker Analyzed®, UK) for another 1 min and air-dried for observation under light microscope (Olympus BX53F, Japan).

3.2.7 Confocal microscopy and surface plots

The co-localization of the bacteria and the structure of the biofilm formed under varying nutrient conditions was analyzed using two different stains: 4′,6-diamino-2-phenylindole (DAPI) (Invitrogen, Thermo Fisher Scientific, USA) for *P. fluorescens* and wheat germ agglutinin (WGA) Texas Red^{TM}- X conjugate (Invitrogen, Thermo-Fischer Scientific, Life Technologies corporation, USA) for *L. monocytogenes* (Zhou, Dong, et al., 2024). Biofilm formed in 10% TSB and full-strength TSB for 72 h at 30°C on polystyrene surfaces was selected for staining and confocal microscopy (Nikon D-eclipse C1, Japan). The polystyrene coupons were washed with phosphate buffer solution (PBS) (Oxoid, Oxoid Ltd, UK) and a staining solution containing 6 μL of DAPI (1 mg/mL) and 6 μL of WGA- Texas red (1 mg/mL) in 6 mL of TSB. The staining was completed in the dark for 60 mins at room temperature, after which the coupons were washed with sterile distilled water and allowed to dry in the dark before proceeding to the confocal imaging. The z-stack sequence was obtained using EZ-C1

(Gold version 3.80 build 860) and processed in ImageJ software (ImageJ 1.54g, National Institute of Health, USA) for surface plots. *P. fluorescens* and *L. monocytogenes* dual-species biofilm was chosen for imaging based on the lowest log reduction of each bacterium (higher sanitizer tolerance) observed compared to other combinations and their single species counterparts (Table 3.2).

3.2.8 Statistical analysis

The significant differences between the samples were determined with one-way ANOVA (IBM SPSS version 29) with 95% confidence ($p<0.05$), together with Tukey analysis for post-hoc analysis. The correlation between the properties of the biofilm was analyzed using Pearson's Correlation Analysis (IBM SPSS version 29). All experiments had at least two biological replicates and six technical replicates, and results were presented as mean ± standard deviation.

3.3 Results

3.3.1 Biofilm formation

All three bacteria formed biofilm on the polystyrene surface under both nutrient conditions (TSB and 10% TSB) as observed through the $O.D_{590}$ nm value after crystal violet staining. Significantly higher biofilm ($p<0.001$) was observed in full-strength TSB compared to 10% TSB for all three bacteria in single and multispecies (Figure 3.1). In 10% TSB, *P. fluorescens* (0.09) and *S. aureus* (0.06) formed comparatively higher biofilm ($p<0.001$) compared to *L. monocytogenes* (0.02) in single species. A similar pattern was observed for single-species biofilm formed in TSB, with *L. monocytogenes* being the poor biofilm former (0.11) compared to *P. fluorescens* (0.21) and *S. aureus* (0.37) (Figure 3.1).

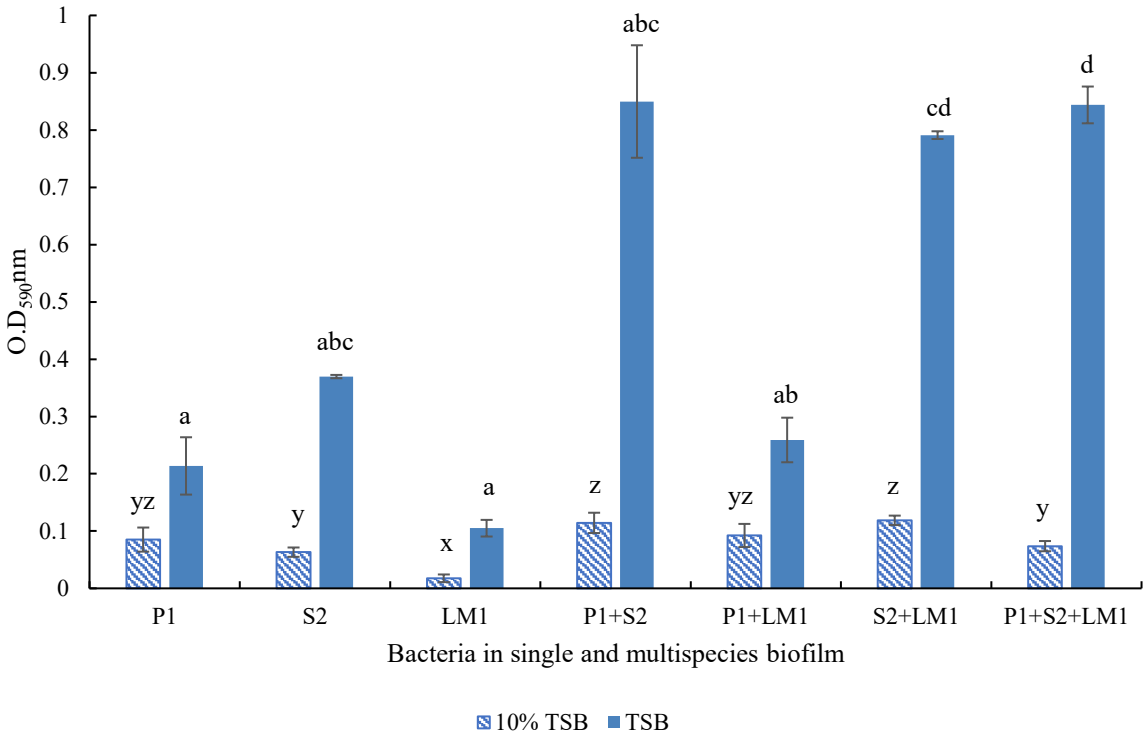

Figure 3.1 Crystal violet values (O.D 590 nm) of *P. fluorescens* (P1), *S. aureus* (S2), and *L. monocytogenes* (LM1) in single, dual, and triple species biofilm (24 h) formed in 10% TSB and full-strength TSB. The lowercase letters x,y,z, and a,b,c,d indicate the significant differences between combinations in 10% TSB and TSB, respectively.

The relationship equation by Ren et al., (2015) provided insight into the interaction between the bacteria in both nutrient-sufficient (TSB) and nutrient-deficient (10% TSB) conditions. In TSB, the combination of *P. fluorescens*, *S. aureus*, and *L. monocytogenes* in dual and triple species biofilm resulted in synergistic interactions except for *P. fluorescens* and *L. monocytogenes* dual species biofilm, which resulted in neutral interaction (0.2) (Table 3.1).

Table 3.1 Interaction between *P. fluorescens* (P1), *S. aureus* (S2), and *L. monocytogenes* (LM1) in dual and triple species biofilm formed in TSB and 10% TSB based on the relationship equation

Media	Sample	Multispecies biofilm MS ($O.D_{590}$ - S. D)	Highest biofilm former- single species SS (O. D_{590} + S. D)	Interaction
TSB	P1+S2	0.75	0.37	Synergistic
	P1+LM1	0.22	0.23	Neutral
	S2+LM1	0.78	0.37	Synergistic
	P1+S2+LM1	0.81	0.37	Synergistic
10% TSB	P1+S2	0.09	0.16	Antagonistic
	P1+LM1	0.07	0.11	Antagonistic
	S2+LM1	0.11	0.07	Synergistic
	P1+S2+LM1	0.06	0.11	Antagonistic

Synergistic interaction: MS ($O.D_{590}$ - S. D) > SS (O. D_{590} + S. D); Neutral interaction: MS ($O.D_{590}$ - S. D) = SS (O. D_{590} + S. D); Antagonistic interaction MS ($O.D_{590}$ - S. D) < SS (O. D_{590} + S. D)

Biofilm formed under 10% TSB resulted in antagonistic interactions between all combinations of dual and triple species, except *S. aureus* and *L. monocytogenes* dual species, indicating the nutrient content-based synergy of the bacteria involved (Table 3.1).

3.3.2 Biofilm formation: Cell concentrations

Under nutrient-limiting concentrations (10% TSB), there was no significant difference ($p>0.05$) in the cell concentration between single and multispecies biofilm for all three bacteria involved (*P. fluorescens*, *S. aureus*, and *L. monocytogenes*). *P. fluorescens*, *S. aureus*, and *L. monocytogenes* reached the cell concentration of 6.1-6.3 $\log_{10}$ CFU/cm^2, 7.4-7.7 $\log_{10}$ CFU/cm^2, and 6.1-7.0 $\log_{10}$ CFU/cm^2, respectively, indicating biofilm formation in both single and multispecies biofilms (Figure 3.2). The co-inoculation of the second bacteria did not impact the cell concentrations of any bacteria involved in the dual and triple species biofilm formed in 10% TSB (Figure 3.2).

In full-strength TSB, the cell concentration of all three bacteria involved, *P. fluorescens*, *S. aureus*, and *L. monocytogenes,* was comparable in single and dual species, reaching 7.0-7.7 $\log_{10}$ CFU/cm^2, 6.5-7.6 $\log_{10}$ CFU/cm^2, and 6.1-6.6 $\log_{10}$ CFU/cm^2, respectively, for each bacterium. Significantly higher cell concentration ($p<0.001$) was observed for *L. monocytogenes* in the three-species biofilm (7.9 $\log_{10}$ CFU/cm^2) compared to its single (6.6 $\log_{10}$ CFU/cm^2) and dual species (6.1-6.4 $\log_{10}$ CFU/cm^2) counterparts (Figure 3.2). There was no significant difference ($p>0.05$) between the cell concentrations of biofilm in TSB and 10% TSB.

In the three-species biofilm, the predominance of the bacteria varied depending on the media used. In the three-species biofilm formed in 10% TSB, the cell concentration of *S. aureus* was higher (7.7 $\log_{10}$ CFU/cm^2) compared to *L. monocytogenes* (6.18 $\log_{10}$ CFU/cm^2) and *P. fluorescens* (6.76 $\log_{10}$ CFU/cm^2), indicating the predominance of *S. aureus*. In contrast, observations showed that the three biofilm species formed in full-strength TSB had no significant differences ($p>0.05$) in the cell concentration among *P. fluorescens* (7.7 $\log_{10}$ CFU/cm^2), *S. aureus* (8.3 $\log_{10}$ CFU/cm^2), and *L. monocytogenes* (7.9 $\log_{10}$ CFU/cm^2) (Figure 3.2).

These mixed species of biofilms showed intermixed cells in the biofilm formed in full strength TSB, as observed through Gram staining (Figure 3.3).

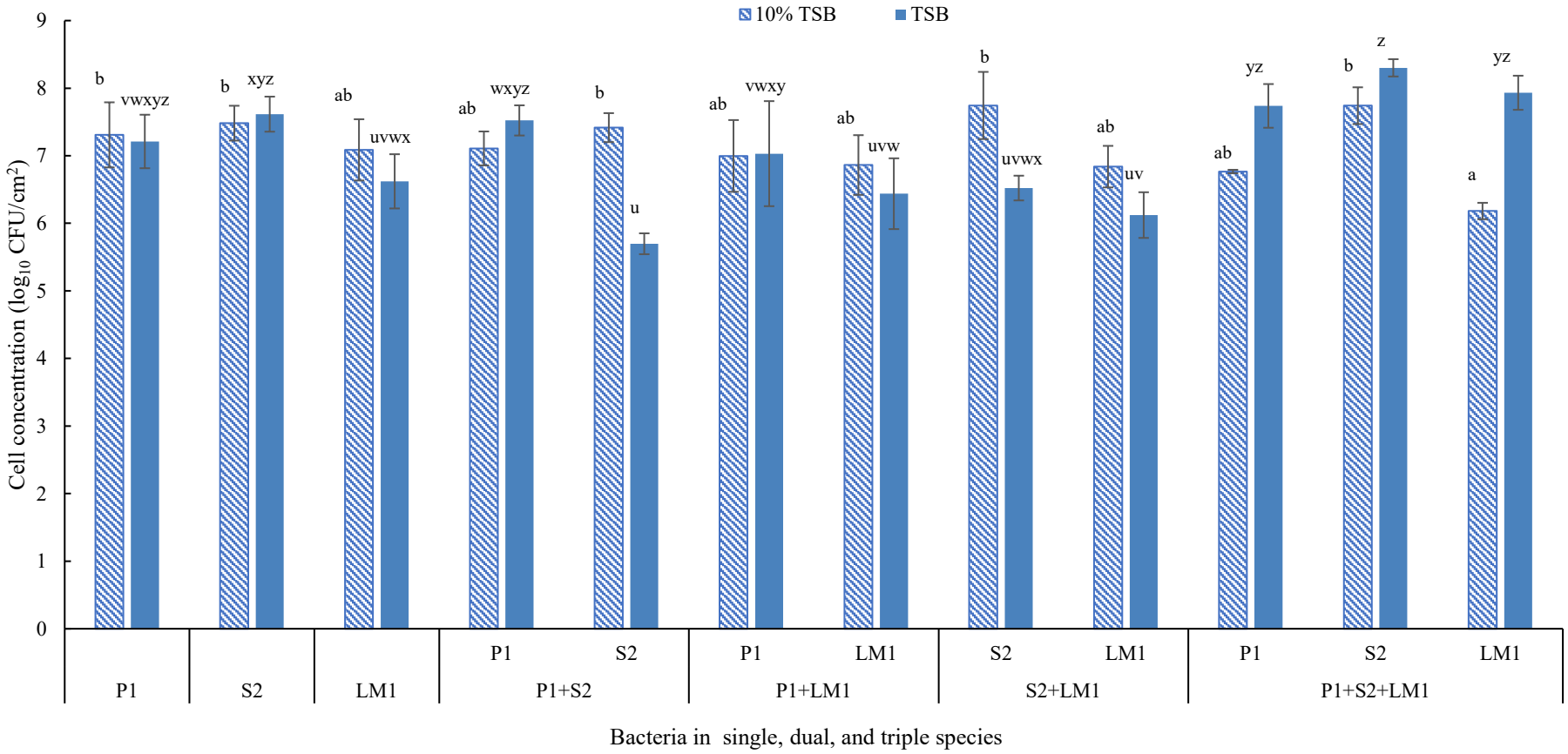

Figure 3.2 Cell concentrations of *P. fluorescens* (P1), *S. aureus* (S2), and *L. monocytogenes* (LM1) in single, dual, and triple species biofilm formed in nutrient-limited conditions (10% TSB) and nutrient-abundant conditions (TSB). The lowercase letters a,b and u-z indicate the significant differences between combinations in 10% TSB and TSB, respectively.

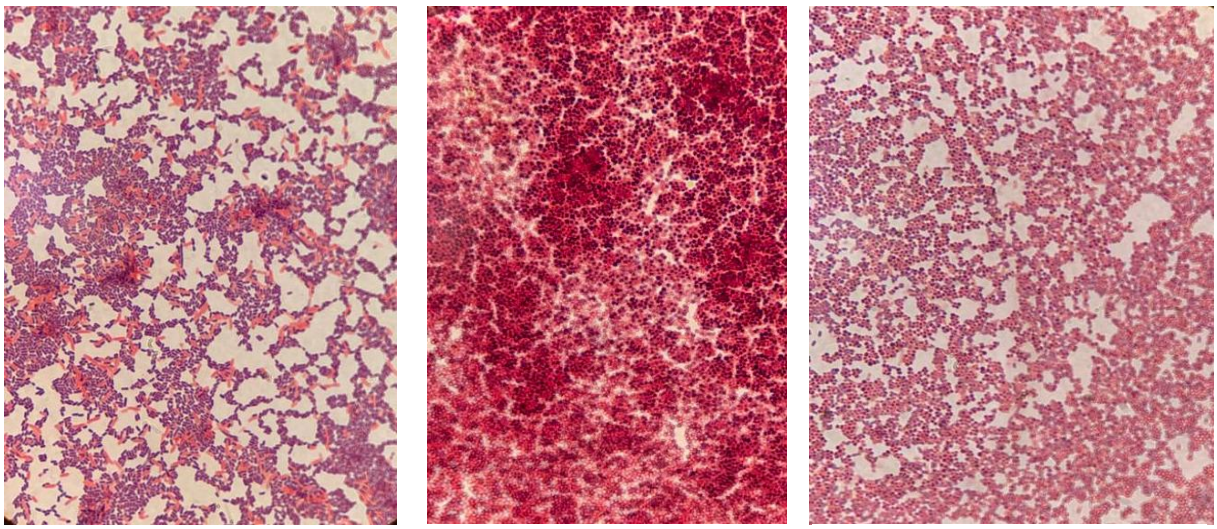

A. *P. fluorescens* (pink rods) and *L. monocytogenes* (purple rods)

B. *P. fluorescens* (pink rods) and *S. aureus* (purple cocci)

C. *S. aureus* (purple cocci) and *L. monocytogenes* (purple rods)

Figure 3.3 Gram-staining images of *P. fluorescens* (pink cylindrical cells), *S. aureus* (purple spherical cells), and *L. monocytogenes* (purple cylindrical cells) dual species biofilm formed in full-strength TSB on polystyrene surface at 30°C for 24 h.

3.3.3 Sanitizer tolerance

The sanitizer treatment of biofilms (single and multispecies) formed in nutrient-limiting conditions (10% TSB) reduced the cell concentration of all three bacteria, *P. fluorescens*, *S. aureus*, and *L. monocytogenes* below the detection limit (<2.1 $\log_{10}$ CFU/cm^2) (Figure 3.4).

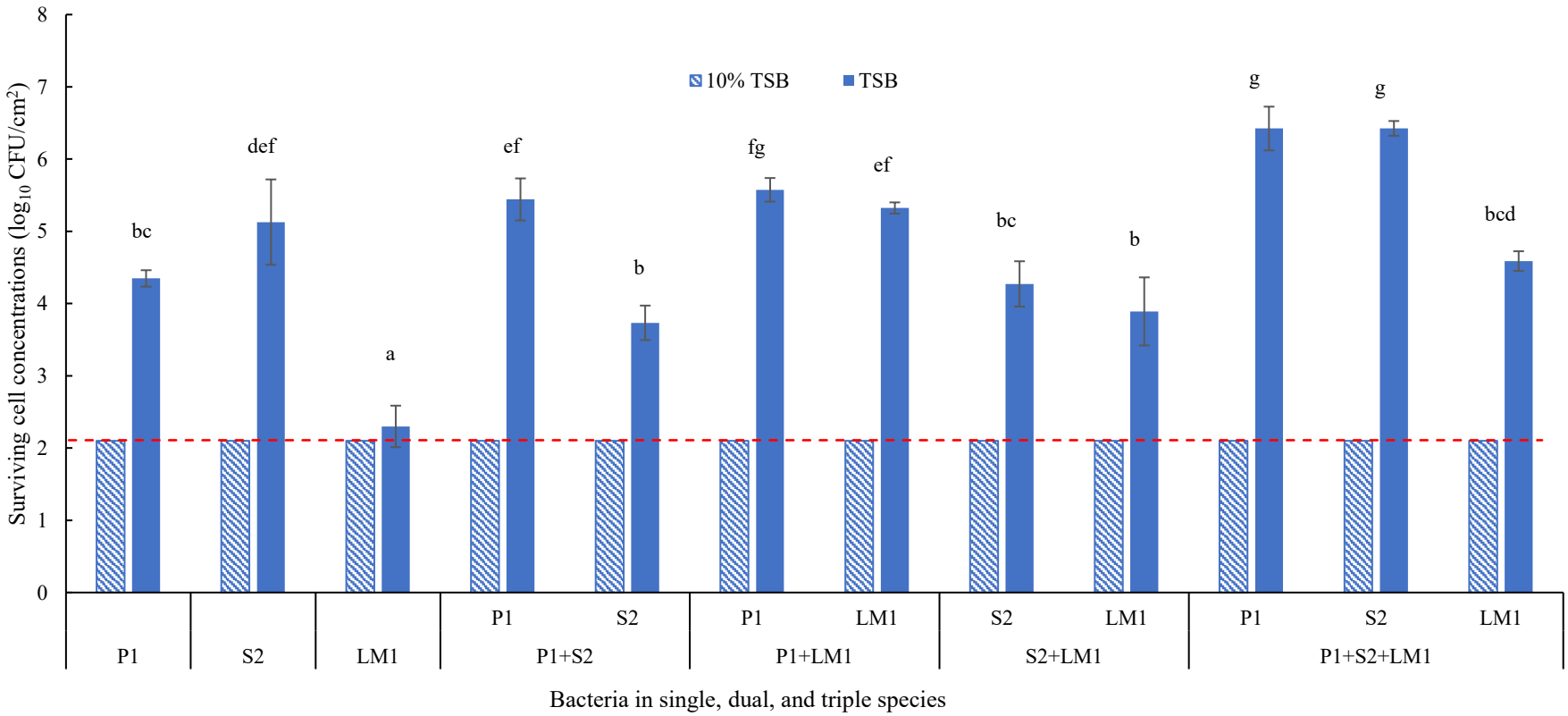

Figure 3.4 Surviving cell concentrations (log_{10} CFU/cm^2) of *P. fluorescens* (P1), *S. aureus* (S2), and *L. monocytogenes* (LM1) in single, dual, and triple species biofilm formed in 10% TSB and full-strength TSB after treatment with sodium hypochlorite (50 ppm/5 mins). The dotted line represents the detection limit (<2.1 log_{10} CFU/cm^2). The lowercase letters a-g indicate the significant differences between combinations in TSB.

In full-strength TSB, the highest reduction post-sanitizer treatment was observed for *L. monocytogenes* in single species (4.3 $\log_{10}$ reduction), this tolerance further improved in dual species, in the presence of *P. fluorescens* (1.1 $\log_{10}$ reduction) and *S. aureus* (2.2 $\log_{10}$ reduction). Similar observations were made for *P. fluorescens* with 2.8 $\log_{10}$ reduction in single species, 2.0 $\log_{10}$ reduction with *S. aureus* in dual species, and 1.4 $\log_{10}$ reduction with *L. monocytogenes* in dual species. The lowest log reduction was observed for *S. aureus* in single species (2.4 $\log_{10}$ reduction), which further improved in dual species (1.9 $\log_{10}$ reduction with *P. fluorescens,* and 2.2 $\log_{10}$ reduction with *L. monocytogenes*) (Table 3.2).

Table 3.2 Log_{10} reduction of *P. fluorescens* (P1), *S. aureus* (S2), and *L. monocytogenes* (LM1) in single, dual, and triple species biofilm formed in 10% TSB and full-TSB.

Biofilm	**Bacteria**	**Log_{10} reduction ($\log_{10}$ CFU/cm^2)**	
		10% TSB	TSB
P. fluorescens		5.21 ± 0.39^{y1}	2.86 ± 0.23^{cd2}
S. aureus		5.38 ± 0.21^{y1}	2.49 ± 0.41^{bcd2}
L. monocytogenes		4.99 ± 0.37^{xy1}	4.32 ± 0.09^{e2}
P. fluorescens + *S. aureus*	*P. fluorescens*	5.01 ± 0.20^{xy1}	2.08 ± 0.42^{abcd2}
	S. aureus	5.32 ± 0.17^{y1}	1.96 ± 0.06^{abc2}
P. fluorescens + *L. monocytogenes*	*P. fluorescens*	4.90 ± 0.43^{xy1}	1.46 ± 0.76^{ab2}
	L. monocytogenes	4.76 ± 0.36^{xy1}	1.12 ± 0.36^{a2}
S. aureus + *L. monocytogenes*	*S. aureus*	5.64 ± 0.40^{y1}	2.25 ± 0.40^{abcd2}
	L. monocytogenes	4.74 ± 0.25^{xy1}	2.23 ± 0.10^{abcd2}
P. fluorescens + *S. aureus* + *L. monocytogenes*	*P. fluorescens*	4.67 ± 0.02^{xy1}	1.31 ± 0.51^{ab2}
	S. aureus	5.64 ± 0.22^{y1}	1.88 ± 0.02^{abc2}
	L. monocytogenes	4.08 ± 0.10^{x1}	3.34 ± 0.09^{de2}

Note: letters (x,y) indicate the significant differences between the $\log_{10}$ reduction of bacteria for biofilm formed in 10% TSB (between rows). Letters (a,b,c,d,e) indicate the significant differences between the $\log_{10}$ reduction of bacteria formed in TSB (between rows). Numbers (1,2) indicate the significant differences between the $\log_{10}$ reduction of bacteria for biofilm formed in 10% TSB and TSB (between columns).

In the three-species biofilm formed in full-strength TSB, the survival of all three bacteria increased with the log reduction ranging 1.3 $\log_{10}$ CFU/cm^2, 1.8 $\log_{10}$ CFU/cm^2, and 3.3 $\log_{10}$ CFU/cm^2 for *P. fluorescens*, *S. aureus*, and *L. monocytogenes,* respectively. This indicated that all three bacteria in this study benefit from the synergy in dual and triple-species biofilm (Figure 3.4).

3.3.4 Exopolysaccharide content

The exopolysaccharide (EPS) content of the biofilm formed under nutrient-abundant conditions (TSB) was significantly higher ($p<0.001$) than that under nutrient-limiting conditions (10% TSB) (Figure 3.5). Under both nutrient conditions, *L. monocytogenes* produced significantly lower exopolysaccharides (2.5-11.8 µg/cm^2) compared to *S. aureus* and *P. fluorescens*. In nutrient-limited conditions, the triple species combination resulted in significantly higher ($p<0.001$) EPS content (16.9 µg/cm^2) compared to their single species counterparts (1.3-8.0 µg/cm^2) but was comparable to their dual species combinations (13.0-15.0 µg/cm^2). A similar observation was made for a multispecies biofilm formed in full-strength TSB, where the three species biofilm showed significantly higher ($p<0.001$) EPS concentration (60.9 µg/cm^2) compared to their single species (11.8-33.5 µg/cm^2) and dual species counterpart (36.7-42.3 µg/cm^2). The EPS concentration (Figure 3.5) reflected the findings of biofilm formation (crystal violet staining) (Figure 3.1).

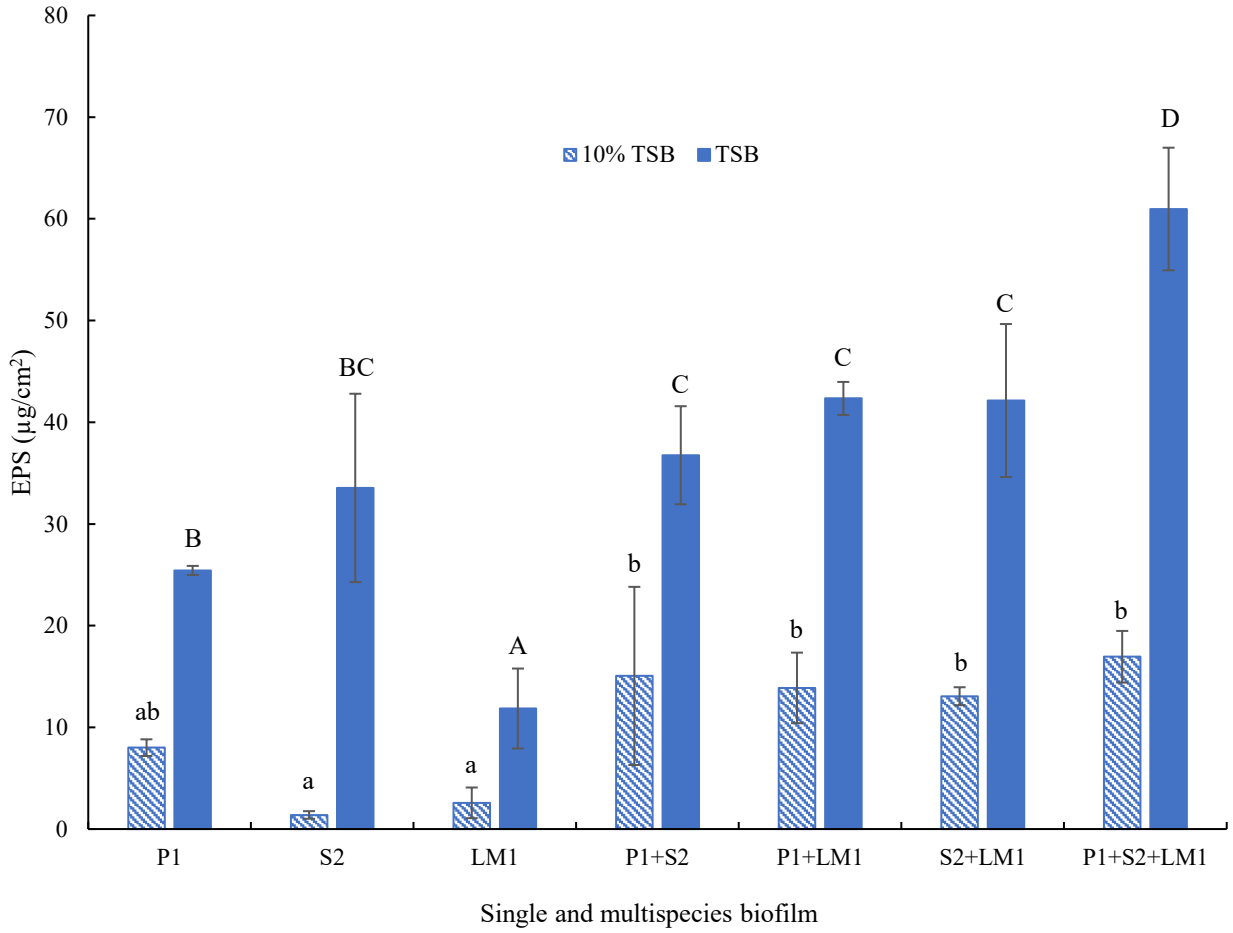

Figure 3.5 Exopolysaccharide concentration (µg/cm^2) of single, dual, and triple species biofilm consisting of *P. fluorescens* (P1), *S. aureus* (S2), and *L. monocytogenes* (LM1). The lowercase letters (a, b) and uppercase letters (A-D) indicate the significant differences between the combinations in 10% TSB and full-strength TSB respectively.

3.3.5 Correlation between biofilm formation and sanitizer tolerance

A significant positive correlation (0.6) was observed between exopolysaccharide content and sanitizer tolerance (Table 3.3), indicating that the higher exopolysaccharide concentration in combinations could be one of the reasons for increased tolerance in multispecies biofilm (Figure 3.4). The cell concentration in the biofilm and the sanitizer tolerance did not have a significant correlation (0.1) (Table 3.3), clarifying the variation between sanitizer tolerance for biofilm formed in 10% TSB and TSB despite having comparable cell concentrations (Figure 3.4).

Table 3.3 Pearson's coefficient analysis between biofilm biomass (CV), biofilm cells, sanitizer tolerance, and the exopolysaccharide concentration

	CV	Biofilm cells	Tolerance	EPS
CV	1	0.247	.555**	.807**
Biofilm cells	0.247	1	0.146	0.284
Tolerance	.555**	0.146	1	.618**
EPS	.807**	0.284	.618**	1

** Correlation is significant at the 0.01 level (2-tailed).

3.3.6 Structural variation as a result of nutrient conditions

The biofilm formed in 10% TSB was observed to consist of mound-like protrusions compared to the compact layers formed in full-strength TSB (Figure 3.6. A and B). The compact biofilm formed in full-strength TSB consisted of higher EPS concentration (Figure 3.5) and higher tolerance to sanitizer (Table 3.2) compared to the biofilm with uneven surfaces formed in 10% TSB.

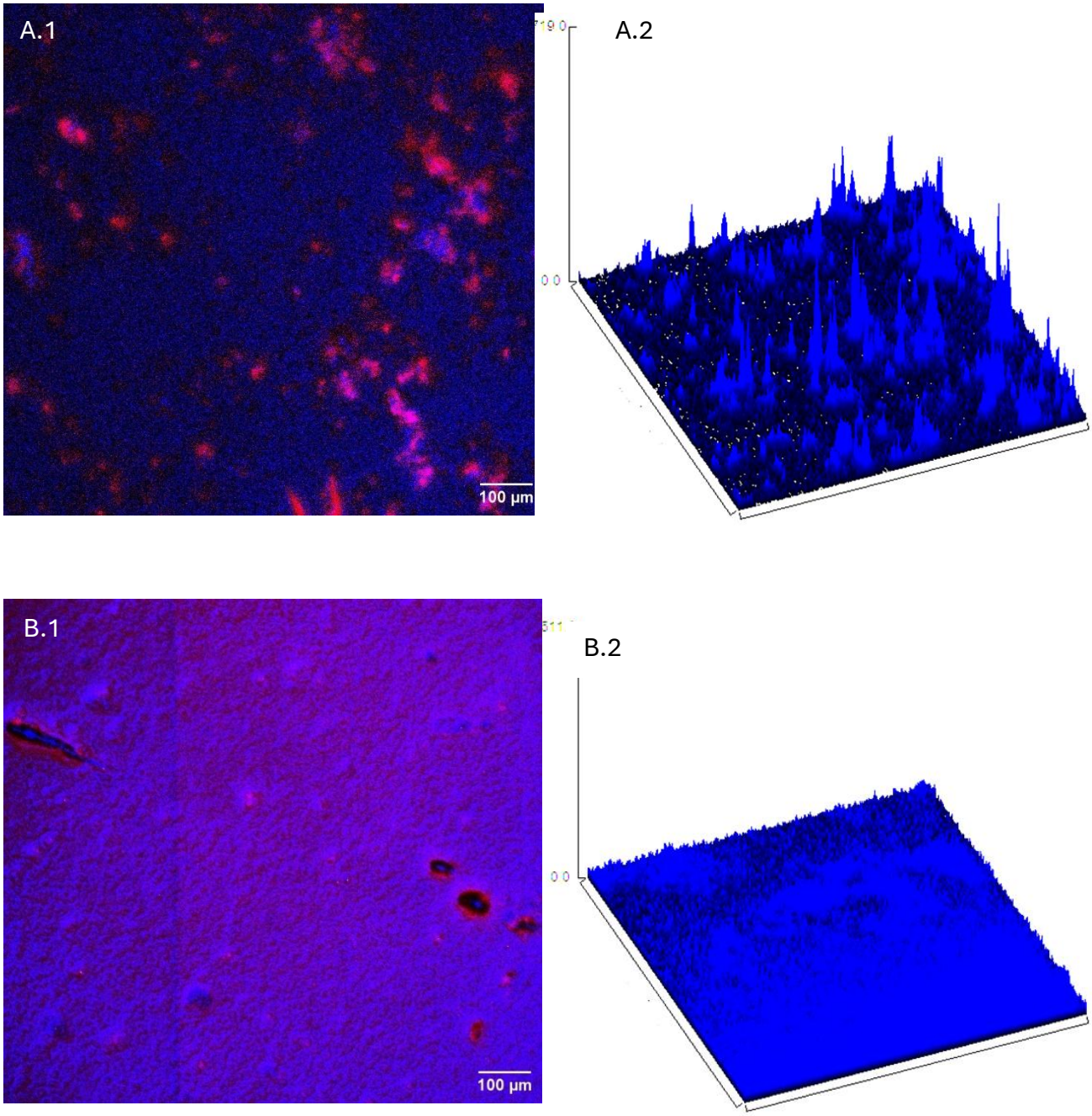

Figure 3.6 Confocal microscopy images showing dual-species biofilm formed with *P. fluorescens* (blue) and *L. monocytogenes* (red) in A) 10% TSB and B) full-strength TSB. A.1 and B.1 are 2-D images obtained from the microscope after dual staining. A.2 and B.2 are the surface plots showing the structural differences between the biofilm formed under varying nutrient conditions for 10% TSB and full-TSB, respectively.

3.4 Discussion

Significantly higher ($p<0.05$) biofilm formation was observed for single and multispecies biofilm formed in full strength TSB, compared to 10% TSB for all three bacteria involved: *P. fluorescens*, *S. aureus*, and *L. monocytogenes,* as observed through crystal violet staining (Figure 3.1) and confirmed by exopolysaccharide concentrations (Figure 3.5). Similar variations in the biofilm as a result of nutrient conditions have been mentioned before. S. Yuan et al., (2020) observed that the increased access to nutrients resulted in biofilms with higher thickness, biovolume, and roughness. Interestingly, the variation in nutrient content had no significant impact ($p>0.05$) on the cell concentrations in single and multispecies biofilms (Figure 3.2). *Pseudomonas* species have been previously reported as one of the major microbial contamination risks in the food industry because of their ability to grow and form biofilm even under low nutrient conditions and at low temperatures (frequently isolated from water - Centre for Disease Control and Prevention) (Xu et al., 2019). The supplementation of media with glucose, sucrose, and sodium chloride yielded higher biofilm (biomass) measured by crystal violet staining for *Staphylococcus* (Liu, Zhang et al., 2020; Singh et al., 2017). A similar observation was made by Karatan & Watnick, (2009) for *S. aureus* and *S. epidermis,* where the presence of added glucose and related sugars in the media resulted in multilayer biofilm formation. Another study shows that the growth and attachment of *Pseudomonas* and *Staphylococcus* in pure and mixed (1:1) cultures in the presence of four different media (Brain Heart Infusion (BHI), Nutrient Broth (NB), Luria Bertani (LB), and Roswell park Memorial Institute (RPMI) 1640) resulted in higher growth and attachment in BHI broth (nutrient rich) (Wijesinghe et al., 2019). Enhanced planktonic growth and biofilm attachment have been positively associated with high nutrient concentrations. In a study of biofilm formation in different media, such as chicken juice and TSB, *L. monocytogenes* showed higher biofilm formation in TSB (Dong et al., 2022). In contrast, Wang et al., (2022) reported the increased production of exopolysaccharides for *L. monocytogenes* strains under nutrient-limiting conditions (dTSB-YE) compared with nutrient-rich conditions (TSB-YE), indicating the response is strain dependent. The order of predominance of bacteria in a three-species biofilm was found to be dependent on the media as well. In 10% TSB media, *S. aureus* predominated the biofilm, followed by *P. fluorescens* and *L. monocytogenes* (Figure 3.2). Previous reports have mentioned the predominance of *P. fragi* and *S. xylosus* in the steady-state multispecies setup containing *P. fragi*, *S. xylosus*, and *L. monocytogenes* in dilute TSB (2g/L) formed in a

constant-depth film fermenter (Norwood & Gilmour, 2000). The order of dominance between *Acinetobacter* and *Enterobacter* in dual-species biofilm was also found to be dependent on the nutrient concentration in an 8-day study (S. Yuan et al., 2020).

In this study, synergistic interaction in multispecies biofilm was observed to be prevalent in high nutrient conditions (full-strength TSB). Under nutrient-deficient conditions, the relationship equations showed higher antagonistic combinations than nutrient-sufficient conditions (Table 3.1). Depending upon the nature of the bacteria, a similar shift in interaction, depending on the nutrient conditions, is noted for a combination of oligotrophic bacteria (stress-preferring) and a fungus, which shifted their interaction from competition to cooperation when evaluated in a low-nutrient environment (Velez et al., 2018). While the 25% TSB did not have a significant effect on the growth of the strains, lower synergy was observed in the multispecies biofilm formed by *Stenotrophomonas rhizophila*, *Xanthomonas retroflexus*, *Microbacterium oxydans*, and *Paenibacillus amylolyticus* compared with the multispecies biofilm formed in full TSB (Olsen et al., 2019). Competitive interactions are reported to occur when there is competition for nutritional niches and space (Parijs & Steenackers, 2018). Hence, under nutrient-limiting conditions, the interaction between the bacteria has been reported to evolve into competition (Xu et al., 2019). The synergistic interaction occurs in many ways: physical interaction (co-aggregation) and metabolite interaction (secretion of enzymes, metabolic cross feeding), but does not necessarily assure higher fitness of the biofilm (Burmølle et al., 2006). The interaction between the dual-species biofilm formed by *P. aeruginosa* and *K. pneumoniae* changed from neutral to competition when the nutrient feeding and waste removal rates decreased (Tan et al., 2017). These observations collectively indicate that the interaction between the bacteria is conditional and dynamic.

In this study, the synergy between the bacteria in the multispecies biofilm provided the increased fitness of the mixed biofilm, showing increased survival of all three bacteria in the multispecies biofilm formed in full-strength TSB (Figure 3.4). The sanitizer tolerance of the pathogen *L. monocytogenes* increased significantly ($p<0.05$) in dual and triple species combinations (Figure 3.4). In a similar disinfection study, eighteen *L. monocytogenes* cultures in single and dual species (with *Pseudomonas*) were treated with peracetic acid and antibiotics. After the disinfection, survival of ten cultures of *Listeria* was noted in dual species, whereas in single species, all eighteen cultures of *Listeria* were reduced to undetectable levels (Thomassen et al., 2023). The dual species of *Pseudomonas* and *S. enteritidis* showed increased tolerance against quaternary ammonium compounds in a dual species combination (Pang et al., 2020).

The protective effect of the binary biofilm of *E. coli* and *P. aeruginosa* against benzalkonium chloride has been noted before (Machado et al., 2012). In addition to the binary biofilm, the persistence of *L. monocytogenes* was also found to be elevated in the presence of *S.* Typhimurium and *P. aeruginosa* against black pepper essential oil in a three-species biofilm (dos Santos et al., 2023). The results show enhanced resistance of the *Listeria* in binary biofilm with *Pseudomonas*, which can be added to the fact that *Pseudomonas* produces higher EPS (thickness and distribution), which acts as a barrier for the sanitizer before it reaches the *Listeria* or *Staphylococcus*, also known as the sheltering effect (Kocot & Olszewska, 2020; Thomassen et al., 2023). The formation of denser biofilm (higher EPS) in multiple species and its correlation with increased sanitizer tolerance has been discussed before (Table 3.2).

In this study, despite the concentration of exopolysaccharide increasing significantly in three species biofilm (Figure 3.5), the surviving bacteria in the three species biofilm after sanitizer treatment were comparable to dual species (Figure 3.4), which might suggest that in addition to exopolysaccharides, the higher survival of *L. monocytogenes* in multispecies biofilm could be the result of quorum sensing, horizontal gene transfer, and/or spatial arrangement with one specific bacterium present in the combination (Wagner et al., 2020). Guillonneau et al., (2018) observed that irrespective of the number of bacteria (dual and triple) in the biofilm, *P. mediterranea* was able to benefit from only one bacterium (*Shewanella* sp.) in the combination. Previous reports have indicated the importance of spatial arrangement on the composition and behavior of multispecies biofilm (Dong et al., 2023; Ibusquiza et al., 2012). In the dual-species biofilm consisting of *P. aeruginosa* and *S. aureus*, *S. aureus* was located at the bottom of the biofilm (facultative anaerobic), whereas *P. aeruginosa* was found on the top layers owing to its aerobic metabolism. The polysaccharide *Psl* produced by *P. aeruginosa* was found to form a protective barrier between *S. aureus* and *P. aeruginosa,* protecting the former bacteria from the lytic effect of the latter (Xu et al., 2019). In addition to sanitizer tolerance, the synergistic interaction in multispecies biofilm has been noted to provide the bacteria with higher resistance towards invasive bacterial species (Burmølle et al., 2006) and surfactant and antibiotics (Lee et al., 2014).

In this study, major structural differences were observed for biofilm formed under different nutrient conditions (Figure 3.6). The *Pseudomonas* biofilm formed under nutrient-abundant conditions had a thick, compact, and uniform structural appearance compared to the biofilm formed under nutrient-deficient conditions, where a porous biofilm containing interstitial channels and voids can be observed (Heydorn et al., 2000). The relationship between the

nutrient content and structure of the biofilm has direct implications for sanitizer tolerance (Bas et al., 2017). Compact biofilm with higher EPS density has been noted to increase resistance against external factors (hydraulic flow, antimicrobials). This has also been previously recognized as rugose (uneven) morphotype vs smooth morphotype in *S.* Typhimurium, observed as the result of continuous exposure to sodium hypochlorite (Bansal et al., 2019). The structure of the biofilm is dependent on the nutrient uptake and diffusion of the nutrient throughout the biofilm. Once the microcolonies are formed, the proliferation of the bacteria is dependent on the nutrient uptake by the bacteria on the outer layer of the structures (Lobo-Cabrera et al., 2024). A porous and heterogeneous structure can be observed when diffusion of the nutrients is limited in the biofilm compared with a homogenous and compact biofilm when the diffusion limitations are absent (Van Loosdrecht et al., 2002). These structural observations are significant because the efficiency of antimicrobials (hydrogen peroxide, chlorine dioxide, and quaternary ammonium compounds) was found to be dependent on the proportion of biofilm coverage on the surface (Bas et al., 2017). Under different nutrient conditions, different genes may be upregulated, leading to differences in the EPS production and hence structural properties (Campanac et al., 2002). This higher EPS production and compact biofilm result in higher proximity of the cells to each other and allow cell-cell interactions and the formation of a synergistic biofilm (Flemming & Wingender, 2010).

3.5 Conclusion

While the $O.D_{595}$ nm was an accurate indicator of the biofilm biomass, the relationship equation based on these values did not correlate with the synergistic interactions in all the cases studied. Among the three bacteria analyzed in this study, *L. monocytogenes* was the weakest biofilm former with the highest susceptibility to sanitizers in single-species and benefited most in the multispecies arrangement. While it's clear that higher exopolysaccharide concentration results in higher tolerance, the uneven log reduction of bacteria in three species biofilm (compared to dual species) indicates that the role of spatial arrangement might be significant in defining which bacteria will be sheltered more in multispecies biofilms. In conclusion, by limiting the nutrient concentration, more impactful removal methodologies can be developed without having to increase the concentration of the chemical sanitizers. Overall, understanding the interactions between bacteria in a multispecies arrangement and their response to sanitizers under different environmental variables can help to develop a targeted, efficient, sustainable cleaning regime.

3.6 Link to the next chapter

While this chapter explores the nutrient variation on polystyrene surfaces under static conditions, providing fundamental information on multispecies arrangements, the interactions on relevant industrial surfaces (e.g., stainless-steel) under dynamic conditions (continuous supply of media/shear stress) might vary. The next chapter (Chapter 4) will explore the single and multispecies biofilm formation on stainless-steel surfaces under static and turbulent flow.

Chapter 4. Single and Multispecies Biofilm Formed in the Static and Continuous Systems

This chapter contains material that was published as a peer-reviewed article:

Pant, K., Palmer, J., & Flint, S. (2025). Evaluation of single and multispecies biofilm formed in the static and continuous systems. *International Journal of Food Microbiology*, 429, 111030.

4.1 Introduction

Listeria monocytogenes, commonly isolated from outbreaks in food products such as milk, soft cheese, and delicatessen meats (pork tongue in jelly) (Leriche & Carpentier, 2000), can adhere to and multiply on industrial surfaces in the presence of *Pseudomonas* (Agustín & Brugnoni, 2018; Fagerlund et al., 2017; Kocot & Olszewska, 2020; Thomassen et al., 2023). Multiple species of planktonic bacteria can come together in the biofilm, which defines the biofilm's characteristics and stability (Brooks & Flint, 2008; Papaioannou et al., 2018). In the food industry, stainless-steel surfaces that are cleaned and sanitized are frequently contaminated with multispecies bacteria within a biofilm, along with nutrient-depleted conditions (Pang et al., 2019). The interactions between the bacteria involved in multispecies biofilm depend on strains of the bacteria, temperature, pH, oxygen content, and hydrodynamic conditions. The hydrodynamic conditions play a significant role in the transport of nutrients, expulsion of waste metabolites, and how the bacteria adapt to the shear stress (Wang et al., 2014). The common niches of *Pseudomonas*, *Staphylococcus*, and *Listeria*, where they might experience dynamic flow conditions through unit operations such as washing has been mentioned before (Figure 2.1). The changes in these variables lead to interactions such as synergistic interactions because of cooperation and utilization of common goods; antagonism because of the competition for nutrients and space (Ramstedt & Burmølle, 2022). Depending on the interaction, exopolysaccharides/metabolites produced by one bacterium in a polymicrobial biofilm can protect other bacteria, resulting in increased survival during cleaning and disinfection (Sanchez-Vizuete et al., 2015).

In the last decade, biofilm research in dynamic conditions has been extensively focused on single species (single strain/multi-strain) (Lineback et al., 2018; Mendez et al., 2020; Mettler et al., 2022; Nkemngong et al., 2020). Considering the dynamic nature of biofilm formation on the food industry surfaces, a continuous system with a multispecies bacterial model provides a more realistic representation of the biofilm (Diarra et al., 2023; L. Yuan, N. Wang, et al., 2020). The viability of the Centre for Disease Control and Prevention (CDC) reactor to replicate the dairy industry settings in laboratory-controlled conditions (Lindsay et al., 2022) and form multispecies biofilms (Prabhukhot et al., 2023) has been mentioned before. This study aimed to understand the effect of flow on the biofilm formation and sanitizer tolerance of *Pseudomonas aeruginosa*, *Staphylococcus aureus*, and *Listeria monocytogenes* in single, dual, and triple-species biofilm using the CDC bioreactor.

4.2 Materials and Methods

4.2.1 Culture preparation

Stock cultures (-80°C) of *Pseudomonas fluorescens* 2614 (P1) (Dairy), *Staphylococcus aureus* subsp. *aureus* Rosenbach (ATCC 9144) (S2), and *Listeria monocytogenes* H1 (LM1) (Environment-soil) were prepared for inoculation into the static system according to section 3.2.1. For the continuous system, 1 mL of ~ 9 $\log_{10}$ CFU/mL in saline solution (0.85%) (Appendix VI) was introduced into the 330 mL bioreactor, consisting of 10% TSB for the final cell concentration of ~ 6 $\log_{10}$ CFU/mL of individual bacteria.

4.2.2 Biofilm formation in the static system

Stainless-steel coupons (316-2B; Advanced Sheetmetals Ltd., Palmerston North) (2.4 cm^2) (Figure 4.1.A) were used as substrates for biofilm formation in the static system. The coupons were prepared by passivation to generate a chromium oxide coat by dipping in 50% nitric acid (Sigma Aldrich, USA) and heating to 70°C for 30 min, followed by washing, drying, and autoclaving (121°C, 15 min). The sterile coupons were introduced vertically into each well (1 mL) of 48-well plate (Costar®, Corning, USA) containing 10% tryptone soy broth (TSB) or full-strength TSB with final bacterial concentration of 6 $\log_{10}$ CFU/mL. A 1:1 and 1:1:1 ratio of each bacterium at the same cell concentration were added for dual species and triple species inoculations respectively. The 48-well plates were incubated for 24 h at 30°C. The media (10% TSB or full-strength TSB) was refreshed every 24 h. The cell count was estimated every 24 h, and exopolysaccharide and microscopic observations were made at 72 h to obtain mature biofilms. The experiment was repeated for at least two biological replicates, and each biological replicate consisted of three technical replicates.

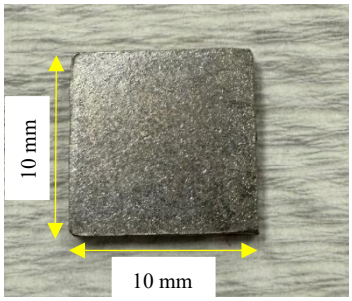

A. Static conditions coupons

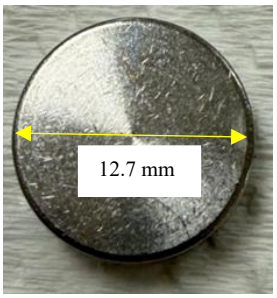

B. Turbulent flow coupons

Figure 4.1 Stainless-steel coupon used as the substrate to form biofilm under static conditions and turbulent flow. Circular grooves can be observed on the surface of circular coupons used for biofilm formation under turbulent flow.

4.2.3 Biofilm formation in the continuous system

The CDC bioreactor® (Biosurface Technologies, USA) was used to form biofilm in a continuous flow system for 72 h. The CDC reactor system consisted of 4 components 1) the influent tank 2) the pump and flow rate control system 3) the bioreactor 4) the effluent tank (Figure 4.2). These components were connected via silicone 16 tubing (Masterflex®, Cole-Parmer®, USA) and passed through the pump using neoprene 16 tubing. The bioreactor consisted of 8 coupon rods, each rod consisting of three circular stainless-steel coupons (2.26 cm^2) passivated and sterilized according to section 4.2.2 (Figure 4.1.B). The media (10% TSB) was prepared in the influent tank and connected to the bioreactor via a pump (Masterflex®, Cole-Parmer®, USA), which fixed the constant flow rate of 5 mL/min. The doubling time for *Pseudomonas*, *Staphylococcus,* and *Listeria* in 10% TSB at 30°C was found to be 1.22 h, 1.5 h, and 1.27 h following the growth curve. The bioreactor was run at 120 rpm and 30°C using a hot plate setup (VWR International, U.S.A). Every 24 h, 2 coupon rods were removed from the bioreactor, and cell counts in the biofilm were calculated per cm^2 of the stainless-steel coupon surface. The system was continuously operated for 3 days for all single species and multiple species combinations. The exopolysaccharide (EPS) content and sanitizer resistance were determined at 72 h to analyze mature biofilm. The experiment was repeated at least twice (2 biological replicates), and three technical replicates were acquired from each biological replicate for analysis.

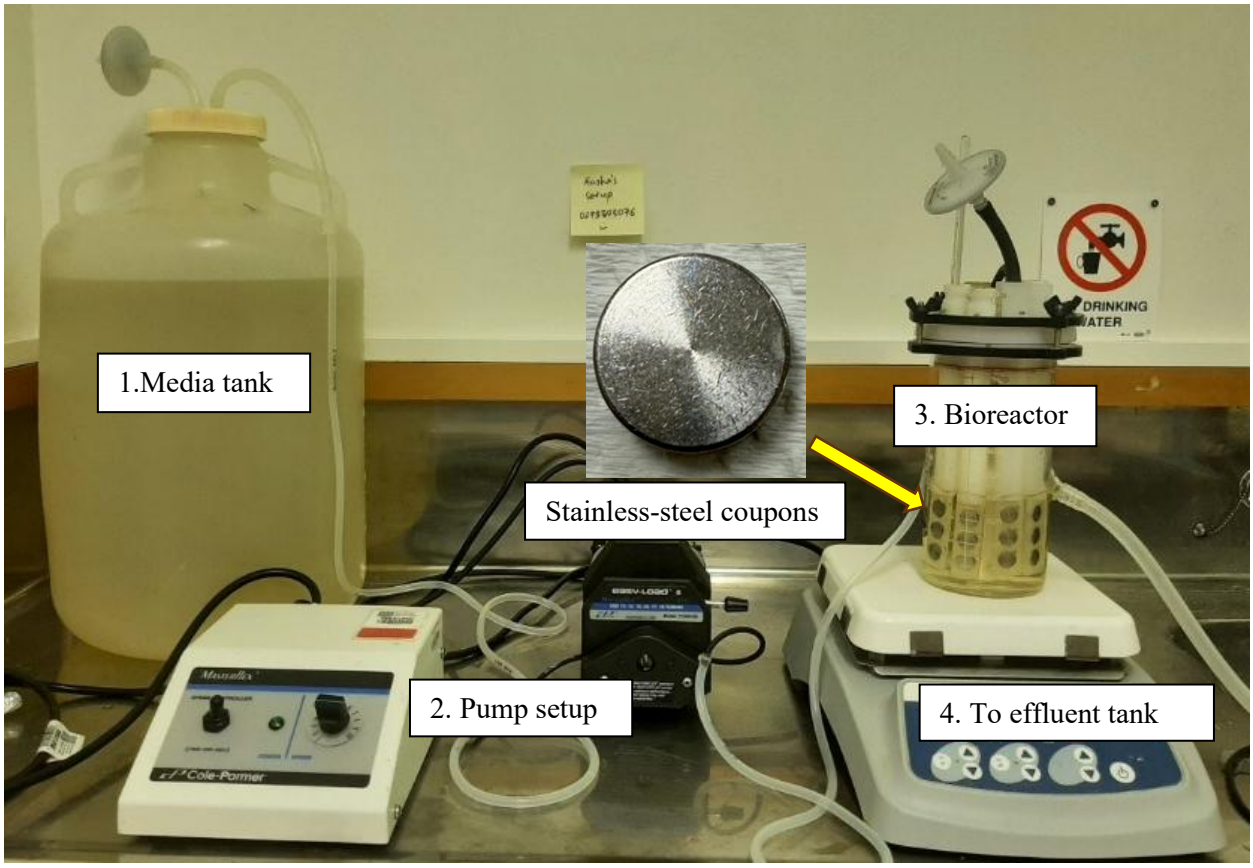

Figure 4.2 CDC bioreactor setup for biofilm formation

The Reynolds number of the fluid through the speed of the impeller in the reactor was determined to estimate the turbulence in the media (Re<2100-laminar, 2100<Re<4000-transient, Re>4000-turbulent) (Prabhukhot, Eggleton, Kim, & Patel, 2024; Prabhukhot, Eggleton, Vinyard, & Patel, 2024). The Reynolds number was calculated according to the modified equation for the tangential velocity of media in the agitated vessel.

$$Re = \frac{v \times Dh}{\mu} \quad (1)$$

Where Re is the Reynold number, v is the hydrodynamic velocity (m/s), Dh is the diameter of the annulus given by 2 (R_o-R_i), R_o (0.03 m) is the outer radius measured from the impeller center to the inner coupon surface, R_i (0.0225 m) is the inner radius measured from the impeller center to the outer edge of the impeller, and μ is the kinematic viscosity (1.0023E-06 m^2/s) (Prabhukhot, Eggleton, Kim, et al., 2024).

The shear stress on the coupons were calculated based on the Colebrook equation (Colebrook et al., 1939) as Equation 2.

$$\frac{1}{\sqrt{f}} = -4.0 \times log10\ (\frac{\in}{Dh} + \frac{4.67}{Re \times \sqrt{f}}) + 2.28 \quad (2)$$

Where $\in$ is the surface roughness of the material (stainless-steel = 0.015×10^{-3} m) and f is the fanning factor. The change in the properties of the material as the result of biofilm formation was not accounted.

The shear stress (τw) can be calculated as (Equation 3) (Prabhukhot, Eggleton, Kim, & Patel, 2024),

$$\tau w = 0.5 \times f \times \rho \times v^2 \quad (3)$$

f is the fanning factor calculated from equation (2), ρ is the density of fluid (998.23 kg/m^3). The shear stress (N/m^2) was used to understand the impact of flow on the biofilm formation formed in bioreactor under turbulent flow.

4.2.4 Sanitizer treatment

The incubated stainless-steel coupons obtained from static and continuous systems incubated for 72 h were washed with saline solution (0.85% w/v) to remove planktonic cells before being treated with sodium hypochlorite (SH) (50 ppm, pH: 6.5-7) (Janola, Australia) (Lindsay et al., 2022; Pang et al., 2019). The sanitizer dilution and preparation were done as mentioned before in section 3.2.4. The coupons with undisturbed biofilms from both static and continuous systems were dipped into 50 mL centrifuge tubes containing 5 mL of sodium hypochlorite sanitizer and treated for 5 mins before being introduced into another tube containing 1% sodium thiosulphate neutralizer with sterile forceps for 1 minute before being washed (10s in 5 mL saline). The coupons containing biofilm were dipped in sterile saline solution instead of sanitizer for untreated samples, followed by sodium thiosulfate neutralizer and surviving cells enumerated according to section 4.2.5. The treatments were conducted in biological duplicates, with each duplicate containing a technical triplicate.

4.2.5 Enumeration of cells from biofilm coupons

The cells were detached from the coupons using the glass bead beating method, vortex mixing with 10 g of sterilized glass beads (diameter -5 mm, Sigma-Aldrich, Germany) with 5 mL saline solution (0.85%), for 5 min. Selective agars were used to enumerate cells (*Pseudomonas* Isolation agar for *Pseudomonas*, Mannitol salt agar for *Staphylococcus,* and Modified Oxford agar for *Listeria*). Similarly, to check the presence of *L. monocytogenes* in macroscopic threads

observed in dual species filamentous biofilm of *S. aureus* and *L. monocytogenes*, the threads were collected using sterile forceps, washed by gentle dipping into sterile saline solution (0.85%), and deposited into a sterile tube containing glass beads (10 g) and saline (5 mL). The sample was mixed by vortex for 5 mins at the highest setting until the threads were not visible in the suspension. The sample was plated using selective agars as mentioned above.

4.2.6 Extracellular polymeric substances (EPS) quantification

The biofilm matrix from the coupon surface was extracted using glass beads and saline solution, along with vortex and sonication, and then quantified using a phenol-sulphuric acid hydrolysis (Zhou, Dong, et al., 2024). Stainless-steel coupons with single and multispecies biofilms were washed (×3) with sterile distilled water to remove planktonic cells. The washed coupons were then mixed by vortex with sterile glass beads (5 g) and sterile distilled water (2 mL) for 5 min at the maximum setting to remove the adhered cells and EPS. This was followed by the sonication (40kHz) of the tubes containing coupons, saline, and glass beads for 5 min. The extraction process was completed by centrifugation at 10,000× g for 5 min. The supernatant was collected for filtration (0.20 µm), whereas the pellet was discarded. To 200 µL of filtrate, 100 µL of 6% phenol, and 500 µL of 98% sulphuric acid were added and left to react for 20 min at room temperature. The optical density reading was taken at 490 nm and compared with the standard curve for dextran (Appendix VII), where the EPS was determined in ug/cm^2 of the stainless-steel coupons.

4.2.7 Microscopy

The coupons obtained from the static and the CDC system at 72 h were washed in sterile distilled water before air drying the surface at room temperature, followed by staining with acridine orange (10 g/L) (BDH, England) for 5 min in the dark (Jha et al., 2020). The coupons were again washed with sterile distilled water and dried at room temperature (dark) before being visualized with an epifluorescence microscope (Nikon Eclipse Ni, USA) at excitation filter 485/20nm and emission filter 500-538 nm (TRITC/filter 3). Three coupons were taken for each biological replicate for microscopic analysis, and at least five images were captured from each coupon across the surface. The observations were made at a magnification of 100 µm. The epifluorescence images were acquired using NIS-elements D software.

The thread-like structures observed in *S. aureus* biofilm formation under turbulent flow were collected with sterile forceps and fixed on a glass-slide before gram staining and observation with light microscopy according to section 3.2.6.

4.3 Statistical analysis

The significant differences between the samples were determined with one-way ANOVA (IBM SPSS version 29) with 95% confidence ($p<0.05$) together with Tukey analysis for a post-hoc test. All experiments had at least two biological replicates, and six technical replicates and results were presented as mean ± standard deviation.

4.4 Results

4.4.1 Biofilm formation in the static system

The impact of nutrient variation in the static system (full strength TSB vs 10% TSB) was limited to *S. aureus* in single species and *P. fluorescens* in dual combinations with *S. aureus*. In nutrient-abundant conditions, the cell concentrations of both *S. aureus* (in single species) and *P. fluorescens* (in dual species with *S. aureus*) were found to be significantly higher ($p<0.05$) (Figure 4.3).

In the static system (10% TSB) (after 48 h), the presence of *S. aureus* and *L. monocytogenes* did not affect the cell concentration of *P. fluorescens* in both dual and triple species (Figure 4.3 and 4.4). The cell concentration of *P. fluorescens* was found to be consistent in single species (6.4 $\log_{10}$ CFU/cm^2), dual species (6.0-6.4 $\log_{10}$ CFU/cm^2), and triple species (6.5 $\log_{10}$ CFU/cm^2). Similar observations were made for *S. aureus* and *L. monocytogenes* in single and multi-species. The cell concentration of *S. aureus* reached 6.9 $\log_{10}$ CFU/cm^2 in single species, 5.8-6.3 $\log_{10}$ CFU/cm^2 in dual species, and 5.6 $\log_{10}$ CFU/cm^2 in triple species biofilm. In single species, the cell concentration of *S. aureus* reached 5.1-6.9 $\log_{10}$ CFU/cm^2 but reduced significantly ($p<0.05$) in dual species (3.7-5.8 $\log_{10}$ CFU/cm^2) with *P. fluorescens*. This trend was observed for dual-species biofilm (*P. fluorescens* and *S. aureus*) formed in both nutrient-abundant (full-strength TSB) (Figure 4.3) and nutrient-deficient (10% TSB) conditions (Figure 4.4).

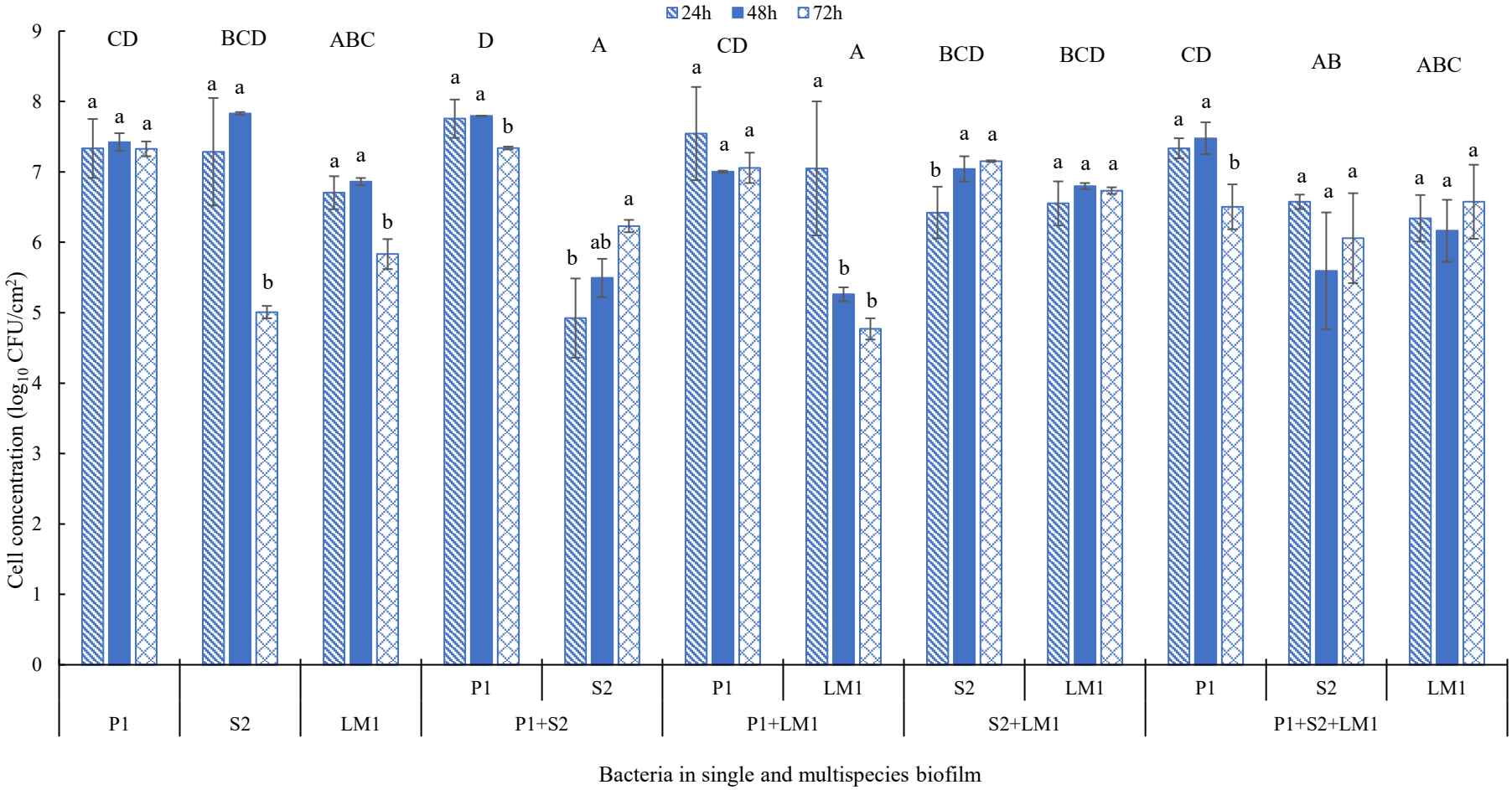

Figure 4.3 Cell concentration (log_{10} CFU/cm^2) of *P. fluorescens* (P1), *S. aureus* (S2), and *L. monocytogenes* (LM1) in single, dual, and triple species biofilm formed in the static system in full-strength TSB at 30°C for 72 h. Note: The lower-case superscripts (a-b) indicate the significant differences in cell concentration of bacteria at different incubation times. The upper-case subscripts (A-D) indicate the significant differences in single and multiple-species biofilm combinations.

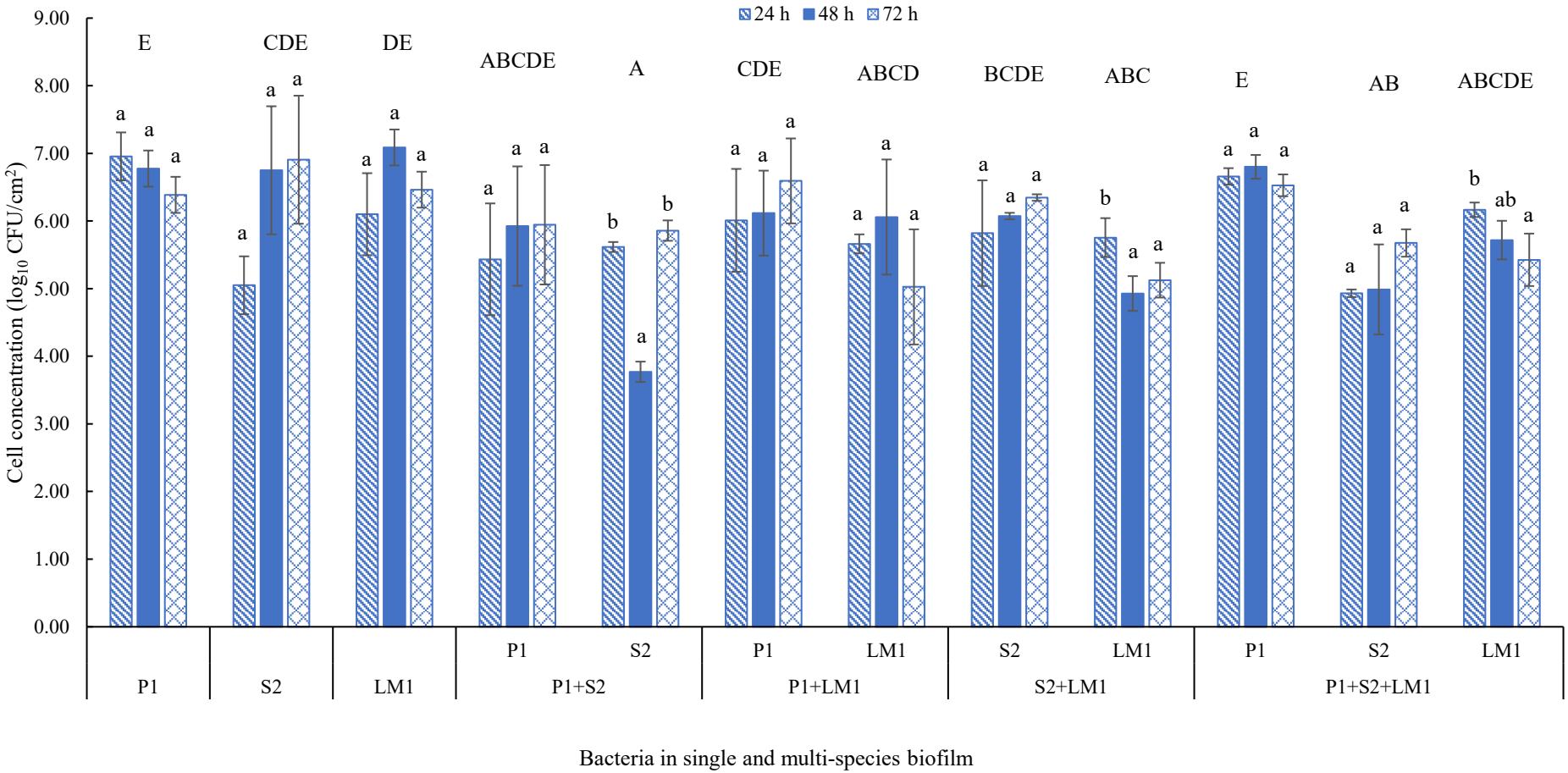

Figure 4.4 Cell concentration (log_{10} CFU/cm^2) of *P. fluorescens* (P1), *S. aureus* (S2), and *L. monocytogenes* (LM1) in single, dual, and triple species biofilm formed in the static system in 10% TSB at 30°C for 72 h. Note: The lower-case superscripts (a-b) indicate the significant differences in cell concentration of bacteria at different incubation times. The upper-case subscripts (A-D) indicate the significant differences in single and multiple-species biofilm combinations.

4.4.2 Biofilm formation in continuous system

The Reynolds number of the agitated media in the bioreactor was > 4000, confirming turbulent flow in the CDC bioreactor. The shear stress at this turbulent flow was found to be 1.44 N/m^2.

A gradual increase of cell concentration in the biofilm can be observed for *S. aureus* and *L. monocytogenes* in both single species and dual species combinations (Figure 4.5). In contrast, for *Pseudomonas,* the cell concentration reached 6.4 $\log_{10}$ CFU/cm^2 at 24 h and stayed comparable over the next 48 h (6.9-7.2 $\log_{10}$ CFU/cm^2) in both single and dual species. At 24 h, the cell concentration of *Staphylococcus* in single species biofilm was below the detection limit (<1.5 $\log_{10}$ CFU/cm^2) but was detected in dual species biofilm with *Pseudomonas* (3.7 $\log_{10}$ CFU/cm^2) as well as with *Listeria* (2.7 $\log_{10}$ CFU/cm^2) and in three-species biofilm (5.5 $\log_{10}$ CFU/cm^2).

The cell concentration of *P. fluorescens* in single species biofilm (6.4, 7.2, and 6.9 $\log_{10}$ CFU/cm^2) was found to be comparable ($p>0.05$) with cell concentration of *Pseudomonas* in dual species (with *Staphylococcus* - 6.0, 6.7, and 6.6 $\log_{10}$ CFU/cm^2 and *Listeria* -7.0, 7.1, and 6.6 $\log_{10}$ CFU/cm^2) and in triple species (6.8, 6.9, and 6.3 $\log_{10}$ CFU/cm^2) at 24 h, 48 h, and 72 h respectively (Figure 4.5). In contrast, at 24 h, significantly ($p<0.05$) higher cell concentration of *Staphylococcus* was observed in dual species biofilm with *Pseudomonas* (3.7 $\log_{10}$ CFU/cm^2), and *Listeria* (3.5 $\log_{10}$ CFU/cm^2) and triple species (5.5 $\log_{10}$ CFU/cm^2) compared to single species biofilm (<1.5 $\log_{10}$ CFU/cm^2). A similar trend of higher biofilm formation of *S. aureus* could be observed for incubation times 48 h and 72 h in combination biofilm (dual and triple species) as well.

Similarly, the presence of a second bacteria (*Pseudomonas*) improved the cell concentration of *Listeria*, increasing it to 7.2 $\log_{10}$ CFU/cm^2 (24 h), 8.2 $\log_{10}$ CFU/cm^2 (48 h), and 8.0 $\log_{10}$ CFU/cm^2 (72 h). For the same incubation time order, the cell concentration of *Listeria* in single species was limited to 4.4 $\log_{10}$ CFU/cm^2, 5.7 $\log_{10}$ CFU/cm^2, and 6.4 $\log_{10}$ CFU/cm^2, respectively. Additionally, the *Listeria* cell concentration in dual species biofilm with *Staphylococcus* was found to be comparable ($p>0.05$) with single species (*Listeria*), with cell concentrations reaching 3.9 $\log_{10}$ CFU/cm^2, 5.2 $\log_{10}$ CFU/cm^2, and 7.3 $\log_{10}$ CFU/cm^2 at 24, 48, and 72 h, respectively. As a result of the influence of *Pseudomonas* (as observed in dual species), the cell concentration of *Listeria* in triple species was found to be significantly higher than single species at 7.2 $\log_{10}$ CFU/cm^2, 8.9 $\log_{10}$ CFU/cm^2, and 8.4 $\log_{10}$ CFU/cm^2 for 24,

48, and 72 h, respectively. Overall, in the three-species biofilm (for all three time periods), the cell concentration of both *Staphylococcus* and *Listeria* improved significantly ($p<0.05$), whereas *Pseudomonas* was consistent with single species.

Owing to the limited motility of cells under turbulent flow, the *P. fluorescens* cells appeared in chains (Figure 4.6) at 48 h, and when further observed at 72 h, the chains were absent. These *P. fluorescens* chains could be observed in dual species biofilm with *S. aureus* as well (Figure 4.10). The lowered biofilm formation observed by *S. aureus* and *L. monocytogenes,* respectively, in single species can be visually observed on the coupon surfaces at 24 h, with minimal observation of bacteria on the surface (Figure 4.7 and Figure 4.8).

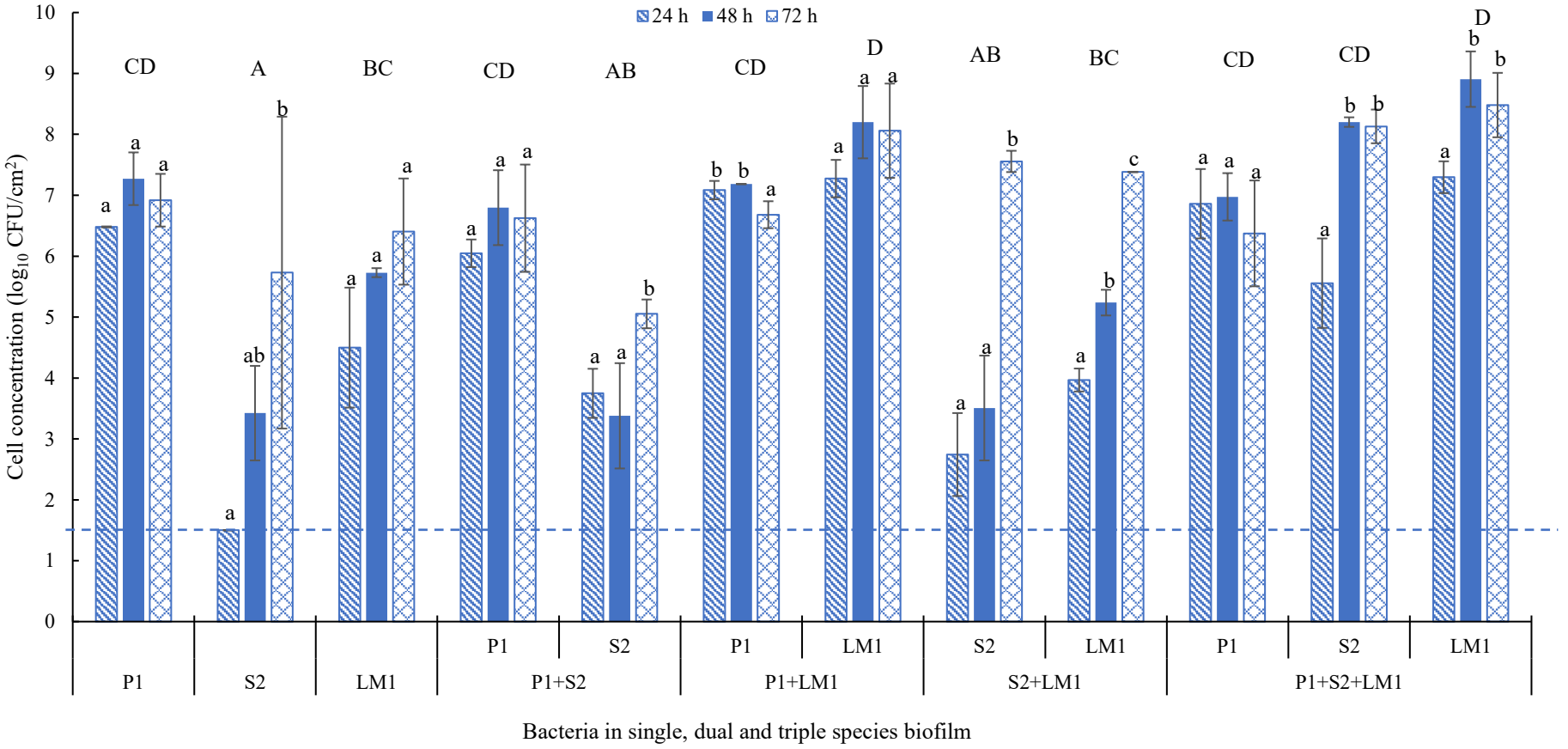

Figure 4.5 Cell concentration (log_{10} CFU/cm^2) of *P. fluorescens* (P1), *S. aureus* (S2), and *L. monocytogenes* (LM1) in single, dual, and triple species biofilm formed in the CDC system in 10% TSB at 30°C over 72 h. Note: The lower-case superscripts (a-b) indicate the significant differences in cell concentration of bacteria at different incubation times. The upper-case subscripts (A-D) indicate the significant differences in single and multiple-species biofilm combinations. The dotted line indicates the detection level (1.5 log_{10} CFU/cm^2).

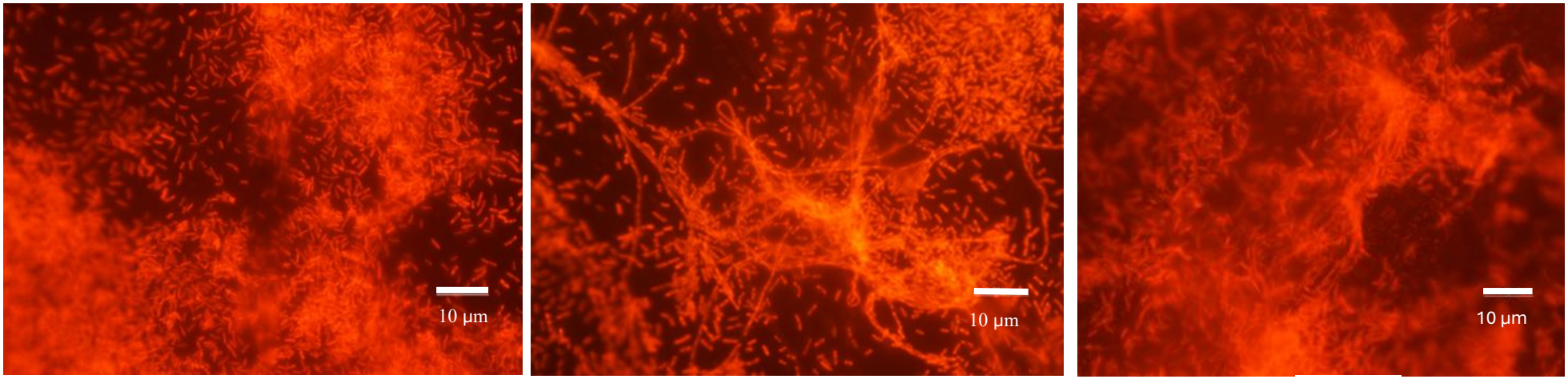

24 h 48 h 72 h

Figure 4.6 *P. fluorescens* biofilm formed on a stainless-steel surface in the CDC bioreactor at 30°C and 10% TSB observed with acridine orange

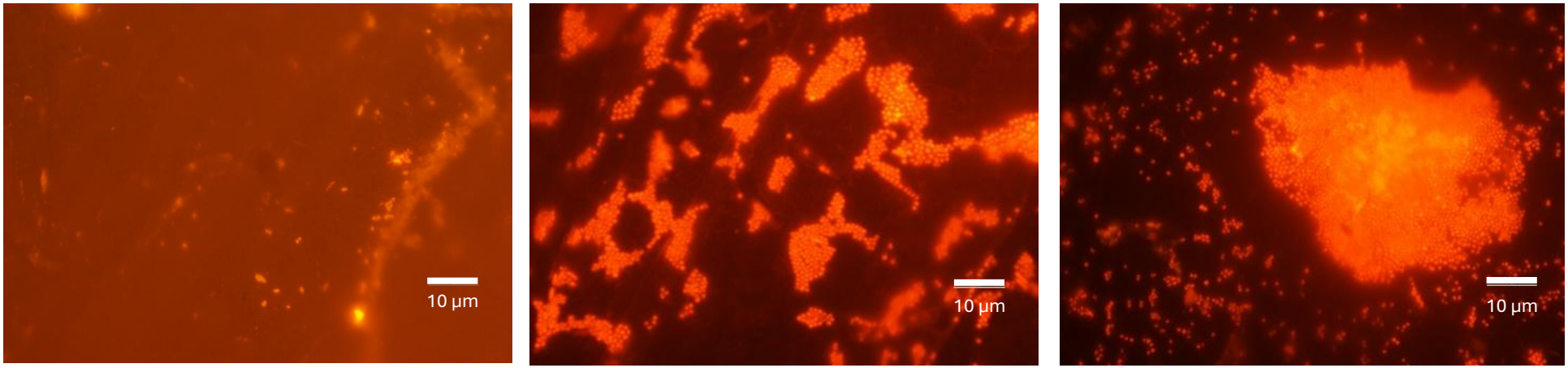

24 h 48 h 72 h

Figure 4.7 *S. aureus* biofilm formed on a stainless-steel surface in the CDC bioreactor at 30°C and 10% TSB observed with acridine orange

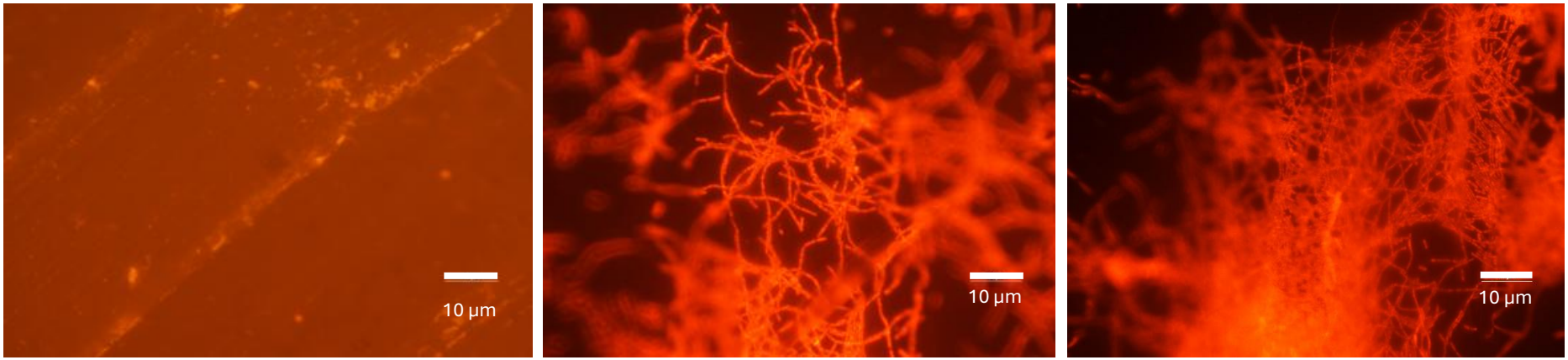

24 h 48 h 72 h

Figure 4.8 *L. monocytogenes* biofilm formed on a stainless-steel surface in the CDC bioreactor at 30°C and 10% TSB observed with acridine orange staining

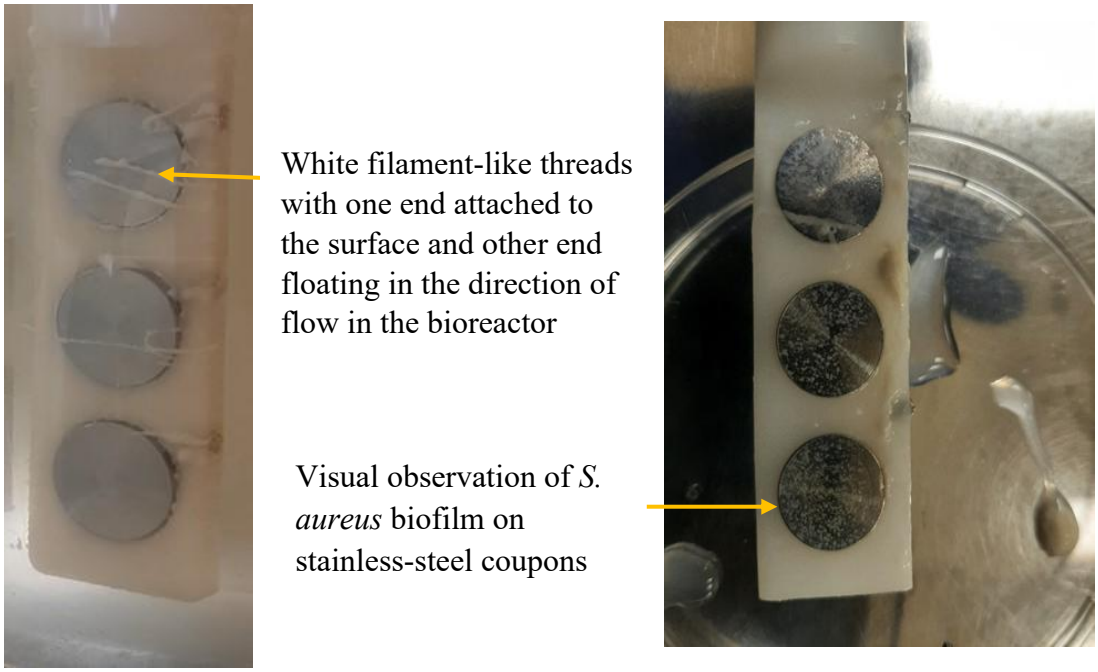

A. Bioreactor rods with 3 stainless-steel coupons taken from the bioreactor with *S. aureus* biofilm after 72 h of incubation under turbulent flow at 30°C.

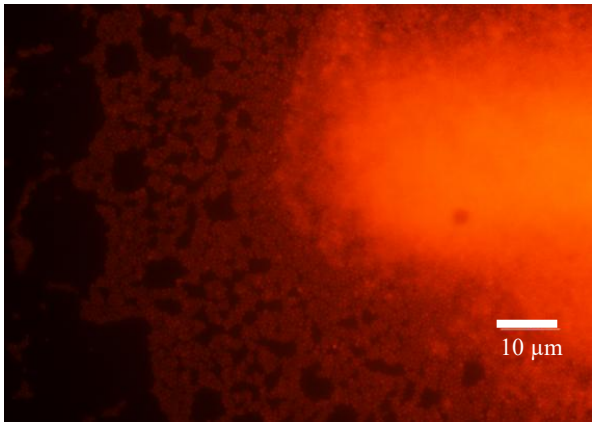

B. *Staphylococcus* observed by acridine orange stain, showing live cells on the free-flowing edge of the threads

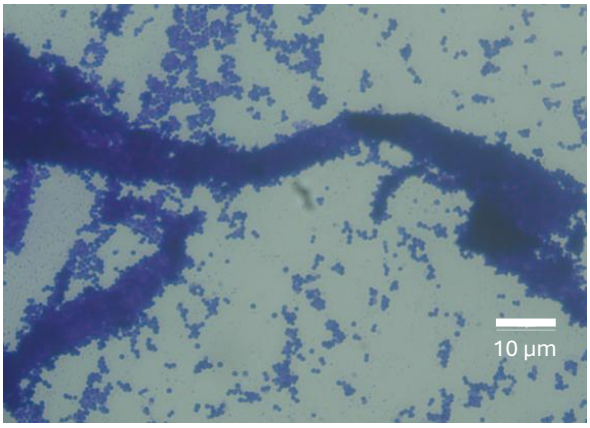

C. *Staphylococcus* threads observed by Gram staining

Figure 4.9 CDC bioreactor rod containing three stainless-steel coupons and a thread-like structure after 48 h of incubation at 30°C.

Acridine orange staining of the single-species *Listeria* biofilm showed filament-like structures at 48 h (Figure 4.8), when the cell concentration reached 5.7 $\log_{10}$ CFU/cm^2. These filamentous structures were absent in the static system at a cell concentration of 7.1 $\log_{10}$ CFU/cm^2. A similar filamentous structure was observed in dual species with *Staphylococcus* (Figure 4.12) at 72 h, where the *Listeria* cell concentration reached 5.2 $\log_{10}$ CFU/cm^2. In contrast, *Listeria*

in dual species with *Pseudomonas* did not appear to have filaments, but instead, a layer of *Pseudomonas* cells could be observed (Figure 4.11). With *Pseudomonas*, the cell concentration of *Listeria* was significantly higher ($p<0.05$) at 8.2 $\log_{10}$ CFU/cm^2. Additionally, the formation of wide channel-like structures was observed in the three species of biofilm formed in a continuous system (Figure 4.13. A). In contrast, the static system showed a different distribution of bacteria with a dense arrangement of bacteria across the surface of the coupon (Figure 4.13. B).

Thread-like structures with one end attached to the coupon rod and another end floating in the impeller direction were observed for *Staphylococcus* biofilm in single and dual species (with *Listeria*) (Figure 4.9). In dual species threads, in addition to *Staphylococcus* at a cell concentration of 7.4 $\log_{10}$ CFU/mL, *Listeria* was also detected at a cell concentration of 7.2 $\log_{10}$ CFU/mL in the threads. These observations have been summarized in Table 4.1.

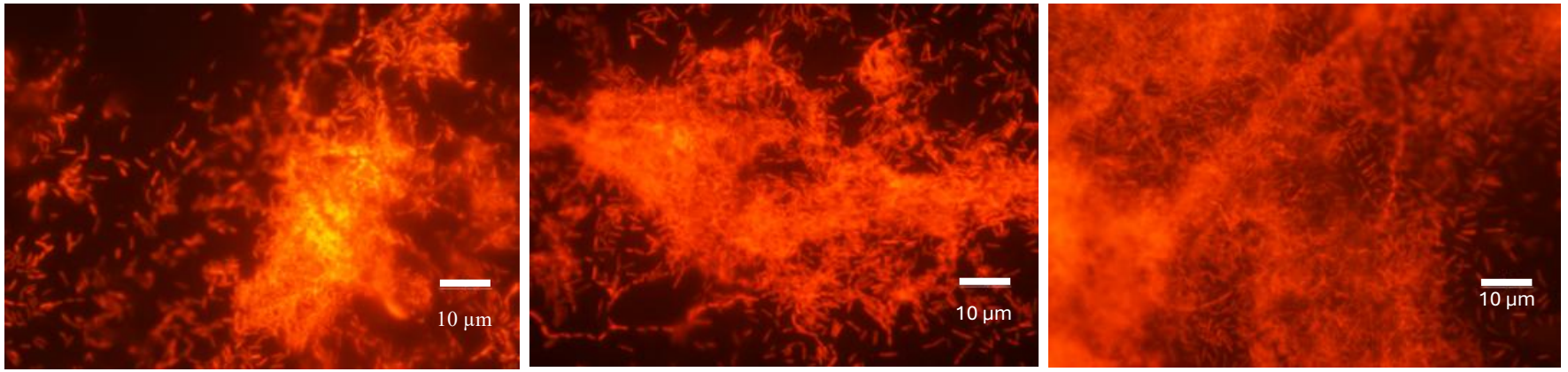

24 h 48 h 72 h

Figure 4.10 *P. fluorescens* and *S. aureus* dual species biofilm formed on a stainless-steel surface in the CDC bioreactor at 30°C and 10% TSB observed with acridine orange staining

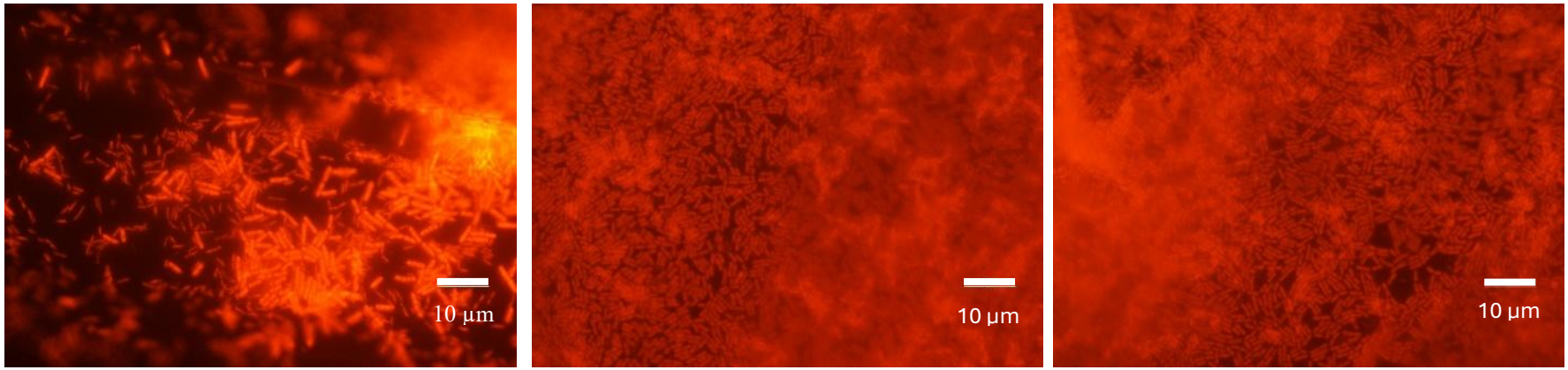

24 h 48 h 72 h

Figure 4.11 *P. fluorescens* and *L. monocytogenes* dual species biofilm formed on a stainless-steel surface in the CDC bioreactor at 30°C and 10% TSB, observed with acridine orange staining

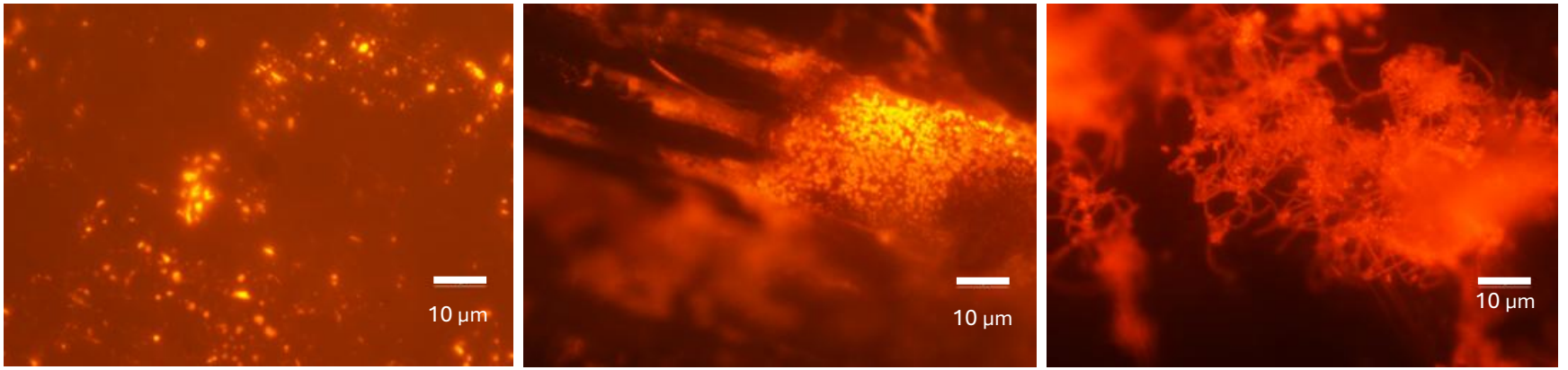

24 h 48 h 72 h

Figure 4.12 *S. aureus* and *L. monocytogenes* dual species biofilm formed on a stainless-steel surface in the CDC bioreactor at 30°C and 10% TSB observed with acridine orange staining.

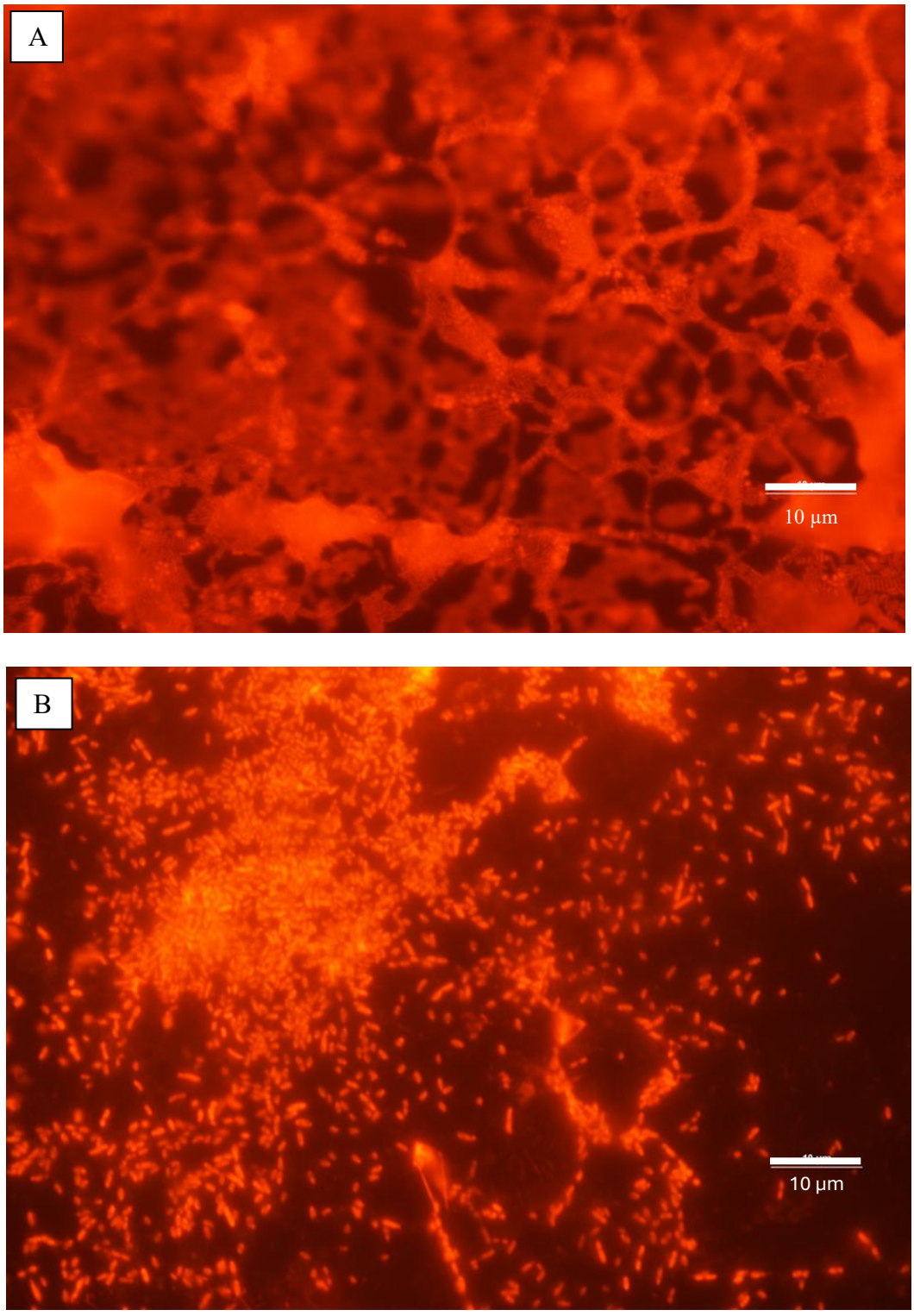

Figure 4.13 Three-species (*P. fluorescens*, *S. aureus*, and *L. monocytogenes*) biofilm formed at 72 h in 10% TSB and 30°C in A) CDC bioreactor system, B) Static system, observed with acridine orange staining and at 10 µm magnification.

Table 4.1 Summary of the microscopic observations for biofilms stained with acridine orange

Bacteria in the biofilm	Incubation time	Microscopic observation
P. fluorescens	24h	Dense cell arrangements over the surface
	48h	Arrangement of chains like structure observed
	72h	No chain structures, surface covered with cells
S. aureus	24h	Sparse arrangement of cells observed
	48h	Surfaces covered with a patchy arrangement of cells
	72h	Sparse ones surround dense clumps of cells on the surface
L. monocytogenes	24h	Low cell numbers were observed on the surface
	48h	Short filaments formation observed
	72h	Long filaments clumped and overlapped on the surface
P. fluorescens + *S. aureus*	24h	Intermixed biofilm with increasing cell densities as incubation time increases
	48h	
	72h	
P. fluorescens + *L. monocytogenes*	24h	Formation of intermixed layers. No chains/filaments observed for both bacteria
	48h	
	72h	
S. aureus + *L monocytogenes*	24h	Sparse distribution of cells on the surface
	48h	Patches of *S. aureus* cell clusters could be observed
	72h	Filamentation of *L. monocytogenes* observed with *S. aureus* intermixed
P. fluorescens + *S. aureus* + *L. monocytogenes*	24h	Observation of cells intermixed and formation of channels with the interstitial voids.
	48h	
	72h	No filaments or chains observed.

4.4.3 Sanitizer tolerance

Biofilms formed in static systems were more susceptible to sodium hypochlorite treatment ($p<0.001$) compared to biofilms formed in a continuous system. In both static and continuous systems, all three bacteria showed significantly higher sanitizer tolerance in dual species biofilm compared to their single species counterpart (Table 4.2).

P. fluorescens cells were more sensitive to sanitizer treatment in single species with log reduction of 4.5-6.9 $\log_{10}$ CFU/cm^2 compared to dual species combination in both static (3.7-3.9 $\log_{10}$ CFU/cm^2) and continuous systems (0.1-2.3 $\log_{10}$ CFU/cm^2). Similarly, for *S. aureus*, the cell survival was found to be higher in dual species with the log reduction of 3.8-5.9 $\log_{10}$ CFU/cm^2 compared to log reduction in single species biofilm (6.1 $\log_{10}$ CFU/cm^2), but this observation was limited to the static system. In the continuous system, the *S. aureus* cells were found to be more sensitive to sanitizer in dual (3.1-5.0 $\log_{10}$ reduction) and triple species (3.3 $\log_{10}$ reduction) compared to single species, with only 0.1 $\log_{10}$ reduction.

Similarly, for *L. monocytogenes*, in the static system, the 5-$\log_{10}$ reduction observed in single species further lowered ($p<0.05$) to 3.3 $\log_{10}$ CFU/cm^2 (with *P. fluorescens*), and 4.7 $\log_{10}$ CFU/cm^2 (with *S. aureus*). In the continuous system, the $\log_{10}$ reduction of *L. monocytogenes* in single species (1.3 $\log_{10}$ CFU/cm^2) was found to be comparable with *L. monocytogenes* in dual species with *S. aureus* (1.3 $\log_{10}$ CFU/cm^2) and *P. fluorescens* (1.0 $\log_{10}$ CFU/cm^2) (Table 4.2).

In three species biofilm (static system), *P. fluorescens* was found to be the predominant bacteria (Figure 4.4) and showed the significant log reduction ($p<0.05$) in triple species (6.5 $\log_{10}$ CFU/cm^2) upon sanitizer treatment compared to single species (4.5 $\log_{10}$ CFU/cm^2) and dual species (3.7-3.9 $\log_{10}$ CFU/cm^2) biofilm. Similarly, *L. monocytogenes* was the predominant bacterium in the continuous system (Figure 4.5) and showed a significant log reduction in triple species (2.6 $\log_{10}$ CFU/cm^2) compared with single (1.3 $\log_{10}$ CFU/cm^2) and dual species counterparts (1.0-1.3 $\log_{10}$ CFU/cm^2).

Table 4.2 Log reduction of *Pseudomonas* (P1), *Staphylococcus* (S2), and *Listeria* (LM1) in single, dual, and triple species 72 h biofilm after treatment with sodium hypochlorite in the static and continuous systems

Biofilm	Bacteria	Log_{10} reduction after sodium hypochlorite treatment	
		Static (log_{10} CFU/cm^2)	Continuous (log_{10} CFU/cm^2)
P1		4.5 ± 1.5^{eA}	6.9 ± 0.4^{jB}
S2		6.2 ± 0.7^{iA}	0.1 ± 0.1^{aB}
LM1		5.1 ± 0.2^{gA}	1.3 ± 0.1^{cB}
P1+S2	P1	3.9 ± 1.5^{cdA}	1.7 ± 0.5^{dB}
	S2	4.0 ± 0.2^{dA}	5.0 ± 0.2^{iB}
P1+LM1	P1	3.7 ± 1.5^{bA}	0.1 ± 0.1^{aB}
	LM1	3.3 ± 1.5^{aA}	1.0 ± 0.1^{bB}
S2+LM1	S2	5.9 ± 0.4^{hA}	3.1 ± 0.1^{gB}
	LM1	4.7 ± 0.4^{fA}	1.3 ± 0.1^{cB}
P1+S2+LM1	P1	6.5 ± 0.2^{jA}	2.3 ± 0.1^{eB}
	S2	3.8 ± 0.2^{cA}	3.3 ± 0.1^{hB}
	LM1	4.7 ± 0.1^{fA}	2.7 ± 0.1^{fB}

Note: The same superscript lowercase letters (a-j) indicate the significant differences between the bacteria within the same column. The same superscript uppercase letters (A-B) indicate the significant differences between the columns (static and continuous).

4.4.4 Exopolysaccharide production

Significantly higher ($p<0.001$) exopolysaccharide was produced by the bacteria in the biofilm formed in the CDC reactor compared with the static system, irrespective of the number of species of bacteria present in the biofilm (Figure 4.14). In the static system, *L. monocytogenes* in single species were found to be the lowest producer (3.2 μg/cm^2) of EPS, followed closely by the dual species combination of *P. fluorescens* and *L. monocytogenes* (3.6 μg/cm^2). Comparatively, *L. monocytogenes* in the CDC system (single species) produced higher EPS (7.6 μg/cm^2). In a continuous system, the dual species combination of *P. fluorescens* + *S. aureus* (6.3 μg/cm^2) and *S. aureus* + *L. monocytogenes* (6.4 μg/cm^2) produced comparable EPS with single species biofilm of *P. fluorescens* (6.0 μg/cm^2) and *S. aureus* (5.9 μg/cm^2). In the

flow systems, there was no significant difference ($p>0.05$) between the EPS produced by the three-species combinations compared with the two-species combinations.

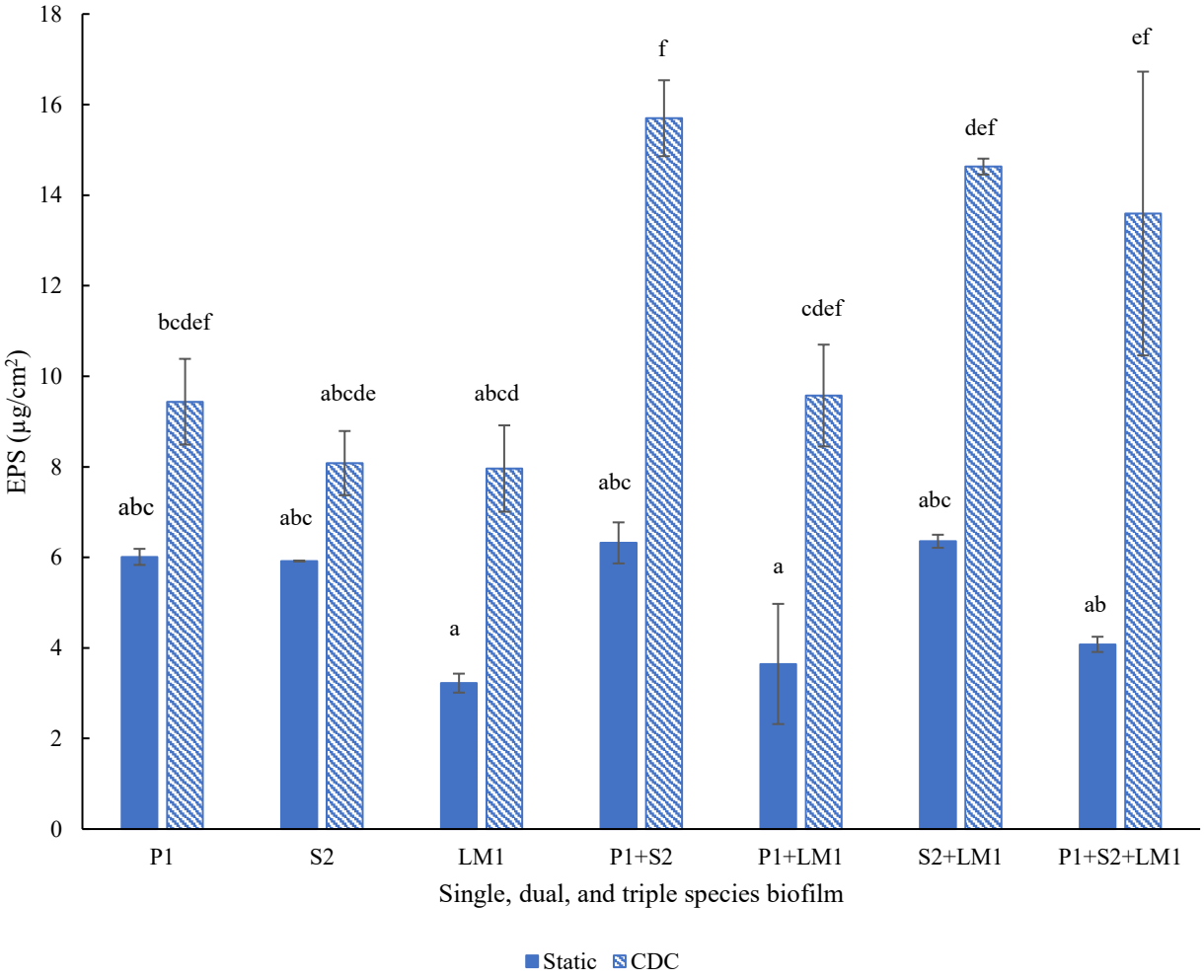

Figure 4.14 Exopolysaccharide content (µg dextran/cm^2) for single, dual, and triple species combinations of *P. fluorescens* (P1), *S. aureus* (S2), and *L. monocytogenes* (LM1) in static and CDC systems.

Note: The lowercase superscript (a-f) indicates the significant differences ($p<0.05$) between the exopolysaccharide content produced by single and multiple species bacteria in static and CDC systems.

4.4.5 Nutrient Flux in the Systems

In addition to the shear stress, another variable that impacts the biofilm formation in the CDC system is the continuous supply of fresh media compared to the static system. This difference in the nutrient supply was calculated as nutrient flux in each system (Table 4.3).

Table 4.3 Nutrient flux in a static and continuous (CDC) system

Parameter	Static system	CDC system
Media (10% TSB)	1 mL	5 mL/min
Area-coupon	2.4 cm^2	2.26 ×24 (8 rods) = 54.24 cm^2
Media/Time	1 mL in 24 h	7200 mL in 24 h
Media (10% TSB) /cm^2	**0.416 mL/cm^2**	**132.74 mL/cm^2**

The CDC system had approximately ×319 times higher influx of nutrients compared to the static system with 10% TSB (Table 4.3) and ×32 times higher influx than the static system with full strength TSB. In addition to the stress under shear, this might have contributed to the higher biofilm formation in the CDC system (Figure 4.5) compared to the static system (Figures 4.3 and 4.4).

4.5 Discussion

Significantly higher ($p<0.05$) exopolysaccharides (Figure 4.14) and tolerance to sodium hypochlorite sanitizer (Table 4.2) were noted for biofilms formed in continuous systems as compared to static systems. The importance of hydrodynamics and flow in the biofilm formation and biofilm community shift in drinking water systems has been stated before (Liu, Shan et al., 2020; Wang et al., 2014). The flow plays a vital role in the access of nutrients, metabolites, shear stress, and oxygen, ultimately shaping the three-dimensional structure of single species biofilm. In addition, the bacteria in the biofilm formed in flow conditions produce higher EPS and are more resistant to detachment from the surface (Paul et al., 2012; Wang et al., 2014). Depending on the bacterial species, the formation of exopolysaccharide is regulated by cyclic-di-guanosine-5′-monophosphate (c-di-GMP), quorum-sensing molecules, and small RNA molecules. When these genetic variables are impacted by the stress factors, variations in the production of matrix compounds such as exopolysaccharides occur (Flemming et al., 2023). In triple species combinations, the highest reduction upon sanitizer treatment was observed for bacteria that exist in predominance in both systems, which could be the result of a higher chance of exposure to the sanitizer in the biofilm. In this study, the three-species

biofilm formed in the continuous system showed the formation of interstitial voids, also known as fluid channels, at 48 h (Figure 4.13.A). This is normally established by the bacteria in the biofilm primarily for the transportation of metabolites, nutrients, and waste (Chitlapilly Dass & Wang, 2022). A study on the biofilm architecture of *P. aeruginosa* revealed a similar formation of open, hydrated structures with large voids in the biofilm structure where fresh media was continuously supplied (Davey et al., 2003). This continued access to nutrients and metabolites could be the reason for the favorable growth of *L. monocytogenes* in the continuous system in this study. In contrast, at the same incubation time for static culture, dense patches of bacteria could be observed where *P. fluorescens* was the predominant species with *S. aureus* and *L. monocytogenes* in the three-species biofilm. Some research has hypothesized that the predominance of *P. fluorescens* in multispecies set-ups is the result of higher EPS production (Chaggar et al., 2024). This study found that even though biofilms in the CDC system had significantly higher EPS content, the predominant species was *L. monocytogenes* (throughout the 72 h incubation), indicating the importance of flow for the order of predominance in a multispecies setup.

The biofilm formation of *S. aureus* and *L. monocytogenes* in single species was found to be lowered in the first 24 h in the presence of flow, indicating that the shear has a higher impact on the weaker biofilm formers as compared to strong biofilm formers (*P. fluorescens*), which remained unaffected. Significantly ($p<0.05$) higher cell concentration of *L. monocytogenes* was observed in dual (with *Pseudomonas*) and triple species in the presence of flow at all time intervals analyzed (24, 48, and 72 h) (Figure 4.5). This could be the result of synergy between the bacteria in the presence of stress factors such as shear. The growth and the interaction of *L. monocytogenes* in multiple species biofilms are known to be different according to the type of stress present (Puga et al., 2016b).

The results showed a significant ($p<0.05$) increase in the tolerance against hypochlorite sanitizer when multiple species of bacteria were present in the biofilm in both static and continuous systems (Table 4.2). Various studies have indicated that the elevated protection of bacteria in single and dual species biofilm is the result of the sheltering effect produced by a higher amount of EPS produced in the combination (Chaggar et al., 2024; Nkemngong et al., 2020). In this study, the EPS produced by single species biofilm was found to be comparable with dual and triple-species biofilms under the flow condition (Figure 4.14) indicating other factors, such as quorum sensing, and spatial organization could be the reasons behind elevated resistance in multiple-species biofilms formed under shear stress. Previous studies have noted

that the biofilm properties (thickness, composition), spatial arrangement, and resistance to the physical removal of the bacteria from the biofilm are significantly impacted by the presence of turbulent flow (Berne et al., 2018; Chawla et al., 2020).

In this study, biofilm streamers were observed for *S. aureus* biofilm in single and dual species (with *L. monocytogenes*) (Figure 4.9). In addition, *L. monocytogenes* could attach itself to the *S. aureus* streamers and reach high cell concentrations, indicating positive interactions between the bacteria. These interactions were found to be highly strain-dependent, as noted in the literature. The inhibitory effect of *L. monocytogenes* by *S. aureus* via the inhibitory compounds has been noted before (Bockelmann et al., 2017; Lynch et al., 2021). With the addition of shear forces going unidirectionally, the formation of filamentous structures referred to as biofilm streamers, formed in a microfluidic channel, has previously been observed for *P. aeruginosa* (Drescher et al., 2013; Secchi et al., 2022; Stoodley et al., 2002) and *S. aureus* (M. K. Kim et al., 2014). The foundation of *P. aeruginosa* biofilm streamers was found to be EPS and eDNA (Secchi et al., 2022), and they elongate by attaching the passing cells onto the EPS in the initial stages (Drescher et al., 2013). Once the initial attachment is complete, the elongation of the streamer depends on the type of biofilm formed. In solid biofilm, further elongation of the streamer is mostly through cell growth rather than attachment from the passing fluid. But, in the case of porous biofilm, the cells flowing through attach themselves to the streamers (Drescher et al., 2013). In addition to the gene expression for enhanced attachment and EPS production, flow is another factor that decides the structure of the *S. aureus* biofilm (M. K. Kim et al., 2014). Like any other type of biofilm, dislodgement of the streamer type of biofilm results in the attachment of the detached biofilm to another site, continuing the process. Additionally, the location of the streamers plays an important role in deciding the flow in a microfluidic channel. The presence of *P. aeruginosa* streamers in the center of the channel results in a significantly decreased flow rate compared to the streamers attached to the wall of the channel (Drescher et al., 2013), which ultimately results in clogging (M. K. Kim et al., 2014) and infection challenges (Secchi et al., 2022) for biofilms formed in medical contexts. Biofilm formed in static conditions with no shear forces often forms biofilm through layering and ends up forming mushroom and tower structures (Secchi et al., 2022).

Another interesting observation was made for the *L. monocytogenes* biofilm formed in a continuous system, where microscopic filamentous structures of *L. monocytogenes* could be observed in single species (Figure 4.8) and dual species (with *S. aureus*) (Figure 4.12) but were absent in the biofilm formed with *P. fluorescens* in dual (Figure 4.11) or in triple species

biofilm (Figure 4.13). In this study, the *L. monocytogenes* filaments were only observed when the cell concentration was <6 $\log_{10}$ CFU/cm^2, indicating the morphological variation might be the result of lowered biofilm formation under stressful conditions. These filamentous structures have previously been observed for *L. monocytogenes* in a planktonic state under sublethal sodium chloride concentrations (Hazeleger et al., 2006; Yamaki et al., 2021), antimicrobial stress (Rocha et al., 2019), alkaline stress (Giotis et al., 2007), and acidic stress in combination with sodium chloride (Bereksi et al., 2002). Furthermore, the filamentous *L. monocytogenes* was found to have higher stress tolerance compared to non-filamentous *L. monocytogenes* and multiplied rapidly once the cells ended the filamentous phase (Yamaki et al., 2021). So far, these filaments have not yet been reported in biofilm form. The formation of stress-resistant filamentous *L. monocytogenes* in the single and dual species biofilm in the continuous system has important implications in the food industry.

4.6 Conclusion

Cell concentration, sanitizer tolerance, and spatial organization of the biofilm are significantly affected by the presence of turbulent flow, indicating the importance of shear stress and access to nutrients in the overall biofilm structure and characteristics. The higher cell concentration of *L. monocytogenes* in multispecies and its ability to attach itself to the *S. aureus* biofilm streamers in the presence of flow is concerning, considering the pathogenicity of *L. monocytogenes*. Additionally, the ability of *L. monocytogenes* to form filamentous cells under flow conditions in single and dual species biofilms with elevated chemical stress tolerance could be a serious concern in food safety. This study concludes that to understand the sanitizer tolerance of bacteria in multiple species biofilms in a dynamic system, in addition to the chemical components (EPS), the spatial arrangement of resistant bacteria in the biofilm architecture and variations in gene expression need to be studied.

4.7 Link to the next chapter

While the nutrient flux explains the higher biofilm formation because of the continuous supply of media into the biofilm, it does not explain the morphological changes observed in *L. monocytogenes* in single species and the lack of this in dual species (*P. fluorescens*) under high shear stress in the biofilm. This will be explored in the next chapter (Chapter 5).

Chapter 5: Shear Stress Adaptation of *Listeria monocytogenes* in Mono and Dual-Species Biofilms

This chapter contains material that was published as a peer-reviewed article:

Pant, K., Palmer, J., & Flint, S. (2025). Shear stress adaptation of *Listeria monocytogenes* in mono and dual-species biofilms. *Food Research International*, 117190.

5.1 Introduction

Listeria monocytogenes is a rod-shaped, non-spore-forming, gram-positive bacteria, and an important foodborne pathogens that commonly cause outbreaks in dairy products (raw milk, ice cream, cheese), meat products (deli meat), fresh fruits (peaches, cantaloupes) (Redding et al., 2024), and vegetables (enoki mushrooms, leafy greens) (Wiktorczyk-Kapischke et al., 2023). They can persist in the food industry, often showing enhanced resistance to adverse conditions such as low temperature (-1.5°C), low nutrients, acidity (pH: 3.3-4.2), salinity (10%), and chemicals (lethal/sublethal) (Melian et al., 2022; Papaioannou et al., 2018; Wiktorczyk-Kapischke et al., 2021). These stress adaptations can be the result of quorum sensing between the bacteria (Zhu et al., 2017), upregulation of stress genes, which are regulated by the sigma factor σ^B (Guerreiro et al., 2020), resulting in the expression of virulence genes, and changes in phenotypic traits (Wiktorczyk-Kapischke et al., 2023).

Homeoviscous (membrane fluidity maintenance) adaptation for low-temperature survival (Miladi et al., 2013), rod to coccoid shape under nutrient stress (Gao & Liu, 2014), and rod to elongated chains under saline stress (Giotis et al., 2007; Shah & Bergholz, 2020) are some examples of stress adaptation by *L. monocytogenes*. The filamentation of planktonic *L. monocytogenes* under saline stress has been correlated with the expression of genes related to the upregulation of the *min* C gene (inhibits septa formation) (Kale et al., 2017), downregulation of *lmo2506* (cell division), *lmo2552* (cell wall synthesis), and *lmo1376* (NADPH production) (Liu, Miller, et al., 2014). The phenotypic change includes the elongation of cells longer than 4 μm as compared to the 'normal' cell length of *L. monocytogenes*, which is 1-2 μm (Yamaki et al., 2021). *L. monocytogenes* isolated from conditions of shear stress have higher adhesion to abiotic surfaces (Mendez et al., 2020) and enhanced tolerance to removal through shear stress (Szlavik et al., 2012; Vázquez-Boland et al., 2001). The formation of filamentous cells under stress can also result in the underestimation of the *L. monocytogenes* cell count in the sample (Bereksi et al., 2002; Jones et al., 2013). Once the stress factor is removed, rapid proliferation of *L. monocytogenes* is observed, contributing to foodborne outbreaks (Yamaki et al., 2021).

The adaptation designed to aid bacteria in surviving multiple stressors is known as cross-tolerance. For example, adapting to cold stress aids in the adhesion of the bacteria to stainless-steel surfaces and resistance to quaternary ammonium compound sanitizer (Miladi et al., 2013).

Similarly, the stress resistance obtained in low-temperature growth improves the cross-tolerance to osmolarity stress (Schmid et al., 2009). The stress-tolerance of *L. monocytogenes* has been positively correlated with the predominance of *L. monocytogenes* in polymicrobial communities in food processing environments (FPEs) (Wang et al., 2023). This synergistic interaction of *L. monocytogenes* with the background microbiota on FPEs enhances biofilm formation and resistance to sanitizers (Gu et al., 2024; Ibusquiza et al., 2012; Puga et al., 2018). Pang & Yuk, (2019) observed higher resistance of *L. monocytogenes* against environmental stresses when it was incorporated into a mature *P. fluorescens* biofilm, indicating the importance of multispecies interactions in biofilm eradication. This can result in the utilization of extracellular matrix components such as exopolysaccharide (EPS) and metabolites produced by the background microbiota, such as *P. fluorescens* (Flemming et al., 2016; Puga et al., 2018). *P. fluorescens* is a major spoilage microorganism frequently isolated from dairy surfaces (Maggio et al., 2021) and has been studied extensively for its role in the synergistic multispecies biofilm (Puga et al., 2018; Zhou, Dong, et al., 2024). *P. fluorescens* has been reported to produce higher proteolytic enzymes in mixed-species biofilm (Teh et al., 2014), harbour weak biofilm formers (Puga et al., 2015), and show enhanced protection of the overall biofilm from desiccation and disinfection (Pang & Yuk, 2019).

So far, studies on the stress response of *L. monocytogenes* have been limited to pH, saline, bile, and nutrients and have focused on planktonic cells, disregarding the most common form of bacteria in nature, the biofilm. The biofilm formation, composition, structure, and finally the difficulty of removal from the surface are dependent on many factors, such as hydrodynamic conditions, properties of the substrate material, nutrient abundance, and temperature (Simões et al., 2022). Flow conditions and nutrient supply to the bacteria are recognized as important variables in biofilm development (Prabhukhot, Eggleton, Kim, & Patel, 2024; Simões et al., 2022; Vázquez-Boland et al., 2001). Another important aspect is understanding the impact of hydrodynamic stress on biofilm formation of pathogens such as *L. monocytogenes* in both single and multi-species communities.

The difficulty in the removal of biofilm formed under flow compared to biofilms formed under static conditions has been mentioned before (Vázquez-Boland et al., 2001). This research aims to understand the effects of shear stress on the biofilm formation of *L. monocytogenes* and the cross-adaptation it develops as the result of shear stress in a single species. The morphology of *L. monocytogenes* under turbulent flow in the presence of *P. fluorescens* on industrially relevant stainless-steel surfaces was also studied.

5.2 Materials and methods

5.2.1 Bacterial strains and culture media used

Pseudomonas fluorescens 2614 (P1) (dairy isolate) and *Listeria monocytogenes* H1 (LM1) (environment-soil isolate) were used for biofilm formation, which are from a previously established culture collection (Food Microbiology Lab, School of Natural Sciences and Food Technology, Massey University, Palmerston North). The cell concentrations for static and bioreactor were prepared according to section 3.2.1. The final cell concentration was set at 8 $\log_{10}$ CFU/mL for inoculation in the bioreactor (Appendix VI). For dual species inoculation, each bacterium was adjusted to this cell concentration and added in a 1:1 concentration during inoculation.

5.2.2 Biofilm formation in static conditions

Single species biofilm of *L. monocytogenes* was formed according to section 4.2.2. The passivated stainless-steel coupons (type 316, 2B finish, 2.4 cm^2) (Advanced Sheetmetals Ltd., Palmerston North) were used for biofilm formation in static conditions (Skowron et al., 2019). The sterile coupons were added to 48-well plates (Costar®, Falcon, USA) containing 10% TSB with a final cell concentration of *L. monocytogenes* adjusted to 6 $\log_{10}$ CFU/mL. The plates were incubated at 30°C for 24 h for further analysis of static biofilm.

5.2.3 Biofilm formation under turbulence

Single and dual species biofilm of *L. monocytogenes* and *P. fluorescens* were formed using CDC bioreactor as mentioned in section 4.2.3. The CDC bioreactor was run for seven days under continuous flow (10% TSB), at 30°C and 250 rpm using a heating magnetic stir plate. Depending on the experiments, rods were taken out at appropriate time intervals for cell concentration analysis, microscopic observations, and genetic analysis.

For the dynamics of the biofilm formation in single and dual species, one rod (three coupons) was taken out of the bioreactor every 24 h for 7 days. The blank rod replaced the coupon rod to maintain the flow. The coupons were saline washed to remove planktonic cells, and the cell concentration in the biofilm was estimated according to section 4.2.5 using bead beating assay

and selective agar. A similar method was repeated for single-species biofilm as well, where the coupons were saline washed, bead-beaten, and plated on tryptone soy agar (TSA) (Difco™, Becton, Dickinson and Company, USA). The bioreactors were run for at least two biological replicates for each sample, and each biological replicate consisted of three technical replicates.

5.2.4 Cross-adaptation: cells from planktonic, static, and turbulent flow

The cells were harvested from the biofilm at 48 h incubation time, formed in turbulent flow (section 5.2.3) and static conditions (section 5.2.2), using glass-bead beating in saline solution (5 min), sonication (5 min), and followed by centrifugation (5 min, 12,000× g) (Niboucha et al., 2022). The cells from the planktonic culture were harvested through centrifugation (5 min, 12,000× g). The supernatant was discarded for both cases, and the cells were washed in saline solution and centrifuged again for 5 min at 12,000× g. The final cell pellet was resuspended in saline solution, and the cell concentration was fixed at 6 $\log_{10}$ CFU/mL before the following analysis was carried out with the harvested cells.

A) Motility

The motility of the cells harvested from planktonic, static, and turbulent flow was observed through swimming agar according to Li et al., (2018) with modifications. A volume of 2 µL inoculum (6 $\log_{10}$ CFU/mL) was stabbed into 0.3% agar in tryptone soy broth (TSB) agar plates, and the diameter of the growth on the agar at 30°C after 24 h was measured using a vernier calliper.

B) Attachment to stainless-steel surface

The variation in the attachment of *L. monocytogenes* cells with filamentation (shear-stressed cells) and without filamentation (static and planktonic) was observed using stainless-steel coupons (Wang et al., 2022). A volume of 100 µL of harvested cells (6 $\log_{10}$ CFU/mL) was inoculated into 10% TSB in a 48-well plate containing stainless-steel coupons and incubated for 5 min at 30°C to investigate the initial attachment of the bacteria harvested from different growth conditions on the stainless-steel surface (Rodriguez et al., 2008). After the incubation, the coupons were removed, washed in saline solution, and cells adhered to the stainless-steel surface were enumerated using the glass bead beating method and plated on TSA using a spread plate method as mentioned in section 4.2.5. The relative attachment of the cells was calculated

by dividing the $\log_{10}$ of the attached bacteria by the $\log_{10}$ of bacteria in the inoculum (Chae & Schraft, 2000).

C) Biofilm-forming ability of harvested cells

The cells harvested from planktonic culture, static biofilm, and turbulent flow biofilms were used as inoculum (adjusted to 6 $\log_{10}$ CFU/mL) to form biofilm on the stainless-steel coupons (type 316, 2B finish, 2.4 cm^2) at 30°C for 24 h in 10% TSB under static conditions according to section 5.2.2. The cells in the biofilm formed were quantified through the glass bead beating method and enumeration on TSA plates as described in section 4.2.5.

5.2.5 Removal of stress from the *L. monocytogenes* biofilms

To observe whether cell filaments in biofilms formed under turbulent flow conditions continued as filamentous cells after the removal of stress, the coupons with filamentous biofilms were incubated in static conditions. The coupons collected from the bioreactor in section 5.2.3 were washed with saline to remove planktonic cells and reintroduced into a 6-well plate with fresh sterile media (10% TSB) (5 mL). The plates were incubated at 30°C for 24 h under static conditions before proceeding with acridine orange staining and microscopic observation according to section 5.2.6.

5.2.6 Epifluorescence- Morphology of the cells

Acridine orange stain was used to visualise the cells in the biofilm after 48 h of incubation on stainless-steel coupons in the CDC bioreactor and on static coupon surfaces as mentioned in the section 4.2.7. For planktonic sample, 24 h *L. monocytogenes* culture was centrifuged (5 min, 12,000× g) for the removal of supernatant followed by the addition of 1 mL of acridine orange solution (10 g/L) to the pellet, mixed by vortex. The tubes were incubated in the dark for 5 mins. After 5 mins, the suspension was centrifuged again (5 min, 12,000× g) and the pellet redissolved in PBS and centrifuged again (5 min, 12,000× g). The final suspension was dropped on a glass slide and air-dried before being observed with epifluorescence microscope.

Picogreen (Quant-iT™ Picogreen™, Thermofisher Scientific, Waltham, Massachusetts, USA) was used to visualise eDNA networks of *L. monocytogenes* for the biofilm formed in the CDC bioreactor. The coupons were removed from the bioreactor with mono-species *L. monocytogenes* biofilm at 48 h and washed with sterile distilled water to remove planktonic

cells. The washed and air-dried coupons were dipped in acridine orange staining solution for 5 min in the dark and washed with sterile distilled water before air-drying. Similarly, for eDNA, the washed and air-dried coupons were stained with pico-green in the dark for 5 min, further washed with sterile distilled water before air-drying. The visualization of the cells/biofilm was done using an epifluorescence microscope (Nikon Eclipse Ni, USA) with TRITC (excitation filter 485/20 nm and emission filter 500–538 nm) and FITC (Excitation 465/490 nm and emission 512 nm) for acridine orange and pico-green, respectively. The NIS-elements D software was used to capture images. Five images were captured from each coupon. Three technical replicates were acquired from each biological replicate. Two biological replicates were used for microscopic analysis. The length of the cells in planktonic, static biofilm, and turbulent biofilm samples was measured using ImageJ (ImageJ 1.54g, National Institute of Health, USA) from the images obtained from the epifluorescence microscope. The length and width of at least 20 cells were measured for each replicate, and the results were presented as mean ± standard deviation.

5.2.7 Fluorescence in situ hybridization (FISH) and confocal microscopy

Dual-species biofilm samples were collected from the bioreactor at 48 h, stained with a fluorescent probe (Custom Taqman®, Life Technologies, CA, USA) (Kocot & Olszewska, 2020) and counterstained with 4′,6-diamino-2-phenylindole (DAPI) (Invitrogen, Thermo Fisher Scientific, USA) and visualised using confocal microscopy (Nikon D-eclipse C1, Japan). Coupons were washed with PBS before fixing in 4% paraformaldehyde (BDH Limited, Poole, England) for 15 min at room temperature. The fixed coupons were treated with lysozyme (1 mg/mL) (Sigma-Aldrich, Belgium) at 37°C for 10 min. The treated coupons were washed with PBS and air-dried before staining with the fluorescent probe at 46°C for 2 h. The coupons were then dipped in wash buffer at 48°C for 15 min before counterstaining with DAPI (1 mg/mL) and incubation in the dark at room temperature for 10 min. The coupons were finally washed with PBS and air dried before visualization of the cells using blue channels for DAPI and red channels for the FISH probe. A 60× water immersion lens was used to observe the images. The images were acquired and overlayed using EZ-C1 software (Gold version 3.80 build 860).

5.2.8 Relative Gene Expression

Based on the observations made above (Section 5.2.4), the variation in the expression of the genes relating to the motility of the cells (*motB*), stress (*sigB*), biofilm formation and adhesion (*mpl*), rod shape (*rodA*), and cell division (*ftsW* and *ftsX*) was observed for samples collected from static and turbulent flow and compared to planktonic cells (Gao et al., 2024). The PCR conditions such as annealing temperature for following genes were optimised from Gao et al., (2024) and Liu, Basu, et al., (2014). 16S rRNA and rpoB genes were reference genes for this experiment (Table 5.1). Despite the internal housekeeping genes, differences in the nucleic acid extraction efficiency and the absence of exogenous internal standard could create variability in gene expression measurements.

Table 5.1 Primer sequences used for gene expression analysis of *Listeria monocytogenes*

Gene	Primer	Sequence	References
16S- reference gene	Forward	ACATCCTTTGACCACTCTGGA	(Gao et al., 2024)
	Reverse	CAACATCTCACGACACGAGC	
rpoB	Forward	CGTCGTCTTCGTTCTGTTGG	(Gao et al., 2024)
	Reverse	GTTCACGAACCACACGTTCC	
motB	Forward	TGCAAAAAAATTCGAACAAATGG	(Gao et al., 2024)
	Reverse	CTGCCGCGCCTTCCT	
sigB	Forward	AAAGAAACGGGTGAACTACTCGAT	(Gao et al., 2024)
	Reverse	CAACGCCTCTCGAAGTTTTTTAA	
mpl	Forward	CGGTTATCCAGTATTCGGCG	(Gao et al., 2024)
	Reverse	TTCCTCTGTGAGTGGAAGCG	
rodA	Forward	CTTCCGCTTGGTCTTGTAGC	(Liu, Basu, et al., 2014)
	Reverse	CAATGAGCGCAATCGAACTA	
ftsW	Forward	GGGATCGCTAGTCTGATTGC	(Liu, Miller, et al., 2014)
	Reverse	TACCAAGCATCATCGACAGC	
ftsX	Forward	AATGGTTGGATGACCTTTGC	(Liu, Miller, et al., 2014)
	Reverse	CGTTGCAAGCTTGTTCATGT	

The cells from the static and turbulent flow biofilms were collected using ice-cold, acid-treated glass beads (Sigma, Germany) and PBS by vortex for 5 min, followed by sonication for 5 min. The sonicated solution was centrifuged (12,000× g) for 5 mins at 4˚C, and the pellets were collected for RNA extraction. The planktonic samples were centrifuged (12,000× g) for 5 mins at 4˚C after 24 h incubation (30°C), and cell pellets were collected for further analysis. The RNA was extracted and purified from the planktonic, static, and shear-stressed samples using NucleoSpin® RNA Plus (Macherey-Nagel, Germany). The integrity of the extracted RNA was analysed using a Nanodrop (Jenway, Bibby Scientific Ltd, UK), and the A_{260}/A_{280} nm ratio of 1.9 and above was selected for RT-qPCR (LightCycler® 480, Roche Diagnostics, Switzerland). A total volume of 20 µl consisted of SYBR@Green mastermix, primers (forward and reverse), DNA template, and PCR-grade water, and the RT-qPCR conditions were set according to Luna® Universal One-step RT-qPCR Kit (New England Biolabs, Ipswich, MA). The fold change was analysed using the $2^{-\Delta\Delta ct}$ for the target genes (Livak & Schmittgen, 2001) with reference gene (16S) as internal control (Table 5.1). The non-template control (NTC) was tested for each set of primers.

5.2.9 Variables in the bioreactor

To further understand whether the variation in the biofilm formation of *L. monocytogenes* under turbulent flow (bioreactor) compared to the static system is due to increased nutrient access or the impact of shear, two different bioreactors, each dealing with a single variable, were set up (Figure 5.1). Bioreactor A was a closed system where there was no continuous supply of fresh media. The bioreactor was emptied every 24 h and replaced with fresh media to replicate the nutrient availability in the static system but with the presence of turbulence (240 rpm). In bioreactor B, a continuous supply of media was provided; however, the impeller was turned off (no turbulent flow).

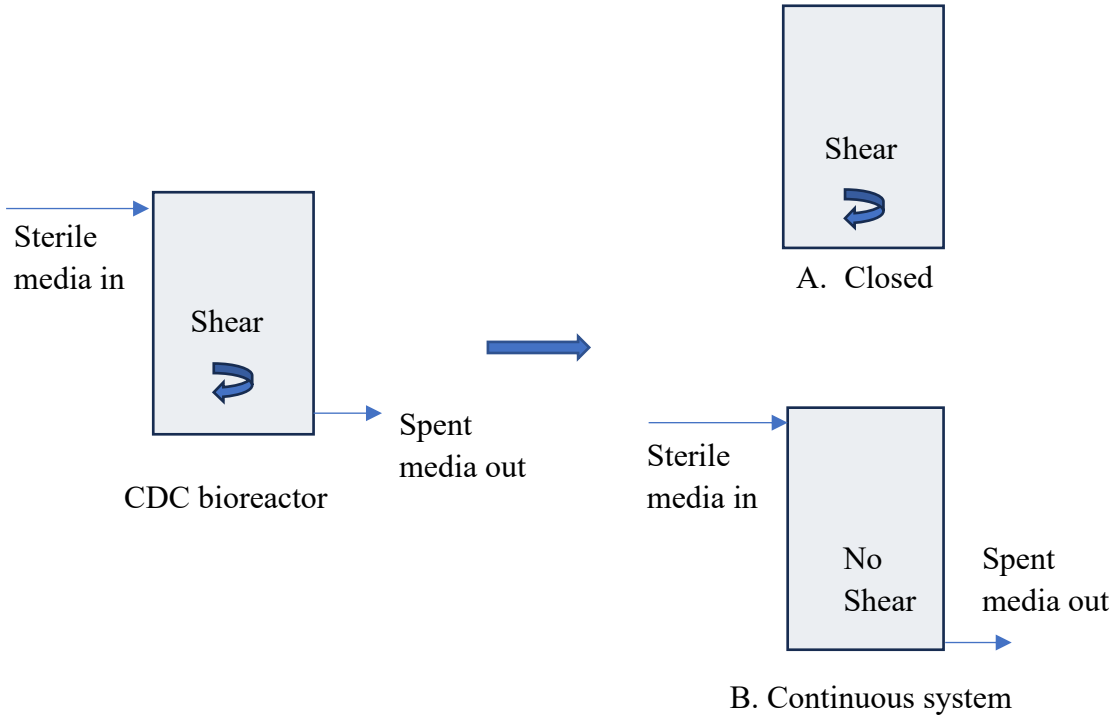

Figure 5.1 Reactor design to understand the influence of nutrient flow and shear as individual factors influencing *L. monocytogenes* biofilm

5.2.10 Statistical analysis

The significant differences ($p<0.05$) between the samples were analysed using one-way ANOVA (IBM SPSS Statistics 29) and post-hoc analysis using Tukey's test, and results were represented as mean ± S.D. The relationship between the length of the cells with motility, adhesion to the stainless-steel coupons, and biofilm formation at 24 h was analysed using Pearson's correlation analysis (IBM SPSS Statistics 29).

5.3 Results

5.3.1 Biofilm formation under turbulent flow

In the single-species biofilm, the cell concentration of *P. fluorescens* at 24 h was 6.3 $\log_{10}$ CFU/cm^2, which gradually increased to 7.8 $\log_{10}$ CFU/cm^2 over the next 6 days of incubation. In the single-species, *L. monocytogenes* showed a gradual increase in cell concentration from 4.7 $\log_{10}$ CFU/cm^2 (day 1) to 6.3 $\log_{10}$ CFU/cm^2 (day 7) (Figure 5.2).

The biofilm formation of *P. fluorescens* was similar in dual species (with *L. monocytogenes*), with cell concentrations ranging from 6.4 to 7.5 $\log_{10}$ CFU/cm^2 during a 7-day incubation period (Figure 5.2). Significantly higher growth ($p<0.05$) of *L. monocytogenes* was observed in dual-species, compared with single-species biofilm (Figure 5.2). While the cell concentration of *L. monocytogenes* in 24 h biofilm was comparable to single (4.7 $\log_{10}$ CFU/cm^2) and dual-species (5 $\log_{10}$ CFU/cm^2), a significant increase ($p<0.005$) was observed at 48 h where the cell concentration of *L. monocytogenes* was significantly higher ($p<0.05$) in dual species (8.7 $\log_{10}$ CFU/cm^2) biofilm as compared to its single species counterpart (5.1 $\log_{10}$ CFU/cm^2). After this initial rise over 48 h in dual species, the cell concentration of *L. monocytogenes* remained consistent over 7 days (8.7-9 $\log_{10}$ CFU/cm^2) (Figure 5.2).

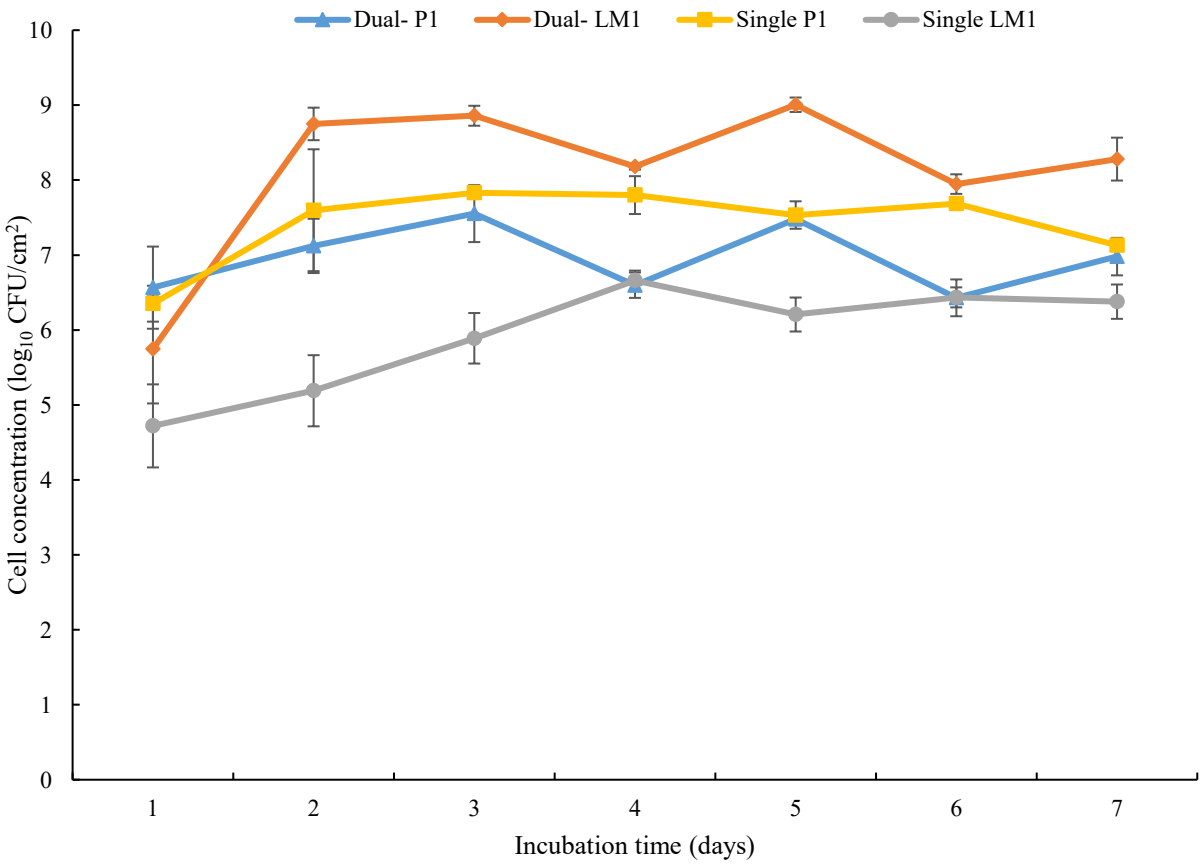

Figure 5.2 Cell concentration of *P. fluorescens* (P1) and *L. monocytogenes* (LM1) in single- and dual-species biofilms formed under turbulent flow in the CDC bioreactor during 7-day incubation at 30°C.

5.3.2 Spatial arrangement and morphology of the cells

A ‘knitted’ or ‘web’ structure (Figure 5.3 A) was observed in 72 h *L. monocytogenes* single species biofilm formed under turbulent flow, which, under higher magnification, was observed to be overlapping of filaments formed by unseparated cells (Figure 5.3 B). This structure was traced with pico green stain specific to extracellular DNA (eDNA) as it is membrane impermeable (Figure 5.4). eDNA is a vital component of the extracellular matrix that plays a role in both initial attachment and biofilm formation of *L. monocytogenes* (Harmsen et al., 2010). While the filament structure was absent in dual-species biofilm formed with *P. fluorescens* under turbulent flow, a ‘web’ structure was observed (Figure 5.6).

The average length of the ‘normal’ *L. monocytogenes* cells in planktonic and static biofilm was 1.3 ± 0.2 µm and 1.4 ± 0.2 µm, respectively ($p>0.05$). In comparison, the length of the shear-stressed cells observed in the bioreactor reached 27.7 ± 6.2 µm (refer to Figure 5.5. C for an example), which increased in length up to 72 h of incubation. The length of the filaments reached as high as 52.3 ± 1.1 µm under the same conditions. In dual-species biofilm formed by *P. fluorescens* and *L. monocytogenes*, filaments were not visible, with the mean cell length of 1.6 ± 0.3 µm under flow conditions, indicating no morphological changes of *L. monocytogenes* in the presence of the second bacterium (*P. fluorescens*) (Figure 5.6). Overall, the bacterial width was unaffected ($p>0.05$) in all growth conditions in single-species biofilm, ranging from 0.48 ± 0.06 µm, 0.46 ± 0.05 µm, and 0.46 ± 0.04 µm for planktonic, static, and turbulent flow, respectively. A similar observation ($p>0.05$) of cell width (0.45 ± 0.07 µm) was made for *L. monocytogenes* cells in a dual-species biofilm with *P. fluorescens*.

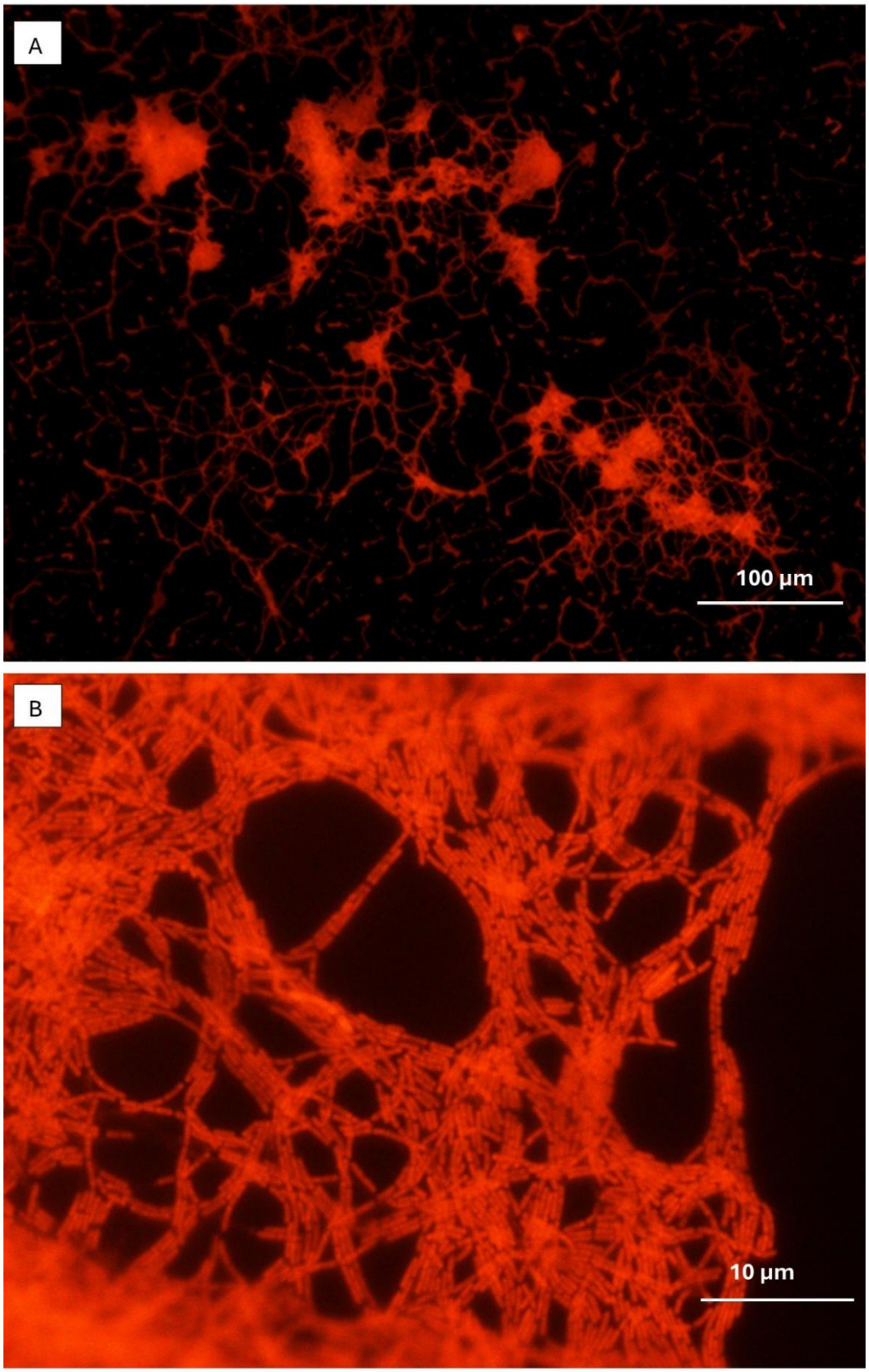

Figure 5.3 Knitted structure of *L. monocytogenes* in single-species biofilm formed under turbulent flow (CDC bioreactor) at 30°C for 72 h, observed with epifluorescence microscopy and acridine orange staining under two different magnifications: A) 400× and B) 1000×

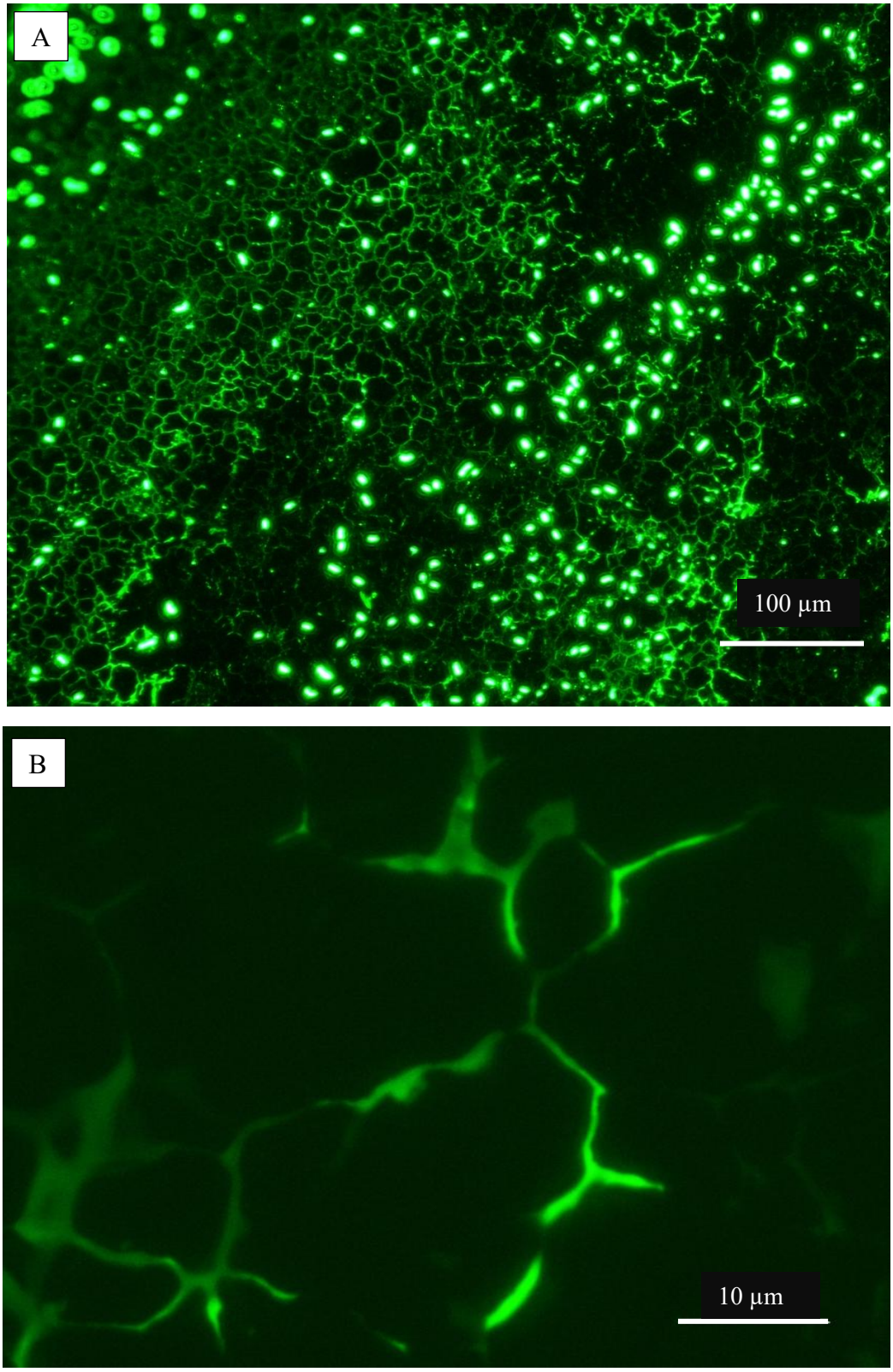

Figure 5.4 Extracellular DNA (eDNA) networks of *L. monocytogenes* biofilm formed under turbulent flow (CDC bioreactor) at 30°C for 72 h, observed with Pico green staining and epifluorescence microscopy under two different magnifications A) 400× and B) 1000×.

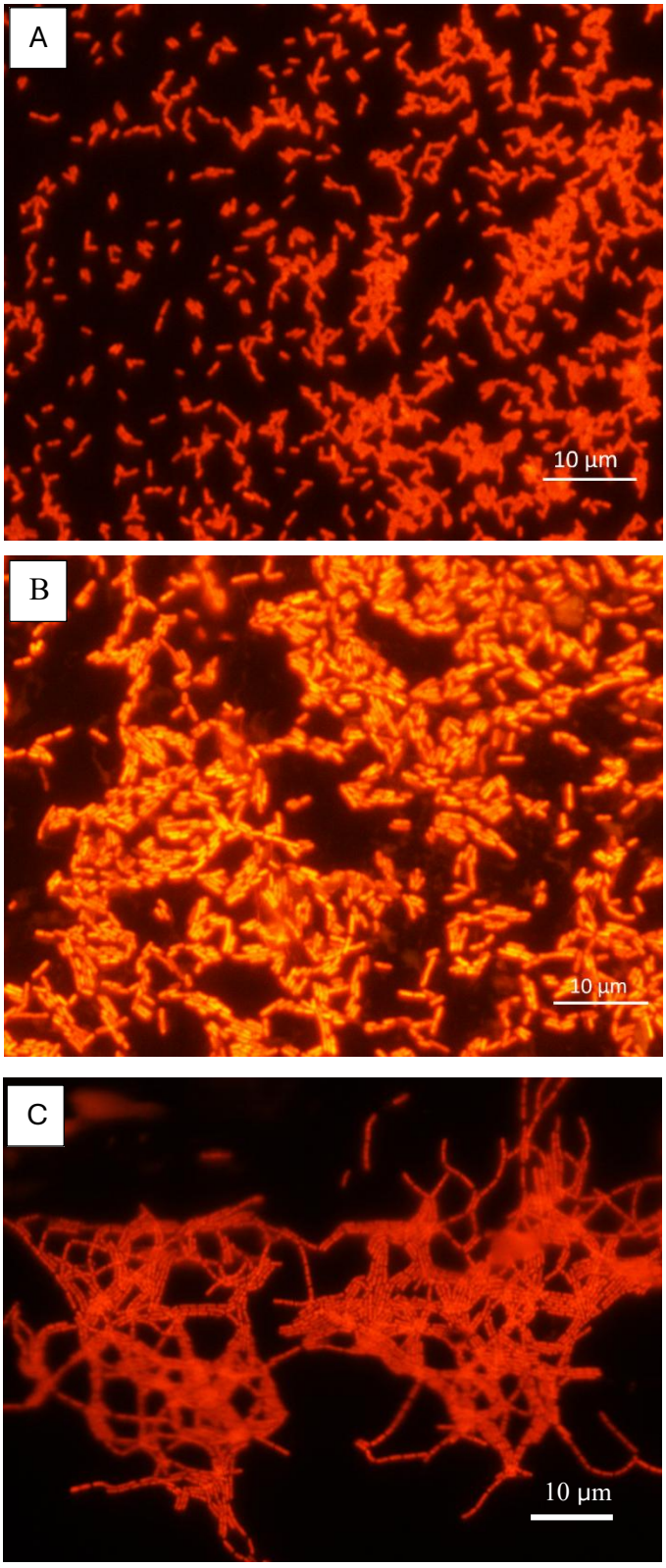

Figure 5.5 *L. monocytogenes* cells morphology under different conditions. A) Cells in 24 h planktonic culture, B) Cells in 48 h static biofilm, C) Cells in 48 h CDC bioreactor, all incubated at 30°C.

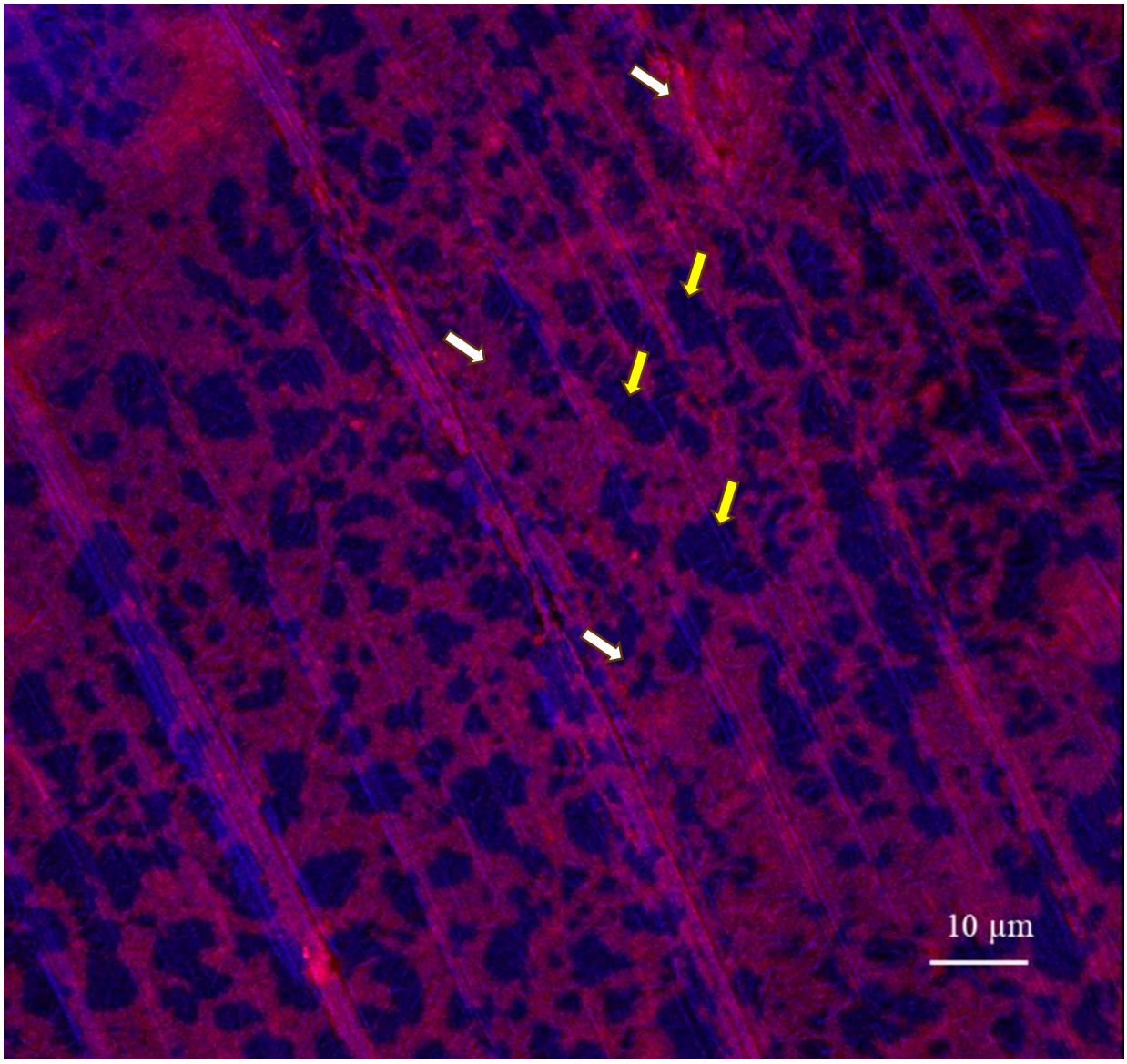

Figure 5.6 Confocal microscopy image (60× immersion lens) showing a web-like structure of *L. monocytogenes* (red-cyanine red probe) on *P. fluorescens* (blue-DAPI) layer, observed for a dual-species biofilm formed in a CDC bioreactor at 30°C. Note: the yellow arrows indicate *P. fluorescens* cells (blue) and the white arrows indicate *L. monocytogenes* cells (red).

5.3.3 Cross-adaptation and correlation

The motility of the cells harvested from biofilm formed under turbulent flow was significantly lower ($p<0.05$) (3.4 ± 0.9 mm) than those harvested from static biofilm (15.3 ± 1.6 mm) and planktonic conditions (21 ± 5.6 mm), observed as the diameter of the growth in 0.3% TSB agar (Figure 5.7.B). The motility negatively correlated (Table 5.2) with the attachment of the

bacteria (5 min) on stainless-steel surfaces in 10% TSB. The highest relative attachment ($p<0.05$) (5 min) was observed for cells from turbulent flow (66.4 ± 7.6%) compared to cells harvested from planktonic (51.8 ± 4.3%) and static systems (51.9 ± 6.7%) (Figure 5.7.A). The higher relative attachment of cells from turbulent flow resulted in lower cell numbers in biofilms ($p<0.05$) in the turbulent flow (6.7 ± 0.07 $\log_{10}$ CFU/cm^2) biofilms compared with static (7.2 ± 0.1 $\log_{10}$ CFU/cm^2) and planktonic systems (7.0 ± 0.1 $\log_{10}$ CFU/cm^2) (Figure 5.7.C).

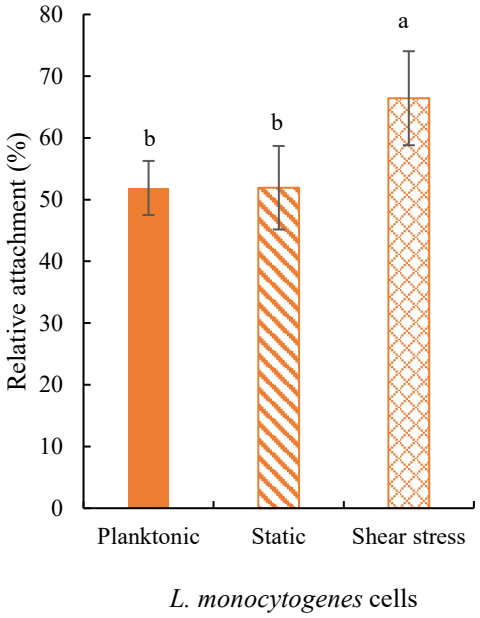

B. Relative attachment of harvested cells

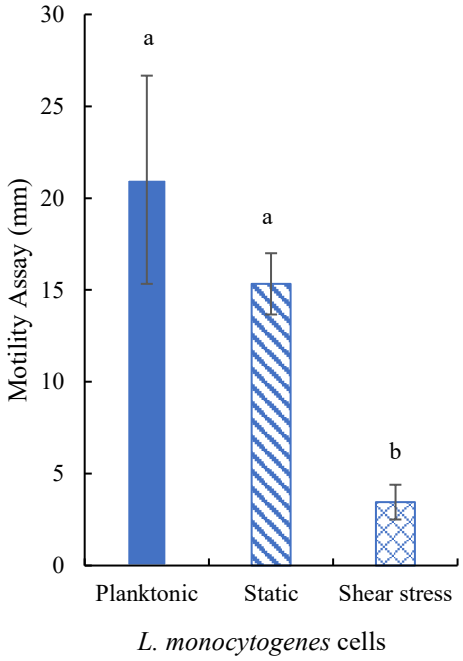

A. Motility assay of harvested cells

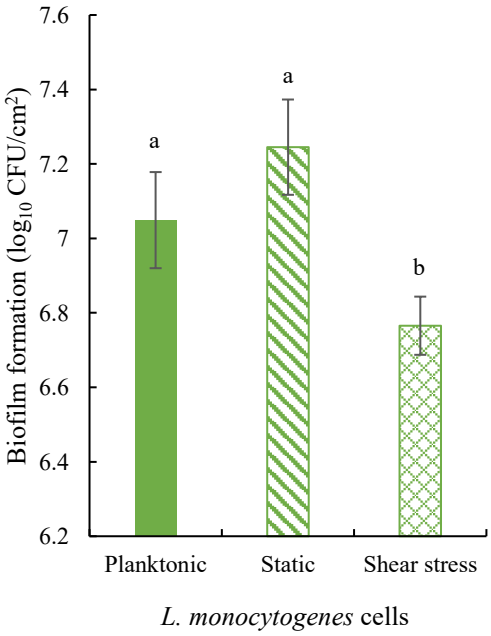

C. Biofilm formation ability of harvested cells

Figure 5.7 Observations made for planktonic, static, and shear-stressed cells at 30°C. The lowercase letters a, b, and c indicate significant differences among cells from three different systems.

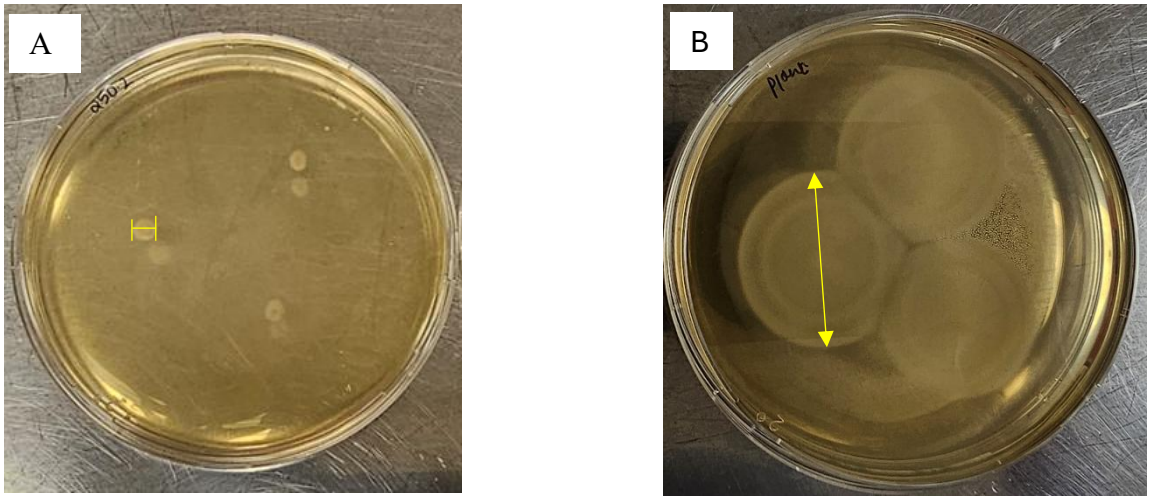

Figure 5.8 Motility assay for cells harvested from A) biofilm formed in a CDC bioreactor B) planktonic cells. The yellow arrows indicate the diameter of the respective colonies.

The concentric rings observed in Figure 5.8.B colonies for planktonic cells show the dense cells on depleted media (inner rings) and active cells with high motility in outer rings. In addition to nutrient depletion, these types of rings have been observed to be a function of cycles of oscillating dark and light (Tiensuu et al., 2013), growth rate, substrate consumption and metabolic activity (Jeanson et al., 2015).

Overall, the length of the cells had a positive impact on attachment and a negative correlation with motility and biofilm formation. Meanwhile, bacteria with higher motility showed reduced attachment, but this had a weak correlation with biofilm. The bacteria's attachment showed a weak negative correlation with biofilm, but the correlation was not statistically significant (Table 5.2).

Table 5.2 Correlation between cell length, motility, attachment, and biofilm formation (24 h) observed with Pearson's coefficient

	Length	**Motility**	**Attachment**	**Biofilm**
Length	1	-0.880**	0.869**	-0.758*
Motility	-0.880**	1	-0.846**	0.49
Attachment	0.869**	-0.846**	1	-0.415
Biofilm	-0.758*	0.49	-0.415	1

** Correlation is significant at the 0.01 level; * Correlation is significant at the 0.05 level

5.3.4 Relative Gene Expression

The cells from the turbulent flow system showed significant ($p<0.001$) downregulation of motility gene (*motB*), stress gene (*sigB*), and cell division genes (*ftsW* and *ftsX*), whereas adhesion gene (*mpl*) and rod shape determining gene (*rodA*) were found to be significantly ($p<0.001$) upregulated, relative to cells harvested from the planktonic and static system (Figure 5.9).

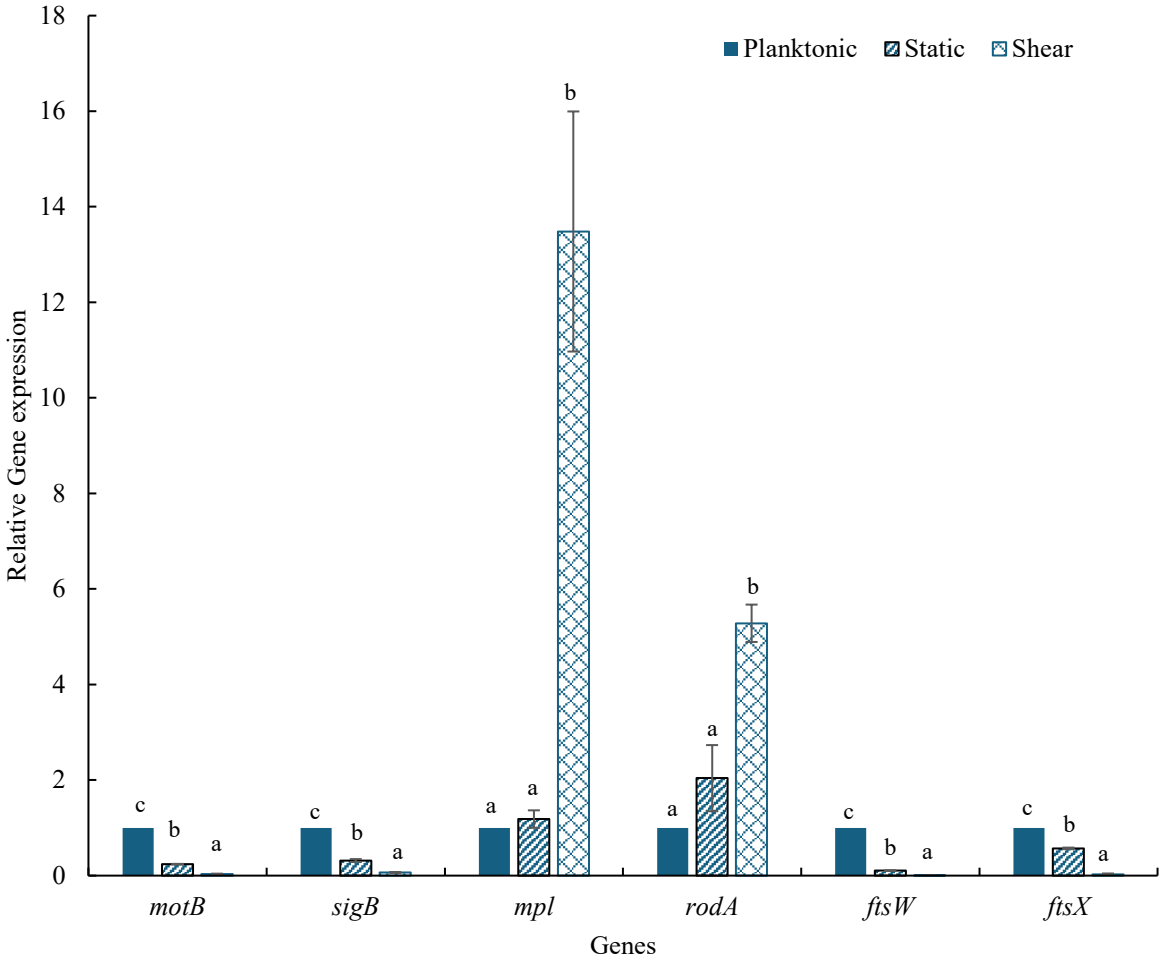

Figure 5.9 The relative gene expression (fold change) of cells from the planktonic system, static biofilm, and biofilm formed under turbulent flow. (Different letters represent significant differences between each bar in a triplicate set – i.e. For each gene)

5.3.5 Filamentation continuity

The coupons removed from the turbulent flow with filamentous biofilm were introduced into the sterile media and incubated for another 24 h under static conditions. The filaments were retained in the biofilm, and further growth of cells around the filaments could be observed. While the filaments did not dismantle immediately, additional growth could be seen around the filaments during the incubation period (Figure. 5.10).

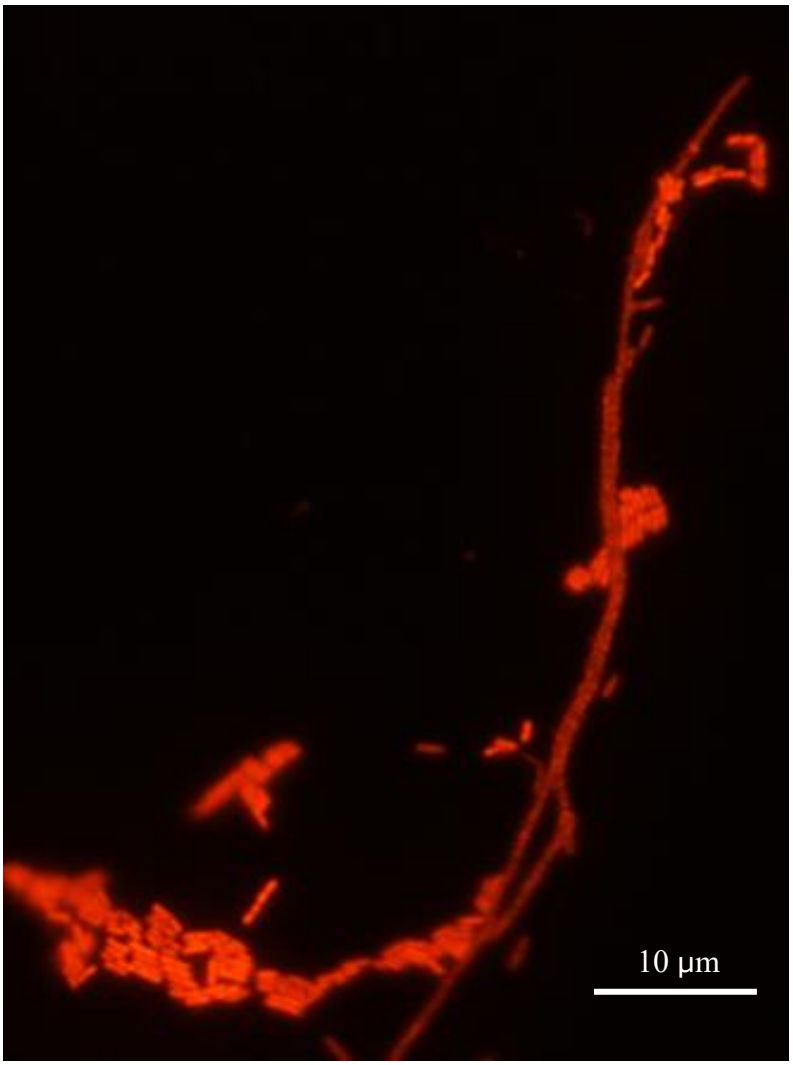

Figure 5.10 The *L. monocytogenes* biofilm (filaments) observed after stress removal and static incubation (in 10% TSB at 30 °C for 24 h).

5.3.6 Variables in the bioreactor

The biofilm formed in the bioreactor with no shear and just the constant supply of media was observed with the highest cell concentration, reaching 8 $\log_{10}$ CFU/cm^2 compared with the

closed system with shear (5.2 $\log_{10}$ CFU/cm^2) and the system with both variables present (5.8 $\log_{10}$ CFU/cm^2) on day 3 of incubation (Figure 5.11). There was a significant difference ($p<0.001$) between the cell concentration in biofilm formed between the closed system (Figure 5.1 A) and the continuous system (Figure 5.1 B).

Among the three models compared for the biofilm formation of *L. monocytogenes,* biofilm formation in the bioreactor (with both variables) was comparable with the biofilm formed in a closed system in shear, indicating the shear stress variable to be the dominating variable in the bioreactor when both variables are present.

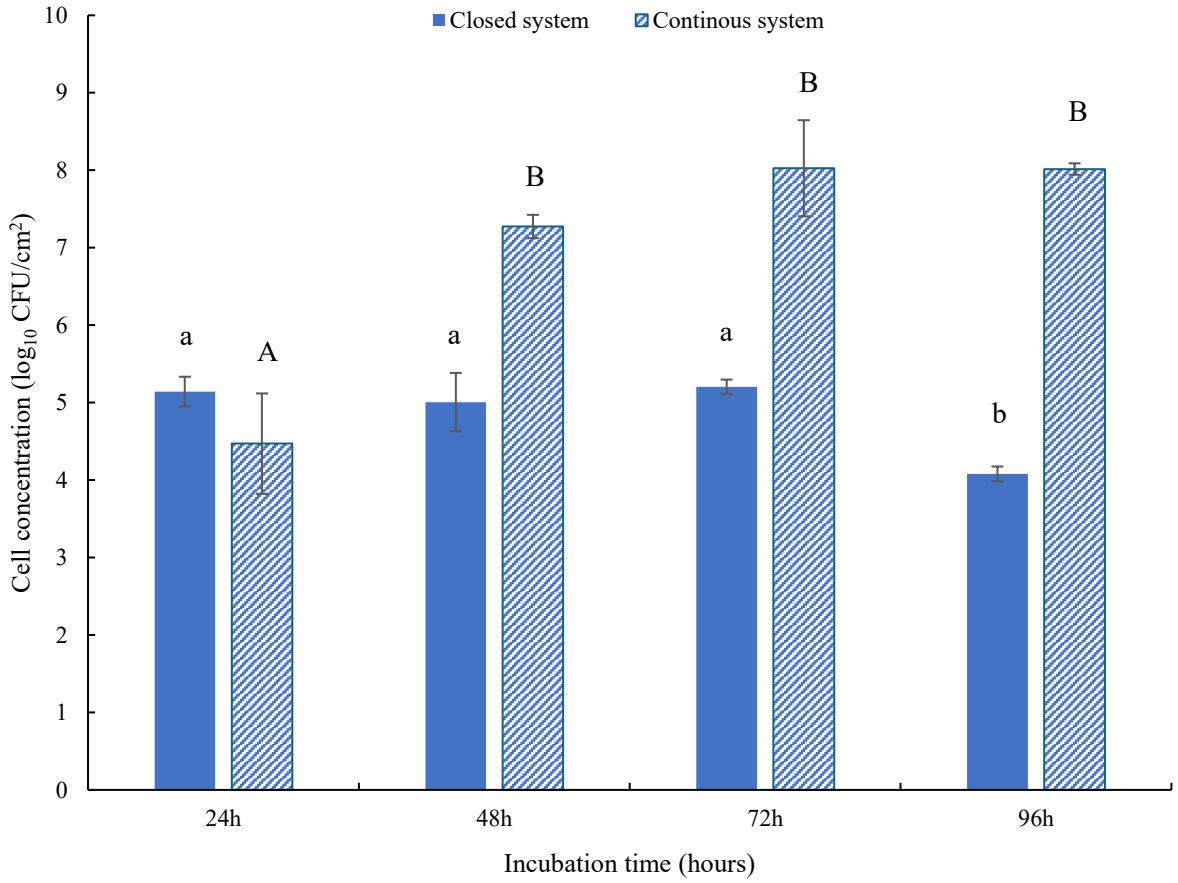

Figure 5.11 The cell concentration of *L. monocytogenes* in single-species biofilm formed under different variables, focusing on shear force and continuous supply of media during 96 h incubation. The lowercase letters a,b, and uppercase letters A,B indicate the significant differences between incubation time for closed and continuous system respectively.

5.4 Discussion

In this study, the cell concentration of *L. monocytogenes* improved significantly ($p<0.05$) in dual-species biofilm compared to its single-species counterpart under turbulent flow during a 7-day incubation period (Figure 5.2). *L. monocytogenes* Scott A was a relatively poor biofilm former under turbulent flow, with its inability to form biofilm under shear stress as noted before (Fagerlund et al., 2021; Puga et al., 2018). Under turbulent flow, the presence of higher exopolysaccharide-producing bacteria (*Pseudomonas*) was found to be more impactful in increasing the biofilm formation of *L. monocytogenes* than the hydrophobicity, surface charge, or the motility of *L. monocytogenes* (Sasahara & Zottola, 1993). A similar observation was made for *Pseudomonas* and *L. monocytogenes* dual-species biofilm formed on the glass coverslips under flow, where improved cell concentration was observed for *L. monocytogenes* in dual-species compared to its mono-species counterpart (Puga et al., 2018). An observation of the spatial arrangement of the bacteria via confocal microscopy showed that *L. monocytogenes* cells embed themselves at the bottom of the biofilm, under the protective layer of *P. fluorescens*, protecting themselves against the shear forces (Puga et al., 2018). In another study of dual-species biofilm formed by *L. monocytogenes* and *P. fragi* under a flow system, the *L. monocytogenes* cells' mobility was limited to a localised surface area and appeared to be trapped between the *P. fragi* cells and the EPS matrix, protected against the flow (Sasahara & Zottola, 1993). Under a different growth condition (static), the cell concentration of *L. monocytogenes* decreased (6.7 $\log_{10}$ CFU/cm^2) in dual-species biofilm formed with *P. fluorescens* compared to its single-species biofilm (7.21 $\log_{10}$ CFU/cm^2), while *P. fluorescens* maintained its cell concentrations (7.5-7.8 $\log_{10}$ CFU/cm^2), indicating the importance of flow on the behaviour of bacteria in multispecies setups (Pang & Yuk, 2019).

The present study observed chain-like filamentation in *L. monocytogenes* cells of the single-species biofilm formed under turbulent flow (Figure 5.3), indicating that this adaptation could be one of the impacts of high hydrodynamic shear stress in the bioreactor. A similar observation was made for *L. innocua* cells under shear stress, where elongation of specific cells was noted for several cells adhered to the stainless-steel surface (Perni et al., 2006). In *L. monocytogenes*, conditional filamentation of bacteria has been attributed to two major conditions: environmental stress and starvation (Karasz et al., 2022). These conditions trigger DNA lesions, and filamentation has been reported as a response to repair these lesions (Jones et al., 2013), resulting in inadequate cell separation and the visualization of filament structures. In addition to the acridine orange, the network of *L. monocytogenes* cells could also be traced with pico-green, indicating the underlying network of eDNA (Figure 5.4). In response to sub-

lethal stress, the release of eDNA of genomic origin can be observed in the biofilm, as a result of lysis or controlled secretion by the cells (Okshevsky & Meyer, 2015). This has been further investigated in the literature by treating the networks of *L. monocytogenes* biofilm formed under stress (nutrient starvation) with DNase I. The DNase I was found to dismantle the network structure and remove the biofilm from the surface, indicating that the eDNA plays a vital role in the adhesion of cells to the surface (Cherifi et al., 2017; Harmsen et al., 2010). In addition to providing extra structural support for cells, this structural eDNA is known to play a key role in adaptation and resistance in response to stress (Olwal et al., 2018).

The average length of *L. monocytogenes* conditioned with 10% NaCl for 3 days was found to be 6.5 ± 3.3 µm (Yamaki et al., 2021), indicating adaptation to salinity stress under sublethal conditions. The plating of the filaments may not necessarily separate the cells during enumeration, leading to an underestimation of the total cell count (Giotis et al., 2007). In this study, the removal of hydrodynamic stress and further incubation in static conditions with fresh media (24 h) did not completely separate the cells in the filaments (Figure 5.10). Once filamentation is triggered, returning to the 'normal' state depends on the type of stress that caused filamentation. For example, alkali-stressed *Listeria* cells required 3 h to revert to normal-sized cells when incubated in fresh media with neutral pH conditions (Giotis et al., 2007), whereas CO_2-stressed *Listeria* cells took longer (2-4 days) to revert to their original morphology (Jydegaard-Axelsen et al., 2005). In addition to the filamentous structure, in the present study, a knitted pattern was observed in 48 h biofilms formed by *L. monocytogenes* in single-species (Figure 5.3.A) and in dual-species (Figure 5.6). A similar observation of a 'web-like' structure was noted for *L. monocytogenes* formed under flow and nutrient stress in a microfluidic system (1/10 BHI) (Cherifi et al., 2017) or 'knitted' structure in flow cell chambers (1% TSB) (Rieu et al., 2008). This pattern changed under the lack of nutrient stress (full-strength BHI), revealing layered bacterial structures instead of 'webs' (Cherifi et al., 2017).

In a dual-species biofilm with *P. fluorescens*, no filamentous structure was observed (Figure 5.6) and was accompanied by significantly ($p<0.001$) higher cell concentrations of *L. monocytogenes* (Figure 5.2). In the case of layering, the upper layer consists of metabolically active cells, while the lower layer contains metabolically inactive cells, as observed in *L. lactis* biofilm (Habimana et al., 2009). This phenomenon has been explained in terms of higher nutrient access to the top of the biofilm compared to the bottom (Habimana et al., 2011). The predominant nature of other bacteria over *L. monocytogenes* has been associated with

differences in growth rates, which result in the smothering of *L. monocytogenes* into the lower layers of the biofilm, leading to competitive inhibition (Habimana et al., 2011). However, in the present study, in the continuous system with *P. fluorescens* and *L. monocytogenes* although *P. fluorescens* predominated, no competitive inhibition was observed for either bacterium over 7 days (Figure 5.2).

While attachment is one of the first steps for biofilm establishment, this study found a weak correlation between attachment (5 min) and biofilm formation (24 h) in terms of cell concentration (Table 5.2). A negative correlation was observed between motility and attachment, resulting in higher attachment of *L. monocytogenes* in filament forms on the stainless-steel surface. In a similar study, *L. monocytogenes* strains with low or no motility were found to form a higher biofilm at 37°C (Fan et al., 2020). Rapid attachment provides the bacteria an opportunity to adhere firmly to the surface and form stronger biofilms before the cleaning and disinfection (Wang et al., 2022). In contrast, the attachment period of 30 min on polystyrene surfaces showed no linear correlation between attachment and motility of *L. monocytogenes* on polystyrene surfaces (microtiter plate) (Takahashi et al., 2010), indicating the importance of duration of adherence. The variation could also be the result of surface hydrophobicity (plastic surfaces). The lack of correlation between *L. monocytogenes* attachment and biofilm formation has been noted before on glass surfaces (3 h) (Chae & Schraft, 2000).

A significant downregulation ($p<0.05$) of the *motB* gene was observed in cells harvested from biofilm under static and flow conditions (Figure 5.9). The motility of the cells is associated with the regulation of the *motB* gene, which regulates the flagella rotation, expressing the swimming and swarming abilities of the bacteria (Fan et al., 2020), and also regulates chemotaxis protein. The downregulation of motility genes results in the paralysis of flagella, resulting in cells with decreased swimming and swarming properties of the bacteria (Jiang et al., 2025). In the present study, motility was positively associated with attachment (5 min) but did not correlate with biofilm formation (24 h) (Table 5.2). Depending on the *L. monocytogenes* strain, media, and growth temperature, a conflicting relationship between motility and biofilm formation can be found in the literature. A positive impact of motility and biofilm formation has been noted for *L. monocytogenes* (Fan et al., 2020; Gao et al., 2024). In contrast, Dong et al., (2022) observed no impact of motility on the biofilm formation for *L. monocytogenes*. The significant upregulation of the *mpl* gene during biofilm formation on stainless-steel surfaces has been noted previously, indicating its importance in biofilm formation (Gao et al., 2024).

The upregulation of the *mpl* gene in the present study, corresponded with significantly higher attachment ($p<0.05$) to the stainless-steel surface for the shear-stressed cells (Figure 5.7.A).

A significant downregulation of the stress-regulating gene (*sigB*) was observed for cells collected from shear-stressed conditions compared to cells collected from planktonic conditions (Figure 5.9). The stress factor gene, *sigB,* controls the general stress response (GSR) (Santos et al., 2019) and is assumed to trigger resistance to environmental and antibiotic stress in *L. monocytogenes,* resulting in cross-tolerance (Poimenidou et al., 2023). Upregulation of the *sigB* genes was observed in the presence of flow (van der Veen & Abee, 2010) and NaCl (2% and 5%). However, reports also suggest that the stressful conditions do not necessarily result in upregulation of *sigB*, but vary depending on the *L. monocytogenes* strains, growth stages, and conditions (van der Veen & Abee, 2010). Under cold stress, higher expression of stress genes was observed for the biofilm during the mature stage (Santos et al., 2019), in contrast to the study by Utratna et al., (2014), where the expression was highest in the early stages of biofilm formation. In the present study, the application of hydrodynamic stress in the continuous system corresponds to the constant influx of fresh media into the bioreactor and removal of waste media from the bioreactor, which could negate the nutritional stress that planktonic cells and static cells encounter in a closed system. In a similar stress study, the *sigB* gene was found to be significantly downregulated in the combined treatment of sodium hypochlorite + peroxyacetic acid and hydrogen peroxide + peroxyacetic acid (Byun et al., 2024), and Quercetin (0.2 mM and 0.8 mM) treatment (Vazquez-Armenta et al., 2020), indicating the role of suppression of *sigB* genes in reduced biofilm formation.

The Fts and RodA proteins belong to the family of SEDS (shape, elongation, division, sporulation) proteins (Rismondo et al., 2019). In the present study, significant downregulation of genes (*ftsW* and *ftsX*) and upregulation of gene *rodA* were observed (Figure 5.9). This correlated with the microscopic observations of biofilm formed under turbulent flow, which showed the formation of filaments with a mixture of divided and non-divided septa (Figure 5.3). In a similar study, *L. monocytogenes* mutant cells lacking the RodA protein were observed to have shorter cell length (1.3 µm) compared to their wild-type strain (1.9 µm), emphasizing the important role of the *rodA* gene in maintaining the rod shape (Rismondo et al., 2019). Two hypotheses have been proposed to explain the elongation of cells as the result of upregulation of the *rodA* gene and downregulation of the *ftsW* gene. An increase in the concentration of RodA leads to the scarcity of proteins required at the cell division site resulting in the overproduction of peptidoglycan on the lateral wall. The second one is that the overproduction

of the RodA protein inhibits the FtsW protein needed for cell division at the site, leading to elongated cells (Rismondo et al., 2019). In another study, downregulation of the cell division gene *ftsX* was observed along with filamentation as a result of salinity stress (2.35% NaCl) after 30 days of storage (Liu, Miller, et al., 2014). Additionally, this gene was found to be upregulated when the cell filaments started dividing, observed at 60 and 90 days (Liu, Miller, et al., 2014). The downregulation of cell division genes indicates adaptation to stressful conditions, as observed in the study regarding *L. monocytogenes* adaptation to a sublethal dose of carnocyclin A (Liu, Basu, et al., 2014). The cell division protein FtsW regulates the gene *ftsW,* which controls the cell division transport system permease protein. Additionally, the *rodA* gene determines the rod shape and the cell division protein in *L. monocytogenes* (Liu, Basu, et al., 2014). The role of FtsW and RodA proteins for the cell shape and morphology has previously been observed for many bacteria, such as *B. subtilis* (Henriques et al., 1998), *S. pneumoniae*, and *E. coli* (Boyle et al., 1997).

The separation of variables (media supply and shear) in two different bioreactors allowed an understanding of the impact of each variable on the biofilms, specifically on *L. monocytogenes* single-species biofilm. *L. monocytogenes* biofilm in closed system under shear (Figure 5.11) had comparable cell concentrations to the *L. monocytogenes* biofilm formed in the bioreactor containing both variables (Figure 5.2), both of which showed reduced biofilm compared with the bioreactor with continuous media supply and no shear (Figure 5.11). This suggests that the dominating variable in the bioreactor containing both variables (flow and nutrient supply) is turbulent flow. The impact of shear on *L. monocytogenes* attachment and biofilm formation has been discussed in the literature (Mendez et al., 2020).

5.5 Conclusion

This study investigated the stress adaptation of *L. monocytogenes* in single and dual-species biofilms with morphological and genetic observations under shear stress and continuous media supply in the CDC bioreactor. The adaptation of *L. monocytogenes* under shear stress was found to be significantly different in single-species biofilm compared to dual-species (with *P. fluorescens*), indicating the importance of considering multispecies in stress response. The gene expression analysis of cells at 48 h incubation time showed that the cells had already adapted to the hydrodynamic stress, possibly aided by the constant inflow of fresh nutrients in the bioreactor, as indicated by the downregulation of the stress gene *sigB* relative to static

conditions (Figure 5.9). Another important observation was the filamentation of the bacteria as a result of stress adaptation in a single species (Figure 5.3), which has been associated with the underestimation of cells in the food chain, posing a critical food safety risk (Yamaki et al., 2021). The elongation of cells and formation of filaments in *L. monocytogenes* have been associated with the variation in susceptibility to antimicrobials (Rismondo et al., 2019). This is crucial information to understand the behaviour of the pathogen *L. monocytogenes* on food processing surfaces under different stressors.

5.6 Link to the next chapter

In this chapter, the variation in the *L. monocytogenes* morphology during the biofilm formation in the bioreactor was concluded to be due to the presence of shear stress caused by the high hydrodynamic flow. Interestingly, this variation was absent in dual-species biofilm. Literature suggests that the attachment, which is the first stage of biofilm formation, is most impacted because of shear. Hence, the attachment and biofilm formation of *L. monocytogenes* on sterile surfaces vs on preformed *P. fluorescens* biofilm surfaces under high shear stress will be explored in the next chapter (Chapter 6).

Chapter 6: Sequential assembly of multispecies biofilm

This chapter contains material that was published as a peer-reviewed article:

Pant, K., Palmer, J., & Flint, S. (2026). Sequential attachment and *Listeria* predominance under turbulent flow. *Biofouling*, 1-16.

6.1 Introduction

One of the reasons for the persistence of pathogens such as *L. monocytogenes* on food processing surfaces has been attributed to the multispecies arrangement, particularly in the presence of high exopolysaccharide-producing spoilage bacteria such as *Pseudomonads* (Y. Wang et al., 2020). The affinity of *Listeria* to colonise preformed mature biofilms of *Pseudomonas* and dictate the interspecies interactions has been reported by several researchers (Puga et al., 2018; Rodríguez-López et al., 2022; Zhou, Liu, et al., 2024). When microbes attach to the surface first in multispecies arrangement as a primary coloniser, they impact and regulate the attachment and biofilm formation of secondary colonisers by the accumulation of exopolysaccharides (EPS), soluble microbial products (SMP) (Hwang et al., 2013), and cell extracts (total cell extract, cytoplasm with cellular debris, periplasmic extract) (Moreira et al., 2017). Bacterial attachment is the first stage of biofilm formation, with early colonisers influencing the overall interactions and ultimately the fate of the multispecies biofilm (Puga et al., 2016b).

The exopolysaccharides produced by the *Pseudomonas aeruginosa,* also defined as 'EPS footprints' after their resistant nature during cleaning and disinfection, can impact sequential bacterial attachment (Liu et al., 2007). Any positive or negative impact on subsequent attachment depends on the composition of the EPS produced by the primary attaching bacteria. For example, a matrix containing high concentrations of polysaccharides was found to increase the attachment of the free-floating bacteria through interactions between surface polymers on the bacteria and the polymers on the EPS on the surface (Hwang et al., 2012). The preconditioning matrix, which contained predominantly protein, was found to decrease the attachment of the bacteria owing to the repulsion between the proteins on the *P. aeruginosa* cell surface and the matrix composition on the surface (Hwang et al., 2012).

Another factor that affects bacterial attachment to the surface is hydrodynamic conditions. Research on the impact of turbulence using annular bioreactors shows that higher turbulent flow can result in the higher attachment and the subsequent formation of biofilms (Tsagkari & Sloan, 2018). The hydrodynamic conditions surrounding the attachment surface influence the transport rate of nutrients into the microcolonies and, subsequently, the mechanical stability of the biofilm (Simoes et al., 2005). The flow also impacts the structure of the biofilm, with

turbulent flow resulting in filamentous biofilm (streamers) (Stoodley et al., 1999) compared to static and non-turbulent flows. In terms of biofilm composition, biofilms formed under flow were found to have a lower thickness, with higher and more compact exopolysaccharides packed into the layers compared to biofilms formed in the absence of turbulent flow (Pereira et al., 2002). The flow had a significant impact on the architecture of the biofilm when the nutrient was limiting during the biofilm formation (≤100 mg glucose/L) (Pereira et al., 2002). The architecture of *P. fluorescens* can vary significantly under flow conditions as observed in different flow systems: flow cell reactor (Pereira et al., 2002) vs microfluidic system (Di Somma et al., 2020), which could impact the subsequently attaching bacteria. The colonisation of *L. monocytogenes* on preformed *P. fluorescens* in a bioreactor with continuous shaking (80 rpm) showed enhanced growth of *L. monocytogenes* and overproduction of exopolysaccharide by *Pseudomonas* (Puga et al., 2018). The biofilm matrix produced by the primary bacteria is bound to be an attachment site for free-floating bacteria (Toté et al., 2009). In addition to a preferable surface for attachment, the leftover matrix can also act as a source of nutrients for the incoming bacteria (Simoes et al., 2005).

As we step into multispecies studies, we must naturally consider a sequence of colonisation, since realistically, not all bacteria may attach at the same time, and some may serve as the foundation for the multispecies biofilm complex, allowing subsequent bacteria to attach. The literature on sequential multispecies biofilm focuses on the colonisation of *Pseudomonas* by *Listeria* on a glass surface under flow (Puga et al., 2016a). While the impact of surface conditioning by primarily attached *P. fluorescens* is clear, it does not delve further into whether it's the cells, the matrix composition, or the architecture of the biofilm that traps the *Listeria* cells into the *Pseudomonas* preformed biofilm. Additionally, the impact of flow on the migration of *Listeria* into deeper layers of *Pseudomonas* biofilm requires the observation of similar sequential biofilm under static conditions and on a more industrially relevant surface, such as stainless-steel. The extracellular matrix (ECM) has been noted to impact the sequential colonisation through the creation of a conditioning film via modification of the surface properties, such as hydrophobicity, surface charge, and roughness (Hwang et al., 2012). A significant research gap exists in how these modifications by the matrix can influence the subsequent attachment of other bacteria and the dynamics of multispecies biofilm formation. This study explores the different stages of biofilm formation (attachment, maturation, and detachment) and spatial arrangement of multispecies biofilm formed by *P. fluorescens* and *L. monocytogenes*, with a focus on sequential colonisation. The impact of the exopolysaccharide

(EPS) conditioning layer was analysed through a range of concentrations of exopolysaccharides (extracted from *P. fluorescens*), which were used as anchoring sites for *L. monocytogenes* attachment under turbulent flow and static environments.

6.2 Materials and methods

6.2.1 Bacteria and media

Pseudomonas fluorescens 2614 (P1) (dairy isolate) and *Listeria monocytogenes* H1 (LM1) (environment-soil isolate) were used for single and dual species biofilm formation, which are from a previously established culture collection (Food Microbiology Lab, School of Natural Sciences and Food Technology, Massey University, Palmerston North). The inoculum was prepared according to section 3.2.1. The final cell concentration was set at 8 $\log_{10}$ CFU/mL for inoculation in the bioreactor (Appendix VI). For dual species inoculation, each bacterium was adjusted to this cell concentration and added in a 1:1 concentration during inoculation.

6.2.2 Biofilm formation system

The static and continuous system were used to form biofilm under three conditions (Figure 6.1):

a) *Pseudomonas* preformed biofilm- *P. fluorescens* was allowed to form biofilm for 48 h before the introduction of *L. monocytogenes* into the system,

b) *Listeria* preformed biofilm- *L. monocytogenes* was allowed to form biofilm for 48 h before the introduction of *P. fluorescens* into the system, and

c) Co-inoculated biofilm where both *P. fluorescens* and *L. monocytogenes* were inoculated at the same time.

The time (48 h) was selected for preformed biofilm to allow for mature biofilm formation by the primary coloniser before the introduction of the secondary coloniser (Daneshvar Alavi & Truelstrup Hansen, 2013; Puga et al., 2016b).

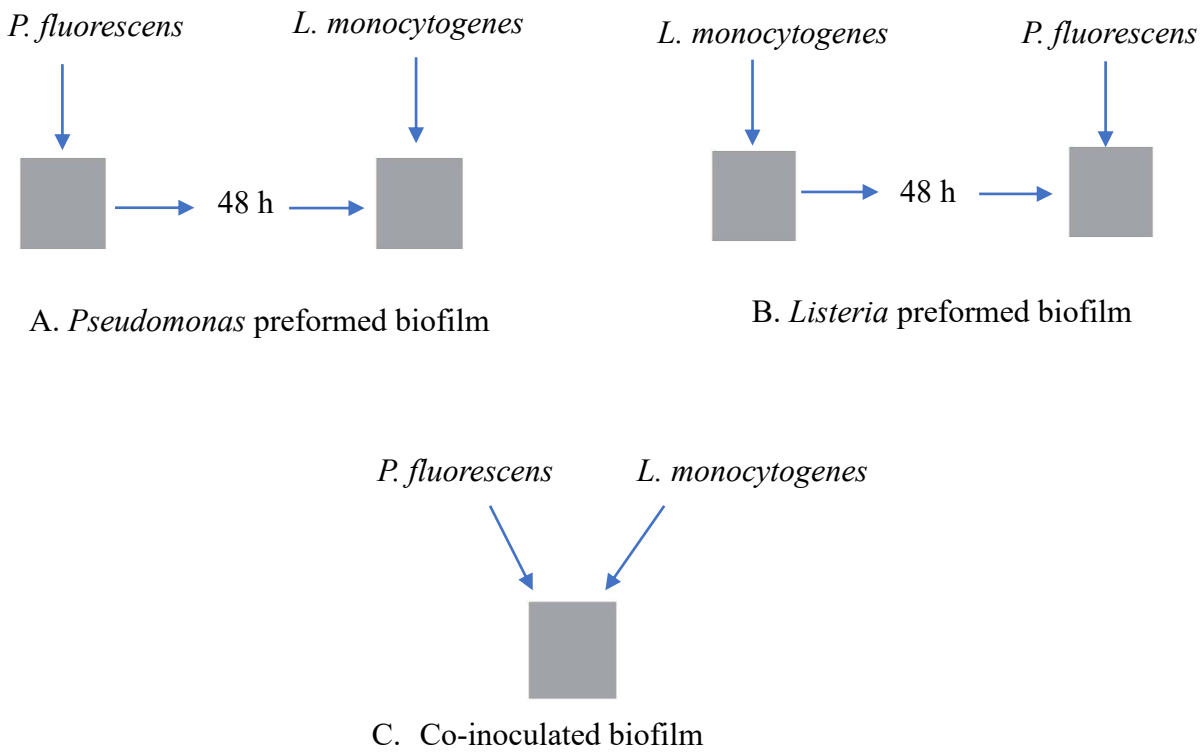

Figure 6.1 The conditions used for dual species biofilm formation in static and continuous system

A) Static system

i) Co-inoculation:

The dual species biofilm under static system was prepared as mentioned in section 4.2.2. Sterile and passivated stainless-steel coupons (2.4 cm^2) were placed vertically on the wells of a 48-well plate containing *P. fluorescens* and *L. monocytogenes* in cell concentrations (1:1) (6 log_{10} CFU/mL) in 10% TSB. The coupons containing wells were incubated for 7 days at 30°C with media refreshed every 24 h. After 30 min of attachment and every 24 h after that, triplicate coupons were used to enumerate cell concentrations in the biofilm using the glass bead beating assay and plating on selective agar according to section 4.2.5. *Pseudomonas* isolation agar was used for *P. fluorescens*, and Modified Oxford *Listeria* agar was used for *L. monocytogenes*.

ii) Sequential:

The sterile stainless-steel coupons (2.4 cm^2) were prepared under the same conditions as mentioned above in the co-inoculation section. The coupons were placed vertically in a 48-well plate with each well containing primary bacteria (*P. fluorescens* or *L. monocytogenes*) (6

$\log_{10}$ CFU/mL) in 10% TSB. The wells were incubated for 48 h at 30°C for mature biofilm formation by the foundation bacteria with media refreshed every 24 h. After 48 h, the coupons were washed with sterile saline solution (0.85%) and placed vertically into a new well containing the secondary coloniser (*P. fluorescens* or *L. monocytogenes*) (6 $\log_{10}$ CFU/mL) in 10% TSB at 30°C. The coupons were analysed for attachment (30 mins) and growth (every 24 h for the next 5 days) on preformed biofilm. The media (10% TSB) was refreshed every 24 h. The cell concentration was analysed using the glass bead beating method and selective agar plating as mentioned above in section 4.2.5.

For single species biofilm formation, coupons were inoculated into wells containing a single species of bacteria (*P. fluorescens* or *L. monocytogenes*) (6 $\log_{10}$ CFU/mL) and incubated for 7 days with media refresh every day. Like the dual species assay, the coupons were collected at 30 min to analyse the attachment on a clean, sterile surface and every 24 h to analyse the dynamics of biofilm formation. The cell concentration was analysed using the glass bead beating method and plated into tryptone soy agar (TSA) as mentioned in section 4.2.5.

B) Continuous system

The Centre for Disease Control (CDC) bioreactor was used to form biofilm under a continuous flow of media (10% TSB) and turbulent flow (Re>4000).

i) Co-inoculation

Both *P. fluorescens* and *L. monocytogenes* were co-inoculated at a cell concentration (1:1) (8 $\log_{10}$ CFU/mL) into the bioreactor (10% TSB) for co-inoculation. The incubation temperature (30°C) and the turbulence (Re>4000) were set using a hot plate magnetic stirrer. After 30 min of run-time, a rod (3 stainless-steel coupons) was removed (replaced with a blank rod) from the bioreactor to analyse attachment during co-inoculation. The cell concentration on the surface was enumerated post-washing with sterile saline solution (0.85%) using the glass bead beating method as mentioned in section 4.2.5. Additionally, the cell count was enumerated every 24 h for the next 7 days.

ii) Sequential:

Using the above CDC setup, mature biofilm (48 h) was formed for primary bacteria, i.e., for single species (*P. fluorescens* or *L. monocytogenes*) in bioreactor A at 30°C. After 48 h of biofilm formation, the rods were removed from the bioreactor A and washed with sterile saline solution (0.85%) to remove planktonic cells and introduced into the sterile bioreactor B with 10% TSB. The sterile bioreactor B was inoculated with the secondary coloniser (*P. fluorescens*

or *L. monocytogenes*) (8 $\log_{10}$ CFU/mL), and the system was run for the next 5 days at 30°C and at 250 rpm (Re > 4000) with a constant supply of fresh media (10% TSB). For the attachment assay, the system was run for 30 min after secondary inoculation and the rods were taken out to analyse the attachment of the secondary coloniser on preformed biofilm, and every 24 h for the next 5 days to analyse the dynamics of biofilm formation using glass bead beating and selective agar plating for the attachment assay as mentioned in section 4.2.5.

For single-species biofilm formation under flow, single species of *P. fluorescens* and *L. monocytogenes* were inoculated into each bioreactor, which was set up as above. The system was run for 7 days with a continuous supply of media (5 mL/min) and under high turbulence (Re>4000) at 30°C. Every 24 h, rods were removed from the bioreactor and replaced with a blank rod. The cell concentration in the biofilm was estimated using the glass bead beating method and plated on tryptone soy agar (TSA) as mentioned in section 4.2.5.

6.2.3 *Pseudomonas* preformed biofilm age and *L. monocytogenes* attachment

To further understand the improved attachment of *L. monocytogenes* on preformed *P. fluorescens* biofilm, *L. monocytogenes* was attached to *P. fluorescens* biofilm of different ages (24 h, 48 h, and 72 h). Single-species biofilm of *P. fluorescens* was formed under static and continuous systems, as explained in section 6.2.2 subsections A and B, respectively. Triplicate coupons (rods) of preformed *Pseudomonas* biofilm were removed from the system at 24 h, 48 h, and 72 h before saline washing and introduced into another system with *L. monocytogenes* inoculum (in 10% TSB). The attachment was allowed for 30 min/30°C under static conditions for preformed biofilm formed under the static system and under turbulent flow for preformed biofilm formed under turbulent conditions. The stainless-steel coupons were then saline washed before proceeding with glass bead beating and cell enumeration using selective agar as mentioned in section 4.2.5.

6.2.4 Extraction, freeze-drying, and quantification of exopolysaccharides

Microtiter plates (96-well plates) (Falcon, USA) were inoculated with *P. fluorescens* (6 $\log_{10}$ CFU/mL) in TSB. After 72 h incubation at 30°C, the media were removed, and the wells were washed with sterile distilled water. Sterile distilled water (100 µl) was added to each well, and the plate was sonicated (40 KHz) for 10 min (Zhou, Dong, et al., 2024). The collected extract was centrifuged at 12,000× g for 10 min, and the supernatant was collected for filtration (0.20

μm) to remove cells. Extracts were freeze-dried (Lab-Kits®, Hong Kong) before redissolving (sterile distilled water) to a range of concentrations for the *L. monocytogenes* attachment assay.

The exopolysaccharide (EPS) was quantified using the phenol sulphuric acid method (Zhou, Dong, et al., 2024) as mentioned in section 4.2.5. To 200 µl of rehydrated EPS solution, 100 µl of 6% phenol was added, immediately followed by 500 µl of 95% sulphuric acid. The reaction was allowed at room temperature for 20 min before the O.D. was analysed at 490 nm using a spectrophotometer. The exopolysaccharide content was determined using a dextran standard curve (Appendix VII).

6.2.5 Preparation of conditioned surfaces and attachment assays

For conditioned surface preparation, the sterile stainless-steel coupons were coated with different concentrations (0-27.5 µg/mL) of rehydrated EPS solution and allowed to air-dry. After the surfaces dried, they were introduced into the static and turbulent systems. Each system consisted of 10% TSB with a *L. monocytogenes* cell concentration of 6 $\log_{10}$ CFU/mL. The attachment assays were run for 30 min at 30°C. After the attachment assay, the coupons were washed with the saline solution to remove planktonic cells, and the adhered cells were enumerated using the glass bead beating method and plated on tryptone soy agar (TSA) according to section 4.2.5.

The adherence of rehydrated EPS on the stainless-steel surfaces was confirmed by staining with calcofluor white (a fluorescent dye that binds with cellulose and chitin to emit blue fluorescence). The coupons coated with rehydrated EPS (sample) and sterile distilled water (blank) were airdried before staining with calcofluor white stain (Fluka® calcofluor white stain, Sigma Aldrich, Canada) for 5 mins in the dark at room temperature. The coupons were washed and air-dried before observation with an epifluorescence microscope with a DAPI filter (Excitation 340-360 nm and Emission 410 nm) (Appendix VIII).

6.2.6 Spatial arrangements via confocal microscopy

The samples collected from section 6.2.2 (static-co, static-P1 pre, static-LM1 pre, continuous-co, continuous-P1 pre, and static-LM1 pre) on their fifth day of incubation were washed with phosphate buffer saline (PBS) and air-dried before staining with wheat germ agglutinin (WGA)-Texas red conjugate (1 mg/mL) and counterstaining with DAPI (1 mg/mL) (Rodríguez-Melcón, Alonso-Hernando, et al., 2021). WGA-Texas red (6 µL) and 6 µL of DAPI

were mixed with 6 mL of TSB and used to stain the coupons at room temperature in the dark for 50 min. After staining, the coupons were washed with PBS and allowed to air-dry before imaging through confocal microscopy (Nikon D-eclipse C1, Japan) (10X) and EZ-C1 software (Gold version 3.80 build 860) for image acquisition.

6.2.7 Statistical analysis

The significant differences between the samples were analysed using one-way ANOVA (IBM SPSS Statistics 29) and post-hoc analysis using Tukey's test. The results were represented as mean ± S.D. The images acquired from the confocal microscope were analysed using ImageJ (ImageJ 1.54g, National Institute of Health, USA). Biological replicates and technical triplicates were repeated for each analysis.

6.3 Results

6.3.1 Sequential biofilm formation under flow

Attachment: The attachment of *L. monocytogenes* on a 48-h preformed *Pseudomonas* biofilm was significantly higher ($p<0.001$) (5.0 $\log_{10}$ CFU/cm^2) (Figure 6.2) compared to its attachment on the sterile stainless-steel surface (4.0 $\log_{10}$ CFU/cm^2), and in co-inoculation (2.57 $\log_{10}$ CFU/cm^2) (with *P. fluorescens*) (Figure 6.4). In contrast, the attachment of *P. fluorescens* on preformed *Listeria* biofilm (2.32 $\log_{10}$ CFU/cm^2) (Figure 6.3) was comparable with attachment in co-inoculation (2.47 $\log_{10}$ CFU/cm^2) with *L. monocytogenes* (Figure 6.4). The attachment of *P. fluorescens* on sterile stainless-steel surfaces in single species was higher compared to other conditions at 4.0 $\log_{10}$ CFU/cm^2.

Maturation: *L. monocytogenes* reached its plateau (8.9 $\log_{10}$ CFU/cm^2) earlier (Day 1 of co-growth) when inoculated onto the *Pseudomonas* preformed biofilm surface (Figure 6.2) compared with co-inoculation mixed species (8.8 $\log_{10}$ CFU/cm^2 on Day 3) (Figure 6.4), and when *L. monocytogenes* was the primary attached bacteria (9.0 $\log_{10}$ CFU/cm^2 on Day 3 of co-growth) (Figure 6.3). *P. fluorescens* did not show preferential growth in any conditions of biofilm formation and reached its plateau 7.5 $\log_{10}$ CFU/cm^2 on Day 3 in co-inoculation (Figure

6.4), 8.0 $\log_{10}$ CFU/cm^2 on Day 2 when *Pseudomonas* was pre-formed (Figure 6.2), and 7.8 $\log_{10}$ CFU/cm^2 on Day 3 when it was inoculated into preformed *Listeria* biofilm (Figure 6.3).

Detachment: A periodic dispersal of cells was observed in dual-species biofilm formed under both co-inoculated (Figure 6.4) and pre-formed biofilm (Figures 6.2 and 6.3) after Day 3 of co-growth. In co-inoculated dual species, the sloughing was observed for both bacteria, i.e, after Day 3, the cell concentration of both *P. fluorescens* and *L. monocytogenes* increased and decreased in parallel, showing a wave-like pattern of periodic cell dispersal (Figure 6.4). Similarly, when *Listeria* was inoculated in a pre-formed *Pseudomonas* biofilm, the detachment pattern showed a slow decline in cell concentration for both bacteria after Day 3 of co-growth (Figure 6.2). In contrast, where *Listeria* was preformed, only *Pseudomonas* showed the wave-like oscillation in cell concentration, while *Listeria* cell concentration remained consistent (8.6-9 $\log_{10}$ CFU/cm^2) throughout the incubation period (Figure 6.3).

In the single-species biofilm formed under flow, the shedding patterns were not observed, with the cell concentrations ranging between 6.3 (Day 1) - 7.1 (Day 7) $\log_{10}$ CFU/cm^2 for *P. fluorescens* and 4.7 (Day 1) – 6.3 (Day 7) $\log_{10}$ CFU/cm^2 for *L. monocytogenes*, respectively. There was no significant reduction ($p<0.001$) in cell concentration during the 7-day biofilm formation under flow.

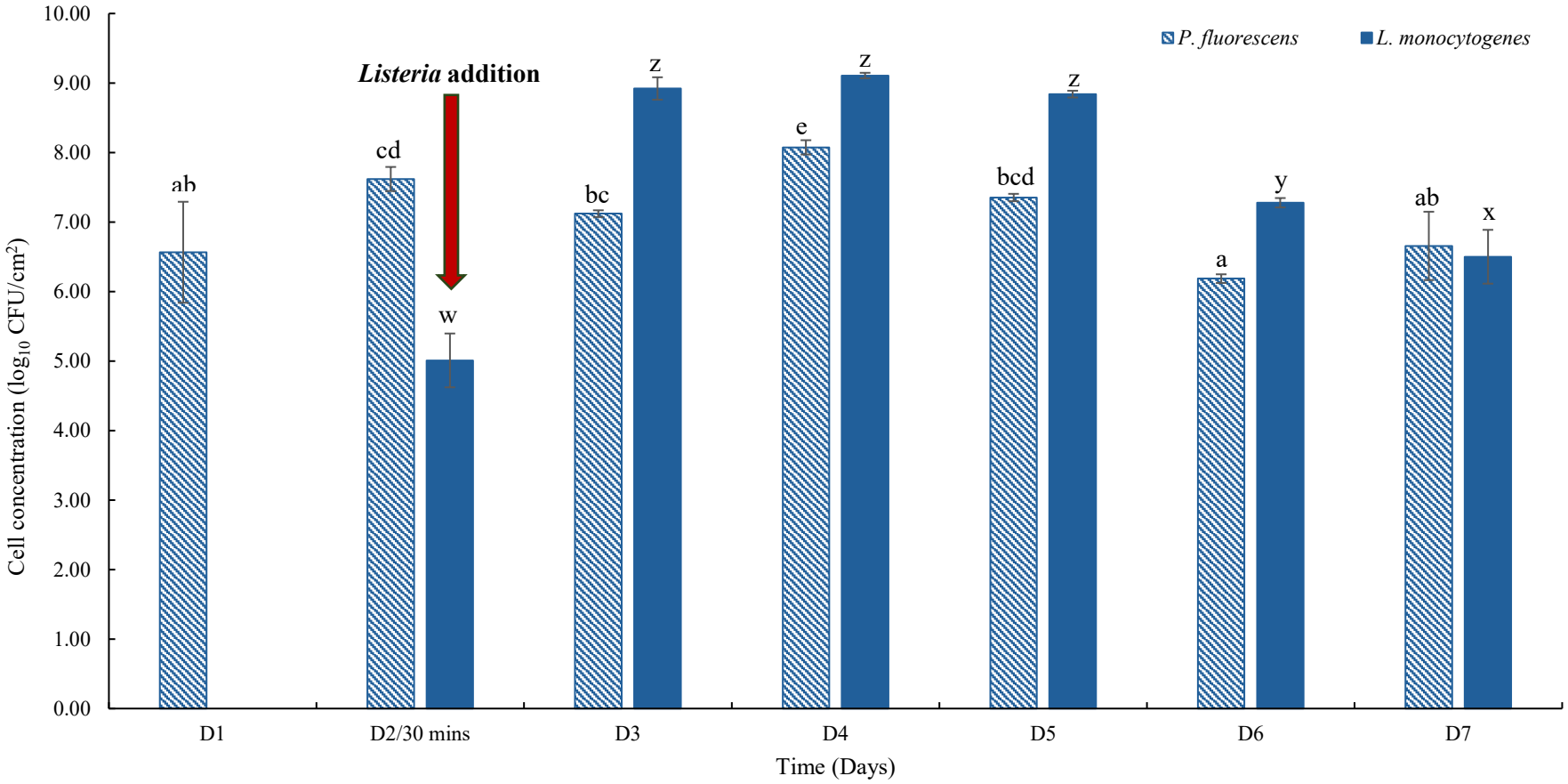

Figure 6.2 The cell concentrations (log_{10} CFU/cm^2) of *P. fluorescens* (P1) and *L. monocytogenes* (LM1) in sequentially formed dual species biofilm under turbulent flow during a 7-day incubation period. The red arrow represents the inoculation of *L. monocytogenes* in *P. fluorescens* 48 h mature biofilm. Note: The superscripts (a-e) and (w-z) indicate the significant differences between cell concentrations during the 7-day incubation period for *P. fluorescens* and *L. monocytogenes*, respectively.

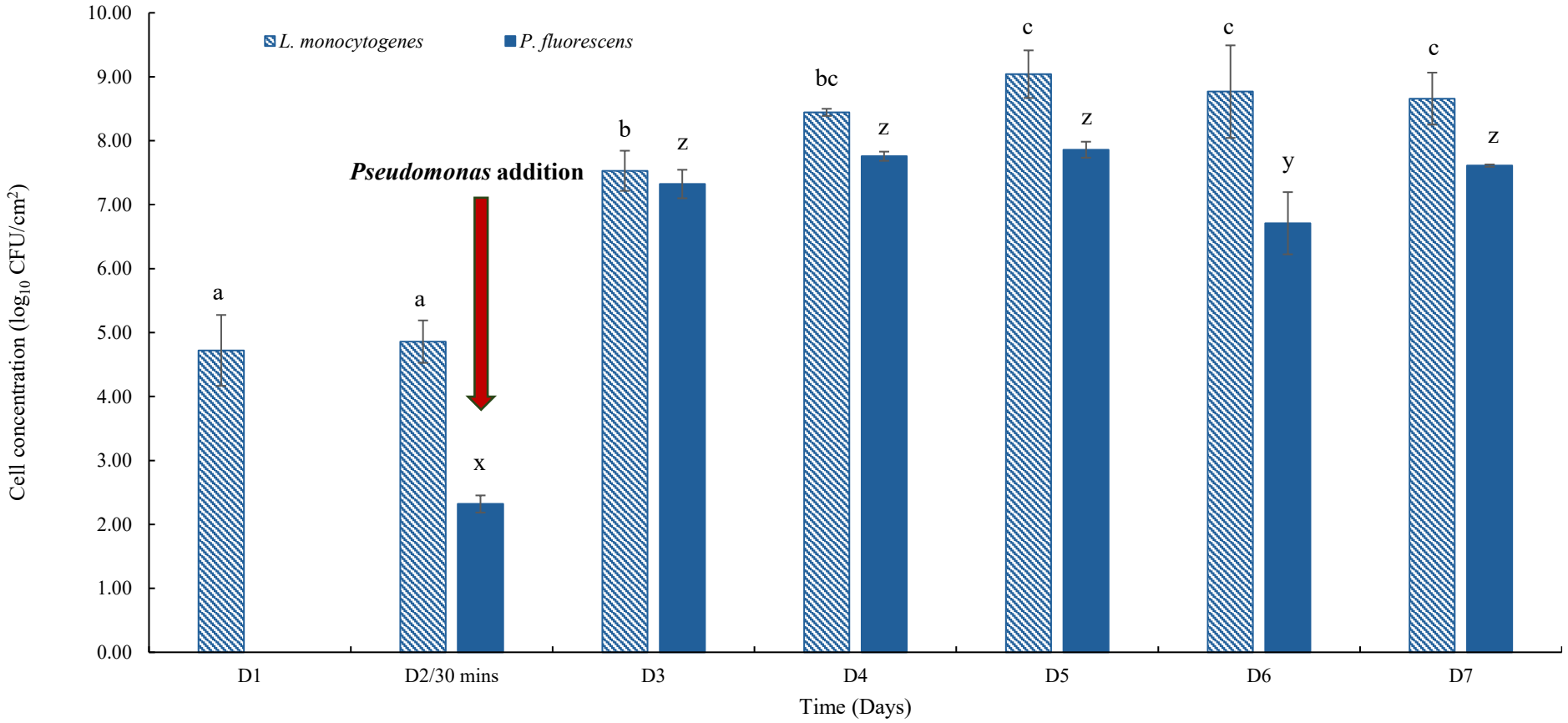

Figure 6.3 The cell concentrations (log_{10} CFU/cm^2) of *L. monocytogenes* (LM1) and *P. fluorescens* (P1) in sequentially formed dual species biofilm under turbulent flow during a 7-day incubation period. The red arrow indicates the inoculation of *P. fluorescens* into the *L. monocytogenes* 48 h biofilm. Note: The superscripts (a-c) and (x-z) indicate the significant differences between cell concentrations during the 7-day incubation period for *L. monocytogenes* and *P. fluorescens*, respectively.

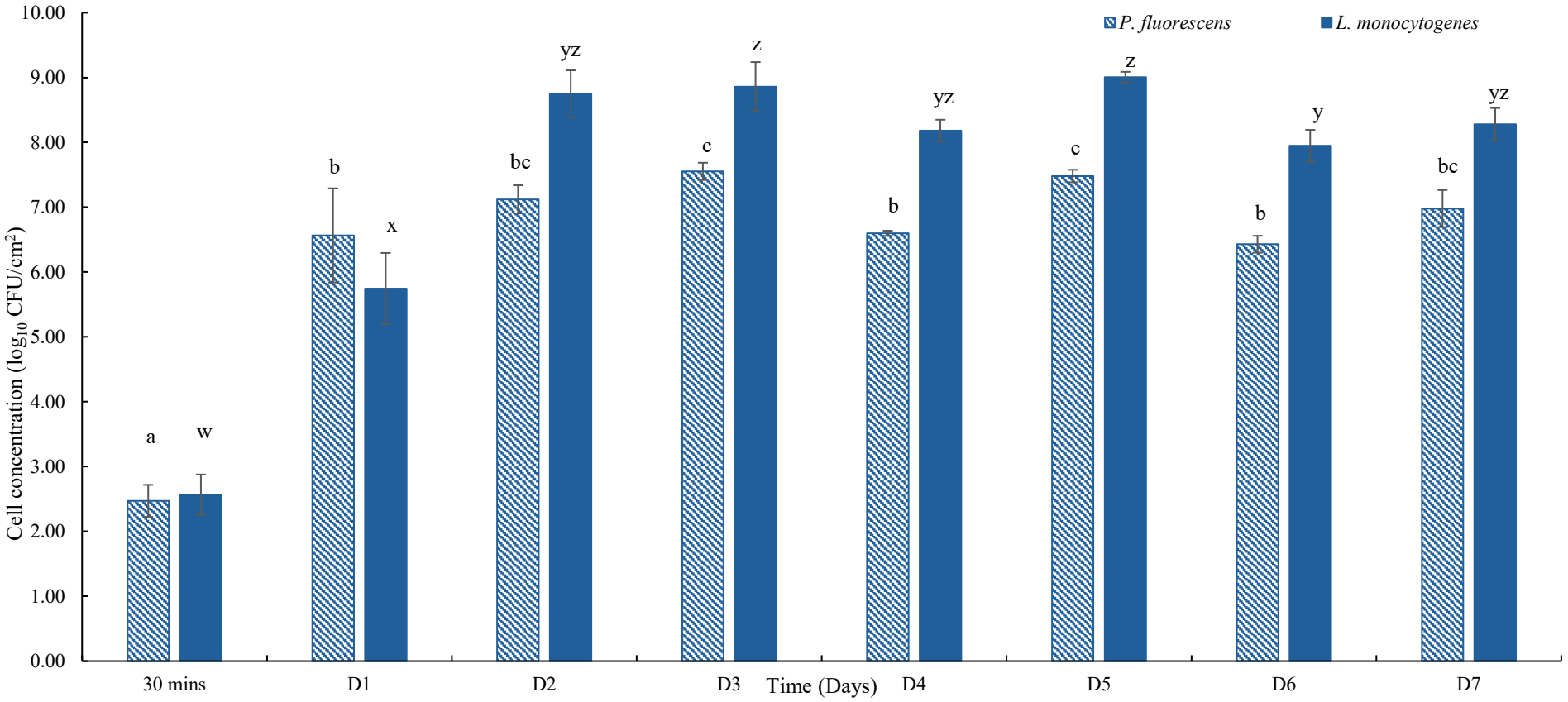

Figure 6.4 The cell concentrations (log_{10} CFU/cm^2) of *P. fluorescens* (P1) and *L. monocytogenes* (LM1) in co-inoculated dual species biofilm during a 7-day incubation period under turbulent flow. Note: The superscripts (a-c) and (w-z) indicate the significant differences between cell concentrations during the 7-day incubation period for *P. fluorescens* and *L. monocytogenes*, respectively.

6.3.2 Sequential biofilm formation under static conditions

Attachment: Under static conditions, the attachment of *L. monocytogenes* was not affected by the presence of preformed *Pseudomonas* biofilm on the surface. In the co-inoculated system, the *L. monocytogenes* attachment was 3.6 $\log_{10}$ CFU/cm^2 (Figure 6.7), which was comparable with *L. monocytogenes* attachment on preformed *Pseudomonas* biofilm (4.3 $\log_{10}$ CFU/cm^2) (Figure 6.5) and in single species (3.6 $\log_{10}$ CFU/cm^2). The attachment of *P. fluorescens* was lower on *Listeria* pre-formed biofilm (3.3 $\log_{10}$ CFU/cm^2) (Figure 6.6) compared to the co-inoculated (4.2 $\log_{10}$ CFU/cm^2) (Figure 6.7) and in single species (4.0 $\log_{10}$ CFU/cm^2).

Maturation: In all three conditions/sequences of biofilm formation, *P. fluorescens* predominated the dual species biofilm formed under static conditions. *P. fluorescens* reached its plateau on Day 2 of co-growth with the cell concentration of 7.5 $\log_{10}$ CFU/cm^2 in *Pseudomonas* preformed (Figure 6.5), 7.1 $\log_{10}$ CFU/cm^2 in *Listeria* preformed (Figure 6.6), and 6.8 $\log_{10}$ CFU/cm^2 in co-inoculation (Figure 6.7), indicating no significant ($p<0.05$) impact of *L. monocytogenes* being introduced at any point in dual species biofilm. Similarly, the cell concentration of *L. monocytogenes* reached its maximum cell concentration on Day 1 of co-growth for all three conditions, ranging between 5.6 and 6.3 $\log_{10}$ CFU/cm^2. In all three attachment conditions, the cell concentration of *L. monocytogenes* reduced after the first 24 h of co-growth (Figures 6.5, 6.6, and 6.7).

Detachment: A 'smothering' effect of *P. fluorescens* on *L. monocytogenes* was observed for the dual species biofilm when *L. monocytogenes* was the primary attaching bacteria, with cell concentration of *L. monocytogenes* reducing to 2.3 $\log_{10}$ CFU/cm^2 (Day 5) from 6.3 $\log_{10}$ CFU/cm^2 (Day 1) (Figure 6.6). Under similar growth conditions (3 days of co-growth), the cell concentration of *L. monocytogenes* in *Pseudomonas* preformed biofilm (3.2 $\log_{10}$ CFU/cm^2) (Figure 6.5) was comparable with co-inoculated dual species biofilm (3.4 $\log_{10}$ CFU/cm^2) (Figure 6.7). A periodic oscillation of cell concentration was observed for *P. fluorescens* during co-growth but was only limited to co-inoculated (Figure 6.7) and *Pseudomonas* preformed conditions (Figure 6.5).

In single-species biofilm formed under static conditions, the cell concentration of single-species biofilm formed by *P. fluorescens* and *L. monocytogenes* was in the range 6.9-7.5 $\log_{10}$ CFU/cm^2 and 6.4-7.3 $\log_{10}$ CFU/cm^2, respectively, during the first 5 days of biofilm formation.

On the 6th day, shedding was observed for both bacteria, where the cell concentration reduced to 5.3 $\log_{10}$ CFU/cm^2 for *P. fluorescens* and 3.8 $\log_{10}$ CFU/cm^2 for *L. monocytogenes*.

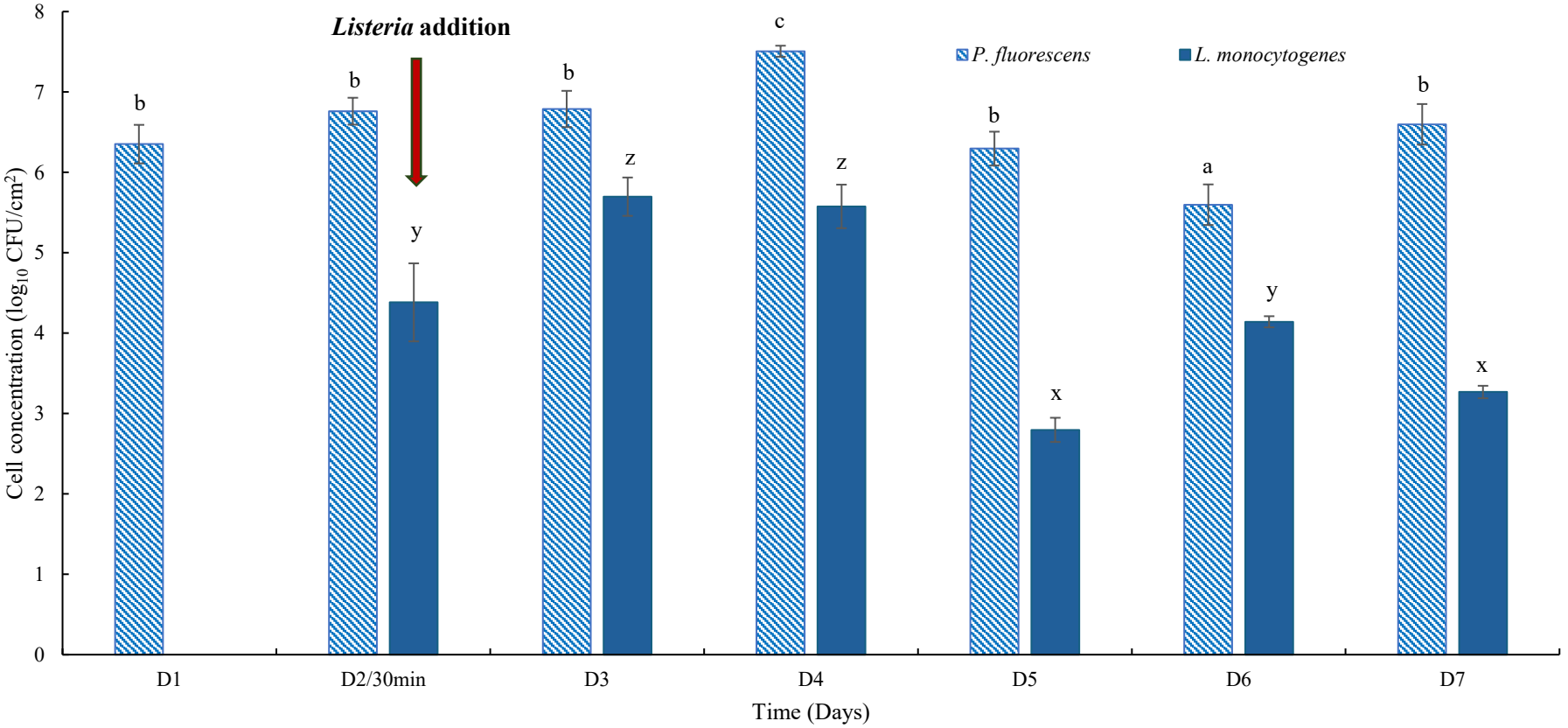

Figure 6.5 The cell concentrations (log_{10} CFU/cm^2) of *P. fluorescens* (P1) and *L. monocytogenes* (LM1) in sequentially formed dual species biofilm under static conditions during a 7-day incubation period. The red arrow represents the inoculation of *L. monocytogenes* in *P. fluorescens* 48h mature biofilm. Note: The superscripts (a-c) and (x-z) indicate the significant differences between cell concentrations during the 7-day incubation period for *P. fluorescens* and *L. monocytogenes,* respectively.

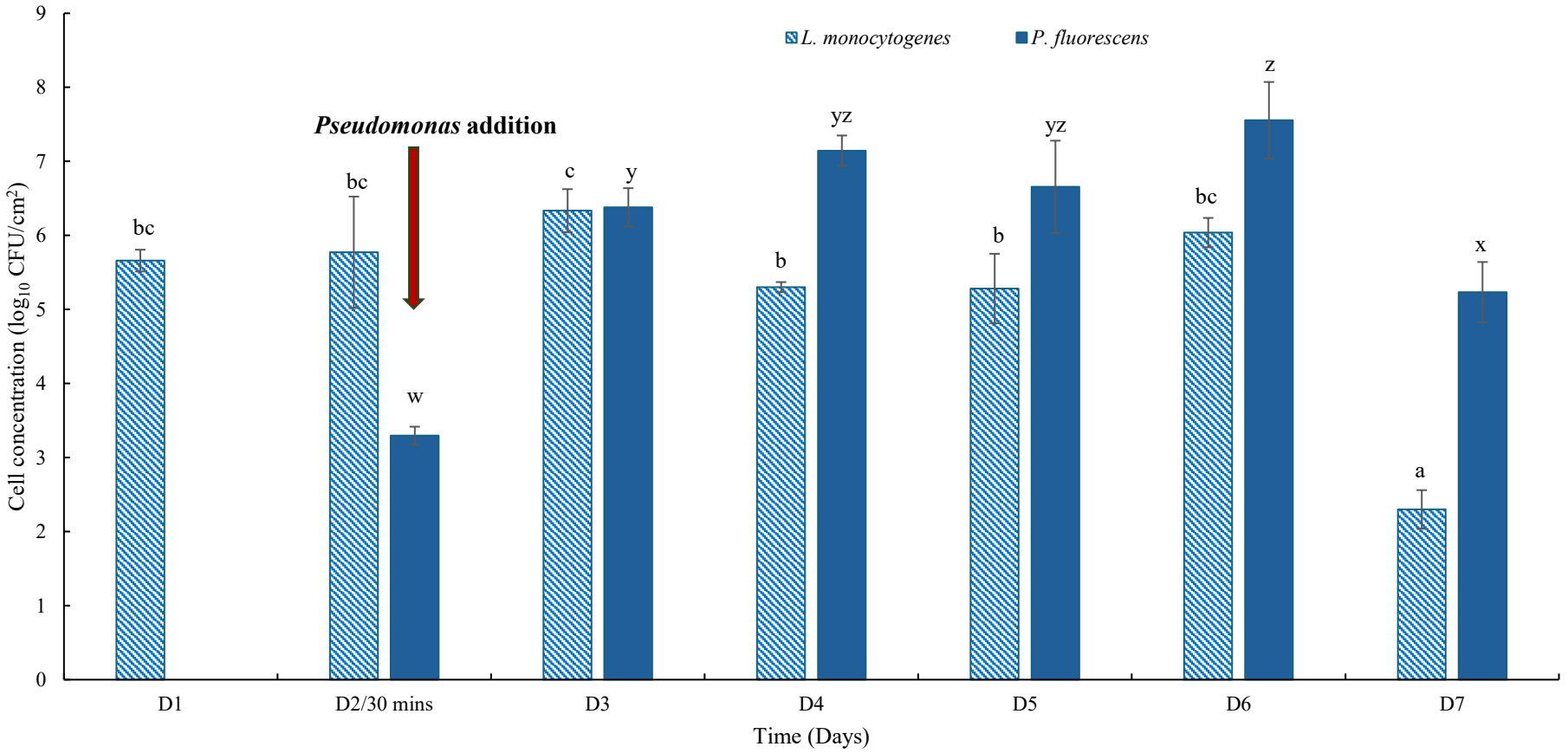

Figure 6.6 The cell concentrations (log_{10} CFU/cm^2) of *L. monocytogenes* (LM1) and *P. fluorescens* (P1) in sequentially formed dual species biofilm under static conditions during a 7-day incubation period. The red arrow represents the inoculation of *P. fluorescens* in *L. monocytogenes* 48h biofilm. Note: The superscripts (a-c) and (w-z) indicate the significant differences between cell concentrations during the 7-day incubation period for *L. monocytogenes* and *P. fluorescens*, respectively.

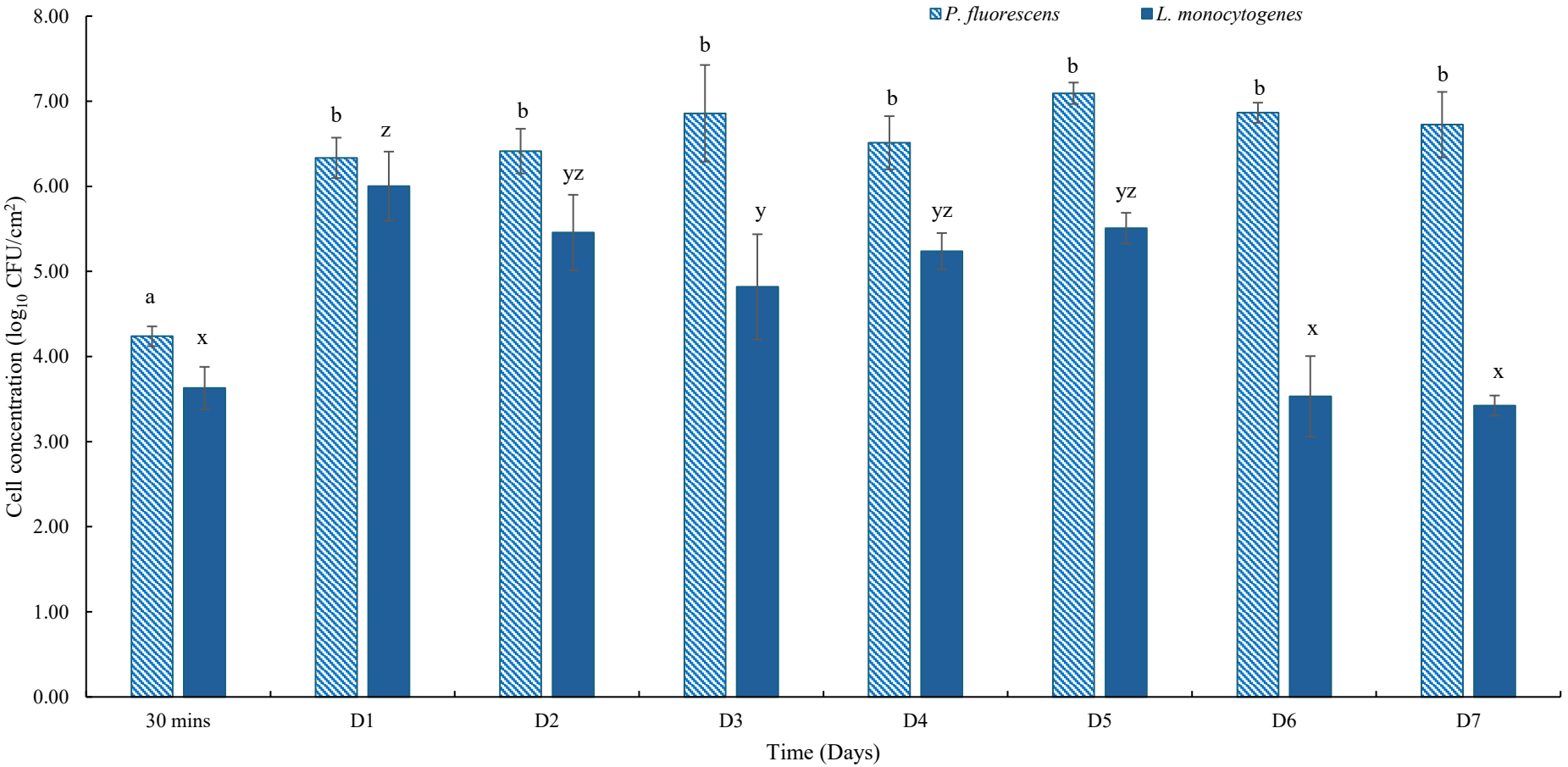

Figure 6.7 The cell concentrations (log_{10} CFU/cm^2) of *P. fluorescens* (P1) and *L. monocytogenes* (LM1) in co-inoculated dual species biofilm during a 7-day incubation period under static conditions. Note: The superscripts (a, b) and (x-z) indicate the significant differences between cell concentrations during the 7-day incubation period for *P. fluorescens* and *L. monocytogenes,* respectively.

6.3.3 Attachment on *Pseudomonas* biofilm and EPS conditioned surfaces

A linear increase (R^2=0.98) ($p<0.05$) in the attachment of *L. monocytogenes* with increasing age of *Pseudomonas* biofilm up to 72 h was observed. The attachment of *L. monocytogenes* on 24 h, 48 h, and 72 h preformed biofilm under turbulent flow was 3.9, 4.6, and 4.9 $\log_{10}$ CFU/cm^2 respectively. The cell concentration of *P. fluorescens* during this attachment for 24 h, 48 h, and 72 h was 6.3, 7.5, and 7.8 $\log_{10}$ CFU/$cm^{2,}$ respectively. In contrast, the *P. fluorescens* biofilm formed under static conditions did not impact the attachment of *L. monocytogenes,* with 5, 4.5, and 4.6 $\log_{10}$ CFU/cm^2 attachment for 24 h, 48 h, and 72 h, respectively, where the cell concentration of *P. fluorescens* ranged from 6.8-7.1 $\log_{10}$ CFU/cm^2. To understand if the increasing exopolysaccharide concentration in the biofilm formed by the primary coloniser under flow is impacting the attachment of the secondary coloniser, attachment of *L. monocytogenes* on surfaces conditioned with different concentrations of EPS was estimated.

The concentration of EPS deposited on the surface for conditioning the stainless-steel surfaces had no significant ($p>0.05$) effect on *L. monocytogenes* attachment (30 min), under both static and turbulent flow conditions. Compared to the turbulent flow system (3.7-4.2 $\log_{10}$ CFU/cm^2), the static system showed significantly higher attachment (30 mins) ($p<0.001$) (4.8-5.1 $\log_{10}$ CFU/cm^2) at all EPS concentrations (0-27.5 µg/mL) (Figure 6.8).

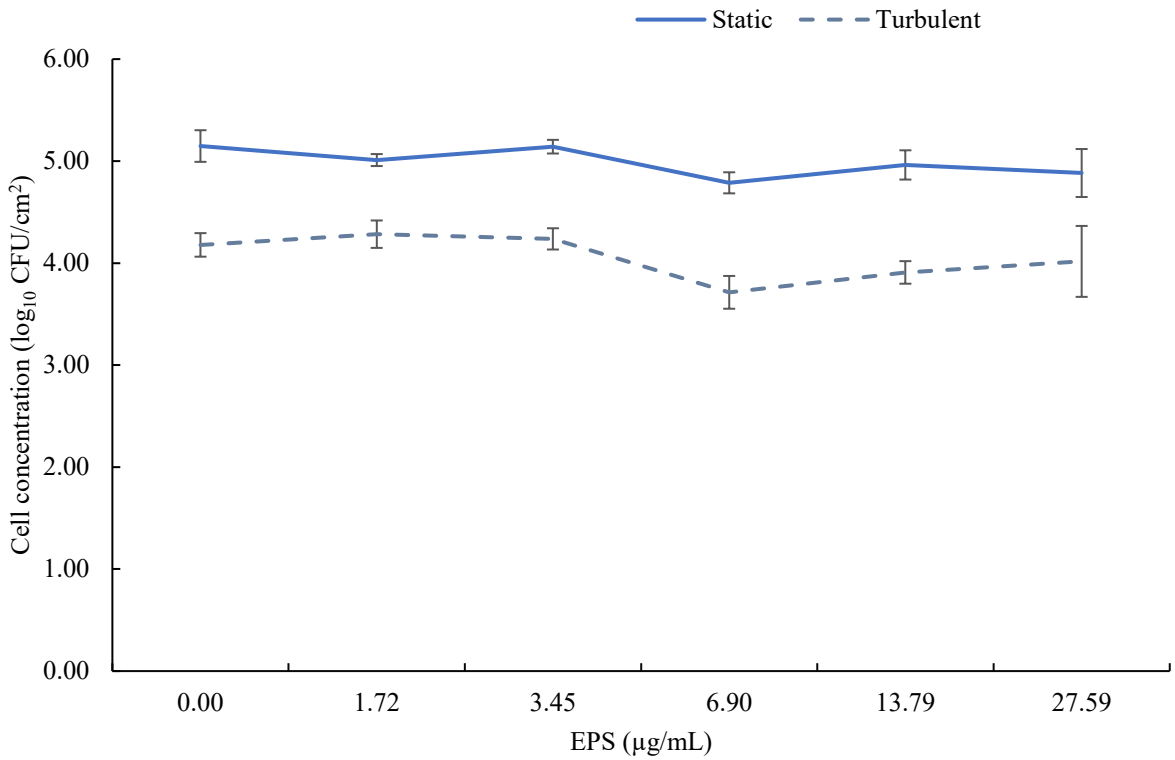

Figure 6.8 The attachment of *L. monocytogenes* (log_{10} CFU/cm^2) to exopolysaccharide (EPS) conditioned stainless-steel surfaces in the range (0-27.59 µg/cm^2) under static and turbulent conditions.

6.3.4 Spatial arrangement of the biofilm in co-inoculated and preformed biofilm

For all three conditions of biofilm formed under turbulent flow, the arrangement of *L. monocytogenes* (red) and *P. fluorescens* (blue) was found to be similar, with *L. monocytogenes* predominating in the biofilm, indicating that these bacteria can rearrange themselves under turbulent flow despite the sequence of attachment (Figure 6.9). This correlated with the higher concentration of *L. monocytogenes* compared to *P. fluorescens* under all three sequence conditions (Figures 6.2, 6.3, and 6.4) under turbulent flow. Visually, the predominance of *L. monocytogenes* (red) does not appear evenly throughout the surfaces (Figure 6.9.A and 6.9.C). The predominance of *L. monocytogenes* in cell counts (Figures 6.2, 6.3, and 6.4) indicates that, in addition to the top layer of the biofilm, *L. monocytogenes* could be localised within the *P. fluorescens* layers. The circular patterns in all three conditions for biofilm formed under flow (Figure 6.9) show the topography of the stainless-steel coupons.

In contrast, visual differences were observed for the dual-species biofilm formed under static conditions, depending on the order of inoculation onto the biofilm. For the condition where *L. monocytogenes* was introduced to *Pseudomonas* preformed biofilm, the *L. monocytogenes* was observed on the top layer (red) (Figure 6.10.B) (3.2 $\log_{10}$ CFU/cm^2) compared to *Listeria* preformed (Figure 6.10.C) (2.3 $\log_{10}$ CFU/cm^2) and co-inoculated (Figure 6.10.A) (3.4 $\log_{10}$ CFU/cm^2) conditions. The decreased concentration of red areas under *Listeria*-preformed conditions (Figure 6.10.C) correlated with the smothering (reduced cell concentration) of *L. monocytogenes* cells in the dual-species biofilm formed under the same conditions (Figure 6.6).

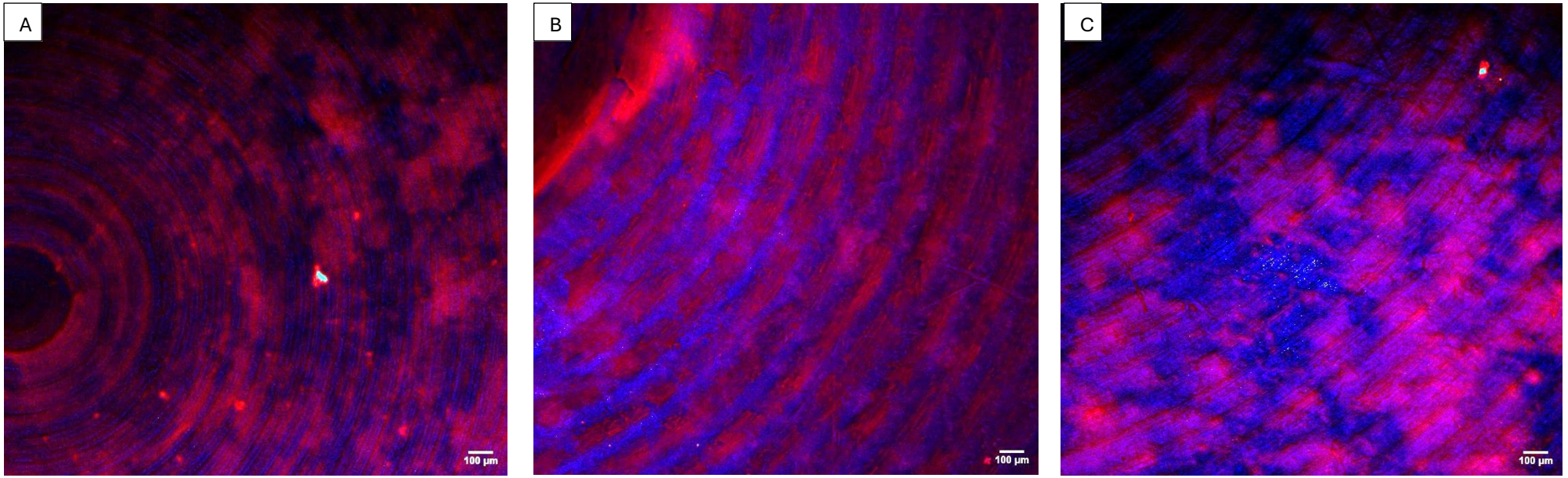

Figure 6.9 The images represent dual-species biofilm formed under turbulent flow in A) Co-inoculation, B) P1 (preformed biofilm) + LM1, and C) LM1 (preformed biofilm) + P1. The red represents *L. monocytogenes* stained with WGA-Texas red conjugate, and the blue represents *P. fluorescens* stained with DAPI. The scale bar represents 100 µm.

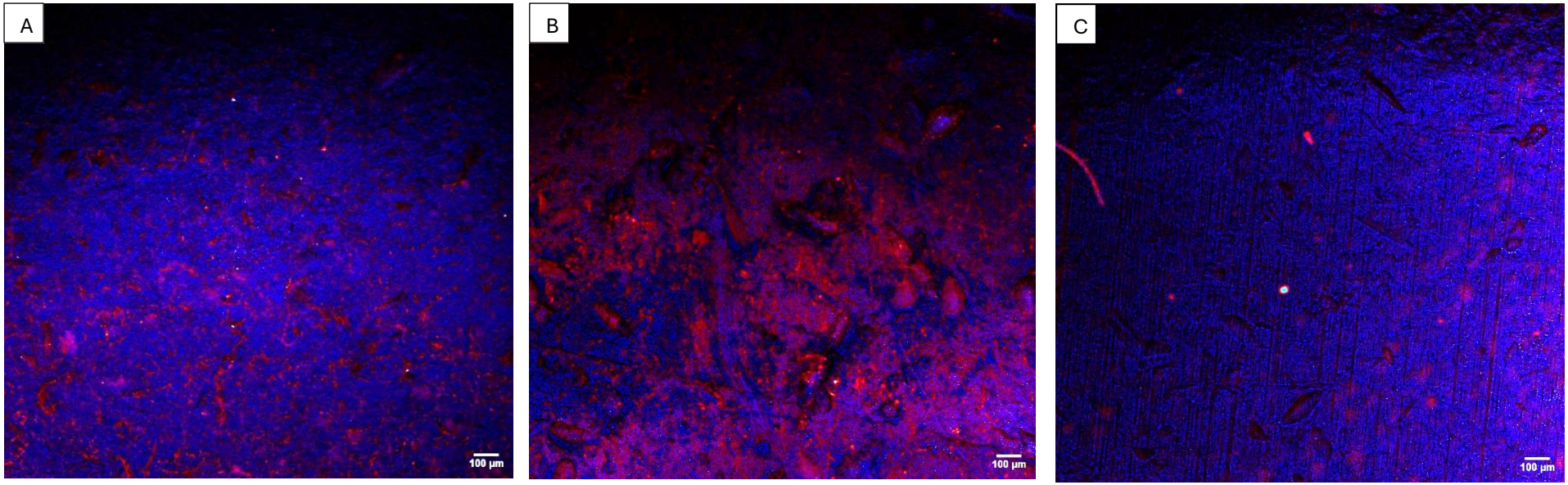

Figure 6.10 The images represent dual-species biofilm formed under static conditions in A) Co-inoculation, B) P1 (preformed biofilm) + LM1, and C) LM1 (preformed biofilm) + P1. The red represents *L. monocytogenes* stained with WGA-Texas red conjugate, and the blue represents *P. fluorescens* stained with DAPI. The scale bar represents 100 µm.

6.4 Discussion

In sequential biofilm formation, *L. monocytogenes* attachment was significantly higher ($p<0.001$) on the preformed *Pseudomonas* biofilm formed under flow (Figure 6.2) compared with attachment during co-inoculation (Figure 6.4) and in single species. In contrast, the presence of preformed *Listeria* biofilm lowered the attachment of *P. fluorescens* (Figure 6.3). Various studies discuss the possibility of enhanced interaction of bacteria in the bulk liquid with the top layer when the *Pseudomonas* biofilm is already present on the surface. Sasahara & Zottola, (1993) observed that *L. monocytogenes* showed enhanced attachment to glass surfaces in the presence of higher EPS producing bacteria such as *P. fragi*. The *L. monocytogenes* cells were observed to have preferential adherence around microcolonies of *P. fragi*, indicating attachment and entrapment of the *L. monocytogenes* cells to the EPS produced by *P. fragi* (Sasahara & Zottola, 1993). Additionally, the attachment of the second bacteria on the surface of the biofilm formed by the primary bacteria can also be influenced by the surface roughness and the structure of the biofilm formed by the primary attaching bacteria (Silva et al., 2024). An EPS producer that forms small aggregates with greater coverage on the surface has a population fitness advantage over late colonisers in a multispecies arrangement. Whereas the formation of larger aggregates by primary bacteria requiring higher energy expenditure on EPS production might result in the predominance of late-arriving colonisers (Jayathilake et al., 2017).

The bacterial attachment under different flow conditions depends on mass transport (sedimentation or diffusion), flow velocity, and topography (roughness) (Chinnaraj et al., 2021; Kreve & Dos Reis, 2021). The 'sedimentation effect' has been reported to impact the attachment of bacteria under static and even low-flow conditions, which might explain the attachment differences observed under flow (Figures 6.2 and 6.3) and static conditions (Figures 6.5 and 6.6) in this study. The microbes interact and settle into these surfaces using appendages (pili, flagella, curli, and fimbriae), forces (van der Waal forces for attraction, electrostatic charges for repulsion), acid-base interactions, and/or through adhesion proteins (Gordon & Wang, 2019). The surface proteins, such as chaperonin, porin, and elongation Tu factors, are affected during the attachment under high shear for bacteria such as *P. aeruginosa* (Hui et al., 2016). The attachment under turbulent flow is also challenged by the reversibility of unsteady bacterial attachment, reduced boundary layer and contact time, and the impact of shear (J. Wang et al., 2020). In a similar study, the attachment of *Sphingomonas rubra*, *Nakamurella*

multipartita, and mixed bacteria was significantly lowered by the presence of shear (100 and 150 rpm) compared to static and low shear (0 and 50 rpm) conditions (J. Wang et al., 2020). After the initial adhesion, motile bacteria can burrow under the mature preformed biofilm through the voids and channels (Houry et al., 2012) formed by the primary bacteria, leading to a stable mixed species biofilm.

Despite having an ecological disadvantage (cell numbers and space), not only is *L. monocytogenes* able to attach itself to the surface, but it also outcompetes the primary bacteria (*P. fluorescens*) (Figure 6.3) under turbulent flow. This observation was found to be specific to biofilm formed under flow. In static conditions, while *L. monocytogenes* can form a biofilm as a secondary coloniser, it cannot outcompete the primary biofilm former (*P. fluorescens*) (Figure 6.5). In addition to architectural protection from the stress, *L. monocytogenes* in dual species also benefits from access to higher nutrients because of the continuous flow of nutrients in the continuous system. The enhanced biofilm formation under the continuous supply of media in a single-species biofilm was observed in the previous chapter (Section 5.3.6). Similar observations of *L. monocytogenes* biofilm formation on multispecies preformed biofilm (*Pseudomonas* predominating) have been observed in a model mimicking a salmon processing surface (Langsrud et al., 2016) under static conditions. In a study by Hascoët et al., (2021), the cell concentration of *L. monocytogenes* was found to be unaffected by the individual preformed biofilm (1 week) of *C. zeylanoides*, *P. luteola*, and *P. fluorescens*, compared to the control (clean surface). In contrast, with shear stress (80 rpm), *L. monocytogenes* were able to modify the structure of the preformed *P. fluorescens* biofilm, resulting in overproduction of exopolysaccharides (Puga et al., 2018) and further protecting from desiccation and disinfection (Pang & Yuk, 2019). Microscopic observations show that *L. monocytogenes* embeds itself into the lower levels of the dual-species biofilm, resulting in added protection against stressors and higher cell concentration (1-2 $\log_{10}$ CFU/cm^2) compared to single-species *L. monocytogenes* biofilm (Puga et al., 2016b). A sequential study on four biofilm-forming bacteria (*Stenotrophomonas rhizophila*, *Xanthomonas retroflexus*, *Microbacterium oxydans*, and *Paenibacillus amylolyticus*) formed in a drip flow reactor (DFR) showed that the prior attachment of a good biofilm former results in a population advantage during sequential attachment (Olsen et al., 2019). Overall, the EPS producing primary coloniser usually has a competitive advantage in the mixed species biofilm (Jayathilake et al., 2017), but the observations varied when shear is present, as noted above.

Despite a spike in the cell concentration of the subsequent coloniser (*L. monocytogenes*), the cell concentration of the resident bacteria (*P. fluorescens*) remained unaffected (Figure 6.2), which could be a result of the synergistic interactions also observed during co-inoculated mixed-species biofilm formation (Figure 6.4). In a mixed-species biofilm consisting of *Pseudomonas* and *Listeria*, the *Pseudomonas* were observed to migrate to the top of the biofilm (Silva et al., 2024), resulting in overproduction of EPS and predominance in cell numbers (Puga et al., 2018; Xavier & Foster, 2007). These observations have been made for mixed-species biofilm, which also explains the sanitizer tolerance and the protection conferred by *Pseudomonas* (Puga et al., 2018).

In this study, the cell concentration of *L. monocytogenes* reached 9 $\log_{10}$ CFU/cm^2 in mixed-species biofilm in all three conditions of sequential attachment (Figures 6.2, 6.3, and 6.4), which is significantly higher ($p<0.001$) compared to *L. monocytogenes* in single species biofilm (6.5 $\log_{10}$ CFU/cm^2) under flow. The following hypotheses may be suggested to explain the rapid increase in cell concentration of *L. monocytogenes* in multispecies under flow. Biofilm formed under low shear stress has a relatively patchy biofilm formation on the surface, whereas the turbulent flow allows the formation of complex structures (filamentous streamers/interstitial voids) (Stoodley et al., 1999). These complex structures could facilitate the entrapment of secondary bacteria and promote better proliferation during longer incubation times and under stressful conditions. In single species, over time, *Listeria* biofilm sheds its cells, revealing the oscillation dynamics of biofilm, but in the presence of *Pseudomonas*, the cells are retained in the EPS matrix, resulting in significantly higher cell concentrations in dual-species compared with a single-species biofilm (Puga et al., 2018). Flow also helps to transport the nutrients into and remove the waste metabolites from the deeper parts of the biofilm and enhances the proliferation of the bacteria in the layers within the biofilm, resulting in a higher cell concentration compared to the static system, where the flow is absent (Tsai, 2005).

In this study, under static conditions, the dual species biofilm where *P. fluorescens* was later inoculated on *Listeria* preformed biofilm resulted in the 'smothering' of *L. monocytogenes* with reductions in cell concentrations from 6.3 $\log_{10}$ CFU/cm^2 (Day 1) to 2.3 $\log_{10}$ CFU/cm^2 (Day 5) over the period of 5 days of co-growth (Figure 6.6). In a similar study, *P. aeruginosa* predominated the dual species biofilm with *L. monocytogenes* and was able to inhibit the growth of *L. monocytogenes* (Dong et al., 2022). Structurally, in a mixed-species biofilm, the bacteria on the top of the biofilm has improved access to nutrients and oxygen (Lee et al., 2014). The predominance of *P. fluorescens* in the dual species biofilm (Figure 6.6) could be

favoured by the condition where *P. fluorescens* attached later, leading to settlement on top layers of the biofilm (better access to nutrients), which can also be observed visually (blue) (Figure 6.10.C).

After the attachment and maturation, the detachment of the multispecies biofilm was also impacted by the sequence of colonisation, as observed under both flow and static conditions. After 3 days of co-growth under flow, biofilm started the shedding cycle for both *Pseudomonas* preformed biofilm (Figure 6.2) and *Listeria* preformed biofilm (Figure 6.3). In *Pseudomonas,* preformed biofilm, biofilm detachment after 3 days of co-growth resulted in a significant reduction of both *P. fluorescens* and *L. monocytogenes* cell concentration (Figure 6.2). Meanwhile, in the *Listeria* preformed biofilm, a significant reduction after 3 days of co-growth was observed only for *P. fluorescens*, with *L. monocytogenes* cell concentration remaining consistent after day 2 of co-growth (Figure 6.3). This difference in detachment might be explained by how each bacterium attaches to the surface under flow. In the previous chapter, we observed that *L. monocytogenes* goes through stress adaptations to attach and form biofilm under turbulent flow (Chapter 5), which might have resulted in a stronger primary attachment of *L. monocytogenes* compared to *P. fluorescens* attachment and hence a lowered detachment. In a similar study, the single and multispecies biofilm formed by *Sphingomonas rubra* and *Nakamurella multipartite* under high shear stress resulted in a more stable biofilm, indicated by the lowered detachment observed after 9 h of incubation (J. Wang et al., 2020). The sloughed biofilm matrix and cells through shear stress retain the biofilm phenotype, whereas the released cells during non-stress conditions show a planktonic cell phenotype (Donlan, 2002). The biofilm matrix, consisting of both cells and EPS, after the detachment, may be protected from the environment and chemical stresses, resulting in a high bacterial load and a fast-tracked process for colonisation of a clean surface (Ghadakpour et al., 2014).

The attachment of *L. monocytogenes* was found to be increasing with the biofilm age of preformed *P. fluorescens* (24 h, 48 h, and 72 h) biofilm under flow. This was absent in biofilm formed under static conditions. In both cases, the cell concentration of *P. fluorescens* in the preformed biofilm is comparable, indicating that either the concentration, composition, or architecture of the extracellular matrix formed by the primary biofilm former (*P. fluorescens*) under turbulent flow is impacting the subsequent attachment of the secondary colonizer (*L. monocytogenes*). In this study, the manually conditioned exopolysaccharide on the stainless-steel surface did not impact the attachment of *L. monocytogenes* (Figure 6.8), despite the concentration range covering five times the EPS concentration at which significantly higher

attachment was observed under flow (Figure 6.2). With the understanding that there is an attachment of rehydrated EPS on the surface (Appendix VIII), the observation that it did not affect the attachment of *L. monocytogenes* could be interpreted in various ways: a) The presence of *P. fluorescens* cells is required in the biofilm for improved attachment of *L. monocytogenes*. b) The freeze-drying and rehydration of EPS to prepare the conditioning film for the stainless-steel surface changes the properties of the exopolysaccharide, and c) The architecture of the biofilm produced is more important than the concentration of the EPS for the attachment of secondary bacteria. Based on the 3-D structure of biofilm formed under flow, observed in the previous chapter (Figure 4.13.A), the architecture of the biofilm could have been a contributing factor in the elevated concentrations of *L. monocytogenes* when attached to *P. fluorescens* biofilm. Contrasting observations have been made for the attachment of poor biofilm-forming bacteria, such as *Listeria,* on the conditioned extracellular matrix produced by higher EPS producing bacteria, such as *Pseudomonas*. The matrix can act as a conditioning film, which can enhance the attachment of bacteria from the bulk fluid, especially under flow. As far as the initial attachment is concerned, in the context of multispecies bacteria, the presence of exopolysaccharide-producing bacteria was found to be more vital than the surface properties, such as hydrophobicity, surface charges, and flagellar movements (Sasahara & Zottola, 1993). The extracellular matrix consists of polysaccharides, proteins, and nucleic acids. The coating of these compounds on the stainless-steel surfaces modifies the surface properties such as hydrophobicity, surface charge, roughness, and surface functional groups (Gubner & Beech, 2000; Tsuneda et al., 2003), which can impact the subsequent attachment of the bacteria. Studies have shown both enhancement and inhibition of subsequent attachment depending on the EPS composition and environmental conditions (Hwang et al., 2012). The conditioning of the surface and metabolic interaction by the preforming bacteria are the most common hypotheses put forward for the increased attachment and growth of subsequently attaching bacteria (Olsen et al., 2019). Hwang et al., (2012) observed that the presence of EPS on the surfaces negatively impacted the initial adhesion of *B. cepacia* and *P. aeruginosa*, owing to the protein compounds present in the coating.

6.5 Conclusion

In conclusion, pathogens like *L. monocytogenes* can integrate into and survive within and even proliferate in an existing biofilm of ubiquitous bacteria such as *P. fluorescens*. In fact, the presence of preformed *Pseudomonas* biofilm improved the attachment of *L. monocytogenes,*

whereas the presence of preformed *Listeria* biofilm reduced the attachment of *P. fluorescens*, indicating the diverse impact of conditioning layer on the attachment patterns of a secondary coloniser under flow. The increased attachment of *L. monocytogenes* led to quicker biofilm formation, with the biofilm reaching a plateau within 24 h of co-growth and outcompeting the primary bacteria (*P. fluorescens*), which suggests that the biofilm matrix produced by one primary bacterium can become anchoring and breeding sites for pathogens such as *L. monocytogenes*. The extracted EPS and manual conditioning of the surface did not have any impact on the attachment of *L. monocytogenes*, implying there are more factors in play in enhanced attachment than just the deposition of exopolysaccharides. Overall, flow was an important variable in understanding the sequentially formed biofilm as it impacted all stages of biofilm formation (attachment, maturation, and detachment) as well as spatial arrangement for all three attachment conditions. Further research on the architecture and composition of the biofilm formed by higher EPS producing bacteria, such as *P. fluorescens,* and its role in the attachment and biofilm formation of subsequently attaching bacteria would be significant in understanding the role of primary biofilm formers on the synergistic multispecies biofilm.

Chapter 7. Discussion

7.1 Final discussion

The dynamics of multispecies biofilms are more complex than those of single-species biofilms **(Chapter 2)**. Overall, the presence of multiple bacteria in the biofilm regulates the population dynamics, exopolysaccharide content, spatial arrangement, and sanitizer tolerance (**Chapter 3**). Understanding the intricate interactions between the bacteria under different variables helps to navigate the complexity of the multispecies biofilms and develop effective and sustainable control methods in their natural environments (Kim et al., 2022).

7.1.1 Impact of nutrient availability in single and multispecies biofilm

The nutrient variations impacted the interspecies interactions between the bacteria, with high nutrient concentrations leading to more synergistic interactions and higher tolerance to sanitizer compared with low nutrient concentrations (Table 3.1). Under the nutrient-abundant conditions, all three bacteria involved showed increased tolerance against sodium hypochlorite sanitizer in the multispecies arrangement compared with their single-species counterparts, with notably higher survival for *L. monocytogenes* (5.3 $\log_{10}$ CFU/cm^2) in a multispecies biofilm compared with its single-species counterpart (2.3 $\log_{10}$ CFU/cm^2). This higher tolerance by pathogens such as *L. monocytogenes* in multispecies (with *Pseudomonas*) is not limited to sodium hypochlorite sanitizer or these specific strains. This pattern of survival has been noted for multiple sanitizers (peroxyacetic acid, benzalkonium chloride) and for strains collected from a variety of multispecies environments (fruit harvest, dairy) (Voloshchuk et al., 2025). The protection provided by *P. fluorescens* to *L. monocytogenes* during stress is not limited to sanitizer treatments either (Chapter 3). Attachment assays showed that in the presence of *P. fluorescens*, *L. monocytogenes* attaches better and multiplies to very high concentrations under shear stress (Chapters 4 and 5). The mechanism of this protection under various stressors has been associated with high exopolysaccharide concentrations, matrix structure, and interspecies interactions (Rodríguez-Melcón, Alonso-Calleja, et al., 2021). When multiple species of bacteria come together in a biofilm, different types of EPS are produced by various bacteria, resulting in a dense and viscous matrix that can serve as an effective barrier against stress (Mann & Wozniak, 2012). However, this changes under low nutrient concentrations (10% TSB). Low nutrient levels led to lower exopolysaccharide concentration per cm^2, and both sanitizer tolerance and additional protection provided by *P. fluorescens* were reduced, with

both bacteria under detectable limits (<2.1 $\log_{10}$ CFU/cm^2) (Figure 3.4). This agrees with the antagonistic interactions observed (Table 3.1) under such conditions as a result of competition for nutrients and space (Sadiq et al., 2021). These interactions could further change when nutrient-rich fresh media is added, resulting in synergy in nutrient-rich conditions (Fu et al., 2020). This finding can be used to understand the impact of frequent cleaning and creating a low-nutrient environment for effective removal of multispecies biofilm from the food processing environments. The interactions between bacteria are a dynamic process that adapts according to the environment, which in this case, is nutrient stress.

7.1.2 Impact of turbulent flow in single and multispecies biofilm

The formation of macroscopic thread-like structures of *S. aureus* (Figure 4.9), microscopic filaments of *L. monocytogenes* (Figure 4.8), and stable biofilm formation of *P. fluorescens* (Figure 4.5) are some of the observations made for single-species biofilm formed under turbulent flow in a CDC bioreactor. The structural observations made for *S. aureus* and *L. monocytogenes* occur concurrently with lowered cell concentrations in single and dual species biofilm, suggesting slow growth and division as a stress response under turbulent flow. However, in the presence of *P. fluorescens* (in dual and triple species biofilms), there are no microscopic filaments (Figure 4.11) or macroscopic thread-like structures for either bacterium, suggesting a form of protection provided by *P. fluorescens* against turbulent flow stress. This protected biofilm formation resulted in significantly ($p<0.001$) higher concentrations of *L. monocytogenes* in dual (with *P. fluorescens*) and triple species with the addition of *S. aureus* (Figure 4.5) under turbulent flow. The dual species biofilm of *S. aureus* and *L. monocytogenes* formed both filaments (Figure 4.12) and thread-like structures (also known as streamers) under turbulent flow, suggesting this dual species combination was still subject to the stress (Wittig et al., 2025) observed in single species biofilm. While nutrient stress forced the bacteria into competition (Chapter 3), the turbulent flow (that also incorporated continuous nutrient flow) resulted in synergy between the bacteria, indicating that the nutrient access for a bacterium and its community interactions might be more important than what we have understood so far. In the CDC bioreactor, there are 2 variables at play: continuous supply of media and shear stress (Figure 5.1). Experiments comparing each variable with the combined one showed that while continuous flux of media supports higher cell concentration in protected biofilms, the dominating variable here is shear stress (Figure 5.11).

Among the three bacteria studied, *L. monocytogenes* had the most interesting response to shear stress. *L. monocytogenes* was able to adapt to the stress by changing its morphology and regulating its gene expression associated with attachment, motility, cell division, stress adaptation, and shape determination (Figure 5.9). This provides insight into how bacteria can survive under hydrodynamic stress in single and multispecies environments. This adaptation and growth are in contrast with the developments in food processing that focus on using mechanical shear to reduce the survivability of *L. monocytogenes* on surfaces (Sheen et al., 2010). While the reduced attachment of *L. monocytogenes* under shear stress has been established, the adaptation of the attached bacteria appears to be overlooked. The transfer of these stress-adapted bacteria into food could prove to be critical in terms of public health (Yamaki et al., 2021). Additionally, the influence of turbulence in multispecies biofilm indicates that further biofilm research regarding processing environments where bacteria are impacted by flow should be best replicated and studied with bioreactors rather than static conditions commonly used so far.

7.1.3 Impact of sequence of colonisation in multispecies biofilm

The stress-adapted bacteria (*L. monocytogenes*) proved to be more strongly adherent to the surface (Figure 6.3) compared to a stable biofilm former (*P. fluorescens*) (Figure 6.2), when inoculated as a foundation bacterium under turbulent flow. The foundation bacterium, also referred to as the primary bacterium in this research, influenced the attachment and growth of subsequently attaching bacteria by conditioning the surface with its cells and extracellular matrix. The preconditioning by *P. fluorescens* resulted in significantly higher ($p < 0.05$) attachment of *L. monocytogenes* (Figure 6.2). This recruitment of the second bacterium is dependent on the surface modifications by the primary attached bacteria. The attachment of *P. fluorescens* was lowered in a surface conditioned with a mature *L. monocytogenes* biofilm (Figure 6.3). *L monocytogenes* is capable of utilizing the overexpression of flagella to attach and burrow itself in the *Pseudomonas* biofilm, irrespective of the order of attachment (Puga et al., 2018). Other factors associated with attachment of bacteria are structural influences from pili, flagella, curli fibres, and fimbriae, and certain ligand-receptor interactions (Rendueles & Ghigo, 2012). Another factor here is the architecture and the composition of the extracellular matrix produced by the primary attaching bacteria. The entrapment of free-floating bacteria into the networks of the biofilm is a possibility, as complex networks with interstitial voids have been observed previously in biofilm formed under turbulent flow in the CDC system

(Figure 4.13). The attachment of *L. monocytogenes* to the freeze-dried exopolysaccharide did not show similar attachment to the matrix containing live cells with undisturbed biofilm (Figure 6.8). This observation is significant when the EPS footprints and subsequent contamination of cleaned surfaces are considered.

These findings can be used to understand the evolution of pathogenic and spoilage bacteria mix on surfaces that undergo nutrient variation and experience flow through mixing, washing, or cleaning.

7.2 Limitations

- In Figure 2.1, the areas where the bacteria co-exist in the biofilm together were shown. In all those surfaces, some form of food soiling, such as milk solids or meat juices, is expected in the food industry, but was not explored in this study.
- The mixing ratio of the bacteria was fixed at 1:1 and 1:1:1 for both dual and triple-species biofilm (Chapters 3-6). While this assumption was vital to reduce the number of variables in this study, this might not simulate the exact nature of multispecies biofilm in natural environments.
- To enumerate the bacteria in multispecies environments after treatment, selective agars were used. This method did not consider injured cells, and only viable surviving cells were calculated.
- Based on the literature, this study considered the exopolysaccharide as the major component of the extracellular matrix and used this constituent to understand the sanitizer tolerance. This might not always be true when it comes to multispecies biofilm formed under different stress conditions. Other components, such as protein and eDNA, could play a significant role in the sanitizer tolerance, sequential attachment, and biofilm formation, which were not investigated in this study.
- Despite many materials being used in industrial floor/drain surfaces, the biofilm formation surfaces were limited to polystyrene surfaces (microtiter plate) and stainless-steel coupons.
- Additionally, as we understand that biofilm formation and composition are very sensitive to the nutrient concentration, this study was limited to 10% TSB and full-strength TSB to create a difference in the nutrient availability and simplify the analysis in static conditions.
- Similarly, in a continuous system, this study limited the inflow media concentration to 10% TSB, based on the literature, and keeping in mind the high cost of nutrient-rich media in a continuous system that runs for 7 days. The implications of nutrient-rich media (full-strength TSB) and starvation conditions (1% TSB) could be different in biofilm formation and interspecies interactions in the continuous system.
- In the continuous system, the objective of this study was limited to turbulent flow based on the literature (Prabhukhot, Eggleton, Kim, & Patel, 2024). The stress adaptation

techniques used by bacteria to deal with the stress from laminar and turbulent flow could be entirely different.

- The amount of exopolysaccharide adhered to the stainless-steel coupons was not determined before deposition of *L. monocytogenes* cells for the attachment assay.

7.3 Future work

While this study has provided new insights regarding multispecies biofilm, it also highlights new areas to consider when it comes to understanding multispecies biofilm, some of which are listed below,

- The concept of biocontrol using a non-pathogenic bacterium to restrict the growth of another has been introduced in recent years (Angoshtari et al., 2023). This study showed that under the right conditions, *P. fluorescens* can smother *L. monocytogenes* in dual-species biofilm (Figure 6.10), which could be explored further.
- A three-fold approach can be taken for the removal of biofilm from food surfaces, disruption of EPS, quorum-sensing inhibition, and disinfection of the surface (Kim et al., 2022). While the present study explored the disruption of EPS, further studies could be important to understand the quorum sensing between multispecies bacteria in the biofilm and how it can be quenched for effective removal.
- As far as the sequence of bacteria was considered, the architecture of the biofilm formed by the primary biofilm former (*P. fluorescens*) was significant in the attachment of later arriving bacteria (*L. monocytogenes*). The attachment of the bacteria on the previously established networks of biofilm could be explored further using imaging techniques, especially because this could also explain the attachment and entrapment of free-floating bacteria on the remnants of the extracellular matrix on cleaned surfaces.

Appendices

Appendix I. Statement of Contribution- Chapter 2

MASSEY UNIVERSITY
TE KUNENGA KI PŪREHUROA
UNIVERSITY OF NEW ZEALAND

GRADUATE RESEARCH SCHOOL

STATEMENT OF CONTRIBUTION
DOCTORATE WITH PUBLICATIONS/MANUSCRIPTS

We, the student and the student's main supervisor, certify that all co-authors have consented to their work being included in the thesis and they have accepted the student's contribution as indicated below in the Statement of Originality.

Student name:	Krisha Pant
Name and title of main supervisor:	Steve Flint
In which chapter is the manuscript/published work?	Chapter 2

Describe the contribution that the student and members of the supervisory team have made to the manuscript/published work:[1]

Krisha Pant: Writing – original draft, Investigation, Formal analysis, Conceptualization. Jon Palmer: Writing – review & editing, Supervision, Methodology. Steve Flint: Writing – review & editing, Supervision, Resources, Project administration, Methodology.

Please select one of the following three options:

- (●) **The manuscript/published work is published or in press**

  Please provide the full reference of the research output:

  Pant, K., Palmer, J., & Flint, S. (2025). Multispecies biofilm cities and the importance of the order of colonization. Food Control, 111319.

- ( ) **The manuscript is currently under review for publication**

  Please provide the name of the journal:

- ( ) **It is intended that the manuscript will be published, but it has not yet been submitted to a journal**

Student's signature:	Krisha Pant — Digitally signed by Krisha Pant, DN: cn=Krisha Pant, email=krishapant@gmail.com, Date: 2026.01.15 11:42:27 +13'00'	Main supervisor's signature:	Steve Flint — Digitally signed by Steve Flint, Date: 2026.01.15 12:04:02 +13'00'

This form should be placed at the beginning of each relevant thesis chapter.

[1] Refer to the Massey University Publishing and Authorship guidelines (OneMassey for staff, Stream for students) and/ or Contributor Roles Taxonomy (CRediT) guidelines for guidance.

Appendix II. Statement of Contribution- Chapter 3

MASSEY UNIVERSITY
TE KUNENGA KI PŪREHUROA
UNIVERSITY OF NEW ZEALAND

GRADUATE RESEARCH SCHOOL

STATEMENT OF CONTRIBUTION
DOCTORATE WITH PUBLICATIONS/MANUSCRIPTS

We, the student and the student's main supervisor, certify that all co-authors have consented to their work being included in the thesis and they have accepted the student's contribution as indicated below in the Statement of Originality.

Student name:	Krisha Pant
Name and title of main supervisor:	Steve Flint
In which chapter is the manuscript/published work?	Chapter 3

Describe the contribution that the student and members of the supervisory team have made to the manuscript/published work:[1]

Krisha Pant: Writing – original draft, Investigation, Formal analysis, Conceptualization. Jon Palmer: Writing – review & editing, Supervision, Methodology, Conceptualization. Steve Flint: Writing – review & editing, Supervision, Resources, Project administration, Methodology.

Please select one of the following three options:

- (●) **The manuscript/published work is published or in press**

  Please provide the full reference of the research output:

  Pant, K., Palmer, J., & Flint, S. (2025). Conditional synergy: Impact of nutrient abundance on multispecies biofilm formation and sanitizer tolerance. Food Microbiology, 104952.

- ( ) **The manuscript is currently under review for publication**

  Please provide the name of the journal:

- ( ) **It is intended that the manuscript will be published, but it has not yet been submitted to a journal**

Student's signature:	Krisha Pant — Digitally signed by Krisha Pant DN: cn=Krisha Pant, email=krishapant@gmail.com Date: 2026.01.15 11:45:44 +13'00'	Main supervisor's signature:	Steve Flint — Digitally signed by Steve Flint Date: 2026.01.15 12:06:29 +13'00'

This form should be placed at the beginning of each relevant thesis chapter.

[1] Refer to the Massey University Publishing and Authorship guidelines (OneMassey for staff, Stream for students) and/ or Contributor Roles Taxonomy (CRediT) guidelines for guidance.

Appendix III. Statement of Contribution- Chapter 4

MASSEY UNIVERSITY
TE KUNENGA KI PŪREHUROA
UNIVERSITY OF NEW ZEALAND

GRADUATE RESEARCH SCHOOL

STATEMENT OF CONTRIBUTION
DOCTORATE WITH PUBLICATIONS/MANUSCRIPTS

We, the student and the student's main supervisor, certify that all co-authors have consented to their work being included in the thesis and they have accepted the student's contribution as indicated below in the Statement of Originality.

Student name:	Krisha Pant
Name and title of main supervisor:	Steve Flint
In which chapter is the manuscript/published work?	Chapter 4

Describe the contribution that the student and members of the supervisory team have made to the manuscript/published work:[1]

Krisha Pant: Writing – original draft, Investigation, Formal analysis, Conceptualization. Jon Palmer: Writing – review & editing, Supervision, Methodology, Conceptualization. Steve Flint: Writing – review & editing, Supervision, Resources, Project administration, Methodology.

Please select one of the following three options:

- (●) **The manuscript/published work is published or in press**

  Please provide the full reference of the research output:

  Pant, K., Palmer, J., & Flint, S. (2025). Evaluation of single and multispecies biofilm formed in the static and continuous systems. International Journal of Food Microbiology, 429, 111030.

- ( ) **The manuscript is currently under review for publication**

  Please provide the name of the journal:

- ( ) **It is intended that the manuscript will be published, but it has not yet been submitted to a journal**

Student's signature:	Krisha Pant Digitally signed by Krisha Pant DN: cn=Krisha Pant, email=krishapant@gmail.com Date: 2026.01.15 11:49:48 +13'00'	Main supervisor's signature:	Steve Flint Digitally signed by Steve Flint Date: 2026.01.15 12:07:25 +13'00'

This form should be placed at the beginning of each relevant thesis chapter.

[1] Refer to the Massey University Publishing and Authorship guidelines (OneMassey for staff, Stream for students) and/ or Contributor Roles Taxonomy (CRediT) guidelines for guidance.

Appendix IV. Statement of Contribution- Chapter 5

MASSEY UNIVERSITY
TE KUNENGA KI PŪREHUROA
UNIVERSITY OF NEW ZEALAND

GRADUATE RESEARCH SCHOOL

STATEMENT OF CONTRIBUTION
DOCTORATE WITH PUBLICATIONS/MANUSCRIPTS

We, the student and the student's main supervisor, certify that all co-authors have consented to their work being included in the thesis and they have accepted the student's contribution as indicated below in the Statement of Originality.

Student name:	Krisha Pant
Name and title of main supervisor:	Steve Flint
In which chapter is the manuscript/published work?	Chapter 5

Describe the contribution that the student and members of the supervisory team have made to the manuscript/published work:[1]

Krisha Pant: Writing – original draft, Investigation, Formal analysis, Conceptualization. Jon Palmer: Writing – review & editing, Supervision, Methodology, Conceptualization. Steve Flint: Writing – review & editing, Supervision, Resources, Project administration, Methodology.

Please select one of the following three options:

- (●) **The manuscript/published work is published or in press**
  Please provide the full reference of the research output:
  Pant, K., Palmer, J., & Flint, S. (2025). Shear stress adaptation of Listeria monocytogenes in mono and dual-species biofilms. Food Research International, 117190.
- ( ) **The manuscript is currently under review for publication**
  Please provide the name of the journal:
- ( ) **It is intended that the manuscript will be published, but it has not yet been submitted to a journal**

Student's signature:	Krisha Pant — Digitally signed by Krisha Pant, DN: cn=Krisha Pant, email=krishapant@gmail.com, Date: 2026.01.15 11:53:43 +13'00'	Main supervisor's signature:	Steve Flint — Digitally signed by Steve Flint, Date: 2026.01.15 12:08:23 +13'00'

This form should be placed at the beginning of each relevant thesis chapter.

[1] Refer to the Massey University Publishing and Authorship guidelines (OneMassey for staff, Stream for students) and/ or Contributor Roles Taxonomy (CRediT) guidelines for guidance.

Appendix V. Statement of Contribution- Chapter 6

MASSEY UNIVERSITY
TE KUNENGA KI PŪREHUROA
UNIVERSITY OF NEW ZEALAND

GRADUATE RESEARCH SCHOOL

STATEMENT OF CONTRIBUTION
DOCTORATE WITH PUBLICATIONS/MANUSCRIPTS

We, the student and the student's main supervisor, certify that all co-authors have consented to their work being included in the thesis and they have accepted the student's contribution as indicated below in the Statement of Originality.

Student name:	Krisha Pant
Name and title of main supervisor:	Steve Flint
In which chapter is the manuscript/published work?	Chapter 6

Describe the contribution that the student and members of the supervisory team have made to the manuscript/published work:[1]

Krisha Pant: Writing – original draft, Investigation, Formal analysis, Conceptualization. Jon Palmer: Writing – review & editing, Supervision, Methodology, Conceptualization. Steve Flint: Writing – review & editing, Supervision, Resources, Project administration, Methodology.

Please select one of the following three options:

- (●) **The manuscript/published work is published or in press**
  Please provide the full reference of the research output:
  Pant, K., Palmer, J., & Flint, S. (2026). Sequential attachment and Listeria predominance under turbulent flow. Biofouling, 1–16.
- ( ) **The manuscript is currently under review for publication**
  Please provide the name of the journal:
- ( ) **It is intended that the manuscript will be published, but it has not yet been submitted to a journal**

Student's signature:	Krisha Pant Digitally signed by Krisha Pant DN: cn=Krisha Pant, email=krishapant@gmail.com Date: 2026.02.25 15:53:53 +13'00'	Main supervisor's signature:	Steve Flint Digitally signed by Steve Flint Date: 2026.02.25 16:04:14 +13'00'

This form should be placed at the beginning of each relevant thesis chapter.

[1] Refer to the Massey University Publishing and Authorship guidelines (OneMassey for staff, Stream for students) and/ or Contributor Roles Taxonomy (CRediT) guidelines for guidance.

Appendix VI. Statistical Analysis

The significant differences between the samples were determined with one-way ANOVA (IBM SPSS version 29) with 95 % confidence ($p < 0.05$) together with Tukey analysis for a post-hoc test. The normality of the data was verified using the Shapiro-walk ($p > 0.05$) and Kolmogorov test ($p > 0.05$) where relevant. All experiments had at least two biological replicates and six technical replicates and results were presented as mean ± standard deviation.

Appendix VII. Cell count

Appendix VII.A Linear relationship between *P. fluorescens* cell count (log_{10} CFU/mL) vs optical density (O.D)

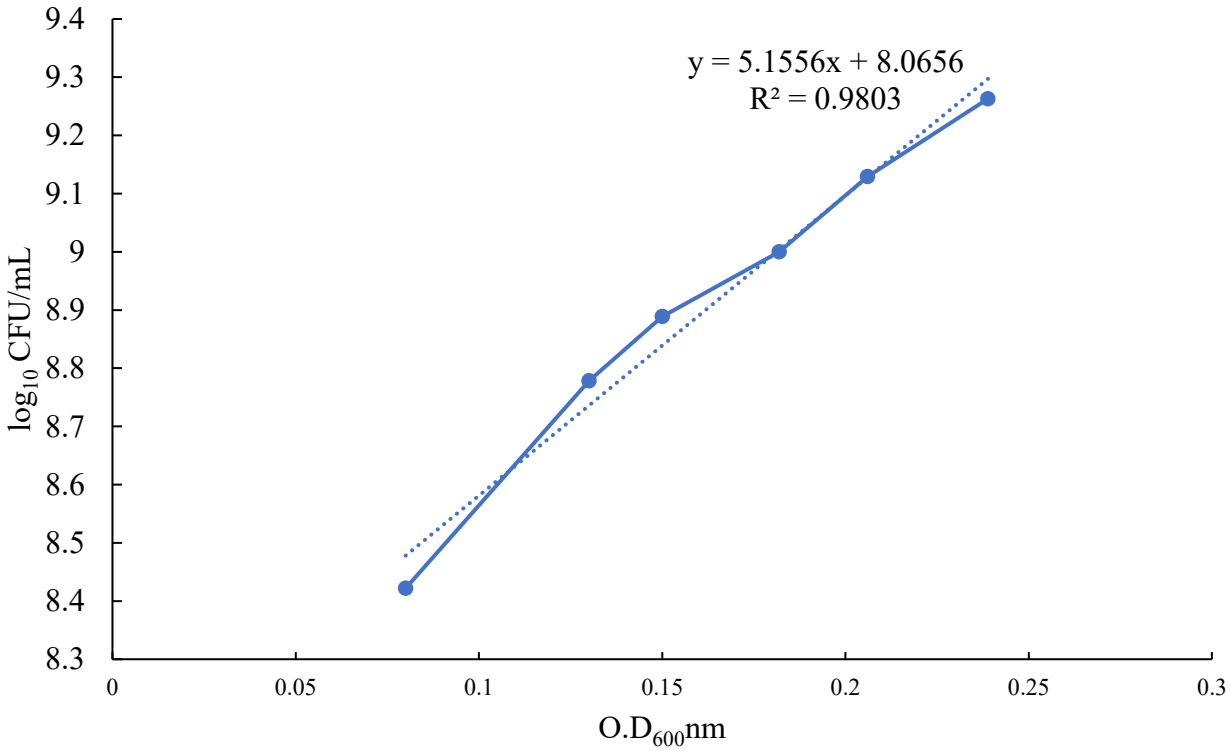

Appendix VII.B Linear relationship between *S. aureus* cell count (log_{10} CFU/mL) vs optical density (O.D)

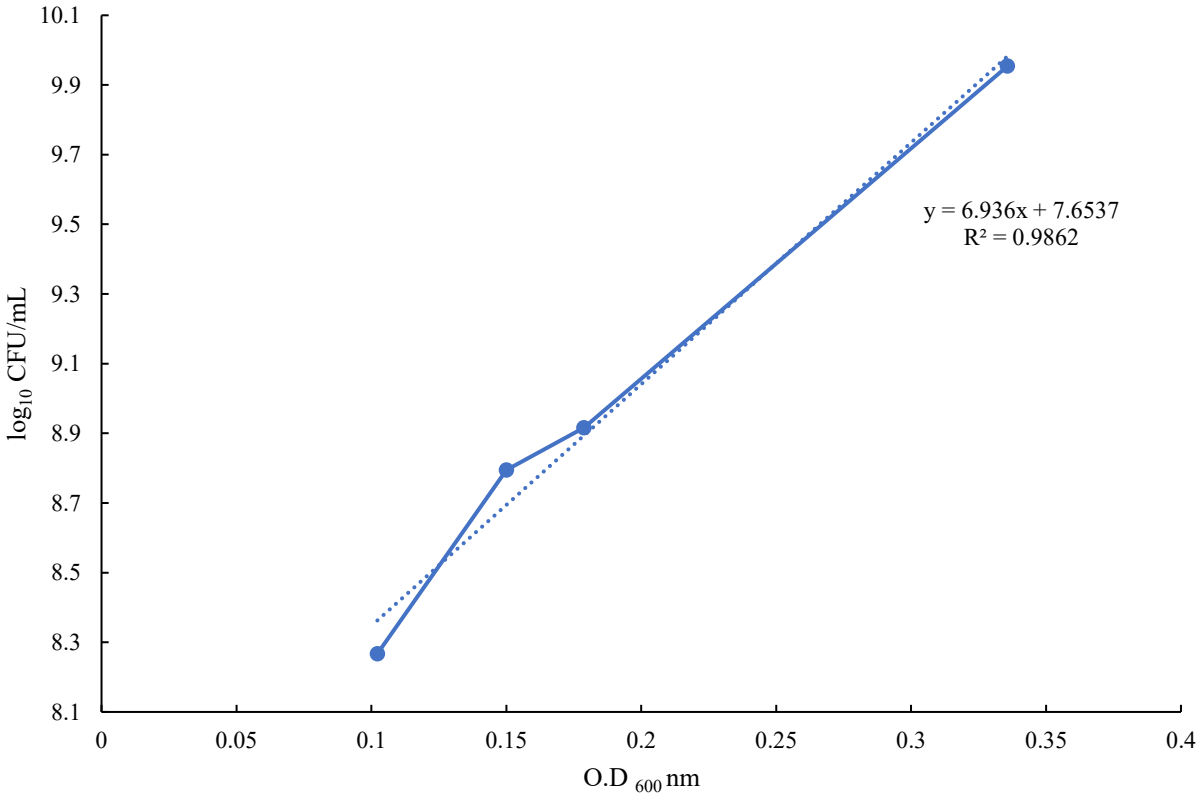

Appendix VII.C *L. monocytogenes* cell count (log_{10} CFU/mL) vs optical density (O.D)

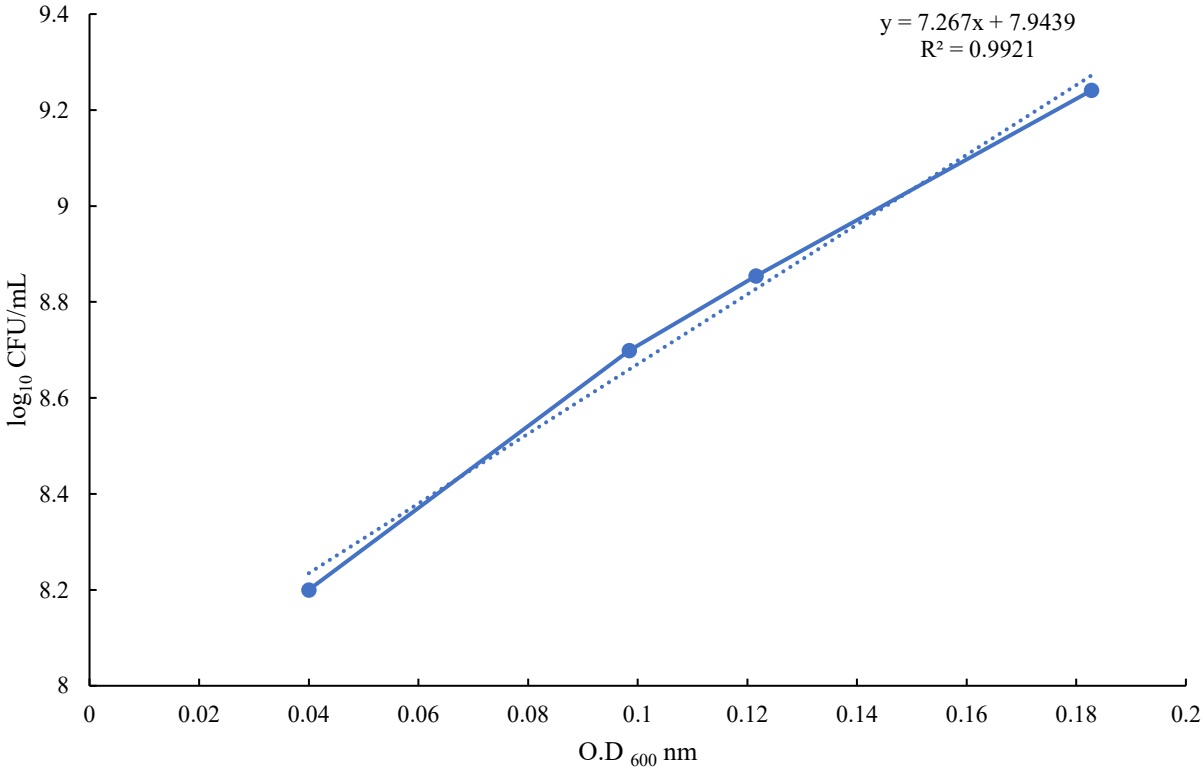

Appendix VIII. Dextrose standard curve

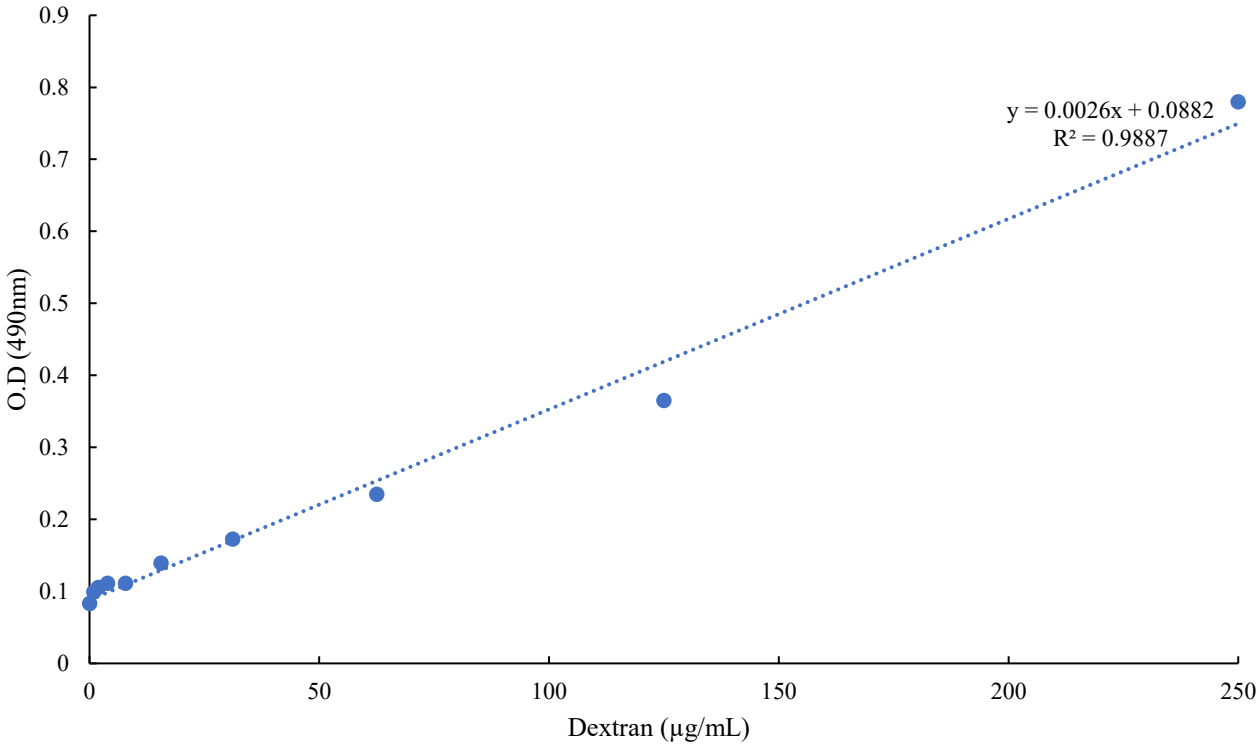

The standard curve of dextran (0.97-250 µg/mL) and optical density at 490nm for exopolysaccharide determination in the biofilm

Appendix IX. Epifluorescence images

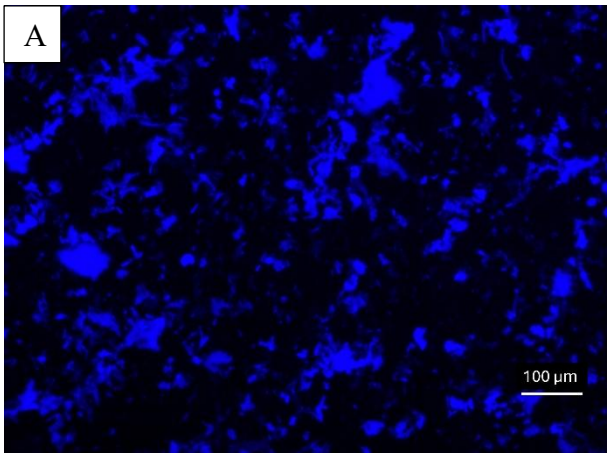

A. EPS coated coupon stained with calcofluor white

B. Blank coupon stained with calcofluor white

References

Aarnisalo, K., Lundén, J., Korkeala, H., & Wirtanen, G. (2007). Susceptibility of *Listeria monocytogenes* strains to disinfectants and chlorinated alkaline cleaners at cold temperatures. *LWT-Food Science and Technology*, *40*(6), 1041-1048.

Abdallah, M., Benoliel, C., Drider, D., Dhulster, P., & Chihib, N.-E. (2014). Biofilm formation and persistence on abiotic surfaces in the context of food and medical environments. *Archives of microbiology*, *196*(7), 453-472.

Abdelli, F., Jardak, M., Elloumi, J., Stien, D., Cherif, S., Mnif, S., & Aifa, S. (2019). Antibacterial, anti-adherent, and cytotoxic activities of surfactin (s) from a lipolytic strain *Bacillus safensis* F4. *Biodegradation*, *30*, 287-300.

Abdullah, Algburi, A., Asghar, A., Huang, Q., Mustfa, W., Javed, H. U., Zehm, S., & Chikindas, M. L. (2021). Black cardamom essential oil prevents *Escherichia coli* O157: H7 and *Salmonella* Typhimurium JSG 1748 biofilm formation through inhibition of quorum sensing. *Journal of Food Science and Technology*, *58*(8), 3183-3191.

Agustín, M., Viceconte, F. R., Vela Gurovic, M. S., Costantino, A., & Brugnoni, L. I. (2019). Effect of quorum sensing molecules and natamycin on biofilms of *Candida tropicalis* and other yeasts isolated from industrial juice filtration membranes. *Journal of Applied Microbiology*, *126*(6), 1808-1820.

Agustín, M. d. R., & Brugnoni, L. (2018). Multispecies biofilms between *Listeria monocytogenes* and *Listeria innocua* with resident microbiota isolated from apple juice processing equipment. *Journal of Food Safety*, *38*(5), e12499.

Al-Sharify, Z. T., Al-Najjar, S. Z., Naser, Z. A., Alsherfy, Z. A. I., & Onyeaka, H. (2025). The Impact of Fluid Flow on Microbial Growth and Distribution in Food Processing Systems. *Foods*, *14*(3), 401.

Alabdullatif, M. (2024). Evaluating the effects of temperature and agitation on biofilm formation of bacterial pathogens isolated from raw cow milk. *BMC Microbiology*, *24*(1), 251.

Almasoud, A., Hettiarachchy, N., Rayaprolu, S., Babu, D., Kwon, Y. M., & Mauromoustakos, A. (2016). Inhibitory effects of lactic and malic organic acids on autoinducer type 2 (AI-2) quorum sensing of *Escherichia coli* O157: H7 and *Salmonella* Typhimurium. *LWT-Food Science and Technology*, *66*, 560-564.

Alomar, J., Loubière, P., Delbes, C., Nouaille, S., & Montel, M.-C. (2008). Effect of *Lactococcus garvieae*, *Lactococcus lactis* and *Enterococcus faecalis* on the behaviour of *Staphylococcus aureus* in microfiltered milk. *Food Microbiology*, *25*(3), 502-508.

Alonso, V. P. P., Harada, A. M. M., & Kabuki, D. Y. (2020). Competitive and/or cooperative interactions of *Listeria monocytogenes* with *Bacillus cereus* in dual-species biofilm formation. *Frontiers in Microbiology*, *11*, 177.

Anand, S., Singh, D., Avadhanula, M., & Marka, S. (2014). Development and control of bacterial biofilms on dairy processing membranes. *Comprehensive Reviews in Food Science and Food Safety*, *13*(1), 18-33.

Angoshtari, R., Scribner, K. T., & Marsh, T. L. (2023). The impact of primary colonizers on the community composition of river biofilm. *PLoS One*, *18*(11), e0288040.

Bai, A. J., & Rai, V. R. (2011). Bacterial quorum sensing and food industry. *Comprehensive Reviews in Food Science and Food Safety*, *10*(3), 183-193.

Bansal, M., Nannapaneni, R., Kode, D., Chang, S., Sharma, C. S., McDaniel, C., & Kiess, A. (2019). Rugose morphotype in *Salmonella* Typhimurium and *Salmonella* Heidelberg induced by sequential exposure to subinhibitory sodium hypochlorite aids in biofilm tolerance to lethal sodium hypochlorite on polystyrene and stainless-steel surfaces. *Frontiers in Microbiology*, *10*, 2704.

Bao, K., Belibasakis, G. N., Selevsek, N., Grossmann, J., & Bostanci, N. (2015). Proteomic profiling of host-biofilm interactions in an oral infection model resembling the periodontal pocket. *Scientific Reports*, *5*(1), 15999.

Barnes, T. M., & Greive, K. A. (2013). Use of bleach baths for the treatment of infected atopic eczema. *Australasian Journal of Dermatology*, *54*(4), 251-258.

Bas, S., Kramer, M., & Stopar, D. (2017). Biofilm surface density determines biocide effectiveness. *Frontiers in Microbiology*, *8*, 2443.

Beaudoin, T., Yau, Y., Stapleton, P., Gong, Y., Wang, P., Guttman, D., & Waters, V. (2017). *Staphylococcus aureus* interaction with *Pseudomonas aeruginosa* biofilm enhances tobramycin resistance. *npj Biofilms and Microbiomes*, *3*(1), 25.

Bencardino, D., Amagliani, G., & Brandi, G. (2021). Carriage of *Staphylococcus aureus* among food handlers: An ongoing challenge in public health. *Food Control*, *130*, 108362.

Bereksi, N., Gavini, F., Benezech, T., & Faille, C. (2002). Growth, morphology and surface properties of *Listeria monocytogenes* Scott A and LO28 under saline and acid environments. *Journal of Applied Microbiology*, *92*(3), 556-565.

Berne, C., Ellison, C. K., Ducret, A., & Brun, Y. V. (2018). Bacterial adhesion at the single-cell level. *Nature Reviews Microbiology*, *16*(10), 616-627.

Bockelmann, W., Koslowsky, M., Goerges, S., Scherer, S., Franz, C. M., & Heller, K. J. (2017). Growth inhibition of *Listeria monocytogenes* by bacteriocin-producing *Staphylococcus equorum* SE3 in cheese models. *Food Control*, *71*, 50-56.

Bonneville, L., Maia, V., Barroso, I., Martínez-Suárez, J. V., & Brito, L. (2021). *Lactobacillus plantarum* in dual-species biofilms with *Listeria monocytogenes* enhanced the anti-*Listeria* activity of a commercial disinfectant based on hydrogen peroxide and peracetic acid. *Frontiers in Microbiology*, *12*, 631627.

Bonsaglia, E., Silva, N., Júnior, A. F., Júnior, J. A., Tsunemi, M., & Rall, V. (2014). Production of biofilm by *Listeria monocytogenes* in different materials and temperatures. *Food Control*, *35*(1), 386-391.

Bottery, M. J., Matthews, J. L., Wood, A. J., Johansen, H. K., Pitchford, J. W., & Friman, V.-P. (2022). Inter-species interactions alter antibiotic efficacy in bacterial communities. *The ISME Journal*, *16*(3), 812-821.

Bottery, M. J., Pitchford, J. W., & Friman, V.-P. (2021). Ecology and evolution of antimicrobial resistance in bacterial communities. *The ISME Journal*, *15*(4), 939-948.

Boyle, D. S., Khattar, M. M., Addinall, S. G., Lutkenhaus, J., & Donachie, W. D. (1997). *ftsW* is an essential cell-division gene in *Escherichia coli*. *Molecular Microbiology*, *24*(6), 1263-1273.

Bremer, P. J., Monk, I., & Osborne, C. M. (2001). Survival of *Listeria monocytogenes* attached to stainless-steel surfaces in the presence or absence of *Flavobacterium* spp. *Journal of Food Protection*, *64*(9), 1369-1376.

Brislawn, C. J., Graham, E. B., Dana, K., Ihardt, P., Fansler, S. J., Chrisler, W. B., Cliff, J. B., Stegen, J. C., Moran, J. J., & Bernstein, H. C. (2019). Forfeiting the priority effect: turnover defines biofilm community succession. *The ISME Journal*, *13*(7), 1865-1877.

Brooks, J. D., & Flint, S. H. (2008). Biofilms in the food industry: problems and potential solutions. *International Journal of Food Science & Technology*, *43*(12), 2163-2176.

Buckingham-Meyer, K., Goeres, D. M., & Hamilton, M. A. (2007). Comparative evaluation of biofilm disinfectant efficacy tests. *Journal of Microbiological Methods*, *70*(2), 236-244.

Burmølle, M., Ren, D., Bjarnsholt, T., & Sørensen, S. J. (2014). Interactions in multispecies biofilms: do they actually matter? *Trends in Microbiology*, *22*(2), 84-91.

Burmølle, M., Webb, J. S., Rao, D., Hansen, L. H., Sørensen, S. J., & Kjelleberg, S. (2006). Enhanced biofilm formation and increased resistance to antimicrobial agents and bacterial invasion are caused by synergistic interactions in multispecies biofilms. *Applied and Environmental Microbiology*, *72*(6), 3916-3923.

Busscher, H. J., & Van Der Mei, H. C. (2006). Microbial adhesion in flow displacement systems. *Clinical Microbiology Reviews*, *19*(1), 127-141.

Byun, K.-H., Han, S. H., Choi, M. W., Kim, B.-H., & Ha, S.-D. (2024). Efficacy of disinfectant and bacteriophage mixture against planktonic and biofilm state of *Listeria monocytogenes* to control in the food industry. *International Journal of Food Microbiology*, *413*, 110587.

Campanac, C., Pineau, L., Payard, A., Baziard-Mouysset, G., & Roques, C. (2002). Interactions between biocide cationic agents and bacterial biofilms. *Antimicrobial Agents and Chemotherapy*, *46*(5), 1469-1474.

Carrascosa, C., Raheem, D., Ramos, F., Saraiva, A., & Raposo, A. (2021). Microbial biofilms in the food industry—A comprehensive review. *International Journal of Environmental Research and Public Health*, *18*(04), 2014.

Castro, M. S. R., da Silva Fernandes, M., Kabuki, D. Y., & Kuaye, A. Y. (2021). Modelling *Pseudomonas fluorescens* and *Pseudomonas aeruginosa* biofilm formation on stainless-steel surfaces and controlling through sanitisers. *International Dairy Journal*, *114*, 104945.

Cervantes-Huamán, B. R. H., Ripolles-Avila, C., Mazaheri, T., & Rodríguez-Jerez, J. J. (2022). Pathogenic mono-species biofilm formation on stainless-steel surfaces: quantitative, qualitative, and compositional study. *LWT*, *159*, 113211.

Chae, M. S., & Schraft, H. (2000). Comparative evaluation of adhesion and biofilm formation of different *Listeria monocytogenes* strains. *International Journal of Food Microbiology*, *62*(1-2), 103-111.

Chaggar, G. K., Bryant, D. B., Chen, R., Fajardo, D., Jules-Culver, Z. A., Drolia, R., & Oliver, H. F. (2024). Development of *Salmonella enterica* serovar Typhimurium, *Listeria monocytogenes*, and *Pseudomonas aeruginosa* multi-species in vitro dry surface biofilm models: Insights into resilience and persistence in low-moisture environments. *Food Control*, *166*, 110703.

Chaves, R. D., Kumazawa, S. H., Khaneghah, A. M., Alvarenga, V. O., Hungaro, H. M., & Sant'Ana, A. S. (2024). Comparing the susceptibility to sanitizers, biofilm-forming ability, and biofilm resistance to quaternary ammonium and chlorine dioxide of 43

Salmonella enterica and *Listeria monocytogenes* strains. *Food Microbiology*, *117*, 104380.

Chawla, R., Gupta, R., Lele, T. P., & Lele, P. P. (2020). A skeptic's guide to bacterial mechanosensing. *Journal of Molecular Biology*, *432*(2), 523-533.

Cheah, H., & Bae, S. (2023). Multichannel Microfluidic Platform for Temporal-Spatial Investigation of Niche Roles of *Pseudomonas aeruginosa* and *Escherichia coli* within a Dual-Species Biofilm. *Applied and Environmental Microbiology*, *89*(7), e00651-00623.

Cherif-Antar, A., Moussa–Boudjemâa, B., Didouh, N., Medjahdi, K., Mayo, B., & Flórez, A. B. (2016). Diversity and biofilm-forming capability of bacteria recovered from stainless-steel pipes of a milk-processing dairy plant. *Dairy Science & Technology*, *96*, 27-38.

Cherifi, T., Jacques, M., Quessy, S., & Fravalo, P. (2017). Impact of nutrient restriction on the structure of *Listeria monocytogenes* biofilm grown in a microfluidic system. *Frontiers in Microbiology*, *8*, 864.

Chinnaraj, S. B., Jayathilake, P. G., Dawson, J., Ammar, Y., Portoles, J., Jakubovics, N., & Chen, J. (2021). Modelling the combined effect of surface roughness and topography on bacterial attachment. *Journal of Materials Science & Technology*, *81*, 151-161.

Chitlapilly Dass, S., & Wang, R. (2022). Biofilm through the looking glass: A microbial food safety perspective. *Pathogens*, *11*(3), 346.

Clarke, E. (2016). Levels of selection in biofilms: multispecies biofilms are not evolutionary individuals. *Biology & Philosophy*, *31*, 191-212.

Cleto, S., Matos, S., Kluskens, L., & Vieira, M. J. (2012). Characterization of contaminants from a sanitized milk processing plant. *PLoS One*, *7*(6), e40189.

Cloete, T. E. (2003). Resistance mechanisms of bacteria to antimicrobial compounds. *International Biodeterioration & Biodegradation*, *51*(4), 277-282.

Colagiorgi, A., Di Ciccio, P., Zanardi, E., Ghidini, S., & Ianieri, A. (2016). A look inside the *Listeria monocytogenes* biofilms extracellular matrix. *Microorganisms*, *4*(3), 22.

Colebrook, C. F., Blench, T., Chatley, H., Essex, E., Finniecome, J., Lacey, G., Williamson, J., & Macdonald, G. (1939). Correspondence. turbulent flow in pipes, with particular reference to the transition region between the smooth and rough pipe laws (includes plates). *Journal of the Institution of Civil Engineers*, *12*(8), 393-422.

Culotti, A., & Packman, A. I. (2014). *Pseudomonas aeruginosa* promotes *Escherichia coli* biofilm formation in nutrient-limited medium. *PLoS One*, *9*(9), e107186.

Cunault, C., Faille, C., Bouvier, L., Föste, H., Augustin, W., Scholl, S., Debreyne, P., & Benezech, T. (2015). A novel set-up and a CFD approach to study the biofilm dynamics as a function of local flow conditions encountered in fresh-cut food processing equipments. *Food and Bioproducts Processing*, *93*, 217-223.

da Silva Fernandes, M., Alvares, A. C. C., Manoel, J. G. M., Esper, L. M. R., Kabuki, D. Y., & Kuaye, A. Y. (2017). Formation of multi-species biofilms by *Enterococcus faecium*, *Enterococcus faecalis*, and *Bacillus cereus* isolated from ricotta processing and effectiveness of chemical sanitation procedures. *International Dairy Journal*, *72*, 23-28.

da Silva Fernandes, M., Kabuki, D. Y., & Kuaye, A. Y. (2015). Behavior of *Listeria monocytogenes* in a multi-species biofilm with *Enterococcus faecalis* and *Enterococcus faecium* and control through sanitation procedures. *International Journal of Food Microbiology*, *200*, 5-12.

Daneshvar Alavi, H. E., & Truelstrup Hansen, L. (2013). Kinetics of biofilm formation and desiccation survival of *Listeria monocytogenes* in single and dual species biofilms with *Pseudomonas fluorescens*, *Serratia proteamaculans* or *Shewanella baltica* on food-grade stainless-steel surfaces. *Biofouling*, *29*(10), 1253-1268.

Davey, M. E., Caiazza, N. C., & O'Toole, G. A. (2003). Rhamnolipid surfactant production affects biofilm architecture in *Pseudomonas aeruginosa* PAO1. *Journal of Bacteriology*, *185*(3), 1027-1036.

Debray, R., Herbert, R. A., Jaffe, A. L., Crits-Christoph, A., Power, M. E., & Koskella, B. (2022). Priority effects in microbiome assembly. *Nature Reviews Microbiology*, *20*(2), 109-121.

Decimo, M., Morandi, S., Silvetti, T., & Brasca, M. (2014). Characterization of gram-negative psychrotrophic bacteria isolated from Italian bulk tank milk. *Journal of Food Science*, *79*(10), M2081-M2090.

Deng, L., Guo, W., Ngo, H. H., Wang, X. C., Hu, Y., Chen, R., Cheng, D., Guo, S., & Cao, Y. (2020). Application of a specific membrane fouling control enhancer in membrane bioreactor for real municipal wastewater treatment: sludge characteristics and microbial community. *Bioresource Technology*, *312*, 123612.

Di Pippo, F., Di Gregorio, L., Congestri, R., Tandoi, V., & Rossetti, S. (2018). Biofilm growth and control in cooling water industrial systems. *FEMS Microbiology Ecology*, *94*(5), fiy044.

Di Somma, A., Recupido, F., Cirillo, A., Romano, A., Romanelli, A., Caserta, S., Guido, S., & Duilio, A. (2020). Antibiofilm properties of temporin-l on *Pseudomonas fluorescens* in static and in-flow conditions. *International Journal of Molecular Sciences*, *21*(22), 8526.

Diarra, C., Goetz, C., Gagnon, M., Roy, D., & Jean, J. (2023). Biofilm formation by heat-resistant dairy bacteria: multispecies biofilm model under static and dynamic conditions. *Applied and Environmental Microbiology*, *89*(10), e00713-00723.

Dong, J., Liu, L., Chen, L., Xiang, Y., Wang, Y., & Zhao, Y. (2023). The Coexistence of Bacterial Species Restructures Biofilm Architecture and Increases Tolerance to Antimicrobial Agents. *Microbiology Spectrum*, *11*(2), e03581-03522.

Dong, Q., Sun, L., Fang, T., Wang, Y., Li, Z., Wang, X., Wu, M., & Zhang, H. (2022). Biofilm formation of *Listeria monocytogenes* and *Pseudomonas aeruginosa* in a simulated chicken processing environment. *Foods*, *11*(13), 1917.

Donlan, R. M. (2001). Biofilm formation: a clinically relevant microbiological process. *Clinical Infectious Diseases*, *33*(8), 1387-1392.

Donlan, R. M. (2002). Biofilms: microbial life on surfaces. *Emerging Infectious Diseases*, *8*(9), 881.

dos Santos, E. A. R., Tadielo, L. E., Schmiedt, J. A., Orisio, P. H. S., Brugeff, E. d. C. L., Possebon, F. S., Pereira, M. O., Pereira, J. G., & dos Santos Bersot, L. (2023). Inhibitory effects of piperine and black pepper essential oil on multispecies biofilm formation by *Listeria monocytogenes*, *Salmonella* Typhimurium, and *Pseudomonas aeruginosa*. *LWT*, *182*, 114851.

Drescher, K., Shen, Y., Bassler, B. L., & Stone, H. A. (2013). Biofilm streamers cause catastrophic disruption of flow with consequences for environmental and medical systems. *Proceedings of the National Academy of Sciences*, *110*(11), 4345-4350.

Dula, S., Ajayeoba, T. A., & Ijabadeniyi, O. A. (2021). Bacterial biofilm formation on stainless-steel in the food processing environment and its health implications. *Folia Microbiologica*, *66*, 293-302.

Dutra, T. V., Fernandes, M. d. S., Perdoncini, M. R. F. G., Anjos, M. M. d., & Abreu Filho, B. A. d. (2018). Capacity of *Escherichia coli* and *Staphylococcus aureus* to produce biofilm on stainless-steel surfaces in the presence of food residues. *Journal of Food Processing and Preservation*, *42*(4), e13574.

Dzieciol, M., Schornsteiner, E., Muhterem-Uyar, M., Stessl, B., Wagner, M., & Schmitz-Esser, S. (2016). Bacterial diversity of floor drain biofilms and drain waters in a *Listeria*

monocytogenes contaminated food processing environment. *International Journal of Food Microbiology*, *223*, 33-40.

Eigentler, L., Kalamara, M., Ball, G., MacPhee, C. E., Stanley-Wall, N. R., & Davidson, F. A. (2022). Founder cell configuration drives competitive outcome within colony biofilms. *The ISME Journal*, *16*(6), 1512-1522.

Elias, S., & Banin, E. (2012). Multi-species biofilms: living with friendly neighbors. *FEMS Microbiology Reviews*, *36*(5), 990-1004.

Eng, T., Herbert, R. A., Martinez, U., Wang, B., Chen, J. C., Brown, J. B., Deutschbauer, A. M., Bissell, M. J., Mortimer, J. C., & Mukhopadhyay, A. (2020). Iron supplementation eliminates antagonistic interactions between root-associated bacteria. *Frontiers in Microbiology*, *11*, 1742.

Evans, C. R., Kempes, C. P., Price-Whelan, A., & Dietrich, L. E. (2020). Metabolic heterogeneity and cross-feeding in bacterial multicellular systems. *Trends in Microbiology*, *28*(9), 732-743.

Fagerlund, A., Langsrud, S., & Møretrø, T. (2021). Microbial diversity and ecology of biofilms in food industry environments associated with *Listeria monocytogenes* persistence. *Current Opinion in Food Science*, *37*, 171-178.

Fagerlund, A., Møretrø, T., Heir, E., Briandet, R., & Langsrud, S. (2017). Cleaning and disinfection of biofilms composed of *Listeria monocytogenes* and background microbiota from meat processing surfaces. *Applied and Environmental Microbiology*, *83*(17), e01046-01017.

Fagerlund, A., Møretrø, T., Jensen, M. R., Langsrud, S., & Moen, B. (2025). Early detection and population dynamics of *Listeria monocytogenes* in naturally contaminated drains from a meat processing plant. *Frontiers in Microbiology*, *16*, 1541481.

Fan, Y., Qiao, J., Lu, Z., Fen, Z., Tao, Y., Lv, F., Zhao, H., Zhang, C., & Bie, X. (2020). Influence of different factors on biofilm formation of *Listeria monocytogenes* and the regulation of cheY gene. *Food Research International*, *137*, 109405.

Fernández-Gómez, P., Oliveira, M., Cobo-Díaz, J. F., González-Raurich, M., Múgica-Vidal, R., Alba-Elías, F., Prieto, M., Alvarez-Ordóñez, A., & López, M. (2023). The background microbiota and sanitization agent drive the fate of *Listeria monocytogenes* in multispecies biofilms formed on a plasma-polymerized coating applied on stainless-steel. *International Journal of Food Microbiology*, *386*, 110017.

Flemming, H.-C., van Hullebusch, E. D., Neu, T. R., Nielsen, P. H., Seviour, T., Stoodley, P., Wingender, J., & Wuertz, S. (2023). The biofilm matrix: multitasking in a shared space. *Nature Reviews Microbiology*, *21*(2), 70-86.

Flemming, H.-C., & Wingender, J. (2010). The biofilm matrix. *Nature Reviews Microbiology*, *8*(9), 623-633.

Flemming, H.-C., Wingender, J., Szewzyk, U., Steinberg, P., Rice, S. A., & Kjelleberg, S. (2016). Biofilms: an emergent form of bacterial life. *Nature Reviews Microbiology*, *14*(9), 563-575.

Floyd, K., Eberly, A., & Hadjifrangiskou, M. (2017). Adhesion of bacteria to surfaces and biofilm formation on medical devices. In *Biofilms and Implantable Medical Devices*, 47-95. Woodhead Publishing.

Foster, J. S., & Kolenbrander, P. E. (2004). Development of a multispecies oral bacterial community in a saliva-conditioned flow cell. *Applied and Environmental Microbiology*, *70*(7), 4340-4348.

Frank, J. F., Gillett, R. A., & Ware, G. O. (1990). Association of *Listeria* spp. contamination in the dairy processing plant environment with the presence of staphylococci. *Journal of Food Protection*, *53*(11), 928-932.

Fu, H., Chen, F., Liu, W., Kong, W., Wang, C., Fang, X., & Ye, J. (2020). Adding nutrients to the biocontrol strain JK-SH007 promotes biofilm formation and improves resistance to stress. *AMB Express*, *10*(1), 32.

Fukami, T. (2015). Historical contingency in community assembly: integrating niches, species pools, and priority effects. *Annual Review of Ecology, Evolution, and Systematics*, *46*(1), 1-23.

Fysun, O., Kern, H., Wilke, B., & Langowski, H.-C. (2019). Evaluation of factors influencing dairy biofilm formation in filling hoses of food-processing equipment. *Food and Bioproducts Processing*, *113*, 39-48.

Gannesen, A., Zhurina, M., Veselova, M., Khmel', I., & Plakunov, V. (2015). Regulation of biofilm formation by *Pseudomonas chlororaphis* in an in vitro system. *Microbiology*, *84*, 319-327.

Gao, B., Cai, H., Xu, B., Yang, F., Dou, X., Dong, Q., Yan, H., Bu, X., & Li, Z. (2024). Growth, biofilm formation, and motility of *Listeria monocytogenes* strains isolated from food and clinical samples located in Shanghai (China). *Food Research International*, *184*, 114232.

Gao, H., & Liu, C. (2014). Biochemical and morphological alteration of *Listeria monocytogenes* under environmental stress caused by chloramine-T and sodium hypochlorite. *Food Control*, *46*, 455-461.

García-Curiel, L., del Rocío López-Cuellar, M., Rodríguez-Hernández, A. I., & Chavarría-Hernández, N. (2021). Toward understanding the signals of bacteriocin production by *Streptococcus* spp. and their importance in current applications. *World Journal of Microbiology and Biotechnology*, *37*, 1-14.

Gensollen, T., Iyer, S. S., Kasper, D. L., & Blumberg, R. S. (2016). How colonization by microbiota in early life shapes the immune system. *Science*, *352*(6285), 539-544.

Ghadakpour, M., Bester, E., Liss, S. N., Gardam, M., Droppo, I., Hota, S., & Wolfaardt, G. M. (2014). Integration and proliferation of *Pseudomonas aeruginosa* PA01 in multispecies biofilms. *Microbial Ecology*, *68*(1), 121-131.

Gibbons, S. M., Kearney, S. M., Smillie, C. S., & Alm, E. J. (2017). Two dynamic regimes in the human gut microbiome. *PLoS Computational Biology*, *13*(2), e1005364.

Giotis, E. S., Blair, I. S., & McDowell, D. A. (2007). Morphological changes in *Listeria monocytogenes* subjected to sublethal alkaline stress. *International Journal of Food Microbiology*, *120*(3), 250-258.

Goeres, D. M., Loetterle, L. R., Hamilton, M. A., Murga, R., Kirby, D. W., & Donlan, R. M. (2005). Statistical assessment of a laboratory method for growing biofilms. *Microbiology*, *151*(3), 757-762.

Gomes, I., Lemos, M., Mathieu, L., Simões, M., & Simões, L. C. (2018). The action of chemical and mechanical stresses on single and dual species biofilm removal of drinking water bacteria. *Science of the Total Environment*, *631*, 987-993.

Gomes, I. B., Lemos, M., Fernandes, S., Borges, A., Simões, L. C., & Simões, M. (2021). The effects of chemical and mechanical stresses on *Bacillus cereus* and *Pseudomonas fluorescens* single-and dual-species biofilm removal. *Microorganisms*, *9*(6), 1174.

Gordon, V. D., & Wang, L. (2019). Bacterial mechanosensing: the force will be with you, always. *Journal of Cell Science*, *132*(7), jcs227694.

Gough, N., & Dodd, C. (1998). The survival and disinfection of *Salmonella* Typhimurium on chopping board surfaces of wood and plastic. *Food Control*, *9*(6), 363-368.

Gounadaki, A. S., Skandamis, P. N., Drosinos, E. H., & Nychas, G.-J. E. (2008). Microbial ecology of food contact surfaces and products of small-scale facilities producing traditional sausages. *Food Microbiology*, *25*(2), 313-323.

Gu, T., Luo, Y., Jia, Z., Meesrison, A., Lin, S., Ventresca, I. J., Brooks, S. J., Sharma, A., Sriram, S., & Yang, M. (2024). Surface topography and chemistry of food contact substances, and microbial nutrition affect pathogen persistence and symbiosis in cocktail *Listeria monocytogenes* biofilms. *Food Control*, *161*, 110391.

Gubner, R., & Beech, I. (2000). The effect of extracellular polymeric substances on the attachment of *Pseudomonas* NCIMB 2021 to AISI 304 and 316 stainless-steel. *Biofouling*, *15*(1-3), 25-36.

Guerreiro, D. N., Wu, J., Dessaux, C., Oliveira, A. H., Tiensuu, T., Gudynaite, D., Marinho, C. M., Boyd, A., García-del Portillo, F., & Johansson, J. (2020). Mild stress conditions during laboratory culture promote the proliferation of mutations that negatively affect sigma B activity in *Listeria monocytogenes*. *Journal of Bacteriology*, *202*(9), 10.1128/jb. 00751-00719.

Guillonneau, R., Baraquet, C., Bazire, A., & Molmeret, M. (2018). Multispecies biofilm development of marine bacteria implies complex relationships through competition and synergy and modification of matrix components. *Frontiers in Microbiology*, 1960.

Haagensen, J. A., Hansen, S. K., Christensen, B. B., Pamp, S. J., & Molin, S. (2015). Development of spatial distribution patterns by biofilm cells. *Applied and Environmental Microbiology*, *81*(18), 6120-6128.

Habimana, O., Guillier, L., Kulakauskas, S., & Briandet, R. (2011). Spatial competition with *Lactococcus lactis* in mixed-species continuous-flow biofilms inhibits *Listeria monocytogenes* growth. *Biofouling*, *27*(9), 1065-1072.

Habimana, O., Meyrand, M., Meylheuc, T., Kulakauskas, S., & Briandet, R. (2009). Genetic features of resident biofilms determine attachment of *Listeria monocytogenes*. *Applied and Environmental Microbiology*, *75*(24), 7814-7821.

Hansen, S. K., Haagensen, J. A., Gjermansen, M., Jørgensen, T. M., Tolker-Nielsen, T., & Molin, S. (2007). Characterization of a *Pseudomonas putida* rough variant evolved in a mixed-species biofilm with Acinetobacter sp. strain C6. *Journal of Bacteriology*, *189*(13), 4932-4943.

Hardie, K. R., & Heurlier, K. (2008). Establishing bacterial communities by 'word of mouth': LuxS and autoinducer 2 in biofilm development. *Nature Reviews Microbiology*, *6*(8), 635-643.

Harmsen, M., Lappann, M., Knøchel, S., & Molin, S. (2010). Role of extracellular DNA during biofilm formation by *Listeria monocytogenes*. *Applied and Environmental Microbiology*, *76*(7), 2271-2279.

Hascoët, A.-S., Ripolles-Avila, C., Cervantes-Huamán, B. R., & Rodríguez-Jerez, J. J. (2021). In vitro preformed biofilms of *Bacillus safensis* inhibit the adhesion and subsequent development of *Listeria monocytogenes* on stainless-steel surfaces. *Biomolecules*, *11*(3), 475.

Hascoët, A.-S., Ripolles-Avila, C., Guerrero-Navarro, A. E., & Rodríguez-Jerez, J. J. (2019). Microbial ecology evaluation of an Iberian pig processing plant through implementing SCH sensors and the influence of the resident microbiota on *Listeria monocytogenes*. *Applied Sciences*, *9*(21), 4611.

Hazeleger, W. C., Dalvoorde, M., & Beumer, R. R. (2006). Fluorescence microscopy of NaCl-stressed, elongated *Salmonella* and *Listeria* cells reveals the presence of septa in filaments. *International Journal of Food Microbiology*, *112*(3), 288-290.

Hekmat, D., Stephan, M., Bauer, R., Feuchtinger, A., & Vortmeyer, D. (2006). Modelling of multispecies biofilm population dynamics in a trickle-bed bioreactor used for waste gas treatment. *Process Biochemistry*, *41*(6), 1409-1416.

Henriques, A. O., Glaser, P., Piggot, P. J., & Moran Jr, C. P. (1998). Control of cell shape and elongation by the rodA gene in *Bacillus subtilis*. *Molecular microbiology*, *28*(2), 235-247.

Heydorn, A., Nielsen, A. T., Hentzer, M., Sternberg, C., Givskov, M., Ersbøll, B. K., & Molin, S. (2000). Quantification of biofilm structures by the novel computer program COMSTAT. *Microbiology*, *146*(10), 2395-2407.

Hilbert, L. R., Bagge-Ravn, D., Kold, J., & Gram, L. (2003). Influence of surface roughness of stainless-steel on microbial adhesion and corrosion resistance. *International Biodeterioration & Biodegradation*, *52*(3), 175-185.

Hobley, L., Harkins, C., MacPhee, C. E., & Stanley-Wall, N. R. (2015). Giving structure to the biofilm matrix: an overview of individual strategies and emerging common themes. *FEMS Microbiology Reviews*, *39*(5), 649-669.

Holt, J. D., Schultz, D., & Nadell, C. D. (2024). Dispersal of a dominant competitor can drive multispecies coexistence in biofilms. *Current Biology*, *34*(18), 4129-4142. e4124.

Hosni, T., Moretti, C., Devescovi, G., Suarez-Moreno, Z. R., Fatmi, M. B., Guarnaccia, C., Pongor, S., Onofri, A., Buonaurio, R., & Venturi, V. (2011). Sharing of quorum-sensing signals and role of interspecies communities in a bacterial plant disease. *The ISME Journal*, *5*(12), 1857-1870.

Houry, A., Gohar, M., Deschamps, J., Tischenko, E., Aymerich, S., Gruss, A., & Briandet, R. (2012). Bacterial swimmers that infiltrate and take over the biofilm matrix. *Proceedings of the National Academy of Sciences*, *109*(32), 13088-13093.

Hua, Z., Younce, F., Tang, J., Ryu, D., Rasco, B., Hanrahan, I., & Zhu, M.-J. (2021). Efficacy of saturated steam against *Listeria innocua* biofilm on common food-contact surfaces. *Food Control*, *125*, 107988.

Huang, H., Peng, C., Peng, P., Lin, Y., Zhang, X., & Ren, H. (2019). Towards the biofilm characterization and regulation in biological wastewater treatment. *Applied Microbiology and Biotechnology*, *103*(3), 1115-1129.

Huang, R., Li, M., & Gregory, R. L. (2011). Bacterial interactions in dental biofilm. *Virulence*, *2*(5), 435-444.

Hui, Y. W., Narayanan, K., & Dykes, G. A. (2016). Control of Attachment of *Pseudomonas aeruginosa* and *Burkholderia cepacia* to Surfaces by Shear Force. *Water Environment Research*, *88*(11), 2040-2046.

Hwang, G., Kang, S., El-Din, M. G., & Liu, Y. (2012). Impact of an extracellular polymeric substance (EPS) precoating on the initial adhesion of *Burkholderia cepacia* and *Pseudomonas aeruginosa*. *Biofouling*, *28*(6), 525-538.

Hwang, G., Liang, J., Kang, S., Tong, M., & Liu, Y. (2013). The role of conditioning film formation in *Pseudomonas aeruginosa* PAO1 adhesion to inert surfaces in aquatic environments. *Biochemical Engineering Journal*, *76*, 90-98.

Ibusquiza, P. S., Herrera, J. J., Vázquez-Sánchez, D., & Cabo, M. L. (2012). Adherence kinetics, resistance to benzalkonium chloride and microscopic analysis of mixed biofilms formed by *Listeria monocytogenes* and *Pseudomonas putida*. *Food Control*, *25*(1), 202-210.

Jacobs, A., & Chenia, H. (2009). Biofilm-forming capacity, surface hydrophobicity and aggregation characteristics of *Myroides odoratus* isolated from South African *Oreochromis mossambicus* fish. *Journal of Applied Microbiology*, *107*(6), 1957-1966.

Jahid, I. K., & Ha, S. D. (2014). The paradox of mixed-species biofilms in the context of food safety. *Comprehensive Reviews in Food Science and Food Safety*, *13*(5), 990-1011.

Jayathilake, P. G., Jana, S., Rushton, S., Swailes, D., Bridgens, B., Curtis, T., & Chen, J. (2017). Extracellular polymeric substance production and aggregated bacteria colonization influence the competition of microbes in biofilms. *Frontiers in Microbiology*, *8*, 1865.

Jeanson, S., Floury, J., Gagnaire, V., Lortal, S., & Thierry, A. (2015). Bacterial colonies in solid media and foods: a review on their growth and interactions with the micro-environment. *Frontiers in Microbiology*, *6*, 1284.

Jha, P. K., Dallagi, H., Richard, E., Benezech, T., & Faille, C. (2020). Formation and resistance to cleaning of biofilms at air-liquid-wall interface. Influence of bacterial strain and material. *Food Control*, *118*, 107384.

Jiang, L., Yue, Y., Zhong, K., Wu, Y., & Gao, H. (2025). Antibiofilm mechanism of pyrrole-2-carboxylic acid by impairing flagellar motility of *Listeria monocytogenes* and its application in cheese. *Food Control*, *168*, 110974.

Jones, T. H., Vail, K. M., & McMullen, L. M. (2013). Filament formation by foodborne bacteria under sublethal stress. *International Journal of Food Microbiology*, *165*(2), 97-110.

Joshi, R. V., Gunawan, C., & Mann, R. (2021). We are one: multispecies metabolism of a biofilm consortium and their treatment strategies. *Frontiers in Microbiology*, *12*, 635432.

Jydegaard-Axelsen, A.M., Aaes-Jørgensen, A., Koch, A. G., Jensen, J. S., & Knøchel, S. (2005). Changes in growth, rRNA content, and cell morphology of *Listeria monocytogenes* induced by CO_2 up-and downshift. *International Journal of Food Microbiology*, 98(2), 145-155.

Kale, S. B., Doijad, S. P., Poharkar, K. V., Garg, S., Pathak, A. D., Raorane, A. V., Rawool, D. B., Kurkure, N. V., & Barbuddhe, S. B. (2017). Elucidation of the role of the minC gene in filament formation by *Listeria monocytogenes* under stress conditions. *International Journal of Current Research and Review*, *9*, 10.

Karasz, D. C., Weaver, A. I., Buckley, D. H., & Wilhelm, R. C. (2022). Conditional filamentation as an adaptive trait of bacteria and its ecological significance in soils. *Environmental Microbiology*, 24(1), 1-17.

Karatan, E., & Watnick, P. (2009). Signals, regulatory networks, and materials that build and break bacterial biofilms. *Microbiology and molecular biology reviews*, *73*(2), 310-347.

Kart, D., Tavernier, S., Van Acker, H., Nelis, H. J., & Coenye, T. (2014). Activity of disinfectants against multispecies biofilms formed by *Staphylococcus aureus*, *Candida albicans* and *Pseudomonas aeruginosa*. *Biofouling*, *30*(3), 377-383.

Kim, D., Sengupta, A., Niepa, T. H., Lee, B.-H., Weljie, A., Freitas-Blanco, V. S., Murata, R. M., Stebe, K. J., Lee, D., & Koo, H. (2017). *Candida albicans* stimulates *Streptococcus*

mutans microcolony development via cross-kingdom biofilm-derived metabolites. *Scientific Reports*, *7*(1), 1-14.

Kim, M. K., Drescher, K., Pak, O. S., Bassler, B. L., & Stone, H. A. (2014). Filaments in curved streamlines: rapid formation of *Staphylococcus aureus* biofilm streamers. *New Journal of Physics*, *16*(6), 065024.

Kim, U., Kim, J.-H., & Oh, S.W. (2022). Review of multi-species biofilm formation from foodborne pathogens: Multi-species biofilms and removal methodology. *Critical Reviews in Food Science and Nutrition*, *62*(21), 5783-5793.

Kim, U., & Oh, S.W. (2024a). Antimicrobial resistance induction potential of grapefruit seed extract on multi-species biofilm of *E. coli* in food industry. *International Journal of Food Microbiology*, *424*, 110849.

Kim, U., & Oh, S.W. (2024b). Characterizing the formation and cross-contamination potential of multi-species biofilms in poultry processing environments: *S*. Enteritidis, *C. jejuni* and *C. perfringens*. *Food Control*, *163*, 110481.

Kim, W., Racimo, F., Schluter, J., Levy, S. B., & Foster, K. R. (2014). Importance of positioning for microbial evolution. *Proceedings of the National Academy of Sciences*, *111*(16), E1639-E1647.

Kirisits, M. J., & Parsek, M. R. (2006). Does *Pseudomonas aeruginosa* use intercellular signalling to build biofilm communities? *Cellular Microbiology*, *8*(12), 1841-1849.

Klančnik, A., Šimunović, K., Sterniša, M., Ramić, D., Smole Možina, S., & Bucar, F. (2021). Anti-adhesion activity of phytochemicals to prevent *Campylobacter jejuni* biofilm formation on abiotic surfaces. *Phytochemistry Reviews*, *20*, 55-84.

Klausen, M., Heydorn, A., Ragas, P., Lambertsen, L., Aaes-Jørgensen, A., Molin, S., & Tolker-Nielsen, T. (2003). Biofilm formation by *Pseudomonas aeruginosa* wild type, flagella and type IV pili mutants. *Molecular Microbiology*, *48*(6), 1511-1524.

Kocot, A. M., & Olszewska, M. A. (2020). Interaction of *Pseudomonas aeruginosa* and *Staphylococcus aureus* with *Listeria innocua* in dual species biofilms and inactivation following disinfectant treatments. *LWT*, *118*, 108736.

Kolenbrander, P. E., Palmer Jr, R. J., Periasamy, S., & Jakubovics, N. S. (2010). Oral multispecies biofilm development and the key role of cell–cell distance. *Nature Reviews Microbiology*, *8*(7), 471-480.

Kreth, J., Merritt, J., Shi, W., & Qi, F. (2005). Competition and coexistence between *Streptococcus mutans* and *Streptococcus sanguinis* in the dental biofilm. *Journal of Bacteriology*, *187*(21), 7193-7203.

Kreve, S., & Dos Reis, A. C. (2021). Bacterial adhesion to biomaterials: What regulates this attachment? A review. *Japanese Dental Science Review*, *57*, 85-96.

Krsmanovic, M., Biswas, D., Ali, H., Kumar, A., Ghosh, R., & Dickerson, A. K. (2021). Hydrodynamics and surface properties influence biofilm proliferation. *Advances in Colloid and Interface Science*, *288*, 102336.

Kumar, H., Franzetti, L., Kaushal, A., & Kumar, D. (2019). *Pseudomonas fluorescens*: a potential food spoiler and challenges and advances in its detection. *Annals of Microbiology*, *69*(9), 873-883.

Kyoui, D., Hirokawa, E., Takahashi, H., Kuda, T., & Kimura, B. (2016). Effect of glucose on *Listeria monocytogenes* biofilm formation, and assessment of the biofilm's sanitation tolerance. *Biofouling*, *32*(7), 815-826.

Langsrud, S., Moen, B., Møretrø, T., Løype, M., & Heir, E. (2016). Microbial dynamics in mixed culture biofilms of bacteria surviving sanitation of conveyor belts in salmon-processing plants. *Journal of Applied Microbiology*, *120*(2), 366-378.

Lapointe, C., Deschênes, L., Ells, T. C., Bisaillon, Y., & Savard, T. (2019). Interactions between spoilage bacteria in tri-species biofilms developed under simulated meat processing conditions. *Food Microbiology*, *82*, 515-522.

Lee, K. W. K., Periasamy, S., Mukherjee, M., Xie, C., Kjelleberg, S., & Rice, S. A. (2014). Biofilm development and enhanced stress resistance of a model, mixed-species community biofilm. *The ISME Journal*, *8*(4), 894-907.

Lee, S. M., Donaldson, G. P., Mikulski, Z., Boyajian, S., Ley, K., & Mazmanian, S. K. (2013). Bacterial colonization factors control specificity and stability of the gut microbiota. *Nature*, *501*(7467), 426-429.

Léguillier, V., Pinamonti, D., Chang, C.-M., Mukherjee, R., Cossetini, A., Manzano, M., Anba-Mondoloni, J., Malet-Villemagne, J., & Vidic, J. (2024). A review and meta-analysis of *Staphylococcus aureus* prevalence in foods. *The Microbe*, *4*, 100131.

Leriche, V., & Carpentier, B. (2000). Limitation of adhesion and growth of *Listeria monocytogenes* on stainless-steel surfaces by *Staphylococcus sciuri* biofilms. *Journal of Applied Microbiology*, *88*(4), 594-605.

Li, H., Yang, Z., Khan, S. A., Walsh, L. J., Seneviratne, C. J., & Ziora, Z. M. (2024). Characteristics of metallic nanoparticles (especially silver nanoparticles) as anti-biofilm agents. *Antibiotics*, *13*(9), 819.

Li, Q., Liu, L., Guo, A., Zhang, X., Liu, W., & Ruan, Y. (2021). Formation of multispecies biofilms and their resistance to disinfectants in food processing environments: a review. *Journal of Food Protection*, *84*(12), 2071-2083.

Li, T., Wang, D., Liu, N., Ma, Y., Ding, T., Mei, Y., & Li, J. (2018). Inhibition of quorum sensing-controlled virulence factors and biofilm formation in *Pseudomonas fluorescens* by cinnamaldehyde. *International Journal of Food Microbiology*, *269*, 98-106.

Lin, Z., Wang, G., Li, S., Zhou, L., & Yang, H. (2022). Dual-species biofilms formed by *Escherichia coli* and *Salmonella* enhance chlorine tolerance. *Applied and Environmental Microbiology*, *88*(22), e01482-01422.

Lindsay, D., Killington, A., Fouhy, K., Loh, M., & Malakar, P. (2022). The CDC biofilm bioreactor is a suitable method to grow biofilms, and test their sanitiser susceptibilities, in the dairy context. *International Dairy Journal*, *126*, 105264.

Lineback, C. B., Nkemngong, C. A., Wu, S. T., Li, X., Teska, P. J., & Oliver, H. F. (2018). Hydrogen peroxide and sodium hypochlorite disinfectants are more effective against *Staphylococcus aureus* and *Pseudomonas aeruginosa* biofilms than quaternary ammonium compounds. *Antimicrobial Resistance & Infection Control*, *7*, 1-7.

Liu, W., Russel, J., Burmølle, M., Sørensen, S. J., & Madsen, J. S. (2018). Micro-scale intermixing: a requisite for stable and synergistic co-establishment in a four-species biofilm. *The ISME Journal*, *12*(8), 1940-1951.

Liu, X., Basu, U., Miller, P., & McMullen, L. M. (2014). Stress response and adaptation of *Listeria monocytogenes* 08-5923 exposed to a sublethal dose of carnocyclin A. *Applied and Environmental Microbiology*, *80*(13), 3835-3841.

Liu, X., Miller, P., Basu, U., & McMullen, L. M. (2014). Sodium chloride-induced filamentation and alternative gene expression of *fts*, *murZ*, and *gnd* in *Listeria monocytogenes* 08-5923 on vacuum-packaged ham. *FEMS Microbiology Letters*, *360*(2), 152-156.

Liu, X., Xia, X., Liu, Y., Li, Z., Shi, T., Zhang, H., & Dong, Q. (2024). Recent advances on the formation, detection, resistance mechanism, and control technology of *Listeria monocytogenes* biofilm in food industry. *Food Research International*, *180*, 114067.

Liu, Y., Shan, R., Chen, G., & Liu, L. (2020). Linking flow velocity-regulated EPS production with early-stage biofilm formation in drinking water distribution systems. *Water Supply*, *20*(4), 1253-1263.

Liu, Y., Yang, C.-H., & Li, J. (2007). Influence of extracellular polymeric substances on *Pseudomonas aeruginosa* transport and deposition profiles in porous media. *Environmental Science & Technology*, *41*(1), 198-205.

Liu, Y., Zhang, H., Wu, C., Deng, W., Wang, D., Zhao, G., Song, J., & Jiang, Y. (2016). Molecular analysis of dominant species in *Listeria monocytogenes*-positive biofilms in the drains of food processing facilities. *Applied Microbiology and Biotechnology*, *100*(7), 3165-3175.

Liu, Y., Zhang, J., & Ji, Y. (2020). Environmental factors modulate biofilm formation by *Staphylococcus aureus*. *Science Progress*, *103*(1), 0036850419898659.

Livak, K. J., & Schmittgen, T. D. (2001). Analysis of relative gene expression data using real-time quantitative PCR and the $2^{-\Delta\Delta CT}$ method. *Methods*, *25*(4), 402-408.

Lobo-Cabrera, F. J., Herrero, M. d. R., Govantes, F., & Cuetos, A. (2024). Computer simulation study of nutrient-driven bacterial biofilm stratification. *Journal of the Royal Society Interface*, *21*(215), 20230618.

Luo, A., Wang, F., Sun, D., Liu, X., & Xin, B. (2022). Formation, development, and cross-species interactions in biofilms. *Frontiers in Microbiology*, *12*, 757327.

Lynch, D., Hill, C., Field, D., & Begley, M. (2021). Inhibition of *Listeria monocytogenes* by the *Staphylococcus capitis*-derived bacteriocin capidermicin. *Food Microbiology*, *94*, 103661.

Machado, I., Lopes, S. P., Sousa, A. M., & Pereira, M. O. (2012). Adaptive response of single and binary *Pseudomonas aeruginosa* and *Escherichia coli* biofilms to benzalkonium chloride. *Journal of Basic Microbiology*, *52*(1), 43-52.

Madsen, J. S., Røder, H. L., Russel, J., Sørensen, H., Burmølle, M., & Sørensen, S. J. (2016). Coexistence facilitates interspecific biofilm formation in complex microbial communities. *Environmental Microbiology*, *18*(8), 2565-2574.

Maggio, F., Rossi, C., Chaves-López, C., Serio, A., Valbonetti, L., Pomilio, F., Chiavaroli, A. P., & Paparella, A. (2021). Interactions between *L. monocytogenes* and *P. fluorescens* in dual-species biofilms under simulated dairy processing conditions. *Foods*, *10*(1), 176.

Maillard, J.-Y., & Centeleghe, I. (2023). How biofilm changes our understanding of cleaning and disinfection. *Antimicrobial Resistance & Infection Control*, *12*(1), 95.

Makovcova, J., Babak, V., Kulich, P., Masek, J., Slany, M., & Cincarova, L. (2017). Dynamics of mono-and dual-species biofilm formation and interactions between *Staphylococcus aureus* and Gram-negative bacteria. *Microbial Biotechnology*, *10*(4), 819-832.

Mann, E. E., & Wozniak, D. J. (2012). *Pseudomonas* biofilm matrix composition and niche biology. *FEMS Microbiology Reviews*, *36*(4), 893-916.

Manville, E., Kaya, E., Yucel, U., Boyle, D., & Trinetta, V. (2023). Evaluation of *Listeria monocytogenes* biofilms attachment and formation on different surfaces using a CDC biofilm reactor. *International Journal of Food Microbiology*, *399*, 110251.

Mazaheri, T., Ripolles-Avila, C., & Rodríguez-Jerez, J. (2023). Elimination of mature *Listeria monocytogenes* biofilms formed on preconditioned and non-preconditioned surfaces after the application of cleaning treatments and their cell regeneration. *LWT*, *173*, 114316.

Meesilp, N., & Mesil, N. (2019). Effect of microbial sanitizers for reducing biofilm formation of *Staphylococcus aureus* and *Pseudomonas aeruginosa* on stainless-steel by cultivation with UHT milk. *Food Science and Biotechnology*, *28*(1), 289-296.

Melian, C., Bentencourt, E., Castellano, P., Ploper, D., Vignolo, G., & Mendoza, L. M. (2022). Biofilm genes expression of *Listeria monocytogenes* exposed to *Latilactobacillus curvatus* bacteriocins at 10° C. *International Journal of Food Microbiology*, *370*, 109648.

Melian, C., Segli, F., Gonzalez, R., Vignolo, G., & Castellano, P. (2019). Lactocin AL705 as quorum sensing inhibitor to control *Listeria monocytogenes* biofilm formation. *Journal of Applied Microbiology*, *127*(3), 911-920.

Mendez, E., Walker, D. K., Vipham, J., & Trinetta, V. (2020). The use of a CDC biofilm reactor to grow multi-strain *Listeria monocytogenes* biofilm. *Food Microbiology*, *92*, 103592.

Mettler, M. K., Parker, C. W., Venkateswaran, K., & Peyton, B. M. (2022). Antimicrobial coating efficacy for prevention of *Pseudomonas aeruginosa* biofilm growth on ISS water system materials. *Frontiers in Microbiology*, *13*, 874236.

Miao, L., Wang, C., Adyel, T. M., Zhao, J., Yan, N., Wu, J., & Hou, J. (2021). Periphytic biofilm formation on natural and artificial substrates: comparison of microbial compositions, interactions, and functions. *Frontiers in Microbiology*, *12*, 684903.

Miladi, H., Ammar, E., Ben Slama, R., Sakly, N., & Bakhrouf, A. (2013). Influence of freezing stress on morphological alteration and biofilm formation by *Listeria monocytogenes*: relationship with cell surface hydrophobicity and membrane fluidity. *Archives of Microbiology*, *195*, 705-715.

Miller, M. B., & Bassler, B. L. (2001). Quorum sensing in bacteria. *Annual Reviews in Microbiology*, *55*(1), 165-199.

Mitik-Dineva, N., Wang, J., Truong, V., Stoddart, P., Malherbe, F., Crawford, R., & Ivanova, E. (2009). Differences in colonisation of five marine bacteria on two types of glass surfaces. *Biofouling*, *25*(7), 621-631.

Molin, S., & Tolker-Nielsen, T. (2003). Gene transfer occurs with enhanced efficiency in biofilms and induces enhanced stabilisation of the biofilm structure. *Current Opinion in Biotechnology*, *14*(3), 255-261.

Moreira, J., Gomes, L., Whitehead, K., Lynch, S., Tetlow, L., & Mergulhão, F. (2017). Effect of surface conditioning with cellular extracts on *Escherichia coli* adhesion and initial biofilm formation. *Food and Bioproducts Processing*, *104*, 1-12.

Mosteller, T., & Bishop, J. (1993). Sanitizer efficacy against attached bacteria in a milk biofilm. *Journal of Food Protection*, *56*(1), 34-41.

Nadell, C. D., Ricaurte, D., Yan, J., Drescher, K., & Bassler, B. L. (2017). Flow environment and matrix structure interact to determine spatial competition in *Pseudomonas aeruginosa* biofilms. *Elife*, *6*, e21855.

Natan, G., Worlitzer, V. M., Ariel, G., & Be'er, A. (2022). Mixed-species bacterial swarms show an interplay of mixing and segregation across scales. *Scientific Reports*, *12*(1), 16500.

Nejadnik, M. R., van der Mei, H. C., Busscher, H. J., & Norde, W. (2008). Determination of the shear force at the balance between bacterial attachment and detachment in weak-adherence systems, using a flow displacement chamber. *Applied and Environmental Microbiology*, *74*(3), 916-919.

Niboucha, N., Goetz, C., Sanschagrin, L., Fontenille, J., Fliss, I., Labrie, S., & Jean, J. (2022). Comparative study of different sampling methods of biofilm formed on stainless-steel surfaces in a CDC biofilm reactor. *Frontiers in Microbiology*, *13*, 892181.

Nielsen, A. T., Tolker-Nielsen, T., Barken, K. B., & Molin, S. (2000). Role of commensal relationships on the spatial structure of a surface-attached microbial consortium. *Environmental Microbiology*, *2*(1), 59-68.

Nkemngong, C. A., Voorn, M. G., Li, X., Teska, P. J., & Oliver, H. F. (2020). A rapid model for developing dry surface biofilms of *Staphylococcus aureus* and *Pseudomonas aeruginosa* for in vitro disinfectant efficacy testing. *Antimicrobial Resistance & Infection Control*, *9*, 1-9.

Norwood, D., & Gilmour, A. (2000). The growth and resistance to sodium hypochlorite of *Listeria monocytogenes* in a steady-state multispecies biofilm. *Journal of Applied Microbiology*, *88*(3), 512-520.

Okshevsky, M., & Meyer, R. L. (2015). The role of extracellular DNA in the establishment, maintenance and perpetuation of bacterial biofilms. *Critical Reviews in Microbiology*, *41*(3), 341-352.

Olsen, N. M. C., Røder, H. L., Russel, J., Madsen, J. S., Sørensen, S. J., & Burmølle, M. (2019). Priority of early colonizers but no effect on cohabitants in a synergistic biofilm community. *Frontiers in Microbiology*, *10*, 1949.

Olwal, C. O., Ang'ienda, P. O., Onyango, D. M., & Ochiel, D. O. (2018). Susceptibility patterns and the role of extracellular DNA in *Staphylococcus epidermidis* biofilm resistance to physico-chemical stress exposure. *BMC microbiology*, *18*(1), 40.

Orazi, G., & O'Toole, G. (2017). *Pseudomonas aeruginosa* alters *Staphylococcus aureus* sensitivity to vancomycin in a biofilm model of cystic fibrosis infection. *mBio* 8: e00873-17.

Palmer, J., Flint, S., & Brooks, J. (2007). Bacterial cell attachment, the beginning of a biofilm. *Journal of Industrial Microbiology and Biotechnology*, *34*(9), 577-588.

Pang, X., Chen, L., & Yuk, H.-G. (2020). Stress response and survival of *Salmonella* Enteritidis in single and dual species biofilms with *Pseudomonas fluorescens* following repeated exposure to quaternary ammonium compounds. *International Journal of Food Microbiology*, *325*, 108643.

Pang, X., Wong, C., Chung, H.-J., & Yuk, H.-G. (2019). Biofilm formation of *Listeria monocytogenes* and its resistance to quaternary ammonium compounds in a simulated salmon processing environment. *Food Control*, *98*, 200-208.

Pang, X., Yang, Y., & Yuk, H. (2017). Biofilm formation and disinfectant resistance of *Salmonella* sp. in mono-and dual-species with *Pseudomonas aeruginosa*. *Journal of Applied Microbiology*, *123*(3), 651-660.

Pang, X., & Yuk, H.-G. (2019). Effects of the colonization sequence of *Listeria monocytogenes* and *Pseudomonas fluorescens* on survival of biofilm cells under food-related stresses and transfer to salmon. *Food Microbiology*, *82*, 142-150.

Papaioannou, E., Giaouris, E. D., Berillis, P., & Boziaris, I. S. (2018). Dynamics of biofilm formation by *Listeria monocytogenes* on stainless-steel under mono-species and mixed-culture simulated fish processing conditions and chemical disinfection challenges. *International Journal of Food Microbiology*, *267*, 9-19.

Parijs, I., & Steenackers, H. P. (2018). Competitive inter-species interactions underlie the increased antimicrobial tolerance in multispecies brewery biofilms. *The ISME Journal*, *12*(8), 2061-2075.

Park, J., Muhammad, B. L., Kim, T., Bui, Q. T. N., Kim, H.-S., Shin, K., Hyun, B., Kang, J.-H., & Ki, J.-S. (2025). Assessment of ship hull-attached marine diatoms: species composition and reattachment. *Marine Pollution Bulletin*, *216*, 117962.

Passos da Silva, D., Schofield, M. C., Parsek, M. R., & Tseng, B. S. (2017). An update on the sociomicrobiology of quorum sensing in gram-negative biofilm development. *Pathogens*, *6*(4), 51.

Paul, E., Ochoa, J. C., Pechaud, Y., Liu, Y., & Liné, A. (2012). Effect of shear stress and growth conditions on detachment and physical properties of biofilms. *Water Research*, *46*(17), 5499-5508.

Paula, A. J., Hwang, G., & Koo, H. (2020). Dynamics of bacterial population growth in biofilms resemble spatial and structural aspects of urbanization. *Nature Communications*, *11*(1), 1354.

Paz-Méndez, A. M., Lamas, A., Vázquez, B., Miranda, J. M., Cepeda, A., & Franco, C. M. (2017). Effect of food residues in biofilm formation on stainless-steel and polystyrene surfaces by *Salmonella enterica* strains isolated from poultry houses. *Foods*, *6*(12), 106.

Pereira, M. O., Kuehn, M., Wuertz, S., Neu, T., & Melo, L. F. (2002). Effect of flow regime on the architecture of a *Pseudomonas fluorescens* biofilm. *Biotechnology and Bioengineering*, *78*(2), 164-171.

Pérez-Ibarreche, M., Castellano, P., Leclercq, A., & Vignolo, G. (2016). Control of *Listeria monocytogenes* biofilms on industrial surfaces by the bacteriocin-producing *Lactobacillus sakei* CRL1862. *FEMS Microbiology Letters*, *363*(12), fnw118.

Periasamy, S., & Kolenbrander, P. E. (2010). Central role of the early colonizer *Veillonella* sp. in establishing multispecies biofilm communities with initial, middle, and late colonizers of enamel. *American Society for Microbiology*.

Periasamy, S., Nair, H. A., Lee, K. W., Ong, J., Goh, J. Q., Kjelleberg, S., & Rice, S. A. (2015). *Pseudomonas aeruginosa* PAO1 exopolysaccharides are important for mixed species biofilm community development and stress tolerance. *Frontiers in Microbiology*, *6*, 851.

Perni, S., Jordan, S. J., Andrew, P. W., & Shama, G. (2006). Biofilm development by *Listeria innocua* in turbulent flow regimes. *Food Control*, *17*(11), 875-883.

Poimenidou, S. V., Caccia, N., Paramithiotis, S., Hébraud, M., Nychas, G.-J., & Skandamis, P. N. (2023). Influence of temperature on regulation of key virulence and stress response genes in *Listeria monocytogenes* biofilms. *Food Microbiology*, *111*, 104190.

Pouget, C., Dunyach-Remy, C., Pantel, A., Schuldiner, S., Sotto, A., & Lavigne, J.P. (2020). Biofilms in diabetic foot ulcers: significance and clinical relevance. *Microorganisms*, *8*(10), 1580.

Prabhukhot, G. S., Eggleton, C. D., Kim, M., & Patel, J. (2024). Impact of surface topography and hydrodynamic flow conditions on single and multispecies biofilm formation by *Escherichia coli* O157: H7 and *Listeria monocytogenes* in presence of promotor bacteria. *LWT*, 116240.

Prabhukhot, G. S., Eggleton, C. D., & Patel, J. (2023). Multispecies bacterial biofilms and their evaluation using bioreactors. *Foods*, *12*(24), 4495.

Prabhukhot, G. S., Eggleton, C. D., Vinyard, B., & Patel, J. (2024). Using Bio-inline reactor to evaluate sanitizer efficacy in removing dual-species biofilms formed by *Escherichia coli* O157: H7 and *Listeria monocytogenes*. *Journal of Food Protection*, 100314.

Puga, C., Orgaz, B., Muñoz, S., & SanJose, C. (2015). Cold stress and presence of *Pseudomonas fluorescens* affect *Listeria monocytogenes* biofilm structure and response to chitosan. *Mol. Genet. Med*, *9*, 1-6.

Puga, C., SanJose, C., & Orgaz, B. (2016). Biofilm development at low temperatures enhances *Listeria monocytogenes* resistance to chitosan. *Food Control*, *65*, 143-151.

Puga, C. H., Dahdouh, E., SanJose, C., & Orgaz, B. (2018). *Listeria monocytogenes* colonizes *Pseudomonas fluorescens* biofilms and induces matrix over-production. *Frontiers in Microbiology*, *9*, 1706.

Puga, C. H., Orgaz, B., & SanJose, C. (2016). *Listeria monocytogenes* impact on mature or old *Pseudomonas fluorescens* biofilms during growth at 4 and 20 C. *Frontiers in Microbiology*, *7*, 134.

Raghupathi, P. K., Liu, W., Sabbe, K., Houf, K., Burmølle, M., & Sørensen, S. J. (2018). Synergistic interactions within a multispecies biofilm enhance individual species protection against grazing by a pelagic protozoan. *Frontiers in Microbiology*, *8*, 2649.

Ramstedt, M., & Burmølle, M. (2022). Can multi-species biofilms defeat antimicrobial surfaces on medical devices? *Current Opinion in Biomedical Engineering*, *22*, 100370.

Ran, Y., Qingmin, C., & Maorun, F. (2019). Chlorine dioxide generation method and its action mechanism for removing harmful substances and maintaining quality attributes of agricultural products. *Food and Bioprocess Technology*, *12*, 1110-1122.

Redding, M., Zheng, J., Mowery, J., Gu, G., Bolten, S., Luo, Y., & Nou, X. (2024). Microscopic and transcriptomic characterization of *Listeria monocytogenes* aggregation and biofilm formation in cantaloupe juice. *Food Control*, *158*, 110243.

Ren, D., Madsen, J. S., Sørensen, S. J., & Burmølle, M. (2015). High prevalence of biofilm synergy among bacterial soil isolates in cocultures indicates bacterial interspecific cooperation. *The ISME Journal*, *9*(1), 81-89.

Rendueles, O., & Ghigo, J.-M. (2012). Multi-species biofilms: how to avoid unfriendly neighbors. *FEMS Microbiology Reviews*, *36*(5), 972-989.

Rickard, A. H., McBain, A. J., Stead, A. T., & Gilbert, P. (2004). Shear rate moderates community diversity in freshwater biofilms. *Applied and Environmental Microbiology*, *70*(12), 7426-7435.

Rieu, A., Briandet, R., Habimana, O., Garmyn, D., Guzzo, J., & Piveteau, P. (2008). *Listeria monocytogenes* EGD-e biofilms: no mushrooms but a network of knitted chains. *Applied and Environmental Microbiology*, 74(14), 4491-4497.

Ripolles-Avila, C., Guitan-Santamaria, M., Pizarro-Giménez, K., Mazaheri, T., & Rodríguez-Jerez, J. J. (2022). Dual-species biofilms formation between dominant microbiota isolated from a meat processing industry with *Listeria monocytogenes* and *Salmonella enterica*: Unraveling their ecological interactions. *Food Microbiology*, *105*, 104026.

Ripolles-Avila, C., Hascoët, A., Guerrero-Navarro, A., & Rodríguez-Jerez, J. (2018). Establishment of incubation conditions to optimize the in vitro formation of mature *Listeria monocytogenes* biofilms on food-contact surfaces. *Food Control*, *92*, 240-248.

Rismondo, J., Halbedel, S., & Gründling, A. (2019). Cell shape and antibiotic resistance are maintained by the activity of multiple FtsW and RodA enzymes in *Listeria monocytogenes*. *MBio*, *10*(4).

Rivett, D. W., Scheuerl, T., Culbert, C. T., Mombrikotb, S. B., Johnstone, E., Barraclough, T. G., & Bell, T. (2016). Resource-dependent attenuation of species interactions during bacterial succession. *The ISME Journal*, *10*(9), 2259-2268.

Rocha, R., Sousa, J. M., Cerqueira, L., Vieira, M. J., Almeida, C., & Azevedo, N. F. (2019). Development and application of peptide nucleic acid fluorescence in situ hybridization for the specific detection of *Listeria monocytogenes*. *Food Microbiology*, *80*, 1-8.

Røder, H. L., Olsen, N. M., Whiteley, M., & Burmølle, M. (2020). Unravelling interspecies interactions across heterogeneities in complex biofilm communities. *Environmental Microbiology*, *22*(1), 5-16.

Røder, H. L., Sørensen, S. J., & Burmølle, M. (2016). Studying bacterial multispecies biofilms: where to start? *Trends in Microbiology*, *24*(6), 503-513.

Rodesney, C. A., Roman, B., Dhamani, N., Cooley, B. J., Katira, P., Touhami, A., & Gordon, V. D. (2017). Mechanosensing of shear by *Pseudomonas aeruginosa* leads to increased

levels of the cyclic-di-GMP signal initiating biofilm development. *Proceedings of the National Academy of Sciences*, *114*(23), 5906-5911.

Rodríguez-Campos, D., Rodríguez-Melcón, C., Alonso-Calleja, C., & Capita, R. (2019). Persistent *Listeria monocytogenes* isolates from a poultry-processing facility form more biofilm but do not have a greater resistance to disinfectants than sporadic strains. *Pathogens*, *8*(4), 250.

Rodríguez-López, P., Rodríguez-Herrera, J. J., & López Cabo, M. (2022). Architectural Features and Resistance to Food-Grade Disinfectants in *Listeria monocytogenes*-*Pseudomonas* spp. Dual-Species Biofilms. *Frontiers in Microbiology*, *13*, 917964.

Rodríguez-López, P., Saá-Ibusquiza, P., Mosquera-Fernández, M., & López-Cabo, M. (2015). *Listeria monocytogenes*-carrying consortia in food industry. Composition, subtyping and numerical characterisation of mono-species biofilm dynamics on stainless-steel. *International Journal of Food Microbiology*, *206*, 84-95.

Rodríguez-Melcón, C., Alonso-Calleja, C., García-Fernández, C., Carballo, J., & Capita, R. (2021). Minimum inhibitory concentration (MIC) and minimum bactericidal concentration (MBC) for twelve antimicrobials (biocides and antibiotics) in eight strains of *Listeria monocytogenes*. *Biology*, *11*(1), 46.

Rodríguez-Melcón, C., Alonso-Hernando, A., Riesco-Peláez, F., García-Fernández, C., Alonso-Calleja, C., & Capita, R. (2021). Biovolume and spatial distribution of foodborne Gram-negative and Gram-positive pathogenic bacteria in mono-and dual-species biofilms. *Food Microbiology*, *94*, 103616.

Rodríguez-Melcón, C., Riesco-Peláez, F., García-Fernández, C., Alonso-Calleja, C., & Capita, R. (2019). Susceptibility of *Listeria monocytogenes* planktonic cultures and biofilms to sodium hypochlorite and benzalkonium chloride. *Food Microbiology*, *82*, 533-540.

Rodriguez, A., Autio, W. R., & Mclandsborough, L. A. (2008). Effect of surface roughness and stainless-steel finish on *Listeria monocytogenes* attachment and biofilm formation. *Journal of Food Protection*, *71*(1), 170-175.

Rolon, M. L., Tan, X., Chung, T., Gonzalez-Escalona, N., Chen, Y., Macarisin, D., LaBorde, L. F., & Kovac, J. (2023). The composition of environmental microbiota in three tree fruit packing facilities changed over seasons and contained taxa indicative of *L. monocytogenes* contamination. *Microbiome*, *11*(1), 128.

Rolon, M. L., Voloshchuk, O., Bartlett, K. V., LaBorde, L. F., & Kovac, J. (2024). Multi-species biofilms of environmental microbiota isolated from fruit packing facilities

promoted tolerance of *Listeria monocytogenes* to benzalkonium chloride. *Biofilm*, *7*, 100177.

Rossi, C., Chaves-López, C., Serio, A., Goffredo, E., Goga, B. T. C., & Paparella, A. (2016). Influence of incubation conditions on biofilm formation by *Pseudomonas fluorescens* isolated from dairy products and dairy manufacturing plants. *Italian Journal of Food Safety*, *5*(3), 5793.

Roy, P. K., Ha, A. J.-W., Mizan, M. F. R., Hossain, M. I., Ashrafudoulla, M., Toushik, S. H., Nahar, S., Kim, Y. K., & Ha, S.-D. (2021). Effects of environmental conditions (temperature, pH, and glucose) on biofilm formation of *Salmonella enterica* serotype Kentucky and virulence gene expression. *Poultry Science*, *100*(7), 101209.

Rückerl, I., Muhterem-Uyar, M., Muri-Klinger, S., Wagner, K.-H., Wagner, M., & Stessl, B. (2014). *L. monocytogenes* in a cheese processing facility: learning from contamination scenarios over three years of sampling. *International Journal of Food Microbiology*, *189*, 98-105.

Rumbaugh, K. P., & Sauer, K. (2020). Biofilm dispersion. *Nature Reviews Microbiology*, *18*(10), 571-586.

Sadekuzzaman, M., Yang, S., Mizan, M., & Ha, S. (2015). Current and recent advanced strategies for combating biofilms. *Comprehensive Reviews in Food Science and Food Safety*, *14*(4), 491-509.

Sadiq, F. A., Burmølle, M., Heyndrickx, M., Flint, S., Lu, W., Chen, W., Zhao, J., & Zhang, H. (2021). Community-wide changes reflecting bacterial interspecific interactions in multispecies biofilms. *Critical Reviews in Microbiology*, *47*(3), 338-358.

Sadiq, F. A., De Reu, K., Burmølle, M., Maes, S., & Heyndrickx, M. (2023). Synergistic interactions in multispecies biofilm combinations of bacterial isolates recovered from diverse food processing industries. *Frontiers in Microbiology*, *14*, 1159434.

Sadiq, F. A., De Reu, K., Yang, N., Burmølle, M., & Heyndrickx, M. (2024). Interspecies interactions in dairy biofilms drive community structure and response against cleaning and disinfection. *Biofilm*, *7*, 100195.

Sadiq, F. A., Flint, S., Yuan, L., Li, Y., Liu, T., & He, G. (2017). Propensity for biofilm formation by aerobic mesophilic and thermophilic spore forming bacteria isolated from Chinese milk powders. *International Journal of Food Microbiology*, *262*, 89-98.

Sanchez-Vizuete, P., Orgaz, B., Aymerich, S., Le Coq, D., & Briandet, R. (2015). Pathogens protection against the action of disinfectants in multispecies biofilms. *Frontiers in Microbiology*, *6*, 705.

Santos, T., Viala, D., Chambon, C., Esbelin, J., & Hébraud, M. (2019). *Listeria monocytogenes* biofilm adaptation to different temperatures seen through shotgun proteomics. *Frontiers in Nutrition*, *6*, 89.

Saraoui, T., Fall, P. A., Leroi, F., Antignac, J.-P., Chéreau, S., & Pilet, M. F. (2016). Inhibition mechanism of *Listeria monocytogenes* by a bioprotective bacteria *Lactococcus piscium* CNCM I-4031. *Food Microbiology*, *53*, 70-78.

Sarjit, A., & Dykes, G. A. (2017). Antimicrobial activity of trisodium phosphate and sodium hypochlorite against *Salmonella* biofilms on abiotic surfaces with and without soiling with chicken juice. *Food Control*, *73*, 1016-1022.

Sasahara, K. C., & Zottola, E. A. (1993). Biofilm formation by *Listeria monocytogenes* utilizes a primary colonizing microorganism in flowing systems. *Journal of Food Protection*, *56*(12), 1022-1028.

Sauer, K., Rickard, A. H., & Davies, D. G. (2007). Biofilms and biocomplexity. *Microbe-American Society for Microbiology*, *2*(7), 347.

Sauer, K., Stoodley, P., Goeres, D. M., Hall-Stoodley, L., Burmølle, M., Stewart, P. S., & Bjarnsholt, T. (2022). The biofilm life cycle: expanding the conceptual model of biofilm formation. *Nature Reviews Microbiology*, *20*(10), 608-620.

Schauder, S., & Bassler, B. L. (2001). The languages of bacteria. *Genes & development*, *15*(12), 1468-1480.

Schilcher, K., & Horswill, A. R. (2020). Staphylococcal biofilm development: structure, regulation, and treatment strategies. *Microbiology and Molecular Biology Reviews*, *84*(3), e00026-00019.

Schlafer, S., & Meyer, R. L. (2017). Confocal microscopy imaging of the biofilm matrix. *Journal of Microbiological Methods*, *138*, 50-59.

Schmid, B., Klumpp, J., Raimann, E., Loessner, M. J., Stephan, R., & Tasara, T. (2009). Role of cold shock proteins in growth of *Listeria monocytogenes* under cold and osmotic stress conditions. *Applied and Environmental Microbiology*, *75*(6), 1621-1627.

Schwibbert, K., Menzel, F., Epperlein, N., Bonse, J., & Krüger, J. (2019). Bacterial adhesion on femtosecond laser-modified polyethylene. *Materials*, *12*(19), 3107.

Secchi, E., Savorana, G., Vitale, A., Eberl, L., Stocker, R., & Rusconi, R. (2022). The structural role of bacterial eDNA in the formation of biofilm streamers. *Proceedings of the National Academy of Sciences*, *119*(12), e2113723119.

Serra, D. O., & Hengge, R. (2014). Stress responses go three dimensional–the spatial order of physiological differentiation in bacterial macrocolony biofilms. *Environmental Microbiology*, *16*(6), 1455-1471.

Shah, M., & Bergholz, T. (2020). Variation in growth and evaluation of cross-protection in *Listeria monocytogenes* under salt and bile stress. *Journal of Applied Microbiology*, *129*(2), 367-377.

Sharma, M., & Anand, S. (2002). Characterization of constitutive microflora of biofilms in dairy processing lines. *Food Microbiology*, *19*(6), 627-636.

Sheen, S., Costa, S., & Cooke, P. (2010). Impact of Mechanical Shear on the Survival of *Listeria monocytogenes* on Surfaces. *Journal of Food Science*, *75*(6), E387-E393.

Shrout, J. D., Tolker-Nielsen, T., Givskov, M., & Parsek, M. R. (2011). The contribution of cell-cell signaling and motility to bacterial biofilm formation. *Mrs Bulletin*, *36*(5), 367-373.

Silva, A. R., Melo, L. F., Keevil, C. W., & Pereira, A. (2024). *Legionella* colonization and 3D spatial location within a *Pseudomonas* biofilm. *Scientific Reports*, *14*(1), 16781.

Simões, L. C., Gomes, I., Sousa, H., Borges, A., & Simões, M. (2022). Biofilm formation under high shear stress increases resilience to chemical and mechanical challenges. *Biofouling*, *38*(1), 1-12.

Simões, M., Pereira, M. O., Sillankorva, S., Azeredo, J., & Vieira, M. J. (2007). The effect of hydrodynamic conditions on the phenotype of *Pseudomonas fluorescens* biofilms. *Biofouling*, *23*(4), 249-258.

Simoes, M., Pereira, M. O., & Vieira, M. J. (2005). Effect of mechanical stress on biofilms challenged by different chemicals. *Water Research*, *39*(20), 5142-5152.

Simões, M., Simões, L. C., & Vieira, M. J. (2010). A review of current and emergent biofilm control strategies. *LWT-Food Science and Technology*, *43*(4), 573-583.

Singh, A. K., Prakash, P., Achra, A., Singh, G. P., Das, A., & Singh, R. K. (2017). Standardization and classification of in vitro biofilm formation by clinical isolates of *Staphylococcus aureus*. *Journal of Global Infectious Diseases*, *9*(3), 93-101.

Skowron, K., Wiktorczyk, N., Grudlewska, K., Kwiecińska-Piróg, J., Wałecka-Zacharska, E., Paluszak, Z., & Gospodarek-Komkowska, E. (2019). Drug-susceptibility, biofilm-forming ability and biofilm survival on stainless-steel of *Listeria* spp. strains isolated from cheese. *International Journal of Food Microbiology*, *296*, 75-82.

Söderling, E. M., Marttinen, A. M., & Haukioja, A. L. (2011). Probiotic lactobacilli interfere with *Streptococcus mutans* biofilm formation in vitro. *Current Microbiology*, *62*(2), 618-622.

Stepanović, S., Ćirković, I., Ranin, L., & Svabić-Vlahović, M. (2004). Biofilm formation by *Salmonella* spp. and *Listeria monocytogenes* on plastic surface. *Letters in Applied Microbiology*, *38*(5), 428-432.

Stewart, E. J., Ganesan, M., Younger, J. G., & Solomon, M. J. (2015). Artificial biofilms establish the role of matrix interactions in staphylococcal biofilm assembly and disassembly. *Scientific Reports*, *5*(1), 13081.

Stewart, E. J., Payne, D. E., Ma, T. M., VanEpps, J. S., Boles, B. R., Younger, J. G., & Solomon, M. J. (2017). Effect of antimicrobial and physical treatments on growth of multispecies staphylococcal biofilms. *Applied and Environmental Microbiology*, *83*(12), e03483-03416.

Stoodley, P., Boyle, J. D., Cunningham, A. B., Dodds, I., Lappin-Scott, H., & Lewandowski, Z. (1999). Biofilm structure and influence on biofouling under laminar and turbulent flows. In *Special Publications of the Royal Society of Chemistry* (Vol. 242). Royal Society of Chemistry.

Stoodley, P., Sauer, K., Davies, D. G., & Costerton, J. W. (2002). Biofilms as complex differentiated communities. *Annual Reviews in Microbiology*, *56*(1), 187-209.

Subramoni, S., Muzaki, M. Z. B. M., Booth, S. C., Kjelleberg, S., & Rice, S. A. (2021). N-acyl homoserine lactone-mediated quorum sensing regulates species interactions in multispecies biofilm communities. *Frontiers in Cellular and Infection Microbiology*, *11*, 646991.

Szlavik, J., Paiva, D. S., Mørk, N., van den Berg, F., Verran, J., Whitehead, K., Knøchel, S., & Nielsen, D. S. (2012). Initial adhesion of *Listeria monocytogenes* to solid surfaces under liquid flow. *International Journal of Food Microbiology*, *152*(3), 181-188.

Tadielo, L. E., Bellé, T. H., dos Santos, E. A. R., Schmiedt, J. A., Cerqueira-Cézar, C. K., Nero, L. A., Yamatogi, R. S., Pereira, J. G., & dos Santos Bersot, L. (2022). Pure and mixed biofilms formation of *Listeria monocytogenes* and *Salmonella* Typhimurium on polypropylene surfaces. *LWT*, *162*, 113469.

Takahashi, H., Suda, T., Tanaka, Y., & Kimura, B. (2010). Cellular hydrophobicity of *Listeria monocytogenes* involves initial attachment and biofilm formation on the surface of polyvinyl chloride. *Letters in Applied Microbiology*, *50*(6), 618-625.

Tamminen, M., Spaak, J., Tlili, A., Eggen, R., Stamm, C., & Räsänen, K. (2022). Wastewater constituents impact biofilm microbial community in receiving streams. *Science of the Total Environment*, *807*, 151080.

Tan, C. H., Lee, K. W. K., Burmølle, M., Kjelleberg, S., & Rice, S. A. (2017). All together now: experimental multispecies biofilm model systems. *Environmental Microbiology*, *19*(1), 42-53.

Teh, K. H., Flint, S., Palmer, J., Andrewes, P., Bremer, P., & Lindsay, D. (2014). Biofilm− An unrecognised source of spoilage enzymes in dairy products? *International Dairy Journal*, *34*(1), 32-40.

Thomassen, G. M. B., Reiche, T., Hjørungnes, M., & Mehli, L. (2023). High disinfectant tolerance in *Pseudomonas* spp. biofilm aids the survival of *Listeria monocytogenes*. *Microorganisms*, *11*(6), 1414.

Tiensuu, T., Andersson, C., Ryden, P., & Johansson, J. (2013). Cycles of light and dark co-ordinate reversible colony differentiation in *Listeria monocytogenes*. *Molecular Microbiology*, *87*(4), 909-924.

Toté, K., Berghe, D. V., Deschacht, M., De Wit, K., Maes, L., & Cos, P. (2009). Inhibitory efficacy of various antibiotics on matrix and viable mass of *Staphylococcus aureus* and *Pseudomonas aeruginosa* biofilms. *International Journal of Antimicrobial Agents*, *33*(6), 525-531.

Truong, V. K., Lapovok, R., Estrin, Y. S., Rundell, S., Wang, J. Y., Fluke, C. J., Crawford, R. J., & Ivanova, E. P. (2010). The influence of nano-scale surface roughness on bacterial adhesion to ultrafine-grained titanium. *Biomaterials*, *31*(13), 3674-3683.

Tsagkari, E., Connelly, S., Liu, Z., McBride, A., & Sloan, W. T. (2022). The role of shear dynamics in biofilm formation. *npj Biofilms and Microbiomes*, *8*(1), 33.

Tsagkari, E., & Sloan, W. (2018). Turbulence accelerates the growth of drinking water biofilms. *Bioprocess and Biosystems Engineering*, *41*, 757-770.

Tsai, Y.P. (2005). Impact of flow velocity on the dynamic behaviour of biofilm bacteria. *Biofouling*, *21*(5-6), 267-277.

Tsuneda, S., Aikawa, H., Hayashi, H., Yuasa, A., & Hirata, A. (2003). Extracellular polymeric substances responsible for bacterial adhesion onto solid surface. *FEMS Microbiology Letters*, *223*(2), 287-292.

Uneputty, A., Dávila-Lezama, A., Garibo, D., Oknianska, A., Bogdanchikova, N., Hernández-Sánchez, J. F., & Susarrey-Arce, A. (2022). Strategies applied to modify structured and

smooth surfaces: A step closer to reduce bacterial adhesion and biofilm formation. *Colloid and Interface Science Communications*, *46*, 100560.

Utratna, M., Cosgrave, E., Baustian, C., Ceredig, R. H., & O'Byrne, C. P. (2014). Effects of Growth Phase and Temperature on σB Activity within a *Listeria monocytogenes* Population: Evidence for RsbV-Independent Activation of σB at Refrigeration Temperatures. *BioMed Research International*, *2014*(1), 641647.

van der Veen, S., & Abee, T. (2010). Importance of SigB for *Listeria monocytogenes* static and continuous-flow biofilm formation and disinfectant resistance. *Applied and Environmental Microbiology*, *76*(23), 7854-7860.

Van Loosdrecht, M., Heijnen, J., Eberl, H., Kreft, J., & Picioreanu, C. (2002). Mathematical modelling of biofilm structures. *Antonie van Leeuwenhoek*, *81*(1), 245-256.

Vazquez-Armenta, F., Hernandez-Oñate, M., Martinez-Tellez, M., Lopez-Zavala, A., Gonzalez-Aguilar, G., Gutierrez-Pacheco, M., & Ayala-Zavala, J. (2020). Quercetin repressed the stress response factor (sigB) and virulence genes (*prfA*, *actA*, *inlA*, and *inlC*), lower the adhesion, and biofilm development of *L. monocytogenes*. *Food Microbiology*, *87*, 103377.

Vázquez-Boland, J. A., Kuhn, M., Berche, P., Chakraborty, T., Domínguez-Bernal, G., Goebel, W., González-Zorn, B., Wehland, J. r., & Kreft, J. r. (2001). *Listeria* pathogenesis and molecular virulence determinants. *Clinical Microbiology Reviews*, *14*(3), 584-640.

Velez, P., Espinosa-Asuar, L., Figueroa, M., Gasca-Pineda, J., Aguirre-von-Wobeser, E., Eguiarte, L. E., Hernandez-Monroy, A., & Souza, V. (2018). Nutrient dependent cross-kingdom interactions: fungi and bacteria from an oligotrophic desert oasis. *Frontiers in Microbiology*, *9*, 358832.

Voloshchuk, O., Rolon, M. L., Bartlett, K. V., Acevedo, M. M., Laborde, L. F., & Kovac, J. (2025). Pseudomonadaceae increased the tolerance of *Listeria monocytogenes* to sanitizers in multi-species biofilms. *Food Microbiology*, *128*, 104687.

von Gillhaussen, P., Rascher, U., Jablonowski, N. D., Plückers, C., Beierkuhnlein, C., & Temperton, V. M. (2014). Priority effects of time of arrival of plant functional groups override sowing interval or density effects: a grassland experiment. *PLoS One*, *9*(1), e86906.

Wagner, E. M., Pracser, N., Thalguter, S., Fischel, K., Rammer, N., Pospíšilová, L., Alispahic, M., Wagner, M., & Rychli, K. (2020). Identification of biofilm hotspots in a meat processing environment: Detection of spoilage bacteria in multi-species biofilms. *International Journal of Food Microbiology*, *328*, 108668.

Wang, C., Miao, L., Hou, J., Wang, P., Qian, J., & Dai, S. (2014). The effect of flow velocity on the distribution and composition of extracellular polymeric substances in biofilms and the detachment mechanism of biofilms. *Water Science and Technology*, *69*(4), 825-832.

Wang, H.-H., Ye, K.-P., Zhang, Q.-Q., Dong, Y., Xu, X.-L., & Zhou, G.-H. (2013). Biofilm formation of meat-borne *Salmonella enterica* and inhibition by the cell-free supernatant from *Pseudomonas aeruginosa*. *Food Control*, *32*(2), 650-658.

Wang, H., Feng, M., Anwar, T. M., Chai, W., Ed-Dra, A., Kang, X., Rantsiou, K., Kehrenberg, C., Yue, M., & Li, Y. (2023). Change in antimicrobial susceptibility of *Listeria* spp. in response to stress conditions. *Frontiers in Sustainable Food Systems*, *7*, 1179835.

Wang, J., Liu, Q., Dong, D., Hu, H., Wu, B., & Ren, H. (2020). In-situ monitoring of the unstable bacterial adhesion process during wastewater biofilm formation: a comprehensive study. *Environment International*, *140*, 105722.

Wang, N., Jin, Y., He, G., & Yuan, L. (2021). Development of multi-species biofilm formed by thermophilic bacteria on stainless-steel immerged in skimmed milk. *Food Research International*, *150*, 110754.

Wang, R., Kalchayanand, N., & Bono, J. L. (2015). Sequence of colonization determines the composition of mixed biofilms by *Escherichia coli* O157: H7 and O111: H8 strains. *Journal of Food Protection*, *78*(8), 1554-1559.

Wang, Y., Hong, X., Liu, J., Zhu, J., & Chen, J. (2020). Interactions between fish isolates *Pseudomonas fluorescens* and *Staphylococcus aureus* in dual-species biofilms and sensitivity to carvacrol. *Food Microbiology*, *91*, 103506.

Wang, Y., Sun, L., Hu, L., Wang, Z., Wang, X., & Dong, Q. (2022). Adhesion and kinetics of biofilm formation and related gene expression of *Listeria monocytogenes* in response to nutritional stress. *Food Research International*, *156*, 111143.

Wang, Z., Xiang, Q., Yang, T., Li, L., Yang, J., Li, H., He, Y., Zhang, Y., Lu, Q., & Yu, J. (2016). Autoinducer-2 of *Streptococcus mitis* as a target molecule to inhibit pathogenic multi-species biofilm formation in vitro and in an endotracheal intubation rat model. *Frontiers in Microbiology*, *7*, 88.

Wetherington, M. T., Nagy, K., Dér, L., Ábrahám, Á., Noorlag, J., Galajda, P., & Keymer, J. E. (2022). Ecological succession and the competition-colonization trade-off in microbial communities. *BMC biology*, *20*(1), 262.

Wicaksono, W. A., Erschen, S., Krause, R., Müller, H., Cernava, T., & Berg, G. (2022). Enhanced survival of multi-species biofilms under stress is promoted by low-abundant

but antimicrobial-resistant keystone species. *Journal of Hazardous Materials*, *422*, 126836.

Wijesinghe, G., Dilhari, A., Gayani, B., Kottegoda, N., Samaranayake, L., & Weerasekera, M. (2019). Influence of laboratory culture media on in vitro growth, adhesion, and biofilm formation of *Pseudomonas aeruginosa* and *Staphylococcus aureus*. *Medical Principles and Practice*, *28*(1), 28-35.

Wiktorczyk-Kapischke, N., Skowron, K., Grudlewska-Buda, K., Wałecka-Zacharska, E., Korkus, J., & Gospodarek-Komkowska, E. (2021). Adaptive response of *Listeria monocytogenes* to the stress factors in the food processing environment. *Frontiers in Microbiology*, *12*, 710085.

Wiktorczyk-Kapischke, N., Skowron, K., Wałecka-Zacharska, E., Grudlewska-Buda, K., Wnuk, K., Buszko, K., & Gospodarek-Komkowska, E. (2023). Assessment of the influence of selected stress factors on the growth and survival of *Listeria monocytogenes*. *BMC microbiology*, *23*(1), 27.

Wittig, C., Wagner, M., Vallon, R., Crouzier, T., van der Wijngaart, W., Horn, H., & Bagheri, S. (2025). The role of fluid friction in streamer formation and biofilm growth. *npj Biofilms and Microbiomes*, *11*(1), 17.

Wood, T. L., Gong, T., Zhu, L., Miller, J., Miller, D. S., Yin, B., & Wood, T. K. (2018). Rhamnolipids from *Pseudomonas aeruginosa* disperse the biofilms of sulfate-reducing bacteria. *npj Biofilms and Microbiomes*, *4*(1), 22.

Xavier, J. B., & Foster, K. R. (2007). Cooperation and conflict in microbial biofilms. *Proceedings of the National Academy of Sciences*, *104*(3), 876-881.

Xavier, J. B., Martinez-Garcia, E., & Foster, K. R. (2009). Social evolution of spatial patterns in bacterial biofilms: when conflict drives disorder. *The American Naturalist*, *174*(1), 1-12.

Xu, Z., Lu, Z., Soteyome, T., Ye, Y., Huang, T., Liu, J., Harro, J. M., Kjellerup, B. V., & Peters, B. M. (2021). Polymicrobial interaction between *Lactobacillus* and *Saccharomyces cerevisiae*: coexistence-relevant mechanisms. *Critical Reviews in Microbiology*, *47*(3), 386-396.

Xu, Z., Xie, J., Soteyome, T., Peters, B. M., Shirtliff, M. E., Liu, J., & Harro, J. M. (2019). Polymicrobial interaction and biofilms between *Staphylococcus aureus* and *Pseudomonas aeruginosa*: an underestimated concern in food safety. *Current Opinion in Food Science*, *26*, 57-64.

Yamaki, S., Kawai, Y., & Yamazaki, K. (2021). Long filamentous state of *Listeria monocytogenes* induced by sublethal sodium chloride stress poses risk of rapid increase in colony-forming units. *Food Control*, *124*, 107860.

Yamamoto, K., Haruta, S., Kato, S., Ishii, M., & Igarashi, Y. (2010). Determinative factors of competitive advantage between aerobic bacteria for niches at the air-liquid interface. *Microbes and Environments*, *25*(4), 317-320.

Yao, S., Hao, L., Zhou, R., Jin, Y., Huang, J., & Wu, C. (2022). Multispecies biofilms in fermentation: Biofilm formation, microbial interactions, and communication. *Comprehensive Reviews in Food Science and Food Safety*, *21*(4), 3346-3375.

Yuan, L., Hansen, M. F., Røder, H. L., Wang, N., Burmølle, M., & He, G. (2020). Mixed-species biofilms in the food industry: Current knowledge and novel control strategies. *Critical Reviews in Food Science and Nutrition*, *60*(13), 2277-2293.

Yuan, L., Sadiq, F. A., Burmølle, M., Liu, T., & He, G. (2018). Insights into bacterial milk spoilage with particular emphasis on the roles of heat-stable enzymes, biofilms, and quorum sensing. *Journal of Food Protection*, *81*(10), 1651-1660.

Yuan, L., Wang, N., Sadiq, F. A., & He, G. (2020). Interspecies interactions in dual-species biofilms formed by psychrotrophic bacteria and the tolerance of sessile communities to disinfectants. *Journal of Food Protection*, *83*(6), 951-958.

Yuan, S., Yu, Z., Pan, S., Huang, J., & Meng, F. (2020). Deciphering the succession dynamics of dominant and rare genera in biofilm development process. *Science of the Total Environment*, *739*, 139961.

Yushina, Y. K., Zaiko, E., Grudistova, M., Semenova, A., Makhova, A., Bataeva, D., Demkina, E., & Nikolaev, Y. A. (2024). Patterns of Biofilm Formation by Members of *Listeria, Salmonella*, and *Pseudomonas* at Various Temperatures and the Role of Their Synergistic Interactions in the Formation of Biofilm Communities. *Microbiology*, *93*(5), 598-609.

Zhao, H., Sun, Y., Shen, Y., Tan, M., & Wang, P. (2024). Inhibition of bacteria adhesion and biofilm formation using a precisely structured nitric oxide-releasing coating with repeatedly renewing antimicrobial and antifouling ability. *Applied Materials Today*, *41*, 102468.

Zhou, G., Dong, P., Luo, X., Zhu, L., Mao, Y., Liu, Y., & Zhang, Y. (2024). Combined effects of cold and acid on dual-species biofilms of *Pseudomonas fluorescens* and *Listeria monocytogenes* under simulated chilled beef processing conditions. *Food Microbiology*, *117*, 104394.

Zhou, G., Liu, Y., Dong, P., Mao, Y., Zhu, L., Luo, X., & Zhang, Y. (2024). Airborne signals of *Pseudomonas fluorescens* modulate swimming motility and biofilm formation of *Listeria monocytogenes* in a contactless coculture system. *Food Microbiology*, *120*, 104494.

Zhu, J., Yan, Y., Wang, Y., & Qu, D. (2019). Competitive interaction on dual-species biofilm formation by spoilage bacteria, *Shewanella baltica* and *Pseudomonas fluorescens*. *Journal of Applied Microbiology*, *126*(4), 1175-1186.

Zhu, Q., Gooneratne, R., & Hussain, M. A. (2017). *Listeria monocytogenes* in fresh produce: outbreaks, prevalence and contamination levels. *Foods*, *6*(3), 21.

Zhu, Y., Li, C., Cui, H., & Lin, L. (2020). Feasibility of cold plasma for the control of biofilms in food industry. *Trends in Food Science & Technology*, *99*, 142-151.

Zhu, Z., Shan, L., Li, X., Hu, F., Yuan, Y., Zhong, D., & Zhang, J. (2020). Effects of interspecific interactions on biofilm formation potential and chlorine resistance: Evaluation of dual-species biofilm observed in drinking water distribution systems. *Journal of Water Process Engineering*, *38*, 101564.